

Magnetic Tomography

On the Nullspace of the Biot-Savart Operator and
Point Sources for Field and Domain Reconstruction

Dissertation

zur Erlangung des Doktorgrades
der Mathematisch-Naturwissenschaftlichen Fachbereiche
der Georg-August-Universität Göttingen

vorgelegt von

Lars Kühn

aus

Dresden

Göttingen 2005

D7

Referent

Prof. Dr. R. Pottthast

Korreferent

Prof. Dr. R. Kress

Tag der mündlichen Prüfung:

Contents

1	Introduction and Basic Definitions	3
1.1	Introduction	3
1.2	Spaces on Lipschitz Domains	11
1.2.1	Continuous Functions and Boundary Regularity	11
1.2.2	Sobolev Spaces	13
1.2.3	Denseness and Imbedding Theorems	16
1.2.4	Spaces of Vector Fields	18
1.3	Trace Operators	20
1.4	Potential Theory	23
1.4.1	Green's Representation Formulas	23
1.4.2	Boundary Value Problems for Laplace's equation	27
1.4.3	Boundary and Volume Potentials	30
1.4.4	The Helmholtz Decomposition	34
2	Magnetic Tomography via the Biot-Savart Operator	37
2.1	Vector analysis for the Biot-Savart operator	39
2.2	Decomposition with Respect to the Nullspace	41
2.2.1	A characterization of $N(W)$	42
2.2.2	A characterization of $N(\mathcal{W})^\perp$	43
2.2.3	More properties of $N(W)^\perp$	45
2.3	Magnetic Tomography for Ohmic Conductors	50
2.3.1	The Anisotropic Impedance Problem	50
2.3.2	Orthogonality of Ohmic Currents	52
2.3.3	A Numerical Study on the Stabilized Inversion	53
2.4	Exterior Field Calculation from Boundary Data	64
3	Magnetic Impedance Tomography	69
3.1	A Homogeneous Conductor with one Inclusion	71
3.1.1	Transmission Boundary Condition	72
3.1.2	Neumann Boundary Condition	74
3.1.3	Numerical Implementation	76
3.2	Field Reconstruction by the Point Source Method	83

3.2.1	The Point Source Approximation	84
3.2.2	Numerical Implementation of the Point Source Method	89
3.3	Shape Reconstruction by the No Response Test	96
3.3.1	Realization of the No Response Test	96
3.3.2	Numerical Examples of the Shape Reconstruction	98
A	Mathematical Background	107
A.1	Tikhonov Regularization	107
A.2	Riesz-Fredholm Theory	109
A.3	Boundary Integral Representation of Harmonic Functions	112
A.4	Boundary Integral Representation of Harmonic Fields	118
A.5	Formulas of Vector Analysis	124
	List of Figures	126
	List of Boundary Value Problems	127
	Bibliography	131

Chapter 1

Introduction and Basic Definitions

1.1 Introduction

Alkaline, hydrogen, and methanol fuel cells are important future technologies. They produce energy through the chemical reaction of hydrogen and oxygen. A fuel cell consists of three layers, the anode layer (a graphite plate), a membrane with catalyst (often platinum) and the cathode layer (again a graphite plate). Hydrogen is induced at the anode, oxygen (usually as part of the air) at the cathode. The hydrogen is decomposed into protons and electrons. Then the protons move through the semipermeable membrane towards the cathode. This leads to an electric potential which drives the electrons through a wire which connects the anode and the cathode. At the cathode the electrons, protons and the oxygen react to water. As a byproduct heat is generated.

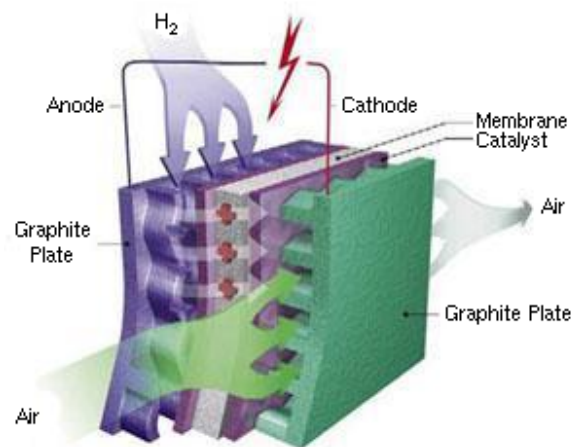


Figure 1.1: Basic principle of a hydrogen fuel cell. Image by Landesinitiative Brennstoffzelle Niedersachsen.

To increase the electric power many fuel cells are connected in series and build a fuel cell stack. For a fuel cell stack, the release of energy is maximal if one can distribute these reactions equally into a stack. Areas of too high reactivity lead to higher temperature and destroy the electrolyte membrane ('burn out') whereas areas of lower reactivity do not achieve their capacity. A reason for different reactivity may be a non-homogeneous supply of hydrogen and oxygen.

One basic problem for fuel cells is to get information about the reactivity which is proportional to the local current density. The best way would be to measure the current distribution at sufficiently many positions inside a fuel cell. This is carried out by different *segmentation methods*, where the fuel cell is segmented into a number of segments in which the current distribution is electrically measured. Of course, by segmenting a fuel cell the original current distribution of a standard fuel cell is changed and it is not clear today whether the current distribution of segmented fuel cells do reflect the true current distribution in unsegmented fuel cells.

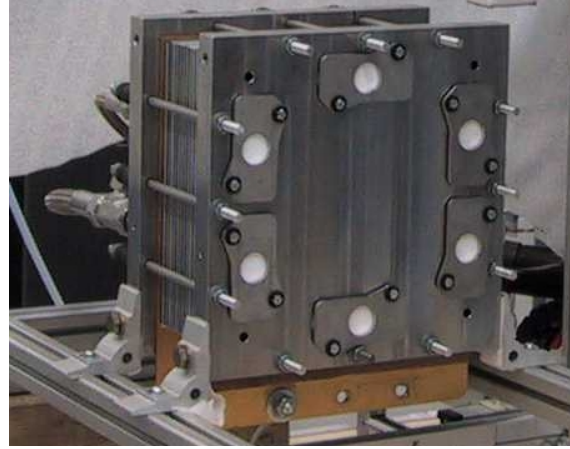


Figure 1.2: Stack consisting of 8 fuel cells, with courtesy by TomoScience GbR, Wolfsburg.

The idea of *magnetic tomography* is to reconstruct the current distribution from its magnetic field measured in the exterior B^e of the fuel cell stack B . Currents and their magnetic fields are related by Maxwell's equations. Since the currents in fuel cells are constant in time, we are interested in the electrostatic case. The *electrostatic Maxwell equations*

$$\operatorname{curl} \mathbf{E} = \mathbf{0}, \quad \operatorname{div} \mathbf{D} = \rho, \quad (1.1)$$

$$\operatorname{curl} \mathbf{H} = \mathbf{j}, \quad \operatorname{div} \mathbf{B} = 0 \quad (1.2)$$

are complemented by the *material equations*

$$\mathbf{D} = \epsilon \epsilon_0 \mathbf{E}, \quad \mathbf{B} = \mu \mu_0 \mathbf{H}. \quad (1.3)$$

For a simpler analysis we will restrict our attention to the case of material constants $\epsilon \in \mathbb{R}^+$ in B and $\mu = 1$ in all \mathbb{R}^3 . In particular, the fuel cell stacks are not allowed to consist of magnetisable materials like iron which is the main restriction in praxis. With these assumptions the *magnetic Maxwell equations* (1.2) reduce to

$$\operatorname{div} \mathbf{H} = 0, \quad \operatorname{curl} \mathbf{H} = \mathbf{j} \quad \text{in } B, \quad (1.4)$$

$$\operatorname{div} \mathbf{H} = 0, \quad \operatorname{curl} \mathbf{H} = \mathbf{0} \quad \text{in } B^e. \quad (1.5)$$

We will derive a phenomenological model for the currents in a fuel cell stack in Section 2.3.1. Modelling the chemical processes in the stack on a macroscopic scale by some *effective conductivity* σ we work with an *anisotropic impedance problem* and develop a variational theory for its solution. We will call currents \mathbf{j}_σ which solve the anisotropic impedance problem *ohmic currents*.

The magnetic field \mathbf{H} of some current distribution \mathbf{j} in a subset B of \mathbb{R}^3 is given by the Biot-Savart's law

$$\mathbf{H}(x) = \frac{1}{4\pi} \int_B \mathbf{j}(y) \times \frac{x-y}{|x-y|^3} dy, \quad x \in \mathbb{R}^3. \quad (1.6)$$

In the easiest case for fuel cell stacks, the set B is a simply-connected rectangular area in \mathbb{R}^3 , i.e. a simply-connected domain with a connected Lipschitz surface. For this reason we will work with trace operators on Lipschitz surfaces in parts of our analysis. The current distribution \mathbf{j} is a three-dimensional vector field with cartesian components \mathbf{j}_k , $k = 1, \dots, 3$. By $\operatorname{div} \operatorname{curl} \mathbf{H} = 0$ via (1.4) we consider currents \mathbf{j} with free divergence. Measurements are taken on the boundary ∂G of some domain G which contains the closure \overline{B} of B in its interior. Following equation (1.6), the mapping of the current distribution onto its magnetic field is described by the *Biot-Savart integral operator*

$$(\mathcal{W}\mathbf{j})(x) := \frac{1}{4\pi} \int_B \mathbf{j}(y) \times \frac{x-y}{|x-y|^3} dy, \quad x \in \partial G. \quad (1.7)$$

A basic task of magnetic tomography is the investigation of the properties of the integral operator \mathcal{W} and the related *Biot-Savart integral equation*

$$\mathcal{W}\mathbf{j} = \mathbf{H}. \quad (1.8)$$

The reconstruction problem to determine \mathbf{j} from \mathbf{H} naturally leads to a number of basic questions.

1. Given some magnetic field, is it possible to uniquely reconstruct the original current distribution \mathbf{j} which generated \mathbf{H} , i.e. is \mathcal{W} injective or does \mathcal{W} have a non-trivial nullspace $N(\mathcal{W})$?
2. If $N(\mathcal{W})$ is non-trivial, can the space be explicitly characterized, i.e. is it possible to describe $N(\mathcal{W})$ without using the operator \mathcal{W} ? In general terms we ask for functions which do not generate a magnetic field in the exterior of B .
3. Is the reconstruction of \mathbf{j} from \mathbf{H} stable? How can we stabilize the calculation of \mathbf{j} ?

First, the authors Kress, Kühn and Potthast have shown in [KrKüPo] that the nullspace of \mathcal{W} is non-trivial and contains the set of all compactly supported vector fields which arise from an component-wise application of the Laplace operator to some sufficiently smooth vector field

$$\{\mathbf{j} = \Delta \mathbf{m} \mid \mathbf{m} \in \mathbf{C}_0^2(B)\}. \quad (1.9)$$

Second, the characterization of $N(\mathcal{W})$ will be carried out in Section 2.2.1 of this work. We will show that the nullspace $N(\mathcal{W})$ is given by the set

$$\{\operatorname{curl} \mathbf{v} \mid \mathbf{v} \in \mathbf{H}_0^1(B), \operatorname{div} \mathbf{v} = 0\}. \quad (1.10)$$

Third, the Biot-Savart integral operator considered as an operator $\mathbf{L}^2(B) \rightarrow \mathbf{L}^2(\partial G)$ has an analytic kernel. Thus, the Biot-Savart integral operator \mathcal{W} is compact, the integral equation (1.8) is ill-posed, and the inverse \mathcal{W}^{-1} cannot be bounded. An application of an unbounded operator to data with measurement errors usually leads to reconstructions which are tampered and do not reflect the true solution. Even small errors in the data may be amplified to uncontrolled errors in the reconstructions. Thus, we need to employ an appropriate stabilization for the solution of the equation.

A well known regularization method for linear integral equations with compact integral operator is the *Tikhonov regularization* which calculates an approximate solution to equation (1.8) by

$$\mathbf{j}_\alpha := (\alpha \mathcal{I} + \mathcal{W}^* \mathcal{W})^{-1} \mathcal{W}^* \mathbf{H} \quad (1.11)$$

with *regularization parameter* $\alpha > 0$. We sum up the relevant facts in Section A.1. Since the operator \mathcal{W}^* maps $\mathbf{L}^2(\partial G)$ onto $N(\mathcal{W})^\perp$, the reconstructed current density \mathbf{j}_α is in the *orthogonal space* $N(\mathcal{W})^\perp$ to the nullspace $N(\mathcal{W})$. This leads to the following important questions for magnetic tomography.

4. Can we explicitly characterize the orthogonal space $N(\mathcal{W})^\perp$? In general terms we ask: which functions (or equivalence classes of functions) do generate a magnetic field outside?
5. What is the relation of ohmic currents to the nullspace $N(\mathcal{W})$ and its orthogonal space $N(\mathcal{W})^\perp$?

The characterization of the orthogonal space $N(\mathcal{W})^\perp$ will be achieved in Sections 2.2.2 and 2.2.3. We will show that

$$N(\mathcal{W})^\perp = \{ \mathbf{j} \in \mathbf{H}_{div=0}(B) \mid \exists q \in L^2(B) : \text{curl } \mathbf{j} = \text{grad } q \}, \quad (1.12)$$

in particular, we show that the components of $\mathbf{j} \in N(\mathcal{W})^\perp$ are solutions to the Laplace equation in a weak sense. Under the assumption of more regularity, the elements of this space are described as solutions to special boundary value problems.

The question 5 is answered in Section 2.3.2, where the *orthogonality relation*

$$\mathbf{j}_\sigma \perp_{\sigma^{-1}} N(\mathcal{W}) \quad (1.13)$$

with the orthogonality $\perp_{\sigma^{-1}}$ with respect to the scalar product

$$\langle \mathbf{u}, \mathbf{v} \rangle_{\sigma^{-1}} := \int_B \sigma(y)^{-1} \mathbf{u}(y) \cdot \mathbf{v}(y) dy \quad (1.14)$$

is proven for ohmic current densities \mathbf{j}_σ . If σ is a multiple of the identity matrix, then this scalar product reduces to the ordinary \mathbf{L}^2 -scalar product and in this case the ohmic current would be in $N(\mathcal{W})^\perp$, i.e. in principle we would be able to fully recover the true

current density. For small perturbations of such a uniform conductivity by continuity of the scalar product we can expect reasonable reconstructions of the true currents.

To prove the reconstructability of faults in a fuel cell stack we have both carried out numerical investigations and real data reconstructions with wire grids and fuel cells ¹. Some results for real data reconstructions are exemplarily documented in Section 2.3.3.

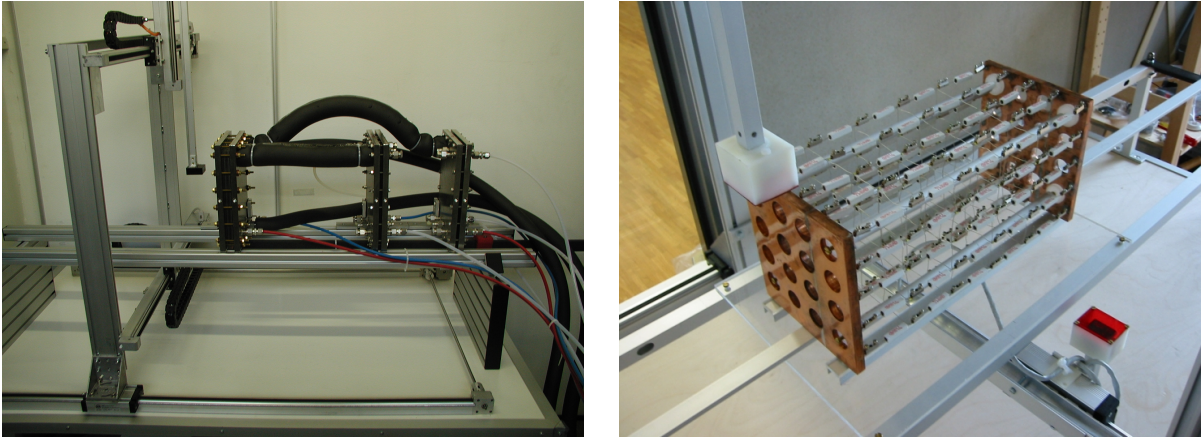


Figure 1.3: Fuel cell, wire grid model and measurement device for magnetic tomography, with friendly permission by TomoScience GbR, Wolfsburg.

So far, we have worked with measurements of the full magnetic field \mathbf{H} on the surface ∂G . Both from a practical and theoretical viewpoint we are lead to another natural question.

6. How much data do we need to measure on ∂G to uniquely determine the magnetic field \mathbf{H} in the exterior B^e ?

The sixth question is investigated in Section 2.4. We first show that the boundary values of \mathbf{H} on ∂G uniquely determine the magnetic field in B^e . Second, we investigate the situation where the normal of the current density \mathbf{j} is known on ∂B . Then, the normal component of \mathbf{H} uniquely determines the magnetic field in B^e , i.e.

$$\nu \cdot \mathbf{j}|_{\partial B} \text{ and } \nu \cdot \mathbf{H}|_{\partial G} \text{ determine } \mathbf{H} \text{ in } B^e. \quad (1.15)$$

Third, it is proven that the knowledge of the tangential components of \mathbf{H} on ∂G is sufficient for the calculation of \mathbf{H} in the exterior. For the latter case we show that the tangential components $\nu \times \mathbf{H}$ on ∂G already determine the normal components of the current density on ∂B , i.e.

$$\nu \times \mathbf{H}|_{\partial G} \text{ determines } \mathbf{H} \text{ in } B^e \text{ and } \nu \cdot \mathbf{j}|_{\partial B}. \quad (1.16)$$

¹Grid reconstructions have been performed in collaboration with TomoScience GbR, Wolfsburg. Measurements on real fuel cells have been done at the Research Center Jülich, again in collaboration with TomoScience.

This result shows the *redundance* of some of the information used in magnetic tomography, where usually the divergence equations and the normal component $\nu \cdot \mathbf{j}$ are exploited in reconstruction algorithms to enhance the quality of the reconstructions.

In the first part of this work we have considered the general magnetic tomography problem where the task is to reconstruct currents from measured magnetic fields. It is shown that this reconstruction has a large nullspace and, in general, it is not possible to reconstruct conductivities from the knowledge of the magnetic field in the exterior domain B^e . This leads to the following two further scientific problems.

First, from other parts of the area of inverse problems it is well known that the reduction of some general reconstruction problem to some particular reduced shape reconstruction problem may yield much better results and uniqueness statements. For this reason in the second part we will study the case where the conductivity takes two different constant values in $B \setminus \bar{D}$ and D with some subdomain $\bar{D} \subset B$.

Second, appropriate measurements of the magnetic field on some surface ∂G do determine \mathbf{H} in B^e , but in general they do not determine \mathbf{H} in the interior B . However, it is reasonable to generate more data and, thus, improve the reconstructability by the measurement of further physical quantities. For the application with fuel cell stacks, the electrical potential on the surface of the stack can be measured and we will provide this additional data

$$\nu \times \mathbf{E}|_{\partial B}. \quad (1.17)$$

It opens the possibility to obtain field reconstructions of \mathbf{H} in some subsets of B and shape reconstructions of D by the application of methods from other areas of inverse problems for partial differential equations.

As a preparation for the analysis of the inverse problems and as a basis for numerical simulations we investigate the *transmission impedance problem* in Section 3.1.1. The case of the *Neumann boundary condition* is treated in Section 3.1.2. For both cases the representation of the magnetic field \mathbf{H} in \mathbb{R}^3 by the Biot-Savart integral operator is transformed into a boundary-layer representation

$$\mathbf{H} = (\sigma_B - \sigma_D)\vec{\mathcal{S}}_D(\nu \times \mathbf{E}) - \sigma_B\vec{\mathcal{S}}_B(\nu \times \mathbf{E}) \quad (1.18)$$

with the single layer potential operator

$$(\vec{\mathcal{S}}_G \mathbf{t})(x) := \frac{1}{4\pi} \int_{\partial G} \frac{1}{|x - y|} \mathbf{t}(y) ds(y), \quad x \in \mathbb{R}^3 \quad (1.19)$$

for some domain G with sufficiently smooth boundary. The numerical implementation of the impedance problem and the boundary potentials is described in Section 3.1.3.

The basic idea of the *point source method* for field reconstructions is the approximation of the fundamental solution

$$\Phi(x, y) = \frac{1}{4\pi} \frac{1}{|x - y|} \quad (1.20)$$

in appropriate field representations and the use of this approximation to replace unknown integral terms by functions of measured quantities. For magnetic impedance tomography, a representation of the magnetic field is provided by (1.18). Here, the domain D and $\nu \times \mathbf{E}|_{\partial D}$ are unknown. It is worked out in Section 3.2.1, how the term $(\sigma_B - \sigma_D)\vec{\mathcal{S}}_D(\nu \times \mathbf{E})$ can be calculated from the knowledge of $\mathbf{H}|_{\partial B}$ and $\nu \times \mathbf{E}|_{\partial B}$ via some approximation of Φ by a single-layer potential over ∂B .

A *numerical study* of the field reconstructions by the point source method is provided in Section 3.2.2. In particular, we demonstrate the pointwise error in the field reconstructions and prove that the point source method is a reasonable method for stable field reconstructions in magnetic tomography.

For general transmission problems with some inclusion D , the magnetic field does not uniquely determine the shape of the inclusion D , since the field alone does not provide any criterion to detect the location of ∂D . Thus, for the shape reconstruction, we will investigate the adaption of the *no response test* introduced by Luke and Potthast [LuPo] for acoustic scattering problems to the magnetic tomography problem. The basic idea of the no response test also starts from (1.18). We multiply the equation by a function $a(x)$, $x \in \partial B$ and integrate over ∂B to obtain

$$\int_{\partial B} \left(\mathbf{H}(x) + \sigma_B \vec{\mathcal{S}}_B(\nu \times \mathbf{E}) \right) a(x) ds(x) = (\sigma_B - \sigma_D) \int_{\partial D} v(y)(\nu \times \mathbf{E})(y) ds(y) \quad (1.21)$$

with

$$v(y) := \int_{\partial B} \Phi(x, y) a(x) ds(x), \quad y \in B. \quad (1.22)$$

The integral (1.21) is called the *response* for probing with the function v or density a , respectively. Given some test domain $G \subset B$ we show in Section 3.2 that it is possible to choose the density a such that v is small on G and has large variations outside of G . Thus, if $D \subset G$, then also the above response (1.21) is small. In general, if $D \not\subset G$, the response is not small. The no response test reconstructs the unknown scatterer as the intersection of test domains such that the response is smaller than some given threshold.

We describe the detailed algorithm of the no response test in Sections 3.3.1 and 3.3.2 and provide numerical examples for reconstructions. In particular, the results show that the no response test can be used to calculate reasonable shape reconstructions for the inverse transmission problem and inverse Neumann problem of magnetic impedance tomography.

During the study of the Biot-Savart operator we have published two papers [KüPo] and [KrKüPo] representing the status at that time. A third paper [HaKüPo] is accepted for publishing. In [KrKüPo] we have shown that the nullspace is not trivial and have characterized the nullspace under the assumption that the current distribution is based on a conductivity distribution by Ohm's law. Furthermore, we have described a method to reconstruct the current distribution using Tikhonov regularization. The underlying

numerical results such as convergence and stability of finite integration techniques applied to magnetic tomography are published in [KüPo]. In [HaKüPo] we have fully characterized the nullspace of the Biot-Savart operator and its orthogonal complement which is the contents of the Section 2.2. Moreover, we have given two examples for an element of the nullspace and an element of its complement in this paper.

A first theoretical result of magnetic tomography was reached by Banks and Kojima [BaKo]. They considered a homogeneous conductor in two dimension with a non-conducting inclusion and tried to detect the boundary curve of the inclusion by minimization of a fit-to-data scalar function.

Magnetic tomography is not only used for monitoring the current distributions in fuel cells and accumulators, respectively. Another approach is biomagnetic imaging, i.e. the visualisation of currents inside a body (especially brain) from their magnetic field. A detailed introduction into the physics is given by Sarvas [Sa]. He models currents from electromotive forces impressed by biological activities. He reduces the problem to a piecewise constant conductivity distribution and consider a Poisson equation with transmission boundary conditions. Tilk and Wach [TiWa] followed this approach and solved the inverse problem by using a regularization scheme as Wiener filter estimation. Further problems on reconstructing currents on surfaces in the brain are treated by Ramon et. al. [Ra1] and [Ra2]. There is a large number of papers on reconstructing magnetic sources in cardiomagnetic inverse problems. As an example we refer to Stroink [Str] and the literature cited therein. Further application fields are geophysics and solar physics where the currents are reconstructed from magnetic satellite data.

A large part of this work has been developed in a cooperation project of the Young Researchers Group "New numerical methods for inverse problems" at the Faculty of Mathematics of the University of Göttingen with the TomoScience GbR (formerly Xcellvision), Wolfsburg. The main task was to build up a measurement device for magnetic fields of fuel cell stacks and to reconstruct the current distribution inside the stacks. Besides physical problems such as magnetism and magnetisability of some materials the typical mathematical problems have arised which we have formulated in the questions 1-6. The chief executive of TomoScience, Dr. Ing. Karl-Heinz Hauer, contacted the young researcher group and a very successful collaboration has developed. Here at this stage, I explicitly thank Karl-Heinz Hauer for the cooperation, and Roland Potthast, the leader of the young researcher group and my doctoral advisor. Both have provided me with the opportunity to write my dissertation in a field of practical importance.

I would also like to thank all the members of the Institute for Numerical and Applied Mathematics for their support of this dissertation. In particular, I profited by the excellent support of the system administrators Dr. G. Siebrasse and R. Wassmann. Last but not least I thank Prof. Dr. Rainer Kress as the second corrector. He was the tutor of my diploma thesis and, during the study of mathematics, he has introduced me into the field of inverse problems.

1.2 Spaces on Lipschitz Domains

In this section we introduce the spaces we require for our analysis. We base our considerations on the concepts of Sobolev spaces. A very detailed treatment can be found in [Adams] or [Gri], where the generalized Sobolev spaces $W^{m,p}(B)$ are investigated. We restrict our attention to the case $p = 2$ with the notation $H^m = W^{m,2}(B)$. We begin with scalar function spaces and afterwards we turn to the spaces of vector fields. Basically in this text, we assume B to be a bounded connected domain with a connected boundary ∂B . The boundary ∂B is Lipschitz continuous. If we require unbounded domains or more regularity on ∂B , we indicate it at the corresponding positions.

We start with introducing continuous functions and the declaration of the regularity of a boundary ∂B in our first subsection. In Subsection 1.2.2 we introduce the Sobolev spaces $H^m(B)$. In order to extend the classical potential theory we sum up denseness results and imbedding theorems in Subsection 1.2.3. Finally, we provide the spaces of vector fields which we need for the analysis of the Biot-Savart operator in Subsection 1.2.4.

1.2.1 Continuous Functions and Boundary Regularity

As basic spaces we need the linear space $C_0^\infty(B)$ of infinitely differentiable functions with compact support in B , and

$$C^\infty(\overline{B}) := \{u|_B \mid u \in C_0^\infty(\mathbb{R}^3)\}, \quad (1.23)$$

the restriction on B of all functions with compact support in \mathbb{R}^3 . We recall the space $C^0(B)$ of continuous functions defined in B and

$$C^m(B) := \{u \in C^0(B) \mid \partial^\alpha u \in C^0(B), \quad \forall |\alpha| \leq m\}, \quad (1.24)$$

the space of m -times continuously differentiable functions. Here, we use the multi-indices $\alpha = (\alpha_1, \dots, \alpha_N) \in \mathbb{N}^N$ with $|\alpha| := \sum_{i=1}^N \alpha_i$ and the usual notation of derivatives

$$\partial^\alpha u := \frac{\partial^{|\alpha|} u}{\partial^{\alpha_1} u \dots \partial^{\alpha_N} u}. \quad (1.25)$$

We remark that $C^m(B)$ functions are not necessarily bounded and introduce $C^m(\overline{B})$ as the space of all functions $u \in C^m(B)$ with bounded and uniformly continuous derivatives $\partial^\alpha u, \forall |\alpha| \leq m$. The space $C^m(\overline{B})$ equipped with the norm

$$\|u\|_{C^m(\overline{B})} := \sum_{i=0}^m \sup_{x \in B} \sup_{|\alpha|=i} |\partial^\alpha u(x)| \quad (1.26)$$

is a Banach space. Sometimes we need more than simple continuity. Let $0 < r \leq 1$ and u be a function defined on B . If the expression

$$\sup_{\substack{x, y \in B \\ x \neq y}} \frac{|u(x) - u(y)|}{|x - y|^r} \quad (1.27)$$

is finite, we call u Hölder continuous with exponent r . Especially, for $r = 1$, we call u Lipschitz continuous. Clearly, if u is Hölder continuous, then u is continuous in B . We denote the linear space of Hölder continuous functions by $C^{0,r}(\overline{B})$. We say u is locally Hölder continuous with exponent r , if expression (1.27) is finite on compact subsets of B and denote this space by $C^{0,r}(B)$. In a certain sense, Hölder continuity may be viewed as fractional differentiability. This suggests a widening of the known spaces of differentiable functions. The Hölder spaces $C^{m,r}(\overline{B})$ and $C^{m,r}(B)$ are defined as the subspaces of $C^m(\overline{B})$ and $C^m(B)$ consisting of functions whose m -th order partial derivatives are Hölder continuous. By setting

$$C^{m,0}(B) = C^m(B), \quad C^{m,0}(\overline{B}) = C^m(\overline{B})$$

we may include the spaces of m -times differentiable functions among the Hölder spaces. The Hölder spaces are Banach spaces with norm

$$\|u\|_{C^{m,r}(\overline{B})} := \|u\|_{C^m(\overline{B})} + \sup_{|\alpha|=m} \sup_{\substack{x,y \in B \\ x \neq y}} \frac{|\partial^\alpha u(x) - \partial^\alpha u(y)|}{|x - y|^r}. \quad (1.28)$$

Now, we are able to give a definition for what we mean by the regularity of the boundary ∂B . By the following one we view ∂B locally as a two dimensional submanifold of \mathbb{R}^3 .

Definition 1.1 *Let B be an open subset of \mathbb{R}^3 . We say ∂B is continuous (resp. Lipschitz continuous, of class C^m , of class $C^{m,1}$ for some $m \in \mathbb{N}_0$) if for every $x \in \partial B$ exists a neighborhood $\Omega(x)$ in \mathbb{R}^3 and new coordinates $y = (y_1, y_2, y_3)$ such that*

- $\Omega(x)$ is a hypercube in the new coordinates

$$\Omega(x) = \{y = (y_1, y_2, y_3)^t \mid -a_i < y_i < a_i, i = 1 \dots 3\}. \quad (1.29)$$

- There exists a continuous (resp. Lipschitz continuous, C^m , $C^{m,1}$) function f defined in

$$\tilde{\Omega}(x) = \{\tilde{y} = (\tilde{y}_1, \tilde{y}_2)^t \mid -a_i < \tilde{y}_i < a_i, i = 1 \dots 2\} \quad (1.30)$$

that satisfies $|f(\tilde{y}_1, \tilde{y}_2)| \leq \frac{a_3}{2}$, $\forall (\tilde{y}_1, \tilde{y}_2) \in \tilde{\Omega}(x)$ and

$$B \cap \Omega(x) = \{y \mid y_3 < f(y_1, y_2)\}, \quad \partial B \cap \Omega(x) = \{y \mid y_3 = f(y_1, y_2)\}. \quad (1.31)$$

Here, ∂B is represented by the mapping $F(y_1, y_2) = (y_1, y_2, f(y_1, y_2))$ from $\tilde{\Omega}(x)$ onto $\partial B \cap \Omega(x)$. Its regularity is determined by that of f . Basically in this work, we consider a Lipschitz continuous boundary ∂B , i.e. f is Lipschitz continuous.

1.2.2 Sobolev Spaces

A measurable function on B is the equivalence class of functions which differs only on a subset of measure zero. By $L^p(B)$, $p \geq 1$ we denote the space consisting of measurable functions f on B for which

$$\|f\|_{L^p(B)} := \left(\int_B |u|^p dx \right)^{\frac{1}{p}} \quad (1.32)$$

is finite. This expression defines a norm on $L^p(B)$, and $L^p(B)$ is a Banach space with respect to (1.32). For $p = \infty$ we declare $L^\infty(B)$ as the space of bounded functions on B with norm

$$\|f\|_{L^\infty(B)} := \operatorname{ess\,sup}_B |u|. \quad (1.33)$$

Let $C_0^\infty(B)^*$ be the dual space of $C_0^\infty(B)$ which is often called the space of distributions on B , and $\langle \cdot, \cdot \rangle$ the duality pairing between $C_0^\infty(B)$ and $C_0^\infty(B)^*$. If u is a locally integrable function, then u can be identified with a distribution by

$$\langle u, v \rangle = \int_B uv dx, \quad \forall v \in C_0^\infty(B). \quad (1.34)$$

Consider $L^2(B)$ and its scalar product $\langle u, v \rangle_{L^2(B)} = \int_B uv dx$. We define the weak derivative (also called ∂^α) by

$$\langle \partial^\alpha u, v \rangle = (-1)^{|\alpha|} \langle u, \partial^\alpha v \rangle, \quad \forall v \in C_0^\infty(B). \quad (1.35)$$

If u is α -times differentiable, the weak derivative definition coincides with the classical definition. Now, we are able to introduce the Sobolev spaces with $m \in \mathbb{N}_0$ by

$$H^m(B) := \{u \in L^2(B) \mid \partial^\alpha u \in L^2(B), \quad \forall |\alpha| \leq m\}, \quad (1.36)$$

especially $H^0(B) = L^2(B)$. $H^m(B)$ is a Hilbert space with the scalar product

$$\langle u, v \rangle_{H^m(B)} := \sum_{|\alpha| \leq m} \int_B \partial^\alpha u \partial^\alpha v dx. \quad (1.37)$$

We denote the corresponding norm by $\|\cdot\|_{H^m(B)}$. By the next definition we extend the Sobolev spaces $H^m(B)$ to non-integer values of m .

Definition 1.2 Let $s > 0$ and $s = m + r$ with $m \in \mathbb{N}_0$ and $0 < r < 1$. We denote by $H^s(B)$ the space of all functions u of $H^m(B)$ such that

$$\int_B \int_B \frac{|\partial^\alpha u(x) - \partial^\alpha u(y)|^2}{|x - y|^{3+2r}} dx dy < \infty, \quad \forall |\alpha| = m. \quad (1.38)$$

The expression (1.38) is often called *Slobodeckii seminorm*. It can be shown that $H^s(B)$ is a Hilbert space with the scalar product

$$\langle u, v \rangle_{H^s(B)} := \langle u, v \rangle_{H^m(B)} + \sum_{|\alpha|=m} \int_B \int_B \frac{\langle \partial^\alpha u(x) - \partial^\alpha u(y), \partial^\alpha v(x) - \partial^\alpha v(y) \rangle}{|x - y|^{3+2r}} dx dy. \quad (1.39)$$

Thus, we have found a way to declare the Sobolev spaces $H^s(B)$ for each non-negative s . If s is an integer we define $H^s(B)$ via (1.36) otherwise $H^s(B)$ is defined by Definition 1.2.

Remark 1.3 *The reader who is familiar with Sobolev spaces notes that there are various notations and definitions which slightly differ from each other. Following [Adams], page 44 the spaces are declared by*

- $W^{m,2}(B) := \{u \in L^2(B) \mid \partial^\alpha f \in L^2(B), \quad \forall |\alpha| \leq m\}$,
- $H^{m,2}(B)$ is the completion of $\{u \in C^m(B) \mid \|u\|_{H^m(B)} < \infty\}$ with respect to the norm $\|\cdot\|_{H^m(B)}$ induced by (1.37).

MEYERS and SERRIN [MeySe] have shown that both definitions are equivalent for a Lipschitz domain $B \subset \mathbb{R}^3$. Of course, there are also several ways to introduce the Sobolev spaces for fractional m . The classical definition of Sobolev spaces is based on the Fourier transform

$$(\mathcal{F}f)(\xi) := \frac{1}{(2\pi)^{3/2}} \int_{\mathbb{R}^3} f(x) e^{-ix\xi} dx, \quad \forall \xi \in \mathbb{R}^3 \quad (1.40)$$

and given by

$$H^s(\mathbb{R}^3) := \{u \in L^2(\mathbb{R}^3) \mid (1 + \xi^2)^{s/2} \mathcal{F}f \in L^2(\mathbb{R}^3)\}, \quad s \geq 0 \quad (1.41)$$

and

$$H^s(B) := \{u \in L^2(B) \mid \exists \hat{u} \in H^s(\mathbb{R}^3) \text{ with } \hat{u}|_B = u\}, \quad s \geq 0. \quad (1.42)$$

We note that this definition makes no difference between integer and non-integer values of s . In the case of a Lipschitz domain B both definitions are equivalent (see Theorem 3.18 and 3.30 in [McL] or Lemma 1.3 in [GiRa]).

In order to introduce $H^{-s}(B)$, $s > 0$ we use define

$$H_0^s(B) := \overline{C_0^\infty(B)}^{H^s(B)}, \quad (1.43)$$

i.e. $H_0^s(B)$ is the closure of $C_0^\infty(B)$ with respect to the norm $\|\cdot\|_{H^s(B)}$. We characterize the space $H^{-s}(B)$ as follows

$$H^{-s}(B) := H_0^s(B)^*, \quad \text{provided } s \neq \left\{ \frac{1}{2}, \frac{3}{2}, \frac{5}{2}, \dots \right\}. \quad (1.44)$$

It means that $H^{-s}(B)$ is the dual space of $H_0^s(B)$ equipped with the norm

$$\|f\|_{H^{-s}(B)} := \sup_{\substack{u \in H_0^s(B) \\ \|u\|_{H_0^s(B)} = 1}} \langle f, u \rangle. \quad (1.45)$$

Remark 1.4 *A detailed treatment of the dual space and the exceptional cases for s can be found in [McL], Chapter 3. Here we give a short summary. Defining*

$$\tilde{H}^s(B) := \overline{C_0^\infty(B)}^{H^s(\mathbb{R}^3)} \quad (1.46)$$

we state for a Lipschitz domain B and $s \in \mathbb{R}$

$$H^{-s}(B) = \tilde{H}^s(B)^* \quad \text{and} \quad H^s(B)^* = \tilde{H}^{-s}(B) \quad (1.47)$$

(see Theorem 3.30 in [McL]). The spaces $H_0^s(B)$, $s > 0$ and \tilde{H}^s are related by

$$\tilde{H}^s(B) = H_0^s(B) \quad \text{provided} \quad s \neq \left\{ \frac{1}{2}, \frac{3}{2}, \frac{5}{2}, \dots \right\} \quad (1.48)$$

(see Theorem 3.33 in [McL]) and

$$\tilde{H}^s(B) = H_0^s(B) = H^s(B), \quad 0 \leq s \leq \frac{1}{2} \quad (1.49)$$

(see Theorem 3.40 in [McL]).

For many applications we want to exclude the constant functions from our consideration. We manage it by the notation

$$H_\circ^2(B) = \left\{ u \in H^s(B) \mid \int_B u \, dx = 0 \right\}. \quad (1.50)$$

For our further analysis we need the Sobolev spaces on boundaries. Definition 1.1 has declared the regularity of boundaries, so we are able to define the space $H^s(\partial B)$ by the following definition.

Definition 1.5 *Let B be a bounded simply-connected domain with boundary ∂B of class $C^{m,1}$, $m \in \mathbb{N}_0$. A function u on ∂B belongs to $H^s(\partial B)$ for $s \leq m + 1$ if $u \circ F$ belongs to $H^s(\tilde{\Omega}) \cap F^{-1}(\partial B \cap \Omega)$ for all possible Ω and F fulfilling the assumptions of Definition 1.1.*

Since the resulting Hilbert norm from this definition would be hard to handle, we shall use equivalent norms as for instance for $s = 0$

$$\|u\|_{L^2(\partial B)}^2 := \int_{\partial B} |u|^2 \, ds, \quad (1.51)$$

where ds denotes the surface measure of ∂B . Other equivalent scalar products for specific Sobolev spaces will be obtained when we investigate the trace operators (see Section 1.3). At this stage, it is worthwhile to point out that the theorems of this section are also valid for the Sobolev spaces $H^s(\partial B)$. In particular, we also use the notation

$$H_\circ^2(\partial B) = \left\{ u \in H^s(\partial B) \mid \int_{\partial B} u \, ds = 0 \right\} \quad (1.52)$$

to exclude constant functions (for negative s the condition is to be understood in the sense of $\langle u, 1 \rangle = 0$).

1.2.3 Denseness and Imbedding Theorems

There is a variety of inclusion, denseness and imbedding theorems in the literature. Here, we want to tailor these theorems to our case of Lipschitz domains and Sobolev spaces $H^s(B)$. In the proofs, we cite the corresponding theorems given in the literature. We start with some simple inclusions.

Theorem 1.6 *For a bounded Lipschitz domain $B \in \mathbb{R}^3$, there hold the inclusions*

$$C^\infty(\overline{B}) \subset C^n(\overline{B}) \subset C^m(\overline{B}) \subset H^a(B) \subset H^b(B) \quad (1.53)$$

and

$$C_0^\infty(B) \subset C^n(\overline{B}) \subset L^\infty(B) \subset L^2(B) \subset L^1(B) \quad (1.54)$$

with $n, m \in \mathbb{N}_0$ and real values $a, b \in \mathbb{R}$ satisfying $n \geq m \geq a \geq b$.

Proof: At first we prove the statement (1.53). The inclusions $C^\infty(\overline{B}) \subset C^n(\overline{B}) \subset C^m(\overline{B})$ are trivial. Let $l \in \mathbb{N}_0$ with $m \geq l \geq a$. Then for all $u \in C^m(\overline{B})$ we have $\partial^\alpha u \in C^0(\overline{B}) \subset L^2(B), \forall |\alpha| \leq l$ by the definition of the partial derivatives. Therefore, $C^m(\overline{B}) \subset H^l(B)$. Since $H^a(B) \subset H^b(B)$ for all real values a, b with $a \geq b$ (see for instance [McL], Theorem 3.27), all of the following inclusions are shown

$$C^\infty(\overline{B}) \subset C^n(\overline{B}) \subset C^m(\overline{B}) \subset H^l(B) \subset H^a(B) \subset H^b(B).$$

In the second statement the inclusion $C_0^\infty(B) \subset C^n(\overline{B})$ is obvious. If $u \in C^n(\overline{B})$ we have $\sup_B |u| \leq \infty$ and thus $u \in L^\infty(B)$. For $u \in L^\infty(B)$ holds $\|u\|_{L^2(B)} \leq C \sup_B |u|$ where C is the volume of B . With the aid of the estimation $\|u\|_{L^1(B)} \leq \sqrt{C} \|u\|_{L^2(B)}$ we conclude $L^2(B) \subset L^1(B)$ and the proof is complete. ■

Theorem 1.7 *For a bounded Lipschitz domain $B \subset \mathbb{R}^3$ holds*

- $C^\infty(B) \cap H^s(B)$ is dense in $H^s(B)$ for all $s \geq 0$.
- $C^\infty(\overline{B})$ is dense in $H^s(B)$ for all $s \geq 0$.
- $C_0^\infty(B)$ is dense in $H_0^s(B)$ for all $s \geq 0$, especially $H_0^0(B) = L^2(B)$.

Proof: A proof of the first statement can be found in [GiTr], Theorem 7.9. For the second one we refer to [Adams], Theorem 3.18. The last statement follows from the definition of $H_0^s(B)$ for $s > 0$ and from characterization (1.49) for $0 \leq s \leq \frac{1}{2}$. ■

From this theorem we conclude that $C^n(B) \cap C^0(\overline{B}), n \in \mathbb{N}_0$ is dense in $L^2(B)$. Looking at the third statement, we have obtained another characterization of $L^2(B)$ as the completion of $C_0^\infty(B)$ in the L^2 -norm. As a consequence, the function space $C_0^n(B), n \in \mathbb{N}_0$ is dense in $L^2(B)$.

Before we turn to the Sobolev imbedding theorem we have to declare what we mean by a continuous imbedding $B_1 \hookrightarrow B_2$:

Definition 1.8 (Imbedding) *A Banach space B_1 is said to be continuously imbedded in a Banach space B_2 if there exists a bounded linear one-to-one mapping $B_1 \hookrightarrow B_2$.*

Theorem 1.9 (Sobolev Imbedding Theorem) *For the following imbeddings we assume B to be a bounded Lipschitz domain in \mathbb{R}^3 .*

- Let $1 \leq q \leq 6$, then

$$H^1(B) \hookrightarrow L^q(B). \quad (1.55)$$

- Suppose $j, k \in \mathbb{N}_0$ with $2k > 3$, then

$$H^{k+j}(B) \hookrightarrow C_{\text{bnd}}^j(B), \quad (1.56)$$

where $C_{\text{bnd}}^m(B)$ is defined by

$$C_{\text{bnd}}^m(B) := \{u \in C^m(B) \mid \partial^\alpha u \in L^\infty(B), \quad \forall |\alpha| \leq m\}. \quad (1.57)$$

- Suppose $j, k \in \mathbb{N}_0$ with $2k > 3 > 2k - 2$, then

$$H^{k+j}(B) \hookrightarrow C^{j,\alpha}(\overline{B}), \quad 0 < \alpha \leq k - \frac{3}{2}. \quad (1.58)$$

Proof: The full theorem and its proof can be found in [Adams], Theorem 5.4 together with Remark 5.5. ■

Remark 1.10 *For the interested reader we refer to [Adams], Theorem 5.4 and Remark 5.5 to get a wide overview of this topic. There one can see that the assumption on the domain B can be weakened in many of the statements, for instance (1.56), (1.58) holds for unbounded domains and only (1.58) requires a Lipschitz boundary ∂B .*

For the weak solutions of boundary value problems we provide well suited spaces. Let \mathcal{P} be a linear (differential) operator defined on $C^\infty(\overline{B})$. If we are able to extend the domain of \mathcal{P} to $H^s(B)$, then we consider the space

$$H_{\mathcal{P}}^s(B) := \{u \in H^s(B) \mid \mathcal{P}u \in L^2(B)\} \quad (1.59)$$

which is a Hilbert space with the Hilbert norm

$$\|u\|_{H_{\mathcal{P}}^s(B)}^2 := \|u\|_{H^s(B)}^2 + \|\mathcal{P}u\|_{L^2(B)}^2. \quad (1.60)$$

Following this idea we consider the Laplacian Δ and define

$$H_{\Delta}^1(B) := \{u \in H^1(B) \mid \Delta u \in L^2(B)\}. \quad (1.61)$$

Theorem 1.11 *Let B be a bounded Lipschitz domain, then the space $C^\infty(\overline{B})$ is dense in $H_{\Delta}^1(B)$.*

Proof: See Theorem 1.5.3.9 in [Gri]. ■

1.2.4 Spaces of Vector Fields

After the introduction of the basic scalar function spaces we turn to the vector field spaces. The usual way is to declare the product spaces, for instance

$$\mathbf{C}^{m,r}(\overline{B}) := [C^{m,r}(\overline{B})]^3, \quad \mathbf{H}^s(B) := [H^s(B)]^3. \quad (1.62)$$

We denote spaces of scalar functions by script letters and their three dimensional analogon by bold letters just as done for scalar functions and vector fields. For example, we write $\mathbf{C}_0^\infty(B)$, $\mathbf{C}^\infty(\overline{B})$, $\mathbf{L}^2(B)$. To avoid confusions with the magnetic field \mathbf{H} , we always note the order when referring to Sobolev spaces. We remark that $\mathbf{H}^s(B)$ is a Hilbert spaces with the scalar product

$$\langle \mathbf{u}, \mathbf{v} \rangle_{\mathbf{H}^s(B)} := \sum_{i=1}^3 \langle u_i, v_i \rangle_{H^s(B)} \quad (1.63)$$

for fields $\mathbf{u} = (u_1, u_2, u_3)^t$, $\mathbf{v} = (v_1, v_2, v_3)^t \in \mathbf{H}^s(B)$. In the same manner we declare the product space of fields on the boundary ∂B . From Definition 1.1 we see that Lipschitz continuous boundaries have almost everywhere a unit vector ν . Thus, we are able to define $\mathbf{L}_t^2(\partial B)$ as the space of all tangential \mathbf{L}^2 vector fields on ∂B . Dependent on the regularity of ∂B it is possible to define surface operators such as surface divergence and spaces with corresponding properties. We come back to those spaces in Section (2.4).

In addition to the elementary products we need some other spaces for which we now introduce the concepts of weak divergence and weak curl. For a field $\mathbf{u} \in \mathbf{L}^2(B)$ we declare the weak divergence (also called $\operatorname{div} \mathbf{u}$) as the distribution for which

$$\int_B \phi \operatorname{div} \mathbf{u} \, dx = \int_B \mathbf{u} \cdot \operatorname{grad} \phi \, dx, \quad \forall \phi \in C_0^\infty(B). \quad (1.64)$$

is satisfied. For a field $\mathbf{u} \in \mathbf{L}^2(\partial B)$ we identify the weak curl as the distribution (also called $\operatorname{curl} \mathbf{u}$) for which holds

$$\int_B \mathbf{v} \cdot \operatorname{curl} \mathbf{u} \, dx = \int_B \mathbf{u} \cdot \operatorname{curl} \mathbf{v} \, dx, \quad \forall \mathbf{v} \in \mathbf{C}_0^\infty(B). \quad (1.65)$$

Of course, if there exist weak derivatives the usual definitions of divergence and curl coincide with the definitions (1.64) and (1.65). As a consequence, the spaces

$$\mathbf{H}_{div}(B) := \{\mathbf{v} \in \mathbf{L}^2(B) \mid \operatorname{div} \mathbf{v} \in \mathbf{L}^2(B)\}, \quad (1.66)$$

$$\mathbf{H}_{curl}(B) := \{\mathbf{v} \in \mathbf{L}^2(B) \mid \operatorname{curl} \mathbf{v} \in \mathbf{L}^2(B)\}. \quad (1.67)$$

are subsets of $\mathbf{H}^1(B)$. Clearly, the space $\mathbf{H}_{div}(B)$ equipped with the scalar product

$$\langle \mathbf{u}, \mathbf{v} \rangle_{\mathbf{H}_{div}(B)} := \langle \mathbf{u}, \mathbf{v} \rangle_{\mathbf{L}^2(B)} + \langle \operatorname{div} \mathbf{u}, \operatorname{div} \mathbf{v} \rangle_{\mathbf{L}^2(B)} \quad (1.68)$$

is a Hilbert space. Introducing the subspace $\mathbf{H}_{div=0}(B)$ of $\mathbf{H}_{div}(B)$ by

$$\mathbf{H}_{div=0}(B) := \{\mathbf{v} \in \mathbf{H}_{div}(B) \mid \operatorname{div} \mathbf{v} = 0\} \quad (1.69)$$

we recognize that $\mathbf{H}_{div=0}(B)$ is a Hilbert space with \mathbf{L}^2 scalar product. In the same way $\mathbf{H}_{curl}(B)$ equipped with the scalar product

$$\langle \mathbf{u}, \mathbf{v} \rangle_{\mathbf{H}_{curl}(B)} := \langle \mathbf{u}, \mathbf{v} \rangle_{\mathbf{L}^2(B)} + \langle \operatorname{curl} \mathbf{u}, \operatorname{curl} \mathbf{v} \rangle_{\mathbf{L}^2(B)} \quad (1.70)$$

is a Hilbert space and

$$\mathbf{H}_{curl=0}(B) := \{\mathbf{v} \in \mathbf{H}_{curl}(B) \mid \operatorname{curl} \mathbf{v} = \mathbf{0}\} \quad (1.71)$$

with \mathbf{L}^2 scalar product is a Hilbert space, too. With the aid of the concepts of weak divergence and curl we have found two Hilbert spaces equipped with the usual \mathbf{L}^2 scalar product. Later, when we need regularization techniques for reconstruction, we are reliant on Hilbert spaces. Thus, $\mathbf{H}_{div=0}(B)$ is an excellent space for our application. The next theorem shows that smooth functions are dense in both spaces.

Theorem 1.12 *Let B be a bounded Lipschitz domain, then the set $\mathbf{C}^\infty(\overline{B})$ is a dense subset of $\mathbf{H}_{div}(B)$ as well as of $\mathbf{H}_{curl}(B)$.*

Proof: See Theorem 2.4 and Theorem 2.10 in [GiRa]. ■

From another point of view we have investigated a three dimensional analogon to the spaces $H_{\mathcal{P}}^s(B)$ from (1.59) with the divergence and curl operator. In the same way we may introduce

$$\mathbf{H}_{\Delta}^1(B) := \{\mathbf{u} \in \mathbf{H}^1(B) \mid \Delta \mathbf{u} \in \mathbf{L}^2(B)\}. \quad (1.72)$$

From Theorem 1.11 we know that $\mathbf{C}^\infty(\overline{B})$ is dense in $\mathbf{H}_{\Delta}^1(B)$.

1.3 Trace Operators

In this section, we investigate the trace operators often called boundary value operators. In preparation for the boundary value problems we study their behavior on a boundary with given regularity.

Definition 1.13 *Let $\phi \in C^\infty(\overline{B})$ be a scalar function and $\mathbf{u} \in \mathbf{C}^\infty(\overline{B})$ a vector field. We define the trace operators*

$$\begin{aligned} \gamma_0 : \phi &\mapsto \phi|_{\partial B} & \text{resp.} & & \gamma_0 : \mathbf{u} &\mapsto \mathbf{u}|_{\partial B}, \\ \partial_\nu : \phi &\mapsto \frac{\partial \phi}{\partial \nu}, \\ \gamma_\nu : \mathbf{u} &\mapsto \nu \cdot \mathbf{u}|_{\partial B}, \\ \gamma_\times : \mathbf{u} &\mapsto \nu \times \mathbf{u}|_{\partial B}, \\ \gamma_T : \mathbf{u} &\mapsto \nu \times \mathbf{u}|_{\partial B} \times \nu. \end{aligned}$$

In this text, we always denote ν as the unit outward normal to ∂B . If we distinguish between trace operators from the interior or exterior, we have to care about the normal direction. We specify the domain of the trace operators (for instance $\gamma_\nu[B], \gamma_\nu[B^e]$), therefore $\gamma_\nu[B]\mathbf{u} = -\gamma_\nu[B^e]\mathbf{u}$ for a vector field $\mathbf{u} \in \mathbf{C}^\infty(\mathbb{R}^3)$. In order to extend the domains of the trace operators γ_0, ∂_ν let us consider the mapping

$$u \mapsto \left\{ \gamma[B]u, \gamma[B]\frac{\partial u}{\partial \nu}, \dots, \gamma[B]\frac{\partial^l u}{\partial \nu^l} \right\} \quad (1.73)$$

which is defined for $u \in C^{k,1}(B)$ and $\partial B \in C^{k,1}$ provided $k \geq l$. We quote the basic trace extension theorem from [Gri].

Theorem 1.14 *Let B be a bounded simply-connected domain of \mathbb{R}^3 with a $C^{k,1}$, $k \in \mathbb{N}_0$ boundary ∂B . Assume that $\frac{1}{2} < s \leq k+1$ and $s - \frac{1}{2} \notin \mathbb{N}_0$. Let $s - \frac{1}{2} = l + r$ with a non-negative integer l and $0 < r < 1$. Then the mapping (1.73) has an unique extension as an operator from*

$$H^s(B) \text{ onto } \prod_{j=0}^l H^{s-j-\frac{1}{2}}(\partial B) \quad . \quad (1.74)$$

Proof: For the proof see Theorem 1.5.1.2 in [Gri]. ■

We explicitly note that the mapping (1.73) is not injective, the following theorem characterizes its kernel.

Theorem 1.15 *Let B be a bounded simply-connected domain of \mathbb{R}^3 with a $C^{k,1}$, $k \in \mathbb{N}_0$ boundary ∂B . Assume that $\frac{1}{2} < s \leq k+1$ and $s - \frac{1}{2} \notin \mathbb{N}_0$. Let $s - \frac{1}{2} = l + r$ with a nonnegative integer l and $0 < r < 1$. Then $u \in H_0^s(B)$ if and only if $u \in H^s(B)$ and*

$$0 = \gamma[B]u = \gamma[B]\frac{\partial u}{\partial \nu} = \dots = \gamma[B]\frac{\partial^l u}{\partial \nu^l}. \quad (1.75)$$

Proof: For the proof we refer to Theorem 1.5.1.6 in [Gri]. ■

Hence, we may give the alternative definitions

$$H_0^1(B) = \{u \in H^1(B) \mid \gamma_0[B]u = 0\}, \quad (1.76)$$

$$H_0^2(B) = \{u \in H^2(B) \mid \gamma_0[B]u = 0, \partial_\nu[B]u = 0\}. \quad (1.77)$$

While the first relation holds for a Lipschitz continuous boundary, we request a $C^{1,1}$ boundary ∂B for the second one. We are able to improve the results of Theorem 1.14 for the trace operators γ_0 and ∂_ν .

Theorem 1.16 *Let B be a Lipschitz domain, then the trace operators*

$$\gamma_0[B] : H^s(B) \rightarrow H^{s-\frac{1}{2}}(\partial B) \quad \text{and} \quad \gamma_0[B] : \mathbf{H}^s(B) \rightarrow \mathbf{H}^{s-\frac{1}{2}}(\partial B) \quad (1.78)$$

are bounded surjective operators for each $s \in (\frac{1}{2}, \frac{3}{2})$.

Proof: For the proof we refer to Theorem 3.38 in [McL]. ■

Theorem 1.17 *Let B be a Lipschitz domain, then the trace operator ∂_ν is a bounded operator*

$$H_\Delta^s(B) \rightarrow H^{s-\frac{3}{2}}(\partial B). \quad (1.79)$$

for $s \in (\frac{1}{2}, \frac{3}{2})$.

Proof: For the proof we refer to Lemma 4.3 of [Co]. ■

For the rest of this subsection we turn to the normal and tangential components of a vector field. For a smooth field \mathbf{v} in \overline{B} we have $\gamma_0 \mathbf{v} = \gamma_T \mathbf{v} + \gamma_\nu \mathbf{v} \nu$. We extend the domain of the trace operators $\gamma_\nu[B]$, $\gamma_\times[B]$ and $\gamma_T[B]$ in the following theorem.

Theorem 1.18 *The linear operators $\gamma_\nu[B]$, $\gamma_\times[B]$, $\gamma_T[B]$, can be extended by continuity to bounded operators*

$$\gamma_\nu[B] : \mathbf{H}_{div}(B) \rightarrow H^{-\frac{1}{2}}(\partial B), \quad (1.80)$$

$$\gamma_\times[B] : \mathbf{H}_{curl}(B) \rightarrow \mathbf{H}^{-\frac{1}{2}}(\partial B), \quad (1.81)$$

$$\gamma_T[B] : \mathbf{H}_{curl}(B) \rightarrow \mathbf{H}^{-\frac{1}{2}}(\partial B). \quad (1.82)$$

Proof: The statements (1.80) and (1.81) are shown in Theorem 2.5 and Theorem 2.11 of [GiRa]. The statement (1.82) follows from $\gamma_T[B] \mathbf{v} = \gamma_\times[B] \mathbf{v} \times \nu$. ■

We see that $\nu \cdot \mathbf{j}$ and $\nu \times \mathbf{j}$ are defined in the spaces $\mathbf{H}_{div}(B)$ and $\mathbf{H}_{curl}(B)$ in a weak sense, that means as extensions of the classical trace operators. For a better readability we keep writing $\partial u / \partial \nu$, $\nu \cdot \mathbf{u}$, $\nu \times \mathbf{u}$ instead of the trace operators which considerably shortens the formulas. Mostly, the meaning can be deduced from the context, but to avoid confusions

and mistakes we refer to the sense if necessary. If we explicitly distinguish between the traces from the exterior or the interior of B then we also use the notations $\nu^+ \cdot \mathbf{u}$ or $\nu^- \times \mathbf{u}$.

Again, we build the closure of $\mathbf{C}_0^\infty(B)$ with respect to the norms $\|\cdot\|_{\mathbf{H}_{div}(B)}$ and $\|\cdot\|_{\mathbf{H}_{curl}(B)}$ and define

$$\mathbf{H}_{0,div}(B) := \overline{\mathbf{C}_0^\infty(B)}^{\mathbf{H}_{div}(B)}, \quad \mathbf{H}_{0,curl}(B) := \overline{\mathbf{C}_0^\infty(B)}^{\mathbf{H}_{curl}(B)}. \quad (1.83)$$

Theorem 1.19 *The operator $\gamma_\nu[B] : \mathbf{H}_{div}(B) \rightarrow H^{-\frac{1}{2}}(\partial B)$ is surjective. Its kernel is given by $\mathbf{H}_{0,div}(B)$.*

Proof: For the nullspace statement we refer to Theorem 2.6 in [GiRa]. The proof of the range can be found in [GiRa], Corollary 2.8. ■

Theorem 1.20 *The nullspace of the operators $\gamma_\times[B], \gamma_T[B] : \mathbf{H}_{curl}(B) \rightarrow \mathbf{H}^{-\frac{1}{2}}(\partial B)$ is given by $\mathbf{H}_{0,curl}(B)$.*

Proof: See Theorem 2.12 in [GiRa]. ■

There exists a similar result for the surjectivity of $\gamma_T[B]$. We present it in Section 2.2.3 after the introduction of spaces with surface divergence on a C^2 -boundary. Similar to the characterization of $H_0^m(B)$ we are able to identify

$$\mathbf{H}_{0,div}(B) = \{\mathbf{u} \in \mathbf{H}_{div}(B) \mid \nu \cdot \mathbf{u} = 0\}, \quad (1.84)$$

$$\mathbf{H}_{0,curl}(B) = \{\mathbf{u} \in \mathbf{H}_{curl}(B) \mid \nu \times \mathbf{u} = 0\}. \quad (1.85)$$

We complete this subsection by a regularity result.

Theorem 1.21 *Let B be a bounded simply-connected domain of \mathbb{R}^3 with a $C^{m,1}$ -boundary ∂B with a non-negative integer m . We have*

$$\mathbf{H}^m(B) = \{\mathbf{v} \in \mathbf{L}^2(B) \mid \operatorname{curl} \mathbf{v} \in \mathbf{H}^{m-1}(B), \operatorname{div} \mathbf{v} \in H^{m-1}(B), \nu \cdot \mathbf{v} \in H^{m-\frac{1}{2}}(\partial B)\} \quad (1.86)$$

with the norm inequality

$$\|\mathbf{v}\|_{\mathbf{H}^m(B)} \leq C \{ \|\mathbf{v}\|_{\mathbf{L}^2(B)} + \|\operatorname{curl} \mathbf{v}\|_{\mathbf{H}^{m-1}(B)} + \|\operatorname{div} \mathbf{v}\|_{H^{m-1}(B)} + \|\nu \cdot \mathbf{v}\|_{H^{m-\frac{1}{2}}(\partial B)} \}. \quad (1.87)$$

Proof: See Corollary 3.7 in [GiRa]. ■

1.4 Potential Theory

The goal of this section is to summarize basic results from potential theory, i.e. the theory of harmonic functions and vector fields. An detailed introduction into classical potential theory can be found in [Kre] or [CoKr1]. The theory of harmonic vector fields is presented in [Ma]. We call a function u *strong* or *classical harmonic* if it fulfills the *Laplace* equation

$$\Delta u(x) = 0 \tag{1.88}$$

pointwise with the *Laplace* operator defined by

$$\Delta = \frac{\partial^2}{\partial x^2} + \frac{\partial^2}{\partial y^2} + \frac{\partial^2}{\partial z^2}. \tag{1.89}$$

For a (*weak*) *harmonic* function u , the Laplace equation $\Delta u = 0$ holds as equation in the Sobolev space $H^s(G)$ with a domain $G \in \mathbb{R}^3$, i.e. the Laplace operator is considered as mapping $H^{s+2}(G) \rightarrow H^s(G)$. We call a vector field \mathbf{u} *strong* or *classical harmonic* if it fulfills

$$\operatorname{curl} \mathbf{u} = \mathbf{0}, \quad \operatorname{div} \mathbf{u} = 0. \tag{1.90}$$

pointwise and (*weak*) *harmonic* if the equations hold as equations in appropriate Sobolev spaces. The formula $\operatorname{curl} \operatorname{curl} = -\Delta + \operatorname{grad} \operatorname{div}$ implies $\Delta \mathbf{u} = \mathbf{0}$ for a harmonic field \mathbf{u} , i.e. a harmonic field has harmonic components. Please note that fields with harmonic components need not be harmonic themselves.

We will show that the exterior magnetic field is a vector field with harmonic components in B^e . Thus, in preparation for the analysis of the Biot-Savart operator, we investigate Gauss' and Stokes theorems as well as Green's identities in the next Subsection 1.4.1. Measuring the magnetic field components on a surface ∂G with a domain G that contains \bar{B} we obtain a boundary value problem for the exterior magnetic field. In order to calculate the exterior magnetic field from various boundary data we study the basic boundary value problems for the Laplace equation in Subsection 1.4.2. In Subsection 1.4.3 we introduce the single, double, and volume potentials. On the one hand, if $\partial B \in C^2$, we are able to represent the solution of the boundary value problems in Subsection 1.4.2 in terms of single and double layer potentials on ∂B which is carried out in Section A.3 and A.4. On the other hand, the magnetic field of an ohmic current based on a piecewise constant conductivity is represented in terms of single layer potentials (see Section 3.1). At the end of this section, we investigate the vector potentials for curl-free vector fields and the Helmholtz decomposition of vector fields.

1.4.1 Green's Representation Formulas

The classical Gauss' divergence and Stokes' theorems hold for smooth boundaries and fields. Here, we need these results in the framework of Lipschitz boundaries and the Sobolev spaces. To this end we present the standard extension technique for further use.

Gauss' divergence theorem

$$\int_B \operatorname{div} \mathbf{u} \, dx = \int_{\partial B} \boldsymbol{\nu} \cdot \mathbf{u} \, ds \quad (1.91)$$

holds for fields $\mathbf{u} \in \mathbf{C}^\infty(\overline{B})$. The left side is a linear continuous mapping $\mathbf{H}_{div}(B) \rightarrow \mathbb{R}$. With the aid of the linear continuous trace operator $\gamma_\nu[B]$ the right side can be written as $\langle \gamma_\nu[B]\mathbf{u}, 1 \rangle$ in the sense of the dual system $\langle H^{-\frac{1}{2}}(\partial B), H^{\frac{1}{2}}(\partial B) \rangle$, i.e. it is also a linear continuous mapping $\mathbf{H}_{div}(B) \rightarrow \mathbb{R}$. Since $\mathbf{C}^\infty(\overline{B})$ is dense in $\mathbf{H}_{div}(B)$, there exists a sequence $(\mathbf{u}_n)_{n \in \mathbb{N}} \subset \mathbf{C}^\infty(\overline{B})$ with $\mathbf{u}_n \rightarrow \mathbf{u}, n \rightarrow \infty$ for every $\mathbf{u} \in \mathbf{H}_{div}(B)$. Then, we derive

$$\begin{aligned} \int_B \operatorname{div} \mathbf{u} \, dx &= \int_B \operatorname{div} \lim_{n \rightarrow \infty} \mathbf{u}_n \, dx = \lim_{n \rightarrow \infty} \int_B \operatorname{div} \mathbf{u}_n \, dx = \lim_{n \rightarrow \infty} \int_B \gamma_\nu[B]\mathbf{u}_n \, dx \\ &= \int_B \gamma_\nu[B] \lim_{n \rightarrow \infty} \mathbf{u}_n \, dx = \int_B \boldsymbol{\nu} \cdot \mathbf{u} \, dx. \end{aligned}$$

Therefore, the equation (1.91) is true for all $\mathbf{u} \in \mathbf{H}_{div}(B)$.

Let us consider the formula $\operatorname{div}(\phi \mathbf{u}) = \mathbf{u} \cdot \operatorname{grad} \phi + \phi \operatorname{div} \mathbf{u}$ which can be applied to $\mathbf{u} \in \mathbf{C}^1(\overline{B}), \phi \in C^1(\overline{B})$. The integration over B and an application of Gauss' divergence theorem for the field $\phi \mathbf{u}$ yield

$$\int_B \operatorname{grad} \phi \cdot \mathbf{u} \, dx + \int_B \phi \operatorname{div} \mathbf{u} \, dx = \int_{\partial B} \phi \boldsymbol{\nu} \cdot \mathbf{u} \, ds. \quad (1.92)$$

The terms on the left are well defined and linear bounded operators $H^1(B) \times \mathbf{H}_{div}(B) \rightarrow \mathbb{R}$. The right side is a linear bounded mapping $H^{1/2}(\partial B) \times H^{-1/2}(\partial B) \rightarrow \mathbb{R}$. Altogether, we are able to extend this relation to functions $\phi \in H^1(B)$ and fields $\mathbf{u} \in \mathbf{H}_{div}(B)$ by the dense approximation technique. The relation (1.92) and all of the following formulas of vector analysis and of partial differentiation including their extensions are listed in the appendix (for instance the equation (1.92) can be found in (A.73)). The Section A.5 shall be a reference, it contains well known rules and their weak forms which we prove in this work.

The next theorems summarize the basic facts from potential theory.

Theorem 1.22 (Green's Identities) *Green's first identity*

$$\int_B u \Delta v + \operatorname{grad} u \cdot \operatorname{grad} v \, dx = \int_{\partial B} u \frac{\partial v}{\partial \boldsymbol{\nu}} \, ds \quad (1.93)$$

and *Green's second identity*

$$\int_B u \Delta v - v \Delta u \, dx = \int_{\partial B} u \frac{\partial v}{\partial \boldsymbol{\nu}} - v \frac{\partial u}{\partial \boldsymbol{\nu}} \, ds \quad (1.94)$$

hold for $u, v \in C^2(B) \cap C^1(\overline{B})$.

Proof: For Green's first identity we apply Gauss' divergence theorem to the field $u \operatorname{grad} v$ and use $\operatorname{div}(u \operatorname{grad} v) = \operatorname{grad} u \cdot \operatorname{grad} v + u \Delta v$. For Green's second identity we use Green's first identity twice, second time with interchanged u, v , and subtract both results. ■

Theorem 1.23 (Green's Representation Formula) *Let $u \in C^2(B) \cap C^1(\bar{B})$. Then we have*

$$u(x) = \int_{\partial B} \Phi(x, y) \frac{\partial u(y)}{\partial \nu} - u(y) \frac{\partial \Phi(x, y)}{\partial \nu(y)} ds(y) - \int_B \Phi(x, y) \Delta u dy, \quad x \in B, \quad (1.95)$$

where the fundamental solution to the Laplacian in three dimension is given by

$$\Phi(x, y) = \frac{1}{4\pi} \frac{1}{|x - y|}, \quad x \neq y. \quad (1.96)$$

Proof: Here, we avoid to go into the technical details of the proof. We refer to [GiTr], pages 17, 18 for instance. ■

Since ∂_ν is a linear bounded operator $H_\Delta^1(B) \rightarrow H^{-\frac{1}{2}}(\partial B)$ we are able to extend Green's first identity to functions $u \in H^1(B), v \in H_\Delta^1(B)$. We will extend Green's representation formula when we treat the boundary and volume potentials. Setting $\Delta u(x) = 0, x \in B$ in (1.95) we arrive at **Green's representation formula for harmonic functions**

$$u(x) = \int_{\partial B} \Phi(x, y) \frac{\partial u(y)}{\partial \nu} - u(y) \frac{\partial \Phi(x, y)}{\partial \nu(y)} ds(y), \quad x \in B. \quad (1.97)$$

Since the integrand is infinitely differentiable and, in fact, also analytic with respect to x , it follows that the harmonic function u is analytic, too. Thus, harmonic functions are analytic throughout their domain of definition.

Corollary 1.24 *For a harmonic function $v \in C^2(B) \cap C^1(\bar{B})$ we have*

$$\int_{\partial B} \frac{\partial v}{\partial \nu} ds = 0. \quad (1.98)$$

Proof: Setting $u \equiv 1$ in (1.93) proves the statement. ■

A further property of harmonic functions which we often use in our analysis is the maximum-minimum principle

Theorem 1.25 (Maximum-Minimum Principle) *A strong harmonic function on a domain cannot attain its maximum or its minimum unless it is constant.*

Proof: See [Kre], Theorem 6.8. ■

Corollary 1.26 *Let B be a bounded domain and u be a strong harmonic function in B and continuous in \bar{B} . Then u attains both its maximum and its minimum on ∂B .*

Just as done for Gauss' divergence theorem we extend **Stokes' theorem**

$$\int_B \operatorname{curl} \mathbf{u} \, dx = \int_{\partial B} \boldsymbol{\nu} \times \mathbf{u} \, ds \quad (1.99)$$

to fields $\mathbf{u} \in \mathbf{H}_{\operatorname{curl}}(B)$, where $\boldsymbol{\nu} \times \mathbf{u}$ has to be understood in the sense of $\gamma_{\times}[B]\mathbf{u}$. As an extension of formula $\operatorname{div}(\mathbf{u} \times \mathbf{v}) = \mathbf{v} \operatorname{curl} \mathbf{u} - \mathbf{u} \operatorname{curl} \mathbf{v}$ we have

$$\int_B \mathbf{v} \cdot \operatorname{curl} \mathbf{u} \, dx - \int_B \mathbf{u} \cdot \operatorname{curl} \mathbf{v} \, dx = \int_{\partial B} \gamma_{\mathbf{T}} \mathbf{v} \cdot \gamma_{\times} \mathbf{u} \, ds \quad (1.100)$$

for $\mathbf{u} \in \mathbf{H}_{\operatorname{curl}}(B)$, $\mathbf{v} \in \mathbf{H}^1(B)$ which can be concluded by denseness of $\mathbf{C}^\infty(\bar{B})$ in $\mathbf{H}_{\operatorname{curl}}(B)$ and $\mathbf{H}^1(B)$, respectively. Again, the expression on the right hand side has to be understood in the dual system $\langle H^{\frac{1}{2}}(\partial B), H^{-\frac{1}{2}}(\partial B) \rangle$.

Subsequently, we state a vector form of Green's identities.

Theorem 1.27 (Green's Vector Identities) *Let $\mathbf{u}, \mathbf{v} \in \mathbf{C}^2(B) \cap \mathbf{C}^1(\bar{B})$, then we have Green's first vector identity*

$$\int_B \mathbf{u} \cdot \Delta \mathbf{v} + \operatorname{curl} \mathbf{u} \cdot \operatorname{curl} \mathbf{v} + \operatorname{div} \mathbf{u} \operatorname{div} \mathbf{v} \, dx = \int_{\partial B} \boldsymbol{\nu} \cdot \mathbf{u} \operatorname{div} \mathbf{v} + \boldsymbol{\nu} \times \mathbf{u} \cdot \operatorname{curl} \mathbf{v} \, ds \quad (1.101)$$

and Green's second vector identity

$$\int_B \mathbf{u} \cdot \Delta \mathbf{v} - \mathbf{v} \cdot \Delta \mathbf{u} \, dx = \int_{\partial B} \boldsymbol{\nu} \cdot \mathbf{u} \operatorname{div} \mathbf{v} + \boldsymbol{\nu} \times \mathbf{u} \cdot \operatorname{curl} \mathbf{v} - \boldsymbol{\nu} \cdot \mathbf{v} \operatorname{div} \mathbf{u} - \boldsymbol{\nu} \times \mathbf{v} \cdot \operatorname{curl} \mathbf{u} \, ds. \quad (1.102)$$

Proof: Consider the field $\mathbf{u} \operatorname{div} \mathbf{v} + \mathbf{u} \times \operatorname{curl} \mathbf{v}$ for $\mathbf{u}, \mathbf{v} \in \mathbf{C}^2(B) \cap \mathbf{C}^1(\bar{B})$. To evaluate the divergence of this field we use the formulas $\operatorname{div}(a\mathbf{b}) = \mathbf{b} \cdot \operatorname{grad} a + a \operatorname{div} \mathbf{b}$ and $\operatorname{div}(\mathbf{a} \times \mathbf{b}) = \operatorname{curl} \mathbf{a} \cdot \mathbf{b} - \mathbf{a} \cdot \operatorname{curl} \mathbf{b}$. Inserting the corresponding expressions and subtracting both results we obtain

$$\begin{aligned} & \operatorname{div} \{ \mathbf{u} \operatorname{div} \mathbf{v} + \mathbf{u} \times \operatorname{curl} \mathbf{v} \} \\ &= \mathbf{u} \operatorname{grad} \operatorname{div} \mathbf{v} + \operatorname{div} \mathbf{u} \operatorname{div} \mathbf{v} - \mathbf{u} \cdot \operatorname{curl} \operatorname{curl} \mathbf{v} + \operatorname{curl} \mathbf{u} \cdot \operatorname{curl} \mathbf{v} \\ &= \mathbf{u} \cdot \Delta \mathbf{v} + \operatorname{div} \mathbf{u} \operatorname{div} \mathbf{v} + \operatorname{curl} \mathbf{u} \cdot \operatorname{curl} \mathbf{v}, \end{aligned} \quad (1.103)$$

where we additionally used $\Delta \mathbf{v} = \operatorname{grad} \operatorname{div} \mathbf{v} - \operatorname{curl} \operatorname{curl} \mathbf{v}$. Now, we apply Gauss' divergence theorem to equation (1.103) and Green's first vector identity (1.101) is proven. To verify Green's second vector identity (1.102) we apply Green's first vector identity twice, the second time with interchanged \mathbf{u}, \mathbf{v} , and subtract both results. ■

Now, we may extend Green's vector identities. For instance, the identity (1.101) holds for $\mathbf{u} \in \mathbf{H}_{div}(B) \cap \mathbf{H}_{curl}(B)$ and $\mathbf{v} \in \mathbf{H}^2(B)$. Then the terms on the right hand side have to be understood in the sense of the trace operators $\gamma_0[B]$, $\gamma_\nu[B]$, $\gamma_\times[B]$ and in corresponding dual systems. Under the given assumption on \mathbf{u} and \mathbf{v} , these terms are well defined. In a view of Theorem 1.21, if the regularity of ∂B is $C^{1,1}$, we may replace the unusual condition $\mathbf{u} \in \mathbf{H}_{div}(B) \cap \mathbf{H}_{curl}(B)$ by $\mathbf{u} \in \mathbf{H}^1(B)$.

1.4.2 Boundary Value Problems for Laplace's equation

In preparation for the calculation of the exterior magnetic field from boundary data we turn our attention to the boundary value problems for the Laplacian. A detailed treatment of scalar elliptic problems in nonsmooth domains can be found in [Gri]. Here, we focus on the Laplacian as a very special case of elliptic problems and investigate the interior and exterior Neumann and Dirichlet boundary value problems. Further, we study two boundary value problems for harmonic fields.

BVP 1 (Interior Dirichlet problem for Laplace's equation) Let $\partial B \in C^{0,1}$. For some given function $f \in H^{\frac{1}{2}}(\partial B)$

$$\text{find } u \in H^1_\Delta(B) \text{ such } \begin{cases} \Delta u = 0 & \text{in } B, \\ u = f & \text{on } \partial B. \end{cases} \quad (1.104)$$

Theorem 1.28 *The interior Dirichlet problem for Laplace's equation (1.104) has an unique solution $u \in H^1_\Delta(B)$.*

Proof: See Theorem 2.5.9 in [Ned]. ■

BVP 2 (Interior Neumann problem for Laplace's equation) Let $\partial B \in C^{0,1}$. For some given function $g \in H^{-1/2}_\circ(\partial B)$

$$\text{find } u \in H^1_\Delta(B) \text{ such } \begin{cases} \Delta u = 0 & \text{in } B, \\ \frac{\partial u}{\partial \nu} = g & \text{on } \partial B. \end{cases} \quad (1.105)$$

Theorem 1.29 *The interior Neumann problem for Laplace's equation (1.105) with boundary values $g \in H^{-1/2}_\circ(\partial B)$ admits an solution $u \in H^1_\Delta(B)$ uniquely determined up to a constant.*

Proof: See Theorem 2.5.10. in [Ned] ■

Usually we force uniqueness of the Neumann problem by an additional condition, for example we require $\int_B u \, dx = 0$ or $\int_{\partial B} u \, ds = 0$.

Next, we turn to the exterior problems. In order to require a certain behavior at infinity we introduce the weighted Sobolev space for $k \in \mathbb{N}_0$

$$W^k(B^e) = \left\{ u \mid (1+r^2)^{\frac{i-1}{2}} \frac{\partial^\alpha u}{\partial x^\alpha} \in L^2(B^e), |\alpha| = 0 \dots k \right\} \quad (1.106)$$

where $r = |x|$. We note that $C^\infty(\overline{B^e})$ is dense in $W^k(B^e)$.

BVP 3 (Exterior Dirichlet problem for Laplace's equation) Let $\partial B \in C^{0,1}$. For some given function $f \in H^{\frac{1}{2}}(\partial B)$

$$\text{find } u \in W^1(B^e) \text{ such } \begin{cases} \Delta u = 0 & \text{in } B^e, \\ u = f & \text{on } \partial B. \end{cases} \quad (1.107)$$

Here, the boundary condition holds in the sense of $\gamma_0[B^e]$.

Theorem 1.30 *The exterior Dirichlet problem for Laplace's equation (1.107) has one and only one solution $u \in W^1(B^e)$.*

Proof: See Theorem 2.5.14. in [Ned]. ■

BVP 4 (Exterior Neumann problem for Laplace's equation) Let $\partial B \in C^{0,1}$. For some given function $g \in H^{-\frac{1}{2}}(\partial B)$

$$\text{find } u \in W^1(B^e) \text{ such } \begin{cases} \Delta u = 0 & \text{in } B^e, \\ \frac{\partial u}{\partial \nu} = g & \text{on } \partial B. \end{cases} \quad (1.108)$$

Theorem 1.31 *The exterior Neumann problem for Laplace's equation (1.107) has one and only one solution $u \in W^1(B^e)$.*

Proof: See Theorem 2.5.15. in [Ned]. ■

Remark 1.32 *We have introduced the space $W^1(B)$ to control the behavior at infinity of harmonic functions defined in B^e . In general, for a strong harmonic function u , we have the behavior*

$$u(x) = u_\infty + O(|x|^{-1}), \quad (1.109)$$

$$\frac{\partial^\alpha u}{\partial x^\alpha} = O(|x|^{-|\alpha|-1}), \quad |\alpha| \geq 1 \quad (1.110)$$

with a constant $u_\infty \in \mathbb{R}$ (see Theorem 3.1 of [Ma]). Therefore, if we require a decay $u(x) \rightarrow 0, |x| \rightarrow \infty$ for a classical solution u of the exterior boundary value problem (1.107) and (1.108) then $u \in W^1(B)$.

A simple application of the Neumann problem for Laplace's equation are the following boundary value problems for harmonic vector fields. We make use of the properties of the scalar potential of a harmonic field which exists since B is a simply-connected domain.

Theorem 1.33 *A field $\mathbf{u} \in \mathbf{L}^2(B)$ satisfies*

$$\operatorname{curl} \mathbf{u} = \mathbf{0} \text{ in } B \quad (1.111)$$

iff there exists a function $q \in H^1(B)$ such that

$$\mathbf{u} = \operatorname{grad} q. \quad (1.112)$$

Moreover, the function q is uniquely determined up to a constant.

Proof: See [GiRa], Theorem 2.9. ■

BVP 5 (Interior normal problem for harmonic fields) Let $\partial B \in C^{0,1}$. For some given function $g \in H_\circ^{-1/2}(\partial B)$

$$\text{find } \mathbf{u} \in \mathbf{H}_{\operatorname{div}}(B) \text{ such } \begin{cases} \operatorname{div} \mathbf{u} = 0, & \operatorname{curl} \mathbf{u} = \mathbf{0} & \text{in } B, \\ \nu \cdot \mathbf{u} = g & & \text{on } \partial B. \end{cases} \quad (1.113)$$

The boundary condition is to be understood in the sense of $\gamma_\nu[B]\mathbf{u} = g$.

Theorem 1.34 *The boundary value problem (1.113) with boundary values $g \in H_\circ^{-1/2}(\partial B)$ has one and only one solution $\mathbf{u} \in \mathbf{H}_{\operatorname{div}}(B)$.*

Proof: Let $q \in H_\Delta^1(B)$ be a solution of the interior Neumann problem (1.105) with boundary condition $\partial_\nu q = g$, then $\mathbf{u} = \operatorname{grad} q$ solves the problem (1.113) and existence is proven. For uniqueness, let \mathbf{u} be a solution of the corresponding homogeneous problem. Then, there exists a function $q \in H^1(B)$ such that $\mathbf{u} = \operatorname{grad} q$. Consequently, the function q satisfies $\Delta q = 0$, $\partial_\nu q = 0$. Green's first identity yields

$$\int_B |\mathbf{u}|^2 dx = \int_B |\operatorname{grad} q|^2 dx = \int_{\partial B} q \partial_\nu q ds = 0$$

from where $\mathbf{u} = \mathbf{0}$ follows. ■

BVP 6 (Exterior normal problem for harmonic fields) Let $\partial B \in C^{0,1}$. For some given function $g \in H^{-\frac{1}{2}}(\partial B)$

$$\text{find } \mathbf{u} \text{ such } \begin{cases} \operatorname{div} \mathbf{u} = 0, & \operatorname{curl} \mathbf{u} = \mathbf{0} & \text{in } B^e, \\ \nu \cdot \mathbf{u} = g & & \text{on } \partial B. \end{cases} \quad (1.114)$$

The boundary condition is to be understood in the sense of $\gamma_\nu[B^e]\mathbf{u} = g$.

The existence and uniqueness of a solution can be proven by reducing the problem to the exterior Neumann problem for Laplace's equation (1.108) by the scalar potential q with $\mathbf{u} = \text{grad } q$ as done in the proof of Theorem 1.34. We set

$$\mathbf{Z} := \text{grad } W^1(B^e) = \left\{ \text{grad } q \in \mathbf{L}^2(B^e) \mid \frac{q}{\sqrt{1+|x|^2}} \in L^2(B^e) \right\} \quad (1.115)$$

Theorem 1.35 *The boundary value problem (1.114) has one and only one solution $\mathbf{u} \in \mathbf{Z}$.*

Remark 1.36 *In general, for a strong harmonic field \mathbf{u} , we have the behavior at infinity*

$$\mathbf{u}(x) = \mathbf{u}_\infty + O(|x|^{-2}), \quad (1.116)$$

$$\frac{\partial^\alpha \mathbf{u}}{\partial x^\alpha} = O(|x|^{-|\alpha|-1}), \quad |\alpha| \geq 1 \quad (1.117)$$

with a constant vector \mathbf{u}_∞ (see Theorem 3.1 of [Ma]). Therefore, it is sufficient to require a decay $\mathbf{u}(x) \rightarrow \mathbf{0}$, $|x| \rightarrow \infty$ for classical solutions of the problem (1.114). In this case, due to the behavior of strong harmonic functions (1.109), there exists just one scalar potential q of \mathbf{u} vanishing at infinity, and this function q has the stronger decay $q(x) = O(|x|^{-1})$. In a view of the definition of \mathbf{Z} we get $\mathbf{u} = \text{grad } q \in \mathbf{Z}$.

1.4.3 Boundary and Volume Potentials

Now we are prepared to introduce some notations and operators which are well known from potential theory. We start with the *single* and *double layer potentials*

$$(\mathcal{S}\phi)(x) := \int_{\partial B} \Phi(x, y) \phi(y) ds(y), \quad x \in \mathbb{R}^3, \quad (1.118)$$

$$(\mathcal{D}\phi)(x) := \int_{\partial B} \frac{\partial \Phi(x, y)}{\partial \nu(y)} \phi(y) ds(y), \quad x \in \mathbb{R}^3 \setminus \partial B. \quad (1.119)$$

Analogously, $\vec{\mathcal{S}}$ is the *vectorial single layer potential* in three dimensions.

Theorem 1.37 *Let $s \in [-\frac{1}{2}, \frac{1}{2}]$. The operator \mathcal{S} and $\vec{\mathcal{S}}$ are linear bounded mappings*

$$\mathcal{S} : H^{s-\frac{1}{2}}(\partial B) \rightarrow H^{s+1}(B_R), \quad (1.120)$$

$$\vec{\mathcal{S}} : \mathbf{H}^{s-\frac{1}{2}}(\partial B) \rightarrow \mathbf{H}^{s+1}(B_R), \quad (1.121)$$

where B_R is a ball with sufficiently large radius R . The double layer potential \mathcal{D} is a linear bounded mapping

$$\mathcal{D} : H^{s+\frac{1}{2}}(\partial B) \rightarrow H^{s+1}(B), \quad H^{s+\frac{1}{2}}(\partial B) \rightarrow H^{s+1}(B^e). \quad (1.122)$$

Proof: We refer to Theorem 6.12 of [McL] for the interval $(\frac{1}{2}, \frac{1}{2})$. For the whole interval see [McL], page 209 and the literature cited there. ■

Remark 1.38 *Of course, if ∂B is smoother, then we get more regularity. Provided $\partial B \in C^{k+1,1}, k \in \mathbb{N}_0$, the results of Theorem 1.37 can be extended for $s \in (\frac{1}{2}, k+1]$ with the modification*

$$\mathcal{S} : H^{s-\frac{1}{2}}(\partial B) \rightarrow H^{s+1}(B), \quad H^{s-\frac{1}{2}}(\partial B) \rightarrow H^{s+1}(B_R \cap B^e), \quad (1.123)$$

$$\vec{\mathcal{S}} : \mathbf{H}^{s-\frac{1}{2}}(\partial B) \rightarrow \mathbf{H}^{s+1}(B), \quad \mathbf{H}^{s-\frac{1}{2}}(\partial B) \rightarrow \mathbf{H}^{s+1}(B^e) \quad (1.124)$$

(see Corollary 6.14 of [McL]).

We state the mapping properties of the evaluations of \mathcal{S} and \mathcal{D} on ∂B in the following theorem and add the mapping property of ∂_ν applied to \mathcal{S} and \mathcal{D} , respectively. Here, $\partial_\nu \mathcal{S}$ is declared as

$$((\partial_\nu \mathcal{S})\phi)(x) = \int_{\partial B} \frac{\partial \Phi(x, y)}{\partial \nu(x)} \phi(y) ds, \quad x \in \partial B, \quad (1.125)$$

where the unit normal vector ν is almost everywhere defined. In the same way we declare $\partial_\nu \mathcal{D}$. We should explicitly make a difference between $\gamma_0[B], \gamma_0, \gamma_0[B^e]$ and $\partial_\nu[B], \partial_\nu, \partial_\nu[B^e]$ respectively because they may lead to different results.

Theorem 1.39 *For the simply-connected domain B with Lipschitz continuous boundary ∂B and $s \in [-\frac{1}{2}, \frac{1}{2}]$ holds*

$$\mathcal{S} : H^{s-\frac{1}{2}}(\partial B) \rightarrow H^{s+\frac{1}{2}}(\partial B), \quad (1.126)$$

$$\mathcal{D} : H^{s+\frac{1}{2}}(\partial B) \rightarrow H^{s+\frac{1}{2}}(\partial B), \quad (1.127)$$

$$\partial_\nu \mathcal{S} : H^{s-\frac{1}{2}}(\partial B) \rightarrow H^{s-\frac{1}{2}}(\partial B), \quad (1.128)$$

$$\partial_\nu \mathcal{D} : H^{s+\frac{1}{2}}(\partial B) \rightarrow H^{s-\frac{1}{2}}(\partial B). \quad (1.129)$$

Proof: See Theorem 1 of [Co]. ■

For every density $\phi \in H^{-\frac{1}{2}}(\partial B)$ we have $\mathcal{S}\phi \in W^1(\mathbb{R}^3)$. Further, the function $\mathcal{S}\phi$ is analytic and harmonic in B and in B^e . The kernel $\Phi(x, y)$ is analytic for $y \in \partial B$ and $x \notin \partial B$. We may interchange differentiation and integration and obtain an analytic function. With the aid of $\Delta_x \Phi(x, y) = 0$ we conclude that $\mathcal{S}\phi$ is a harmonic function in B and in B^e . In the same way we can show that $\mathcal{D}\psi$ is a harmonic function in B, B^e for each density $\psi \in H^{\frac{1}{2}}(\partial B)$. This property makes the single and double layer potential to excellent tools to solve boundary value problems for Laplace's equation.

We will show that the Biot-Savart operator can be represented as curl of the *volume potential*

$$(\mathcal{V}f)(x) := \int_B \Phi(x, y) f(y) dy, \quad x \in \mathbb{R}^3. \quad (1.130)$$

Thus, we study the mapping properties of \mathcal{V} .

Theorem 1.40 *Given two bounded domains D and G , the volume potential $\mathcal{V} : L^2(D) \mapsto H^2(G)$ is a linear bounded operator.*

Proof: For the statement we refer to Theorem 8.2 in [CoKr1]. In this theorem, the more general case of Helmholtz' equation is considered. ■

At this stage we can show continuity of $\mathcal{V}f$ in a very easy way. For $z \in B^e$ and $x \rightarrow z$ we are able to estimate $|(\mathcal{V})f(x) - (\mathcal{V}f)(z)|$ against $C\|f\|_{L^1(B)}|x - z|$ with a constant $C \in \mathbb{R}^+$ depending on $\text{dist}(x, B)$. Thus, we have continuity in B^e . An application of Theorem 1.40 to the Lipschitz domains B and G with $\overline{B} \subset G$ yields $\mathcal{V}f \in H^2(G)$. From the Sobolev imbedding Theorem 1.9 we obtain $H^2(G) \subset C^0(\overline{G})$, i.e. $\mathcal{V}f$ is continuous in \overline{G} . Together with $\overline{B} \subset G$ we have continuity in \mathbb{R}^3 . Moreover, the integral kernel $\Phi(x, y)$ is analytic for $x \in B^e$ and $y \in B$. By interchanging differentiation and integration we derive the analyticity of $\mathcal{V}f$ in B^e . Now, we are able to formulate

Theorem 1.41 *The volume potential \mathcal{V} with density $f \in L^2(B)$ is continuous in \mathbb{R}^3 and analytic in B^e .*

Theorem 1.42 *For the volume potential \mathcal{V} with density $f \in L^2(B)$ the equations*

$$\Delta \mathcal{V}f = 0 \text{ in } B^e, \quad (1.131)$$

$$\Delta \mathcal{V}f = -f \text{ in } B \quad (1.132)$$

are satisfied.

Proof: Equation (1.131) can be shown by using the analyticity of the integral kernel together with $\Delta \Phi(x, y) = 0$ for $x \in B^e, y \in B$. For the statement (1.132) we refer to [Jost], Satz 9.1.1. ■

Now, we are in a position to extend Green's representation formula

$$u(x) = \int_{\partial B} \Phi(x, y) \frac{\partial u(y)}{\partial \nu} - u(y) \frac{\partial \Phi(x, y)}{\partial \nu(y)} ds(y) - \int_B \Phi(x, y) \Delta u dy, \quad x \in B$$

to functions $u \in H_{\Delta}^1(B)$. We rewrite it as a sum of single layer, double layer, and volume potentials

$$u = \mathcal{S}(\partial_{\nu}u) - \mathcal{D}(\gamma_0 u) - \mathcal{V}(\Delta u). \quad (1.133)$$

The terms are well defined and bounded for $u \in H_{\Delta}^1(B)$ because $\partial_{\nu}[B]u \in H^{-\frac{1}{2}}(B)$, $\gamma_0[B]u \in H^{\frac{1}{2}}(B)$, and $\Delta u \in L_2(B)$. Finally, Green's representation formula (1.95) holds for $u \in H_{\Delta}^1(B)$ by a dense approximation argument from Theorem 1.11. Applying this formula to harmonic functions which are weak in L^2 -sense, we obtain a representation

$$u = \mathcal{S}(\partial_{\nu}u) - \mathcal{D}(\gamma_0 u). \quad (1.134)$$

As argued above, the single and double layer potential are analytic and strong harmonic functions inside B , and thus, u is a strong harmonic function. Summarizing we state: *weak harmonic functions are strong harmonic functions and strong harmonic functions are analytic functions.*

We complete the analysis of the scalar boundary integrals by giving a short outline of the injectivity of \mathcal{S}, \mathcal{D} . Let $u \equiv 1$ in B , then $\partial_\nu[B]u = 0$. We apply Green's representation of harmonic functions (1.134) to conclude $1 = -\mathcal{D}1$ in B . For any $x \in B^e$, the function $\Phi(x, \cdot)$ is harmonic in \overline{B} . We apply Green's first identity (1.93) to the functions $u \equiv 1$ and $v = \Phi(x, \cdot)$ and obtain $0 = \mathcal{D}1$ for $x \in B^e$. Together we have shown

$$\mathcal{D}1 = \begin{cases} -1, & x \in B, \\ 0, & x \in B^e. \end{cases} \quad (1.135)$$

Therefore, \mathcal{D} can not be continuous across ∂B . Moreover, $\mathcal{D}\phi = 0$ in B^e does not imply that ϕ vanishes. For the single layer potential we state.

Theorem 1.43 *If $\phi \in H^{-\frac{1}{2}}(\partial B)$ satisfy $\mathcal{S}\phi = 0$ on ∂B , then $\phi = 0$.*

Proof: A proof can be found in [McL], Theorem 8.11. ■

For our vector analysis we need to introduce the three dimensional analogon $\vec{\mathcal{V}}$ of the volume potential \mathcal{V} . In this text, we focus on volume potentials with divergence-free fields. Such volume potentials are not divergence-free in general as we will see in the next theorem.

Theorem 1.44 *Let B_R be a ball with sufficiently large radius R and $\mathbf{j} \in \mathbf{H}_{div}(B)$. Then we have $\operatorname{div}(\vec{\mathcal{V}}\mathbf{j}) \in \mathbf{H}^1(B_R)$ and*

$$\operatorname{div}(\vec{\mathcal{V}}\mathbf{j}) = -\mathcal{S}(\nu \cdot \mathbf{j}) + \mathcal{V}(\operatorname{div} \mathbf{j}). \quad (1.136)$$

Further, the relation (1.136) holds pointwise in B^e .

Proof: From Theorem 1.40 we get $\vec{\mathcal{V}}\mathbf{j} \in \mathbf{H}^2(B_R)$ and $\operatorname{div}(\vec{\mathcal{V}}\mathbf{j}) \in H^1(B_R)$. Let $\mathbf{j} \in \mathbf{C}^\infty(\overline{B})$, then we calculate

$$\begin{aligned} \operatorname{div}(\vec{\mathcal{V}}\mathbf{j})(x) &= \int_B \operatorname{div}_x \{\Phi(x, y)\mathbf{j}(y)\} dy = - \int_B \operatorname{grad}_y \Phi(x, y)\mathbf{j}(y) dy \\ &= - \int_B \operatorname{div}_y (\Phi(x, y)\mathbf{j}(y)) dy + \int_B \Phi(x, y) \operatorname{div} \mathbf{j}(y) dy \\ &= -(\mathcal{S}(\nu \cdot \mathbf{j}))(x) + (\mathcal{V}(\operatorname{div} \mathbf{j}))(x) \end{aligned} \quad (1.137)$$

for $x \in B_R$. Both sides are well defined and linear bounded operators $\mathbf{H}_{div}(B) \rightarrow H^1(B_R)$. Hence, the statement (1.136) holds for $\mathbf{j} \in \mathbf{H}_{div}(B)$ by the dense approximation technique together with denseness of $\mathbf{C}^\infty(\overline{B})$ in $\mathbf{H}_{div}(B)$ (see Theorem 1.12).

For the exterior of B , we know that $\vec{\mathcal{V}}\mathbf{j}$ is analytic for $\mathbf{j} \in \mathbf{H}_{div}(B)$ accordant to Theorem 1.41. Hence, the calculation (1.137) holds for $\mathbf{j} \in \mathbf{H}_{div}(B)$ and $x \in B^e$. ■

As a consequence, the volume potential with density $\mathbf{j} \in \mathbf{H}_{div=0}(B)$ is divergence-free provided $\nu \cdot \mathbf{j} = 0$.

1.4.4 The Helmholtz Decomposition

For every curl-free field \mathbf{u} there exists a function q called *scalar potential* with $\mathbf{u} = \text{grad } q$. Analogously, for every divergence-free field \mathbf{w} there exists a field \mathbf{v} called *vector potential* that satisfies $\text{curl } \mathbf{v} = \mathbf{w}$. The vector potential \mathbf{w} of \mathbf{v} is not uniquely determined, we may add a constant vector. It is also a well known fact that we are able to choose a divergence-free field \mathbf{v} among the vector potentials. The following theorem states that every divergence-free field has a divergence-free vector potential with vanishing normal component.

Theorem 1.45 *Let $\mathbf{w} \in \mathbf{H}_{div=0}(B)$. There exists one and only one divergence-free vector potential $\mathbf{u} \in \mathbf{H}_{curl}(B)$ of \mathbf{w} with $\nu \cdot \mathbf{u} = 0$. If ∂B is of class $C^{1,1}$, then $\mathbf{u} \in \mathbf{H}^1(B)$.*

Proof: The proof can be found in [GiRa], Theorem 3.5. ■

For the classical magnetostatic problem (1.4) the magnetic field \mathbf{H} is a divergence-free vector potential of the current distribution \mathbf{j} . In the sequel we also consider vector potentials different from those defined by Theorem 1.45. As an further example, consider a current distribution $\mathbf{j} \in \mathbf{H}_{div}(B)$ with harmonic components, then there exists a vector potential in the form of a vectorial single layer potential $\vec{\mathcal{S}}\mathbf{a}$ with a density \mathbf{a} (see Subsection 2.2.3).

The next theorem gives another characterization of the vector potential defined by Theorem 1.45 if in addition we assume that the normal component vanishes.

Theorem 1.46 *Let $\mathbf{w} \in \mathbf{H}_{div=0}(B)$ with $\nu \cdot \mathbf{w} = 0$. There exists one and only one divergence-free vector potential \mathbf{v} of \mathbf{w} with $\nu \times \mathbf{v} = \mathbf{0}$. This vector potential can be characterized as the unique solution to the boundary value problem*

$$\mathbf{v} \in \mathbf{H}_{curl}(B) : \begin{cases} -\Delta \mathbf{v} = \text{curl } \mathbf{w} & \text{in } \mathbf{H}^{-1}(B), \\ \text{div } \mathbf{v} = 0 & \text{in } B, \\ \nu \times \mathbf{v} = 0 & \text{on } \partial B. \end{cases} \quad (1.138)$$

Moreover, if ∂B is of class $C^{1,1}(B)$ or a convex polyhedron, then \mathbf{v} belongs to $\mathbf{H}^1(B)$.

Proof: We refer to Theorem 3.6 of [GiRa]. ■

Remark 1.47 *It can be shown that for a field $\mathbf{w} \in \mathbf{H}_{0,div}(B)$ with $\text{div } \mathbf{w} = 0$ the characterizations from Theorems 1.45 and 1.46 lead to the same vector potential (see proof of Theorem 3.6 of [GiRa]).*

An interesting application of Theorem 1.46 is the decomposition of vector fields also called Helmholtz' decomposition in the literature. It expresses that every field $\mathbf{w} \in L^2(B)$ may be written as a sum of a gradient and a curl field, i.e. there exist $q \in H^1(B)$ and $\mathbf{v} \in \mathbf{H}^1(B)$ such that $\mathbf{w} = \text{grad } q + \text{curl } \mathbf{v}$. For the moment, assume that the existence is proven. Then $\mathbf{w} - \text{grad } q$ is a divergence-free field of $\mathbf{H}_{div}(B)$ and $\nu \cdot (\mathbf{w} - \text{grad } q)$ is well defined. Now, there exists a vector potential for $\mathbf{w} - \text{grad } q$. If we require $\nu \cdot (\mathbf{w} - \text{grad } q) = 0$ in $H^{-\frac{1}{2}}(B)$ we may choose the vector potential defined by (1.138) which has the property $\nu \cdot \text{curl } \mathbf{v} = \nu \cdot (\mathbf{w} - \text{grad } q) = 0$. The following version from [GiRa] puts the condition $\nu \cdot (\mathbf{w} - \text{grad } q) = 0$ in other terms.

Theorem 1.48 (Helmholtz' Decomposition) *For each vector field $\mathbf{w} \in \mathbf{L}^2(B)$, there exists a function $q \in H^1(B)$ and a function $\mathbf{v} \in \mathbf{H}^1(B)$ such that*

$$\mathbf{w} = \text{grad } q + \text{curl } \mathbf{v} \quad (1.139)$$

with \mathbf{v} being the only solution of (1.138) and $q \in H^1(B)$ being a solution of

$$\int_B (\text{grad } q - \mathbf{v}) \cdot \text{grad } \phi \, dx = 0 \quad \forall \phi \in H^1(B). \quad (1.140)$$

Moreover, the functions $\text{curl } \mathbf{v}$ and $\text{grad } q$ are orthogonal in $\mathbf{L}^2(B)$.

Proof: The theorem and its proof can be found in [GiRa], Corollary 3.4. ■

Chapter 2

Magnetic Tomography via the Biot-Savart Operator

The main ingredient of magnetic tomography is the Biot-Savart operator

$$(\mathcal{W}\mathbf{j})(x) = \frac{1}{4\pi} \int_B \mathbf{j}(y) \times \frac{x-y}{|x-y|^3} dy = \int_B \text{grad}_x \Phi(x, y) \times \mathbf{j}(y) dy, \quad (2.1)$$

which maps a current distribution \mathbf{j} onto its magnetic field \mathbf{H} . The basic task to reconstruct a current density \mathbf{j} from its magnetic field \mathbf{H} leads to the investigation of the mapping properties of the operator \mathcal{W} . In the introduction, we have developed six questions as core problems of this investigation.

1. Given some magnetic field, is it possible to uniquely reconstruct the original current distribution \mathbf{j} which generated \mathbf{H} , i.e. is \mathcal{W} injective or does \mathcal{W} have a non-trivial nullspace $N(\mathcal{W})$?
2. If $N(\mathcal{W})$ is non-trivial, can the space be explicitly characterized, i.e. is it possible to describe $N(\mathcal{W})$ without using the operator \mathcal{W} ? In general terms we ask: which functions do not generate a magnetic field in the exterior B^e ?
3. Is the reconstruction of \mathbf{j} from \mathbf{H} stable? How can we stabilize the calculation of \mathbf{j} ?
4. Can we explicitly characterize the orthogonal space $N(\mathcal{W})^\perp$? In general terms this question reads: which functions (or equivalence classes of functions) do generate a magnetic field outside?
5. What is the relation of ohmic currents to the nullspace $N(\mathcal{W})$ and its orthogonal space $N(\mathcal{W})^\perp$?
6. How much data do we need to measure on ∂G to uniquely determine the magnetic field \mathbf{H} in the exterior B^e ?

The task of this chapter is to provide detailed answers to each question.

In the first section of this chapter we establish some mapping properties of the Biot-Savart operator. For instance we show that the Biot-Savart operator does not satisfy the Maxwell equation in general.

Questions 1., 2. and 4. are investigated in Section 2.2. It is shown that the nullspace $N(\mathcal{W})$ is non-trivial, and then characterizations of the spaces $N(\mathcal{W})$ and $N(\mathcal{W})^\perp$ are developed. The space $N(\mathcal{W})$ contains all current densities which do not generate a magnetic field in the exterior B^e of the domain B . The set $N(\mathcal{W})^\perp$ describes the set of equivalence classes

$$\mathbf{j} + N(\mathcal{W}), \quad \mathbf{j} \in N(\mathcal{W})^\perp \quad (2.2)$$

which do produce the same magnetic field in the exterior B^e .

The space $N(\mathcal{W})^\perp$ also is of great interest for the reconstructability of the currents from its exterior magnetic field \mathbf{H} . As an integral operator with analytic kernel the Biot-Savart operator \mathcal{W} is not continuously invertible, i.e. the inversion is *unstable*. This answers the first part of question 3. We use the Tikhonov regularization scheme to stabilize the inversion of the equation $\mathcal{W}\mathbf{j} = \mathbf{H}$. It is well known that the classical Tikhonov regularization

$$\mathbf{j}_\alpha := (\alpha\mathcal{I} + \mathcal{W}^*\mathcal{W})^{-1}\mathcal{W}\mathbf{H} \quad (2.3)$$

in the limit $\alpha \rightarrow 0$ for exact data reconstructs a projection of \mathbf{j} onto $N(\mathcal{W})^\perp$. Thus, the characterization of $N(\mathcal{W})^\perp$ also provides a basis to investigate best-possible reconstructions for some given current density \mathbf{j} as an appropriate projection into the equivalence class $\mathbf{j} + N(\mathcal{W})$.

Question 5 is investigated in Section 2.3. We first formulate and solve an anisotropic conductivity problem which is used to model 'realistic' currents. Indicating this particular model based on Ohm's law, we call these currents *ohmic currents*. Then we show that these ohmic currents are orthogonal to the nullspace $N(\mathcal{W})$ with respect to the scalar product (1.14). Please note that these results go one step further than the orthogonality results which have already been achieved in [KrKüPo].

Finally, we investigate the amount of data which is necessary for reconstructions, i.e. we treat question 6. Here, three different settings are investigated. In the first setting the *full three-dimensional magnetic field* \mathbf{H} is measured on some exterior surface ∂G with $B \subset G$. As shown in [KrKüPo], these measurements already uniquely determine \mathbf{H} in the exterior set B^e . Second, we investigate the case where the flux $\nu \cdot \mathbf{j}|_{\partial B}$ is known and show that the knowledge of the *normal components* $\nu \cdot \mathbf{H}|_{\partial G}$ uniquely determines the magnetic field in B^e . Third, we assume that the *tangential components* $\nu \times \mathbf{H}|_{\partial G}$ are known. These data also uniquely determine \mathbf{H} in B^e . Further, we show that the tangential components determine the current flux $\nu \cdot \mathbf{j}|_{\partial B}$.

2.1 Vector analysis for the Biot-Savart operator

The Biot-Savart operator has a weakly singular kernel and as shown in Theorem A.12 in the appendix is a linear compact mapping $\mathcal{W} : \mathbf{L}^2(B) \rightarrow \mathbf{L}^2(B)$.

Theorem 2.1 *The operator \mathcal{W} with density $\mathbf{j} \in \mathbf{L}^2(B)$ may be written as*

$$\mathcal{W}\mathbf{j} = \operatorname{curl}(\vec{\mathcal{V}}\mathbf{j}). \quad (2.4)$$

Proof: It follows by the transformation

$$(\mathcal{W}\mathbf{j})(x) = \int_B \operatorname{grad}_x \Phi(x, y) \times \mathbf{j}(y) dy = \int_B \operatorname{curl}_x \{\Phi(x, y)\mathbf{j}(y)\} dy = \operatorname{curl}(\vec{\mathcal{V}}\mathbf{j})(x)$$

for $x \in \mathbb{R}^3$. ■

Let G be a bounded Lipschitz domain with $\overline{B} \subset G$. Then, the Biot-Savart operator maps $\mathbf{L}^2(B)$ into $\mathbf{L}^2(G)$ and equation (2.4) holds in $\mathbf{L}^2(G)$. Moreover, the operator \mathcal{W} maps $\mathbf{L}^2(B)$ continuously into $\mathbf{H}^1(G)$ which can be derived as follows. The vector-valued volume potential $\vec{\mathcal{V}}$ maps $\mathbf{L}^2(B)$ into $\mathbf{H}^2(G)$ since the scalar-valued volume potential is a mapping $\mathcal{V} : L^2(B) \rightarrow H^2(G)$ from Theorem 1.40. Therefore, we have $\operatorname{curl} \vec{\mathcal{V}}\mathbf{j} \in \mathbf{H}^1(G)$. The trace operators $\gamma_0[B]$ and $\gamma_0[B^e]$ applied to $\mathcal{W}\mathbf{j}$ coincide. Since $\vec{\mathcal{V}}\mathbf{j}$ is analytic in B^e the field $\mathcal{W}\mathbf{j} = \operatorname{curl} \vec{\mathcal{V}}\mathbf{j}$ is also analytic. We summarize these results in the following theorem.

Theorem 2.2 *The operator \mathcal{W} is a linear bounded mapping*

$$\mathcal{W} : \mathbf{L}^2(B) \rightarrow \mathbf{H}^1(B). \quad (2.5)$$

Moreover, the operator \mathcal{W} is analytic in B^e and continuous across ∂B in the sense that

$$\gamma_0[B]\mathcal{W}\mathbf{j} = \gamma_0[B^e]\mathcal{W}\mathbf{j} \quad (2.6)$$

for each $\mathbf{j} \in \mathbf{L}^2(B)$.

In preparation for the nullspace decomposition we focus on current distributions \mathbf{j} with weak divergence, then the current flux $\nu \cdot \mathbf{j}$ is well defined. We introduce the operator

$$(\mathcal{S}^\nabla \mathbf{j})(x) := \operatorname{grad} \mathcal{S}(\nu \cdot \mathbf{j})(x) = \operatorname{grad} \int_{\partial B} \Phi(x, y)(\nu \cdot \mathbf{j})(y) ds(y) \quad (2.7)$$

which is well defined for $\mathbf{j} \in \mathbf{H}_{div}(B)$ since $\gamma_\nu[B]\mathbf{j} \in H^{-\frac{1}{2}}(\partial B)$ and \mathcal{S} is well defined on $H^{-\frac{1}{2}}(\partial B)$.

Theorem 2.3 *For the Biot-Savart operator \mathcal{W} with density $\mathbf{j} \in \mathbf{H}_{div}(B)$ we have*

$$\operatorname{div}(\mathcal{W}\mathbf{j}) = 0, \quad \operatorname{curl}(\mathcal{W}\mathbf{j}) = \mathbf{j} - \mathcal{S}^\nabla \mathbf{j} + \operatorname{grad} \mathcal{V}(\operatorname{div} \mathbf{j}) \quad \text{in } B, \quad (2.8)$$

$$\operatorname{div}(\mathcal{W}\mathbf{j}) = 0, \quad \operatorname{curl}(\mathcal{W}\mathbf{j}) = -\mathcal{S}^\nabla \mathbf{j} + \operatorname{grad} \mathcal{V}(\operatorname{div} \mathbf{j}) \quad \text{in } B^e. \quad (2.9)$$

Proof: Looking at the representation $\mathcal{W}\mathbf{j} = \operatorname{curl} \vec{\mathcal{V}}\mathbf{j}$ the divergence statements are clear. For the curl statements, we will repeat the proof from [KrKüPo], Lemma 8.

Let $\mathbf{j} \in \mathbf{C}^\infty(\overline{B})$. Using $\operatorname{curl} \operatorname{curl} \vec{\mathcal{V}}\mathbf{j} = -\Delta \vec{\mathcal{V}}\mathbf{j} + \operatorname{grad} \operatorname{div} \vec{\mathcal{V}}\mathbf{j}$ together with $\operatorname{div} \vec{\mathcal{V}}\mathbf{j} = -\mathcal{S}(\nu \cdot \mathbf{j}) + \mathcal{V}(\operatorname{div} \mathbf{j})$ from Theorem 1.44 we obtain

$$\begin{aligned} \operatorname{curl} \mathcal{W}\mathbf{j} &= \operatorname{curl} \operatorname{curl} \vec{\mathcal{V}}\mathbf{j} = -\Delta \vec{\mathcal{V}}\mathbf{j} + \operatorname{grad} \operatorname{div} \vec{\mathcal{V}}\mathbf{j} \\ &= -\Delta \vec{\mathcal{V}}\mathbf{j} - \mathcal{S}^\nabla(\nu \cdot \mathbf{j}) + \operatorname{grad} \mathcal{V}(\operatorname{div} \mathbf{j}). \end{aligned} \quad (2.10)$$

For the interior domain B we have $\Delta \vec{\mathcal{V}}\mathbf{j} = -\mathbf{j}$ and

$$\operatorname{curl} \mathcal{W}\mathbf{j} = \mathbf{j} - \mathcal{S}^\nabla \mathbf{j} + \operatorname{grad} \mathcal{V}(\operatorname{div} \mathbf{j}).$$

Now, the curl statement of (2.8) follows from the denseness of $\mathbf{C}^\infty(\overline{B})$ in $\mathbf{H}_{div}(B)$. Considering the equation (2.10) in the exterior domain B^e we have $\Delta \vec{\mathcal{V}}\mathbf{j} = 0$ and

$$\operatorname{curl} \mathcal{W}\mathbf{j} = -\mathcal{S}^\nabla \mathbf{j} + \operatorname{grad} \mathcal{V}(\operatorname{div} \mathbf{j}),$$

which holds for $\mathbf{j} \in \mathbf{H}_{div}(B)$ by denseness of $\mathbf{C}^\infty(\overline{B})$ in $\mathbf{H}_{div}(B)$. ■

From these equations we see that the Biot-Savart operator in general does not satisfy the magnetic Maxwell equations in linear media

$$\operatorname{curl} \mathbf{H} = \mathbf{j}, \quad \operatorname{div} \mathbf{H} = 0 \quad (2.11)$$

It is a solution provided $-\mathcal{S}^\nabla \mathbf{j} + \operatorname{grad} \mathcal{V}(\operatorname{div} \mathbf{j}) = 0$. The additional terms $\mathcal{S}^\nabla \mathbf{j}$ and $\operatorname{grad} \mathcal{V}(\operatorname{div} \mathbf{j})$ take into account boundary effects and current sources. If we assume that there are no sources in B , the curl equation of (2.9) reduces to $\operatorname{curl}(\mathcal{W}\mathbf{j}) = -\mathcal{S}^\nabla \mathbf{j}$. The term $\mathcal{S}^\nabla \mathbf{j}$ vanishes if and zero only if $\nu \cdot \mathbf{j} = 0$, that is for closed systems (see decay at infinity and injectivity of \mathcal{S}).

The question for a harmonic exterior magnetic field $\mathcal{W}\mathbf{j}$ is of practical interest. If $\mathcal{W}\mathbf{j}$ is harmonic (and solves Maxwell's equations) we are able to calculate $\mathcal{W}\mathbf{j}$ from the normal component $\nu \cdot \mathcal{W}\mathbf{j}|_{\partial G}$ on a boundary of a domain G with $B \subset G$, i.e. we need to measure one scalar function. The accordant exterior boundary value problem is investigated in Theorem 1.35. From a practical point of view, it would decrease the cost of measurements. In Subsection 2.3.3 we present a study on *difference reconstruction* where $\mathbf{j}_1, \mathbf{j}_2$ are current distributions with same current flux in a homogeneous fuel cell and a fuel cell with a defect inclusion, respectively. Then, by $\mathbf{j} := \mathbf{j}_2 - \mathbf{j}_1$, the field $\mathcal{W}\mathbf{j}$ is harmonic in B^e and uniquely determined by the measurement of $\nu \cdot \mathcal{W}\mathbf{j}|_{\partial G}$.

2.2 Decomposition with Respect to the Nullspace

It has already been shown by Kress, Kühn, Potthast [KrKüPo] that the nullspace $N(\mathcal{W})$ contains the set

$$\mathbf{M} := \{\mathbf{j} = \Delta \mathbf{m} \mid \mathbf{m} \in \mathbf{C}_0^2(B)\}, \quad (2.12)$$

i.e. the nullspace is non-trivial. The proof shows that the set \mathbf{M} is included in the nullspace of operator $\vec{\mathcal{V}}$. Together with $\mathcal{W} = \text{curl } \vec{\mathcal{V}}$ we have $\mathbf{M} \subset N(\mathcal{W})$. This answers question 1. The goal for this section is to characterize the nullspace $N(\mathcal{W})$ and its orthogonal complement where \mathcal{W} is considered as a mapping

$$\mathcal{W} : \mathbf{H}_{\text{div}=0}(B) \rightarrow \mathbf{L}^2(B^e). \quad (2.13)$$

Here, the behavior at infinity ensures that $\mathcal{W}\mathbf{j}$ is square integrable in B^e .

Trivially, if \mathbf{j} is an element of $N(\mathcal{W})$, then $\mathcal{W}\mathbf{j}$ solves Maxwell's equation in B^e . The following statements show some more consequences.

Theorem 2.4 *Let $\mathbf{j}_0 \in \mathbf{H}_{\text{div}}(B)$ such that $\mathcal{W}\mathbf{j}_0 = \mathbf{0}$ in B^e , then*

$$\mathcal{S}(\nu \cdot \mathbf{j}_0) = \mathcal{V}(\text{div } \mathbf{j}_0) \quad (2.14)$$

is satisfied in B^e . Furthermore, if $\mathbf{j}_0 \in \mathbf{H}_{\text{div}=0}(B)$ satisfies $\mathcal{W}\mathbf{j}_0 = \mathbf{0}$ in B^e , then $\nu \cdot \mathbf{j}_0 = 0$ on ∂B .

Proof: Let $\mathbf{j}_0 \in \mathbf{H}_{\text{div}}(B)$. The assumption $\mathcal{W}\mathbf{j}_0 = \mathbf{0}$ in B^e implies $\text{curl } \mathcal{W}\mathbf{j}_0 = \mathbf{0}$. Inserting this in (2.9) entails

$$\mathbf{0} = \text{curl } \mathcal{W}\mathbf{j}_0 = -\mathcal{S}^\nabla \mathbf{j}_0 + \text{grad } \mathcal{V}(\text{div } \mathbf{j}_0) = -\text{grad } \mathcal{S}(\nu \cdot \mathbf{j}_0) + \text{grad } \mathcal{V}(\text{div } \mathbf{j}_0).$$

Therefore, $\mathcal{V}(\text{div } \mathbf{j}_0) - \mathcal{S}(\nu \cdot \mathbf{j}_0)$ must be constant. From the behavior of the single layer potential and volume potential at infinity we conclude $\mathcal{S}(\nu \cdot \mathbf{j}_0) = \mathcal{V}(\text{div } \mathbf{j}_0)$ in B^e . If furthermore $\text{div } \mathbf{j}_0 = 0$, then we have $\mathcal{S}(\nu \cdot \mathbf{j}_0) = 0$ in B^e and $\mathcal{S}(\nu \cdot \mathbf{j}_0) = 0$ on ∂B . The injectivity of \mathcal{S} from Theorem 1.43 implies $\nu \cdot \mathbf{j}_0 = 0$ on ∂B . ■

Corollary 2.5 *Let $\mathbf{j}_0 \in \mathbf{H}_{\text{div}}(B)$ such that $\mathcal{W}\mathbf{j}_0 = \mathbf{0}$ in B^e , then Maxwell's equations for the exterior*

$$\text{div}(\mathcal{W}\mathbf{j}_0) = 0, \quad \text{curl}(\mathcal{W}\mathbf{j}_0) = \mathbf{0} \quad \text{in } B^e \quad (2.15)$$

are satisfied. Furthermore, if $\mathbf{j}_0 \in \mathbf{H}_{\text{div}=0}(B)$, then we have

$$\text{div}(\mathcal{W}\mathbf{j}_0) = 0, \quad \text{curl}(\mathcal{W}\mathbf{j}_0) = \mathbf{j}_0 \quad \text{in } B. \quad (2.16)$$

Proof: Let $\mathbf{j} \in \mathbf{H}_{\text{div}}(B)$ satisfy $\mathcal{W}\mathbf{j}_0 = \mathbf{0}$ in B^e . Theorem 2.4 implies $\mathcal{S}(\nu \cdot \mathbf{j}_0) = \mathcal{V}(\text{div } \mathbf{j}_0)$. Inserting this in equation (2.9) proves the statement (2.15). If furthermore $\text{div } \mathbf{j}_0 = 0$, then $\nu \cdot \mathbf{j}_0 = 0$ and the term $\mathcal{S}(\nu \cdot \mathbf{j}_0)$ as well as $\mathcal{V}(\text{div } \mathbf{j}_0)$ vanishes. In this case equation (2.9) leads to (2.16) and the proof is complete. ■

As a further preparation step, we use the Helmholtz decomposition for the current \mathbf{j} and apply the Biot-Savart operator to the gradient term and the curl term of the decomposition separately. Let $\mathbf{v} \in \mathbf{C}^\infty(\overline{B})$, we calculate

$$\begin{aligned}
\mathcal{W}(\operatorname{curl} \mathbf{v})(x) &= \operatorname{curl} \mathcal{V}(\operatorname{curl} \mathbf{v})(x) = \operatorname{curl} \int_B \Phi(x, y) \operatorname{curl} \mathbf{v}(y) dy \\
&\stackrel{(A.76)}{=} \operatorname{curl} \int_B \operatorname{curl}_y \{ \Phi(x, y) \mathbf{v}(y) \} dy - \operatorname{curl} \int_B \operatorname{grad}_y \Phi(x, y) \times \mathbf{v}(y) dy \\
&\stackrel{(1.99)}{=} \operatorname{curl} \vec{\mathcal{S}}(\nu \times \mathbf{v})(x) + \operatorname{curl} \int_B \operatorname{grad}_x \Phi(x, y) \times \mathbf{v}(y) dy \\
&\stackrel{(2.1)}{=} \operatorname{curl} \vec{\mathcal{S}}(\nu \times \mathbf{v})(x) + \operatorname{curl} (\mathcal{W}\mathbf{v})(x), \quad x \in \mathbb{R}^3
\end{aligned} \tag{2.17}$$

where we have used formula (A.76), Stokes' theorem (1.99) and the representation of \mathcal{W} (2.1). This equation can be extended by dense approximation to fields $\mathbf{v} \in \mathbf{H}_{\operatorname{curl}}(B)$. For $q \in C^\infty(\overline{B})$ we derive

$$\begin{aligned}
\mathcal{W}(\operatorname{grad} q)(x) &= \int_B \operatorname{grad}_x \Phi(x, y) \times \operatorname{grad} q dy = - \int_B \operatorname{grad}_y \Phi(x, y) \times \operatorname{grad} q dy \\
&\stackrel{(A.76)}{=} - \int_B \operatorname{curl}_y \{ \Phi(x, y) \operatorname{grad} q \} dy \\
&\stackrel{(1.99)}{=} - \vec{\mathcal{S}}(\nu \times \operatorname{grad} q),
\end{aligned} \tag{2.18}$$

which holds for $q \in H^1(B)$ by a dense approximation argument again. Now, we put both results together. Let $\mathbf{j} = \operatorname{grad} q + \operatorname{curl} \mathbf{v}$ be a Helmholtz decomposition with $\mathbf{v} \in \mathbf{H}^1(B)$, $\operatorname{div} \mathbf{v} = 0$, $\nu \times \mathbf{v} = \mathbf{0}$ and $q \in H^1(B)$, $\partial_\nu q = \nu \cdot \mathbf{j}$. Applying the above calculations to the exterior B^e of B we derive

$$\begin{aligned}
\mathcal{W}\mathbf{j} &= \mathcal{W}(\operatorname{grad} q + \operatorname{curl} \mathbf{v}) = \mathcal{W}(\operatorname{grad} q) + \mathcal{W}(\operatorname{curl} \mathbf{v}) \\
&\stackrel{(2.18), (2.17)}{=} - \vec{\mathcal{S}}(\nu \times \operatorname{grad} q) + \operatorname{curl} \mathcal{S}(\nu \times \mathbf{v}) + \operatorname{curl} \mathcal{W}\mathbf{v} \\
&\stackrel{(2.9)}{=} - \vec{\mathcal{S}}(\nu \times \operatorname{grad} q) - \mathcal{S}^\nabla \mathbf{v}.
\end{aligned} \tag{2.19}$$

2.2.1 A characterization of $N(W)$

We are now prepared to answer question 3, i.e. we characterize the nullspace $N(W)$.

Lemma 2.6 *For every $\mathbf{j}_0 \in N(W)$ exists a field $\mathbf{v} \in \mathbf{H}_0^1(B)$, $\operatorname{div} \mathbf{v} = 0$ that satisfies $\operatorname{curl} \mathbf{v} = \mathbf{j}_0$.*

Proof: Define $\mathbf{v} := \mathcal{W}\mathbf{j}_0$, then $\mathbf{v} \in \mathbf{H}^1(B)$. Since $\mathbf{j}_0 \in N(W)$ the field \mathbf{v} vanishes in B^e . Together with $\gamma_0[B]\mathbf{v} = \gamma_0[B^e]\mathbf{v}$ we have $\mathbf{v} \in \mathbf{H}_0^1(B)$. Furthermore, we obtain

$$\operatorname{div} \mathbf{v} = 0, \quad \operatorname{curl} \mathbf{v} = \mathbf{j}_0 \quad \text{in } B$$

from Corollary 2.5. ■

The question arises if all divergence-free fields \mathbf{v} with vanishing trace $\gamma_0[B]\mathbf{v}$ produce a field $\text{curl } \mathbf{v}$ such that $\mathcal{W}(\text{curl } \mathbf{v})$ vanishes outside B . To verify this, we use equation (2.19) for $\text{curl } \mathbf{v}$ with $\text{div } \mathbf{v} = 0$, $\gamma_0[B]\mathbf{v} = \mathbf{0}$ to conclude

$$\mathcal{W}(\text{curl } \mathbf{v}) = \mathbf{0} \quad \text{in } B^e. \quad (2.20)$$

To simplify notations we introduce the space

$$\mathbf{X} := \{ \text{curl } \mathbf{v} \mid \mathbf{v} \in \mathbf{H}_0^1(B) : \text{div } \mathbf{v} = 0 \}$$

and have proven the following theorem.

Theorem 2.7 *The nullspace $N(\mathcal{W})$ is given by the space \mathbf{X} , i.e.*

$$N(\mathcal{W}) = \mathbf{X}. \quad (2.21)$$

As the nullspace of the linear continuous operator \mathcal{W} the space \mathbf{X} is a closed subspace of $\mathbf{H}_{\text{div}=0}(B)$ and therefore complete. Moreover, \mathbf{X} is a Hilbert space equipped with the L^2 -scalar product.

2.2.2 A characterization of $N(\mathcal{W})^\perp$

We have the decomposition

$$\mathbf{H}_{\text{div}=0}(B) = N(\mathcal{W}) \oplus N(\mathcal{W})^\perp, \quad (2.22)$$

where the orthogonality is related to the scalar product of $\mathbf{H}_{\text{div}=0}(B)$ which is in fact the L^2 scalar product. It means

$$N(\mathcal{W})^\perp := \{ \mathbf{j} \in \mathbf{H}_{\text{div}=0}(B) \mid \langle \mathbf{j}, \mathbf{j}_0 \rangle_{L^2(B)} = 0 \quad \forall \mathbf{j}_0 \in N(\mathcal{W}) \}.$$

We search for a characterization of $N(\mathcal{W})^\perp$ without using the operator \mathcal{W} . At first, we convince ourselves that harmonic fields are elements of $N(\mathcal{W})^\perp$.

Theorem 2.8 *Harmonic vector fields are elements of the space $N(\mathcal{W})^\perp$, i.e.*

$$\{ \mathbf{j} \in \mathbf{H}_{\text{div}=0}(B) \mid \text{curl } \mathbf{j} = \mathbf{0} \} \subset N(\mathcal{W})^\perp. \quad (2.23)$$

Proof: Let $\mathbf{j} \in \mathbf{H}_{\text{div}=0}(B)$ satisfy $\text{curl } \mathbf{j} = \mathbf{0}$. For each $\mathbf{j}_0 \in N(\mathcal{W})$ we have $(\mathcal{W}\mathbf{j}_0)|_{\partial B} = \mathbf{0}$. With the aid of formula (A.75) and equation (2.16) we obtain

$$\begin{aligned} \langle \mathbf{j}, \mathbf{j}_0 \rangle_{L^2(B)} &= \int_B \mathbf{j} \cdot \mathbf{j}_0 \, dx \\ &\stackrel{(2.16)}{=} \int_B \mathbf{j} \cdot \text{curl}(\mathcal{W}\mathbf{j}_0) - (\mathcal{W}\mathbf{j}_0) \cdot \text{curl } \mathbf{j} \, dx \\ &\stackrel{(A.75)}{=} \int_{\partial B} \mathbf{j} \cdot (\nu \times \mathcal{W}\mathbf{j}_0) \, ds = 0, \end{aligned} \quad (2.24)$$

i.e. $\mathbf{j} \perp \mathbf{j}_0$. ■

The reverse inclusion of Theorem 2.8 is not true. We will show that fields with harmonic components are contained in the space $N(\mathcal{W})^\perp$. For this purpose we quote a lemma from [GiRa] which is a special consequence of the theorem proved by De Rham in [deRham]: *if a distribution vector field \mathbf{u} satisfies $\langle \mathbf{u}, \mathbf{v} \rangle_{\mathbf{L}^2(B)} = 0$ for all divergence-free fields of B then $\mathbf{u} = \text{grad } \phi$ for a distribution ϕ .*

Lemma 2.9 *If $\mathbf{f} \in \mathbf{H}^{-1}(B)$ satisfies*

$$\int_B \mathbf{f} \cdot \mathbf{v} \, dx = 0, \quad \forall \mathbf{v} \in \mathbf{H}_0^1(B) \text{ with } \text{div } \mathbf{v} = 0, \quad (2.25)$$

then there exists a $q \in L^2(B)$ such that

$$\mathbf{f} = \text{grad } q. \quad (2.26)$$

Proof: The lemma is taken from [GiRa], Lemma 2.1 ■

We introduce the space

$$\mathbf{Y} := \{ \mathbf{j} \in \mathbf{H}_{\text{div}=0}(B) \mid \exists q \in L^2(B) : \text{curl } \mathbf{j} = \text{grad } q \} \quad (2.27)$$

where $\text{curl } \mathbf{j} = \text{grad } q$ holds as equation in $\mathbf{H}^{-1}(B)$, i.e. in the sense of

$$\int_B \mathbf{j} \cdot \text{curl } \mathbf{v} \, dx = \int_B q \, \text{div } \mathbf{v} \, dx, \quad \forall \mathbf{v} \in \mathbf{H}_0^1(B). \quad (2.28)$$

Theorem 2.10 *The space $N(\mathcal{W})^\perp$ is given by the space \mathbf{Y} , i.e.*

$$N(\mathcal{W})^\perp = \mathbf{Y}. \quad (2.29)$$

Proof: Before we show the inclusions $N(\mathcal{W})^\perp \subset \mathbf{Y}$ and $\mathbf{Y} \subset N(\mathcal{W})^\perp$ we provide a basic formula. Consider the formula of partial differentiation $\text{div}(\mathbf{j} \times \mathbf{v}) = \mathbf{v} \text{curl } \mathbf{j} - \mathbf{j} \text{curl } \mathbf{v}$ which implies

$$\int_B \mathbf{v} \cdot \text{curl } \mathbf{j} \, dx = \int_B \mathbf{j} \cdot \text{curl } \mathbf{v} \, dx \quad (2.30)$$

for $\mathbf{j} \in \mathbf{C}^\infty(\overline{B})$, $\mathbf{v} \in \mathbf{C}_0^\infty(B)$. This equation can be extended to $\mathbf{j} \in \mathbf{H}_{\text{div}}(B)$ and $\mathbf{v} \in \mathbf{H}_0^1(B)$ since $\mathbf{C}^\infty(\overline{B})$ is dense in $\mathbf{H}_{\text{div}}(B)$ and $\mathbf{C}_0^\infty(B)$ is dense in $\mathbf{H}_0^1(B)$. In this case, the left side holds in the sense of dual system $\langle \mathbf{H}_0^1(B), \mathbf{H}^{-1}(B) \rangle$.

We start with the proof of the inclusion $N(\mathcal{W})^\perp \subset \mathbf{Y}$. Let $\mathbf{j} \in N(\mathcal{W})^\perp$, then the characterization of the nullspace $N(\mathcal{W})$ from Theorem 2.7 implies $\langle \mathbf{j}, \text{curl } \mathbf{v} \rangle_{\mathbf{L}^2(B)} = 0$ for each $\mathbf{v} \in \mathbf{H}_0^1(B)$, $\text{div } \mathbf{v} = 0$. We use the formula (2.30) to verify

$$\int_B \mathbf{v} \cdot \text{curl } \mathbf{j} \, dx \stackrel{(2.30)}{=} \int_B \mathbf{j} \cdot \text{curl } \mathbf{v} \, dx = 0 \quad \forall \mathbf{v} \in \mathbf{H}_0^1(B) \text{ with } \text{div } \mathbf{v} = 0$$

in the sense of the dual system $\langle \mathbf{H}_0^1(B), \mathbf{H}^{-1}(B) \rangle$. Now, we apply Lemma 2.9 to conclude that there exists a $q \in L^2(B)$ with $\operatorname{curl} \mathbf{j} = \operatorname{grad} q$ and the first part of the proof is complete.

The second part is the proof of inclusion $\mathbf{Y} \subset N(\mathcal{W})^\perp$. Let $\mathbf{j}_0 \in N(\mathcal{W})$, then there exists a field $\mathbf{v} \in \mathbf{H}_0^1(B)$, $\operatorname{div} \mathbf{v} = 0$ with $\operatorname{curl} \mathbf{v} = \mathbf{j}_0$. With the aid of Gauss' divergence theorem (1.92) we obtain

$$\int_B \mathbf{v} \cdot \operatorname{grad} q \, dx = \int_{\partial B} q \nu \cdot \mathbf{v} \, dx - \int_B q \operatorname{div} \mathbf{v} \, dx = 0 \quad (2.31)$$

for $q \in C^\infty(\overline{B})$. Since $C^\infty(\overline{B})$ is a dense subset of $L^2(B)$ this equation holds for $q \in L^2(B)$ in the sense of the dual system $\langle \mathbf{H}_0^1(B), \mathbf{H}^{-1}(B) \rangle$. Finally, let $\mathbf{j} \in \mathbf{Y}$, then there exists a function $q \in L^2(B)$ with $\operatorname{curl} \mathbf{j} = \operatorname{grad} q$ for a $q \in L^2(B)$. Putting the results (2.31) and (2.30) together we derive

$$\langle \mathbf{j}, \mathbf{j}_0 \rangle_{L^2(B)} = \int_B \mathbf{j} \cdot \operatorname{curl} \mathbf{v} \, dx \stackrel{(2.30)}{=} \int_B \mathbf{v} \cdot \operatorname{curl} \mathbf{j} \, dx = \int_B \mathbf{v} \cdot \operatorname{grad} q \, dx \stackrel{(2.31)}{=} 0. \quad (2.32)$$

This shows $\mathbf{j} \perp \mathbf{j}_0$ and $\mathbf{Y} \subset N(\mathcal{W})^\perp$. ■

2.2.3 More properties of $N(\mathcal{W})^\perp$

We want to have a closer look at the elements of the space $N(\mathcal{W})^\perp$. From $\operatorname{curl} \mathbf{j} = \operatorname{grad} q$ we have

$$\Delta \mathbf{j} = \operatorname{grad} \operatorname{div} \mathbf{j} - \operatorname{curl} \operatorname{curl} \mathbf{j} = \operatorname{curl} \operatorname{grad} q = 0 \quad (2.33)$$

for $\mathbf{j} \in N(\mathcal{W})^\perp$, which holds as equation in $\mathbf{H}^{-2}(B)$. It means that the elements of the space $N(\mathcal{W})^\perp$ have components satisfying the Laplace equation in H^{-2} sense. Under further regularity assumptions, these elements are uniquely determined by the tangential component $\nu \times \mathbf{j}|_{\partial B}$. In this Subsection, we investigate the corresponding boundary value problem for the equation $\Delta \mathbf{j} = \mathbf{0}$, $\operatorname{div} \mathbf{j} = 0$. Additionally, in preparation of the boundary value problems in Section 3.1, we make ourselves familiar with the special boundary value type and the solution methods.

We assume that the boundary ∂B is of class C^2 . We give a brief introduction of the surfacic operators GRAD, DIV, CURL called the *surface gradient*, *surface divergence*, and the scalar *surface rotational* of a vector field on ∂B . A detailed introduction can be found in [Ned], Section 2.5.6. We follow [CoKr1], page 167 and assume a parametric representation

$$x(t) = (x_1(t_1, t_2), x_2(t_1, t_2), x_3(t_1, t_2)) \quad (2.34)$$

of a surface patch of ∂B . In these local coordinates the surface gradient is defined by

$$\operatorname{GRAD} f := \sum_{i,j=1}^2 g^{ij} \frac{\partial f}{\partial t_i} \frac{\partial f}{\partial t_j} \quad (2.35)$$

where g^{ij} is the inverse of the first fundamental matrix

$$g_{ij} = \frac{\partial x}{\partial t_i} \cdot \frac{\partial x}{\partial t_j}, \quad i, j = 1, 2 \quad (2.36)$$

of differential geometry. For a continuous differentiable function in a neighborhood of ∂B we have the relation

$$\text{grad } f = \text{GRAD } f + \frac{\partial f}{\partial \nu} \nu. \quad (2.37)$$

For a continuously differentiable tangential field \mathbf{a} with the representation

$$\mathbf{a} = \mathbf{a}_1 \frac{\partial x}{\partial t_1} + \mathbf{a}_2 \frac{\partial x}{\partial t_2} \quad (2.38)$$

we define the *surface divergence* by

$$\text{DIV } \mathbf{a} := \frac{1}{\sqrt{g}} \left\{ \frac{\partial}{\partial t_1} (\sqrt{g} \mathbf{a}_1) + \frac{\partial}{\partial t_2} (\sqrt{g} \mathbf{a}_2) \right\} \quad (2.39)$$

where g denotes the determinant of the matrix g_{ij} . Now, from the definitions (2.35) and (2.39) we conclude the product rule

$$\text{DIV } (f \mathbf{a}) = \mathbf{a} \cdot \text{GRAD } f + f \text{DIV } \mathbf{a}. \quad (2.40)$$

With the aid of

$$\int_{\partial B} \text{DIV } \mathbf{b} \, ds = 0 \quad (2.41)$$

for each tangential field \mathbf{b} (see for instance [Ma], page 74), we obtain

$$\int_{\partial B} f \text{DIV } \mathbf{a} \, ds = - \int_{\partial B} \mathbf{a} \cdot \text{GRAD } f \, ds. \quad (2.42)$$

which we use for the following definition.

Definition 2.11 *A tangential field \mathbf{a} has weak divergence if there exists an integrable scalar denoted by $\text{DIV } \mathbf{a}$ such that (2.42) is satisfied for all $f \in C^1(\partial B)$.*

The definition (2.35) holds for a function $f \in H^s(\partial B)$ where the partial differentials $\partial f / \partial t_i, i = 1, 2$ have to be understood as weak partial differentials on the C^2 boundary ∂B . This way we have introduced the weak surface gradient. Next, we define the weak scalar rotational $\text{CURL } \mathbf{a}$ of a tangential field \mathbf{a} by

$$\text{CURL } \mathbf{a} := - \text{DIV } (\nu \times \mathbf{a}). \quad (2.43)$$

Let $\mathbf{L}_t^2(\partial B)$ be the space of all square-integrable tangential fields and $\mathbf{H}_t^s(\partial B)$ the space of all tangential \mathbf{H}^s -fields on ∂B . Then we introduce

$$\mathbf{H}_{t,\text{CURL}}^s(\partial B) := \{\mathbf{a} \in \mathbf{H}_t^s(\partial B) \mid \text{CURL } \mathbf{a} \in \mathbf{H}_t^s(\partial B)\}, \quad (2.44)$$

$$\mathbf{H}_{t,\text{CURL}=0}^s(\partial B) := \{\mathbf{a} \in \mathbf{H}_{t,\text{CURL}}^s(\partial B) \mid \text{CURL } \mathbf{a} = 0\}, \quad (2.45)$$

$$\mathbf{H}_{t,\text{DIV}}^s(\partial B) := \{\mathbf{a} \in \mathbf{H}_t^s(\partial B) \mid \text{DIV } \mathbf{a} \in H^s(\partial B)\}, \quad (2.46)$$

$$\mathbf{H}_{t,\text{DIV}=0}^s(\partial B) := \{\mathbf{a} \in \mathbf{H}_{t,\text{DIV}}^s(\partial B) \mid \text{DIV } \mathbf{a} = 0\}. \quad (2.47)$$

The following relations between the surface operators with a field $\mathbf{v} \in \mathbf{H}_{\text{curl}}(B)$ and a tangential field $\mathbf{a} \in \mathbf{H}_{t,\text{CURL}}^s(\partial B)$ hold

$$\begin{aligned} \text{CURL GRAD } \mathbf{a} &= 0, \\ \gamma_\nu \mathbf{w} &= \text{CURL } \gamma_{\text{T}} \mathbf{v} \quad \text{for } \mathbf{w} := \text{curl } \mathbf{v}, \end{aligned}$$

see for instance [Ned], Theorem 2.5.19. and [CoKr1], relation (6.38).

Theorem 2.12 *Let $\partial B \in C^2$. The trace operator γ_{T} is a linear bounded and surjective operator from $\mathbf{H}_{\text{curl}}(B)$ onto $\mathbf{H}_{t,\text{CURL}}^{-1/2}(\partial B)$. For every $\mathbf{a} \in \mathbf{H}_{t,\text{CURL}}^{-1/2}(\partial B)$ exists a divergence-free field $\mathbf{v} \in \mathbf{H}_{\text{curl}}(B)$ with $\gamma_{\text{T}} \mathbf{v} = \mathbf{a}$.*

The trace operator γ_\times is a linear bounded and surjective operator from $\mathbf{H}_{\text{curl}}(B)$ onto $\mathbf{H}_{t,\text{DIV}}^{-1/2}(\partial B)$. For every $\mathbf{a} \in \mathbf{H}_{t,\text{DIV}}^{-1/2}(\partial B)$ exists a divergence-free field $\mathbf{v} \in \mathbf{H}_{\text{curl}}(B)$ with $\gamma_\times \mathbf{v} = \mathbf{a}$.

Proof: See Theorem 5.4.2. in [Ned]. ■

We define the so called *Laplace-Beltrami* operator acting on tangential fields by

$$\Delta_{\partial B} \mathbf{a} := \text{DIV GRAD } \mathbf{a} \quad (2.48)$$

which is an isomorphism of $H_o^{1/2}(\partial B)$ onto $H_o^{-3/2}(\partial B)$ (see for instace [Ned], page 216 in Section 5.4.1) for the connected C^2 boundary ∂B .

After this brief excursus on surface operators we turn back to the characterization of the elements of $N(\mathcal{W})^\perp$. The harmonic vector fields are contained in $N(\mathcal{W})^\perp$ and can be uniquely determined by its tangential component, i.e. we consider the

BVP 7 (Interior tangential problem for harmonic fields) Let $\partial B \in C^2$. For some given field $\mathbf{g} \in \mathbf{H}_{t,\text{DIV}}^{-1/2}(\partial B)$

$$\text{find } \mathbf{j} \in \mathbf{H}_{\text{curl}}(B) \cap \mathbf{H}_{\text{div}}(B) \text{ such } \begin{cases} \text{curl } \mathbf{j} = \mathbf{0}, & \text{div } \mathbf{j} = 0 & \text{in } B, \\ \nu \times \mathbf{j} = \mathbf{g} & & \text{on } \partial B. \end{cases} \quad (2.49)$$

The boundary condition holds as $\gamma_\times[B]\mathbf{j} = \mathbf{g}$.

Theorem 2.13 *The boundary value problem (2.49) admits an uniquely determined solution $\mathbf{j} \in \mathbf{H}_{curl}(B) \cap \mathbf{H}_{div}(B)$, provided*

$$\text{DIV } \mathbf{g} = 0. \quad (2.50)$$

Proof: Let q be the scalar potential of \mathbf{j} , then the solvability condition follows from

$$\text{DIV } \mathbf{g} = \text{DIV} (\nu \times \text{grad } q) = -\text{CURL GRAD } q|_{\partial B} = 0. \quad (2.51)$$

At first we prove uniqueness. Let $\mathbf{j} \in \mathbf{H}_{curl}(B) \cap \mathbf{H}_{div}(B)$ be a solution of the corresponding homogeneous problem and $q \in H^1(B)$ its scalar potential. The homogeneous boundary condition implies $\nu \times \text{GRAD } q|_{\partial B} = \mathbf{0}$ and consequently $\text{GRAD } q|_{\partial B} = 0$. Therefore, the function $q|_{\partial B}$ must be constant. Now, by $\text{div } \mathbf{u} = \Delta q$, the function q solves the interior Dirichlet problem of Laplace's equation with constant boundary values $q|_{\partial B}$. Its unique solvability implies that q is constant in B . Finally, we have $\mathbf{j} = \text{grad } q = \mathbf{0}$.

For the existence of a solution we reduce the problem 2.49 to the interior Dirichlet problem of Laplace equation

$$\text{find } q \in H^1(B) \text{ such } \begin{cases} \Delta q = 0 & \text{in } B, \\ q|_{\partial B} = f & \text{on } \partial B \end{cases} \quad (2.52)$$

with boundary value $f \in H_o^{1/2}(\partial B)$ determined by $\Delta_{\partial B} f = \text{CURL } \mathbf{g}$. We show that a solution of problem (2.52) induces a solution of (2.49) by $\mathbf{j} = \text{grad } q$.

The function $\text{CURL } \mathbf{g} \in H^{-3/2}(\partial B)$ fulfills

$$\langle \text{CURL } \mathbf{g}, 1 \rangle = \int_{\partial B} \text{DIV} (\nu \times \mathbf{g}) ds = 0. \quad (2.53)$$

The isomorphism property of the Laplace-Beltrami operator implies that the equation $\Delta_{\partial B} f = \text{CURL } \mathbf{g}$ has an unique solution $f \in H_o^{1/2}(\partial B)$. Now, we use the unique solvability of problem (2.52) shown in Theorem 1.28. Let $q \in H_{\Delta}^1(B)$ be the unique solution of (2.52), then $\text{grad } q$ solves the problem (2.49) which can be shown as follows. The equations $\text{div grad } q = 0$ and $\text{curl grad } q = \mathbf{0}$ are easy to check, so we prove the boundary condition by

$$\text{DIV} (\nu \times \text{GRAD } f - \mathbf{g}) = -\text{CURL GRAD } f - \text{DIV } \mathbf{g} = 0, \quad (2.54)$$

$$\text{CURL} (\nu \times \text{GRAD } f - \mathbf{g}) = \text{DIV GRAD } f - \text{CURL } \mathbf{g} = 0. \quad (2.55)$$

Since ∂B is a connected boundary, there exists a surface function g with $\text{GRAD } g = \nu \times \text{GRAD } f - \mathbf{g}$. Equation (2.54) implies $\Delta_{\partial B} g = 0$. Hence, g must be constant and $\nu \times \text{GRAD } f - \mathbf{g} = \text{GRAD } g = \mathbf{0}$. Finally, we have $\nu \times \text{grad } q = \nu \times \text{GRAD } f = \mathbf{g}$. ■

Remark 2.14 *The prove of the Theorem 2.13 constructs a solution $\mathbf{j} = \text{grad } q$ where q is the solution of $\Delta q = 0, q|_{\partial B} = f$ and $f \in H_o^{1/2}(\partial B)$ the solution of $\Delta_{\partial B} f = \text{CURL } \mathbf{g}$. Then we obtain that $q \in H_{\Delta}^1(B)$ is a weak harmonic function, and thus, analytic. Altogether, the unique solution \mathbf{j} has more regularity: it is analytic in B .*

In general, if an element of $N(W)^\perp$ has a tangential component $\mathbf{g} \in \mathbf{H}_{t,\text{DIV}}^{-1/2}(\partial B)$, it can be characterized as the solution of the boundary value problem

BVP 8 (Interior tangential problem for the 3d-Laplace equation) Let $\partial B \in C^2$. For some given function $\mathbf{g} \in \mathbf{H}_{t,\text{DIV}}^{-1/2}(\partial B)$

$$\text{find } \mathbf{j} \in \mathbf{H}_{\text{curl}}(B) \cap \mathbf{H}_{\text{div}}(B) \text{ such } \begin{cases} \text{curl curl } \mathbf{j} = \mathbf{0}, & \text{div } \mathbf{j} = 0 & \text{in } B, \\ \nu \times \mathbf{j} = \mathbf{g} & & \text{on } \partial B. \end{cases} \quad (2.56)$$

The boundary condition holds in the sence of $\mathbf{t}[B]\mathbf{j} = \mathbf{g}$.

Theorem 2.15 *The boundary value problem (2.56) admits an uniquely determined solution $\mathbf{j} \in \mathbf{H}_{\text{curl}}(B) \cap \mathbf{H}_{\text{div}}(B)$.*

Proof: For the proof of uniqueness let \mathbf{j} be a solution of the corresponding homogeneous problem, then $\nu \times \mathbf{j} = \mathbf{0}$. Further, $\gamma_T \mathbf{j} = \mathbf{0} \in \mathbf{H}_{t,\text{DIV}}^{-1/2}(B)$, and since the space

$$\left\{ \mathbf{v} \mid \mathbf{v} \in \mathbf{H}_{\text{curl}}(B); \mathbf{v} \in \mathbf{H}_{\text{div}}(B); \gamma_T \mathbf{v} \in \mathbf{H}_{t,\text{DIV}}^{-1/2}(B) \right\} \quad (2.57)$$

is included in $\mathbf{H}^1(B)$ (see Theorem 5.4.3 in [Ned]), the field \mathbf{j} belongs to $\mathbf{H}^1(B)$. From the calculation

$$\begin{aligned} \int_B |\text{curl } \mathbf{j}|^2 dx &= \int_B -\mathbf{j} \text{curl curl } \mathbf{j} + \text{curl } \mathbf{j} \text{curl } \mathbf{j} dx \\ &= \int_B \text{div } \{ \mathbf{j} \times \text{curl } \mathbf{j} \} dx = \int_{\partial B} \text{curl } \mathbf{j} \cdot \nu \times \mathbf{j} dx = 0 \end{aligned}$$

we conclude that $\text{curl } \mathbf{j}$ vanishes. Now, \mathbf{j} solves the problem (2.49) with homogeneous boundary condition. The unique solveability implies $\mathbf{j} = \mathbf{0}$.

Due to Theorem 2.12, there exists a $\mathbf{v} \in \mathbf{H}_{\text{curl}}(B)$, $\text{div } \mathbf{v} = 0$ with $\nu \times \mathbf{v} = \mathbf{g}$. Now, we have $\nu \cdot \text{curl } \mathbf{v} \in H^{-\frac{1}{2}}(\partial B)$ and $\langle \nu \cdot \text{curl } \mathbf{v}, 1 \rangle = 0$. The interior Neumann problem for Laplace equation

$$\begin{cases} \Delta p = 0 & \text{in } B, \\ \partial_\nu p = \nu \cdot \text{curl } \mathbf{v} & \text{on } \partial B \end{cases} \quad (2.58)$$

admits a solution p uniquely determined up to a constant, see Theorem 1.29. We observe that the field $\text{curl } \mathbf{v} - \text{grad } p$ has free divergence and vanishing normal component. From Theorem 1.46, there exists an unique determined vector potential \mathbf{w} of the field $\text{curl } \mathbf{v} - \text{grad } p$ with $\text{div } \mathbf{w} = 0$ and $\nu \times \mathbf{w} = \mathbf{0}$. Finally, we verify

$$\text{curl curl } (\mathbf{v} - \mathbf{w}) = \text{curl } (\text{curl } \mathbf{v} - \text{grad } p - \text{curl } \mathbf{w}) = \mathbf{0}, \quad (2.59)$$

$$\text{div } (\mathbf{v} - \mathbf{w}) = 0, \quad (2.60)$$

$$\nu \times (\mathbf{v} - \mathbf{w}) = \nu \times \mathbf{v} = \mathbf{g}, \quad (2.61)$$

i.e. $\mathbf{j} := \mathbf{v} - \mathbf{w}$ solves (2.56). ■

For an integral representation of the solution of problem (2.56) with boundary values $\mathbf{g} \in \mathbf{L}_{t,\text{DIV}}^2(B)$ we summarize the results of Section A.4. The field

$$\mathbf{j} = \text{curl } \vec{\mathcal{S}}\mathbf{a} \quad (2.62)$$

with density $\mathbf{a} \in \mathbf{L}_{t,\text{DIV}}^2(B)$ as the unique solution of $(\mathcal{I} - \mathcal{M})\mathbf{a} = -2\mathbf{g}$ solves the problem (2.56). Moreover, if $\text{DIV } \mathbf{g} = 0$ then this solution is curl-free, i.e. the fields $\mathbf{j} = \text{curl } \vec{\mathcal{S}}\mathbf{a}$ with $\mathbf{a} = (\mathcal{I} - \mathcal{M})^{-1}\mathbf{g}$ is a solution of problem (2.49).

2.3 Magnetic Tomography for Ohmic Conductors

The results of the last section are true for all currents independent of their physical nature. The decomposition with respect to the nullspace is valid for currents (and their magnetic fields) in the corona of the sun as well as for currents in ohmic conductors. For our applications, as described in the introduction after equation (1.5), we model current distributions to be based on a conductivity distribution. This leads to a reconstruction problem where we measure the magnetic field of a current distribution of an ohmic conductor.

Let B be the domain with a conductivity distribution and g the current flux into B . In the following Section 2.3.1 we show that under appropriate assumptions the current distribution \mathbf{j} is uniquely determined via an anisotropic impedance problem. In Section 2.3.2 we will develop some orthogonality relation for these ohmic currents which provides at least a partial answer to question 5.

2.3.1 The Anisotropic Impedance Problem

We consider a conductivity distribution σ in B . Generally, it is a matrix of the form

$$\sigma(x) = \begin{pmatrix} \sigma_{11}(x) & \sigma_{12}(x) & \sigma_{13}(x) \\ \sigma_{21}(x) & \sigma_{22}(x) & \sigma_{23}(x) \\ \sigma_{31}(x) & \sigma_{32}(x) & \sigma_{33}(x) \end{pmatrix}, \quad x \in B.$$

We assume that σ is strict coercive, i.e., there exists a constant $c > 0$ such that

$$\mathbf{a} \cdot \sigma \mathbf{a} \geq c|\mathbf{a}|^2, \quad \forall \mathbf{a} \in \mathbb{R}^3. \quad (2.63)$$

As a consequence, σ is invertible with bounded inverse σ^{-1} . Further, we restrict the analysis to symmetric conductivities, so we define the set of symmetric and strict coercive matrix functions by

$$\Sigma := \left\{ \sigma = \begin{pmatrix} \sigma_{11} & \sigma_{12} & \sigma_{13} \\ \sigma_{12} & \sigma_{22} & \sigma_{23} \\ \sigma_{13} & \sigma_{23} & \sigma_{33} \end{pmatrix} \mid \sigma \text{ is strict coercive in } B \right\}. \quad (2.64)$$

For a $\sigma \in \Sigma$ and $g \in H_o^{-\frac{1}{2}}(\partial B)$ the current distribution fulfills the condition

$$\operatorname{curl} \sigma^{-1} \mathbf{j} = \mathbf{0}, \quad \operatorname{div} \mathbf{j} = 0 \quad \text{in } B, \quad (2.65)$$

$$\nu \cdot \mathbf{j} = g \quad \text{on } \partial B, \quad (2.66)$$

which follow from Maxwell's equations $\operatorname{curl} \mathbf{E} = \mathbf{0}$, $\operatorname{curl} \mathbf{H} = \mathbf{j}$ and Ohm's law $\mathbf{j} = \sigma \mathbf{E}$. Since B is simply-connected, there is an electric potential ϕ_e such that $\mathbf{E} = \operatorname{grad} \phi_e$. Now, we are able to formulate:

BVP 9 (Interior Neumann problem for the impedance equation) Let $\partial B \in C^{0,1}$. For some given $\sigma \in \Sigma$ and $g \in H_o^{-\frac{1}{2}}(\partial B)$

$$\text{find } \phi_e \in H_{\text{circ}}^1(B) \text{ such } \int_B \operatorname{grad} \psi \cdot \sigma \operatorname{grad} \phi_e \, dx = \int_{\partial B} \psi g \, ds, \quad \forall \psi \in H^1(B). \quad (2.67)$$

Theorem 2.16 *The boundary value problem (2.67) has an unique solution $\phi_e \in H_o^1(B)$.*

Proof: See [KüPo], Theorem 1. ■

Let ϕ_e be a solution of (2.67), then $\mathbf{j} := \sigma \operatorname{grad} \phi_e$ satisfies $\operatorname{div} \mathbf{j} = 0$, $\nu \cdot \mathbf{j} = g$ in a weak sense, i.e.

$$\int_B \mathbf{j} \cdot \operatorname{grad} \psi \, ds = \int_{\partial B} \psi g \, ds, \quad \forall \psi \in H^1(B). \quad (2.68)$$

On the other hand, if \mathbf{j} is a solution of (2.65), then there exists a scalar potential $\phi \in H^1(B)$ such that $\operatorname{grad} \phi = \sigma^{-1} \mathbf{j}$. The assumption implies $\operatorname{div} (\sigma \operatorname{grad} \phi) = 0$, $\nu \cdot (\sigma \operatorname{grad} \phi) = g$. Integrating the first equation over ∂B , using the second equation and Gauss' divergence theorem yields that ϕ is a solution of (2.67).

The left hand side of (2.67) is a scalar product on $\mathbf{L}^2(B)$. Hence, we define

$$\langle \mathbf{E}_1, \mathbf{E}_2 \rangle_\sigma := \int_B \mathbf{E}_1 \cdot \sigma \mathbf{E}_2 \, dx \quad (2.69)$$

and

$$\langle \mathbf{j}_1, \mathbf{j}_2 \rangle_{\sigma^{-1}} := \int_B \mathbf{j}_1 \cdot \sigma^{-1} \mathbf{j}_2 \, dx, \quad (2.70)$$

respectively. We note that the first scalar product generates the so called energy norm $\|\cdot\|_\sigma$ by

$$\|\mathbf{E}\|_\sigma^2 = \int_B \mathbf{E} \cdot \sigma \mathbf{E} \, dx = \int_B \mathbf{E} \cdot \mathbf{j} \, dx. \quad (2.71)$$

We remark that $\mathbf{E} \cdot \mathbf{j}$ is called the energy density (evaluating $\|\mathbf{j}\|_{\sigma^{-1}}$ we derive the same expression by setting $\mathbf{E} = \sigma^{-1} \mathbf{j}$, so both scalar products can be seen as 'energy scalar products').

2.3.2 Orthogonality of Ohmic Currents

Every current distribution \mathbf{j} may be split into $\mathbf{j}_0 + \mathbf{j}_\perp$ with elements $\mathbf{j}_0 \in N(\mathcal{W})$ and $\mathbf{j}_\perp \in N(\mathcal{W})^\perp$. Here, we answer the question 5, where we ask for the relation between ohmic current distributions and the spaces $N(\mathcal{W})$ and $N(\mathcal{W})^\perp$.

Definition 2.17 *We call a current distribution $\mathbf{j} \in \mathbf{L}^2(B)$ an ohmic current distribution if \mathbf{j} is a solution of (2.65) for some $\sigma \in \Sigma$ and some $g \in H^{\frac{1}{2}}(B)$. We use the notation \mathbf{j}_σ for an ohmic current distribution whenever $\sigma \in \Sigma$ and $\mathbf{j}_\sigma \in \mathbf{L}^2(B)$ satisfy $\text{curl } \sigma^{-1} \mathbf{j}_\sigma = 0$ in B .*

Note that the conductivity distribution σ is not uniquely determined by \mathbf{j}_σ . If $\sigma \in \Sigma$ solves $\text{curl } \sigma^{-1} \mathbf{j}_\sigma = 0$ then $c\sigma$ with $c \in \mathbb{R}^+$ satisfies this relation, too.

The next theorems show that the ohmic current distribution is orthogonal to the nullspace of the Biot-Savart operator in some sense.

Theorem 2.18 *Let \mathbf{j}_σ be an ohmic current distribution, then*

$$\mathbf{j}_\sigma \perp_{\sigma^{-1}} (\mathcal{I} - \mathcal{S}^\nabla)N(\mathcal{W}). \quad (2.72)$$

with respect to the scalar product defined by (2.70).

Proof: See [KrKüPo], Theorem 9. Please note that their definition of the scalar product is different from (2.70). ■

We are able to upgrade this statement. Recalling the result $\mathcal{S}^\nabla \mathbf{j}_0 = \mathbf{0}$ for a current distribution $\mathbf{j}_0 \in N(\mathcal{W})$, then from Theorem 2.5 we have $\mathcal{S}^\nabla(N(\mathcal{W})) = \mathbf{0}$.

Corollary 2.19 *Let \mathbf{j}_σ be an ohmic current distribution. Then holds*

$$\mathbf{j}_\sigma \perp_{\sigma^{-1}} N(\mathcal{W}). \quad (2.73)$$

Let \mathbf{j}_σ be an ohmic current distribution, we may rewrite (2.73) as $\sigma^{-1} \mathbf{j}_\sigma \perp N(\mathcal{W})$. That means the electric field $\mathbf{E} = \sigma^{-1} \mathbf{j}_\sigma$ is perpendicular to $N(\mathcal{W})$. For an ohmic current distribution $\tilde{\mathbf{j}}$, which does not generate a magnetic field in the exterior domain B^e of B , we have

$$\int_B \tilde{\mathbf{j}} \cdot \tilde{\mathbf{E}} dx = \int_B \tilde{\mathbf{j}} \cdot \sigma^{-1} \tilde{\mathbf{j}} dx = \langle \tilde{\mathbf{j}}, \tilde{\mathbf{j}} \rangle_{\sigma^{-1}} = 0 \quad (2.74)$$

with the electric field $\tilde{\mathbf{E}} = \sigma^{-1} \tilde{\mathbf{j}}$ related to $\tilde{\mathbf{j}}$. In a physical point of view, the current distribution $\tilde{\mathbf{j}}$ has no electric power (and must vanish). Finally, we are able to prove

Corollary 2.20 *An ohmic current distribution that generates no magnetic field in the exterior B^e of B must vanish.*

Proof: From the calculation (2.74) we have

$$\|\tilde{\mathbf{j}}\|_{\sigma^{-1}} = 0 \quad (2.75)$$

for a current distribution $\tilde{\mathbf{j}}$ which is an ohmic current distribution and belongs to $N(\mathcal{W})$. Since $\|\cdot\|_{\sigma^{-1}}$ defines a norm on $\mathbf{L}^2(B)$ the field $\tilde{\mathbf{j}}$ must vanish. ■

2.3.3 A Numerical Study on the Stabilized Inversion

This section gives an overview on the results we have reached in the cooperation projects of the Young Researchers Group "New numerical methods for inverse problems" with the TomoScience GbR (formerly Xcellvision), Wolfsburg. We present some photographic pictures of fuel cells and wire grid models to get an idea of our measurements and of our work in praxis. Some figures show that basically we are able to reconstruct the currents from the their magnetic field by the stabilized inversion of the Biot-Savart operator. In addition, this subsection shall show that the work in the young researcher group contains even more than the theoretical investigation. We applied and proof the results in practise. For this verification we had to study and solve practical problems combined with the measurements of physical properties. Thus, by an extensive study, we should investigate the accuracy of the stabilized inversion of the Biot-Savart operator. Here, we discuss some of the results.

First, we describe the discretization model for the direct problem. In a view of the fuel cell application we have decided for the finite integration technique. Second, we present two reconstruction algorithms, the *difference* and the *absolute reconstruction algorithm*. Basically, they arise from the practical opportunities of the measurement of the magnetic field. The first one is well suited for the situation where we want to compare the reconstructed current with a known current flow as for instance a homogeneous one. Moreover, we explain how we take into account the free divergence of the reconstructed current distribution.

At first we apply the stabilized inversion of the Biot-Savart operator to simulated magnetic field, i.e. we calculate the current distribution based on a given conductivity distribution and its magnetic field. In the light of some figures we compare the stabilized inversion via Tikhonov-regularization and the simulated currents.

Next, we present a numerical study on the reconstruction of currents in a wire grid model from their magnetic field. A first advantage is that a wire grid does agree with the discretization model such that we can neglect discretization errors and may focus on practical errors. A second advantage is that we are able to calculate and measure the current distribution (in contradiction to the fuel cell application) and may compare it to the reconstructed current. For fuel cells, the contacts between the layers (for instance between a graphite plate and the membrane with the platin catalyst) may cause a different conductivity distribution as assumed which influence and change the current distribution inside the fuel cell such that our simulated current flow does not agree with the real current flow.

Furthermore, we present the reconstruction results of a prepared fuel cell. Here, a graphite layer between the anode and cathode plate is segmented into a number of segments. This method is called *segmentation method*. For each segment the currents can be electrically measured, and altogether we obtain an overview of the currents in z -direction. This way we are able to compare the reconstructed current. Moreover, the segmentation can be used for a test of the stabilized inversion as well the segmentation method. If we

cut off some segments, both results must reflect the removed segments. We discuss two reconstruction pictures for such a test. They do not show any reconstruction pictures of segmented fuel cells in practice since their interpretation requires detailed knowledge of the fuel cell technology.

Discretization model

From our industrial application, a fuel cell stack is a rectangular domain

$$B = \left\{ x = (x_1, x_2, x_3) \in \mathbb{R}^3 \mid |x_1| < \frac{a_1}{2}, |x_2| < \frac{a_2}{2}, |x_3| < \frac{a_3}{2} \right\} \quad (2.76)$$

where the currents are fed in at the base surface, i.e. for $x_3 = -a_3/2$ and are taken from the top surface, i.e. for $x_3 = a_3/2$. Hence, for a simple characterization of the fuel cell stack (where are areas of higher and lower reactivity) it is sufficient to analyse the currents in x_3 -direction. For the grid model we use a rectangular grid \mathcal{G} with n_1, n_2, n_3 points in x_1, x_2 and x_3 -direction, respectively. The knot points are defined by

$$p_{klm} := (x_{1,k}, x_{2,l}, x_{3,m}) \quad (2.77)$$

for

$$k = 0, \dots, n_1 - 1, \quad l = 0, \dots, n_2 - 1, \quad m = 0, \dots, n_3, \quad (2.78)$$

with

$$x_{s,t} := -\frac{a_s}{2} + t \frac{a_s}{n_s - 1}, \quad s = 1, 2, 3, t = 0, \dots, n_s - 1 \quad (2.79)$$

We call the virtual (or real) wire between a point p_{klm} and a neighbor knot point $p_{(k+1)lm}$, $p_{k(l+1)m}$, $p_{kl(m+1)}$ parallel to the x_1, x_2, x_3 axis by $s_{klmx}, s_{klmy}, s_{klmz}$ and denote the current flowing in this wires by

$$I_{klmx}, I_{klmy}, I_{klmz} \quad (2.80)$$

From the *conservation law* we demand

$$\sum_{kl} I_{kl}^{in} = \sum_{kl} I_{kl}^{out} \quad (2.81)$$

for the given current input I_{kl}^{in} and output I_{kl}^{out} at the bottom and top surface points $p_{kl0}, p_{kl n_3}$, respectively. For the index of the currents which are fed in the base surface we use the index $k = -1$. Then we define

$$I_{kl(-1)z} := I_{kl}^{in}, \quad I_{klmz} := I_{kl}^{out} \quad (2.82)$$

for k, l as in (2.78). The current input and output at the shell surface points $p_{0lm}, p_{n_1lm}, p_{k0m}, p_{kn_2m}$ vanishes, i.e. we set

$$I_{(-1)lmx} := I_{n_1lmx} = 0, \quad I_{k(-1)my} := I_{kn_2my} = 0, \quad (2.83)$$

for k, l, m as in (2.78). Now, we have the classical conservation law also called knot rule

$$I_{(k-1)lmx} + I_{k(l-1)my} + I_{kl(m-1)z} = I_{klmx} + I_{klmy} + I_{klmz} \quad (2.84)$$

for all k, l, m as in (2.78), i.e. the sum of incoming and outflowing currents of a knot point is zero. Due to the assumption (2.81) all equations of (2.84) are linear dependent, thus, we drop the last of the knot rules, i.e. for $k = n_1 - 1, m = n_2 - 1, n_3 - 1$.

For the discrete model we assume that the ohmic resistance of the wire $s_{klm\zeta}$ for $\zeta \in \{x, y, z\}$ is given by a scalar $R_{klm\zeta} > 0$. The voltage between the point p_{klm} and its neighbor points in positive ζ -direction is denoted by $U_{klm\zeta}$ and defined by Ohm's law

$$U_{klm\zeta} = I_{klm\zeta} \cdot R_{klm,\zeta} \quad (2.85)$$

The *mesh theorem* states that the sum of the voltages over each closed path vanishes. Here, we restrict ourselves to the elementary meshes of \mathcal{G} , then we have the mesh equations

$$U_{klmx} + U_{(k+1)lmy} - U_{k(l+1)mx} - U_{klmy} = 0, \quad (2.86)$$

$$U_{klmx} + U_{(k+1)lmz} - U_{kl(m+1)x} - U_{klmz} = 0, \quad (2.87)$$

$$U_{klmx} + U_{k(l+1)mz} - U_{kl(m+1)y} - U_{klmz} = 0. \quad (2.88)$$

We note that some of these equations are linearly dependent. A complete and linearly independent set of mesh equations are for instance given by all possible xz-mesh equations (2.87), all yz-mesh equations (2.88), and the xz mesh equations on the top, i.e. for $m = n_3 - 1$.

In the presented discretization model each corner of the elementary meshes is a knot point. The Figure 2.1 shows the cube $(-1, 1)^3$ and the virtual wires of the grid model for a discretization of 4 elementary meshes in each direction, i.e. for $n_1 = n_2 = n_3 = 5$. Thus, we call it a $[4, 4, 4]$ discretization although we have 5 knot points in each direction. Moreover, the blue arrows in Figure 2.1 indicates the currents in the grid for a homogeneous resistance distribution and centred input/outflow.

These introduction into the finite integration technique is taken from our paper [KüPo], a detailed discription can be found there. In addition, solvability and convergence as well as consistency and stability is proven in this paper. Finally, the total magnetic field is calculated by the Biot-Savart operator using a simple rectangular rule for each elementary mesh.

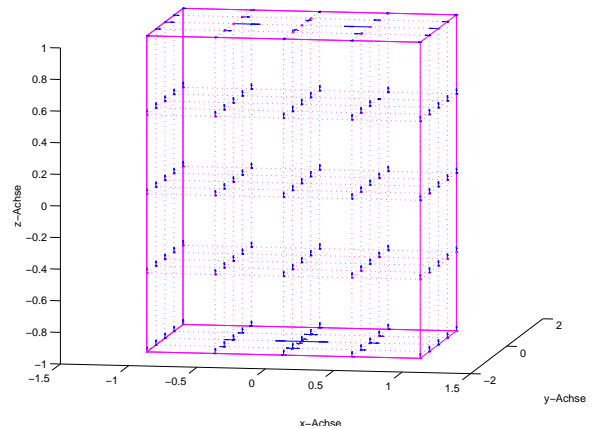


Figure 2.1: Discretization model with 5 points in each direction

Reconstruction algorithm

In praxis, the magnetic flux $\mathbf{B}(x)$ at the point $x \in \mathbb{R}^3$ is a sum of many influences

$$\mathbf{B}(x) = \mathbf{B}_{earth}(x) + \mathbf{B}_{cs}(x) + \mathbf{B}_{fc}(x). \quad (2.89)$$

\mathbf{B}_{earth} denotes the earth magnetic flux (which can be locally disturbed for instance by some steel girders in the walls of the building where we have measured etc.). \mathbf{B}_{cs} is the magnetic flux of the current supply of the fuel cell, and \mathbf{B}_{fc} is the magnetic flux of the fuel cell we are interested in. In general, the fields $\mathbf{B}_{earth}, \mathbf{B}_{cs}$ are not known but we assume that the fields are constant in time. Therefore, a very easy way of reconstruction is the *difference reconstruction*. Here, we subtract two measurements from each other where the first one is a reference measurement (for the wire grid application it can be a homogeneous grid) denoted by \mathbf{B}_{ref} . Then we have

$$\mathbf{B}_2(x) - \mathbf{B}_1(x) = \mathbf{B}_{ref}(x) - \mathbf{B}_{fc}(x), \quad (2.90)$$

We have to convert the magnetic flux into the magnetic field where we use the linear material relation

$$\mathbf{B} = \mu\mu_r\mathbf{H} \quad (2.91)$$

for the exterior of the fuel cell which is usually air with a material constant $\mu_r \approx 1$, thus we have

$$\mathbf{H}_2 - \mathbf{H}_1 = \frac{1}{\mu}(\mathbf{B}_2 - \mathbf{B}_1). \quad (2.92)$$

Since the Biot-Savart operator is a linear operator we obtain

$$\mathbf{H}_2 - \mathbf{H}_1 = \mathcal{W}(\mathbf{j}_{ref} - \mathbf{j}_{fc}), \quad (2.93)$$

i.e. we are able to reconstruct the difference current distribution. This is a very feasible way of reconstruction since we are interested in areas of higher and lower reactivity in fuel cells (in comparison to a homogeneous reactivity distribution).

For the stabilized inversion we use the Tikhonov regularization. An introduction into the regularization of inverse problems is attached in the appendix in Section A.1. We note that the plane Tikhonov regularization scheme

$$\mathbf{j}_{reg} := (\alpha\mathcal{I} + \mathcal{W}^*\mathcal{W})^{-1}\mathcal{W}^*\mathbf{H} \quad (2.94)$$

applied to the equation $\mathcal{W}\mathbf{j}_\sigma = \mathbf{H}$ maps onto $N(\mathcal{W})^\perp$. In the last Subsection we derived the relation

$$\mathbf{j}_\sigma \perp_{\sigma^{-1}} N(\mathcal{W}), \quad (2.95)$$

see (2.19). For a homogeneous conductivity distribution σ this relation reduces to

$$\mathbf{j}_\sigma \perp N(\mathcal{W}), \quad (2.96)$$

and due to the continuity we additionally expect a good approximation $\mathbf{j}_{reg} \approx \mathbf{j}_\sigma$ for a conductivity distribution with small perturbations as for instance small non-conducting inclusions. Therefore,

$$\mathbf{j}_{reg,diff} := (\alpha\mathcal{I} + \mathcal{W}^*\mathcal{W})^{-1}\mathcal{W}^*(\mathbf{H}_2 - \mathbf{H}_1) \quad (2.97)$$

is an approximation of $\mathbf{j}_{ref} - \mathbf{j}_{fc}$ from (2.93) if \mathbf{j}_{ref} and \mathbf{j}_{fc} are current distributions based on a homogeneous conductivity and a conductivity with small inclusions, respectively.

Usually, we do not have a "perfect" fuel cell (or we do not know if the fuel cell is working perfectly), therefore we use another algorithm called *absolute reconstruction algorithm*. Again we have two measurements, for the reference measurement we replace the fuel cell by a conductor whose current distribution as well as its magnetic field \mathbf{B}_{sw} can be calculated and measured, respectively. We denote the calculated magnetic field by $\mathbf{H}_{sw,calc}$. Usually, we short-circuit the current injection points of the fuel cell by a straight wire. Then we obtain

$$\mathbf{B}_1(x) = \mathbf{B}_{earth}(x) + \mathbf{B}_{cs}(x) + \mathbf{B}_{fc}(x), \quad (2.98)$$

$$\mathbf{B}_2(x) = \mathbf{B}_{earth}(x) + \mathbf{B}_{cs}(x) + \mathbf{B}_{sw}(x), \quad (2.99)$$

and the magnetic field of the fuel cell can be calculated by

$$\mathbf{H}_{fc}(x) = \mathbf{H}_1(x) - \mathbf{H}_2(x) + \mathbf{H}_{sw,calc}(x) \quad (2.100)$$

where we assume $\mathbf{H}_{sw}(x) = \mathbf{H}_{sw,calc}(x)$.

Finally, we use the information about the free divergence of the current distribution as constraint for the minimization of the Tikhonov functional

$$\|\mathcal{W}\mathbf{j} - (\mathbf{H}_2 - \mathbf{H}_1)\|_{\mathbf{L}^2(B)} + \alpha\|\mathbf{j}\|_{\mathbf{L}^2(B)} \quad (2.101)$$

to gain a better approximation. We call this method *divergence-free Tikhonov regularization*. In detail, we have the linear constraint (the discretized divergence equation is the knot rule (2.84)) which can be expressed by

$$Aj = r \quad (2.102)$$

where j is the vector of currents $I_{klm\zeta}$ and r the right hand side which contains the incoming and outflowing currents. The general solution of this equation is

$$j = j_0 + N \cdot t \quad (2.103)$$

with a certain solution of (2.102) and a matrix N building a base of the nullspace of A . Inserting this result in the discretized Tikhonov regularization we obtain

$$(\alpha \cdot I + W^*W) \cdot Nt = W^*(H_2 - H_1) - (\alpha \cdot I + W^*W)j_0. \quad (2.104)$$

From the reconstructed t we calculate the current j via (2.103).

Current reconstruction from simulated data

For a given conductivity distribution we calculate the current distribution approximately as described in the previous paragraphs. Afterwards we calculate the magnetic field \mathbf{H} and the magnetic flux \mathbf{B} , respectively, on the shell surface of a cylinder that contains the stack. The Figure 2.2 shows the current distribution from Figure 2.1 and its magnetic field (red arrows) on the shell of a cylinder.

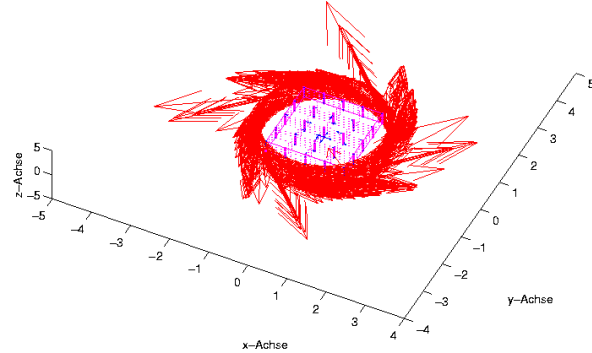


Figure 2.2: Magnetic field of a current distribution on the shell of a cylinder

Since the current is fed in at the base surface and taken from the top surface we are interested in the currents in the z -direction. Thus, we represent the currents I_{klmz} in the grid model as colored plots on the $n_3 - 1$ slices defined by the points p_{klm} for each $m = 0 \dots n_3 - 2$. Note that $I_{kl(n_3-1)}$ are the outflowing currents, and therefore, we do not represent them. In this way, the Figure 2.3 describes how the current I_z of a fuel cell with an electric insulation is represented by a colored plot on 3 slices. Here, the figure shows a difference reconstruction of $\mathbf{j}_{reg} - \mathbf{j}_{hom}$ where \mathbf{j}_{hom} is a current distribution based on a homogeneous conductivity distribution. Thus, the yellow color indicates areas of large currents in negative z -direction, red areas show small currents.

Figure 2.4 shows an example where we compare the simulated (on the left columns) with the reconstructed currents. For both images we used the same conductivity distribution function in \mathbb{R}^3 with one electric insulation close to one of the corner at the top surface. For the first image we took a $[5, 5, 5]$ grid, for the second a $[7, 7, 7]$ -grid. We added a noise of one percent to the calculated magnetic field data and took a regularization parameter $\alpha = 10^{-2}$. Both images reflect the characteristic area of lower currents which is the effect of the low conductivities in this area. In addition, both images have small artefacts at the base of the stack. Altogether, this example shows that we are able to reconstruct defect inclusions near the boundary of the stack.

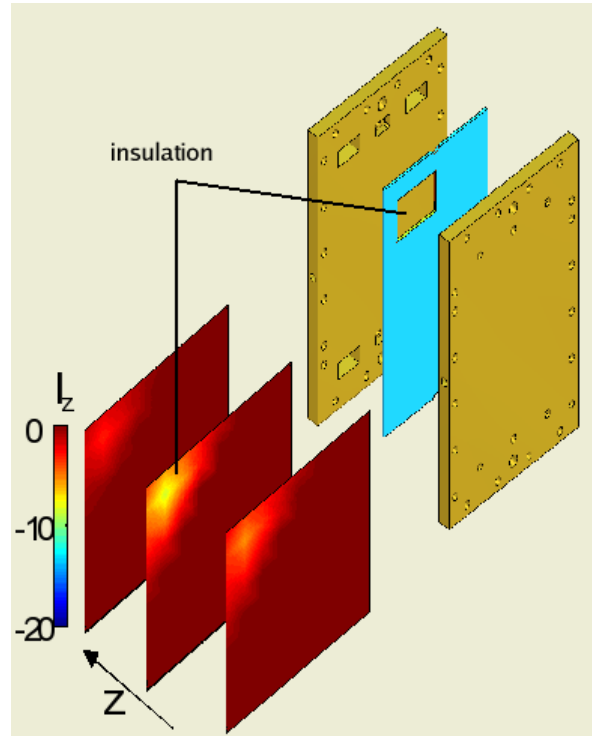


Figure 2.3: Our way of the current representation in 3d. Image by TomoScience GbR.

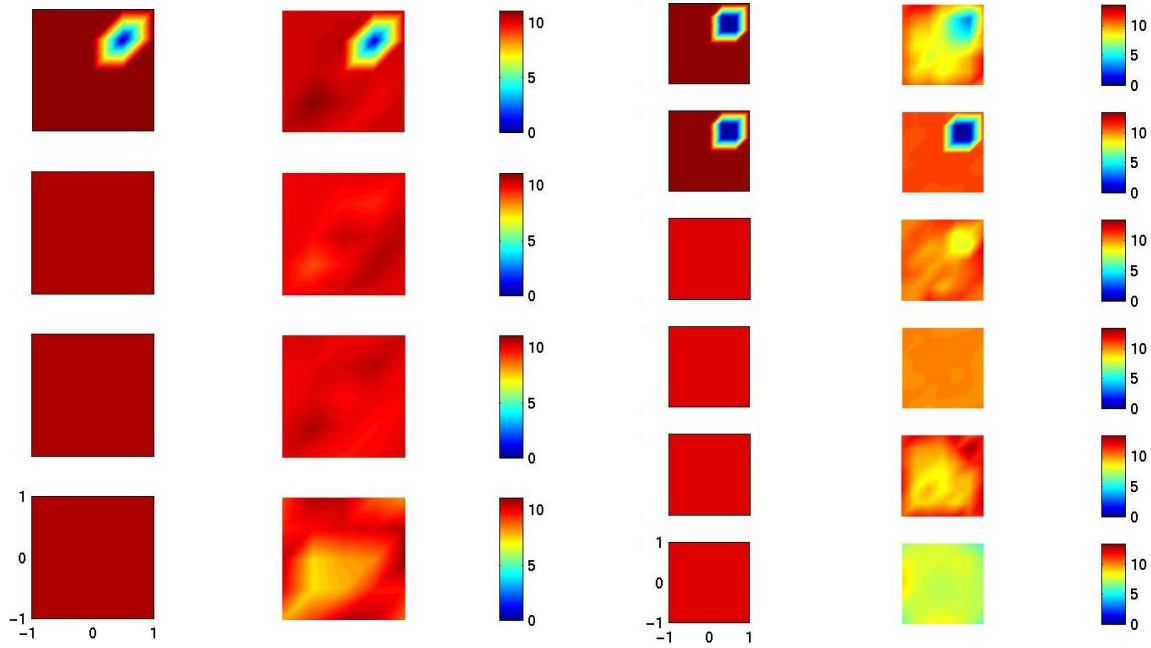
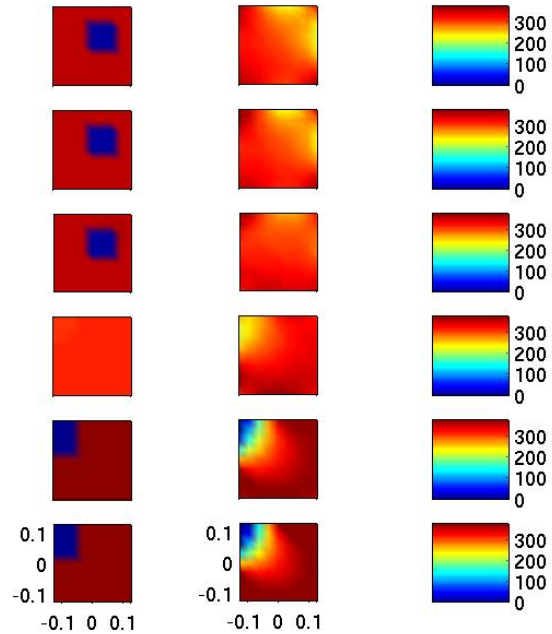


Figure 2.4: Simulated (left columns) and reconstructed current distributions for a $[5, 5, 5]$ grid (left side) and a $[7, 7, 7]$ grid.

In the next example we demonstrate that the reconstruction of an interior defect, i.e. a defect far from the boundary, is much more difficult. For the inverse problem of Figure 2.5 we added a noise of 0.001 to the magnetic field data and chose a regularization parameter $\alpha = 10^{-5}$. The conductivity distribution of this example is zero in two areas. The first area (blue colored in the lower slices) is close to the boundary whereas the second one (blue colored in the upper slices) is pretty far away from the boundary. The first defect is reconstructed pretty well as we can see in the right image of Figure 2.5 but the second defect is hardly recognizable. A larger data error would lead to a result which does not reflect the second defect. In addition, a larger parameter α would smooth the result and we get blurred images, whereas for a too small parameter typical artefacts would mask the defects.



A complete study on the influences of the grid size, the regularization parameter, the data error and the location of the defect inclusion can be found in the paper [KrKüPo].

Figure 2.5: Simulated (left) and reconstructed current distributions from data with a noise level of 0.001.

Reconstruction of currents in wire grids

Here, we get the magnetic field data from measurements of the magnetic flux. A measurement device can be seen in Figure 2.6. Thus, we have to care about problems such as calibration of the sensors, determination of a system of coordinates, adjustment of the fuel cells and wire grids, respectively, and the initialization of the measurement device. We do not deal these problems here and refer to [HPSW].

The left image of Figure 2.7 shows a self-made wire grid with a discretization of 3, 3, 2 points in x, y, z direction and the resistors of 1Ω along the z -wires. The magnetic field of the currents of the grid is calculated on points of the surface of a cuboid enclosing the wire grid (see the right image). For the simple discretization of $3 \times 3 \times 2$ knot points we calculated the magnetic field exactly, i.e. we do not use a cubature rule for the Biot-Savart operator. Instead we calculate the magnetic field part for each current $I_{klm\zeta}$ in the wire $s_{klm\zeta}$ and sum it up.

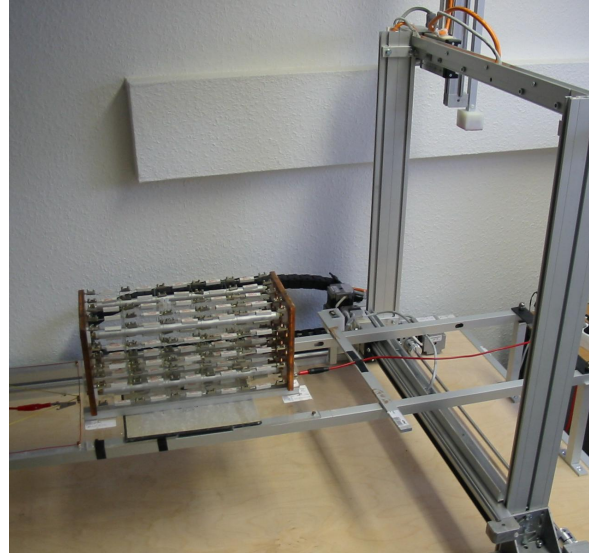


Figure 2.6: Wire grid with 125 resistors and $5 \times 5 \times 6$ knot points

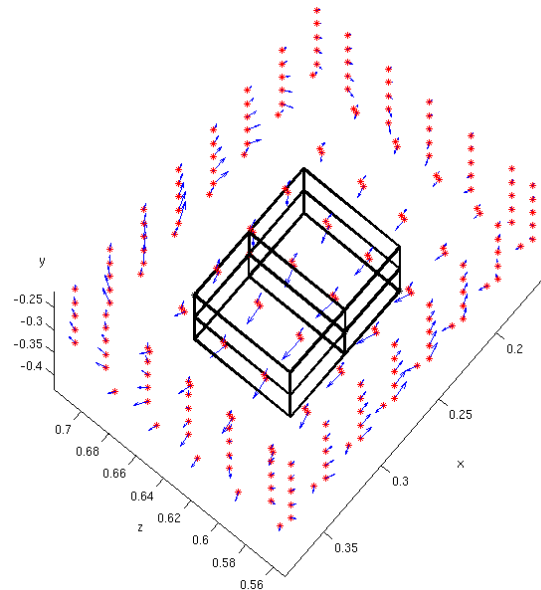
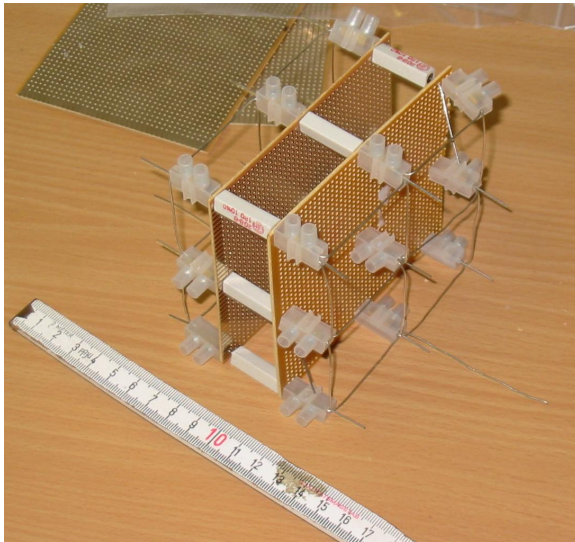


Figure 2.7: Wire grid with $3 \times 3 \times 2$ knot points and simulated magnetic field (red arrows)

We base the following example on the wire grid shown in Figure 2.7. Here, we use the absolute reconstruction algorithm as described above. We remove two of the resistors in

z -direction from the wire grid, inject a current of $6A$ at the base (it is the point p_{110} , the longer wire in the left image of Figure 2.7 indicates the position) and take it from the top surface of the wire grid (the opposite point of the injection point). Figure 2.8 compares the simulated currents I_{klmz} (left image) with the reconstructed currents.

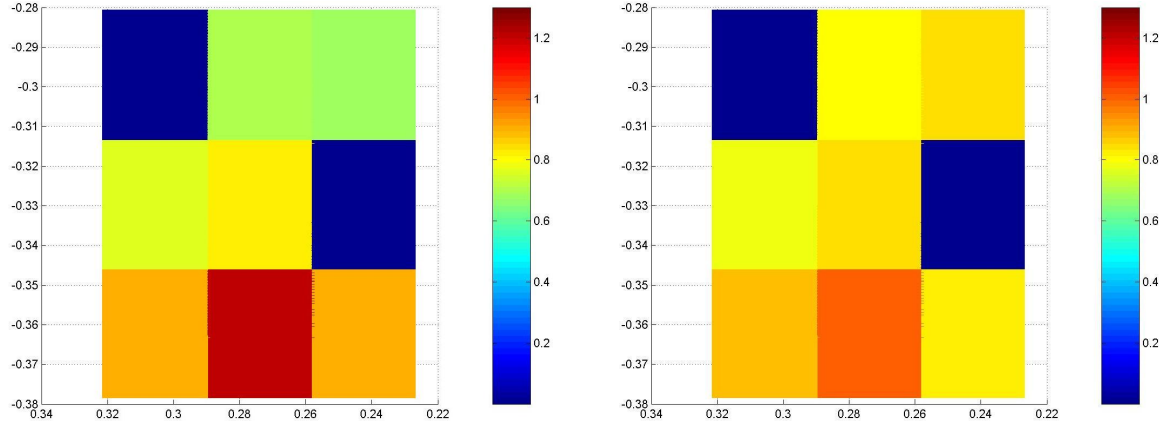


Figure 2.8: Simulated (left columns) and reconstructed current distributions in a wire grid with $3 \times 3 \times 2$ knot points and with two defects

For the second example we refer to the wire grid with 5, 5, 6 points in x, y, z direction and 125 resistors which is shown in Figure 2.6. Here, we use the difference reconstruction algorithm. As reference measurement we take the magnetic field data \mathbf{H}_1 of the current distribution which bases on the default isotropic conductivity distribution, i.e. all resistors in z -direction have a resistance of 1Ω . The red wire in the picture indicates the current supply of $40A$. Since the current supply is very large and the conductivities in z -direction are much smaller than in x, y -direction we achieve an almost homogeneous current distribution. For the second measurement we remove two of the resistors. The Figure 2.9 shows a comparison of the simulated difference current (left column) and the reconstructed one.

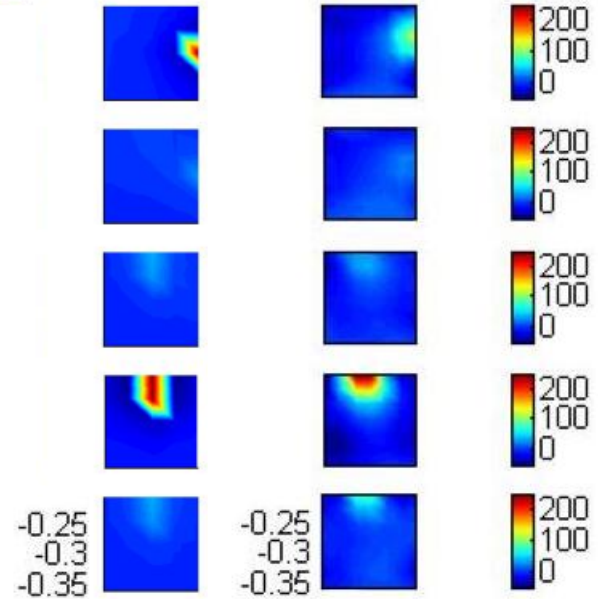


Figure 2.9: Comparison of a difference reconstruction (right) with the simulated z -currents

The two examples demonstrate that we are able to reconstruct defect inclusions in a wire grid from real measurement data. The difficulties of this method arise from the practical preparations of the measurement device (sensor calibration, system of coordinates, the exact replacement for the second

device)

measurement etc.) and the influence of data errors. Thus, as mentioned in the paragraph *Reconstruction of simulated currents* interior defects are hardly reconstructable, but we see that basically the reconstruction method works for real data.

Current reconstruction of a segmented fuel cell

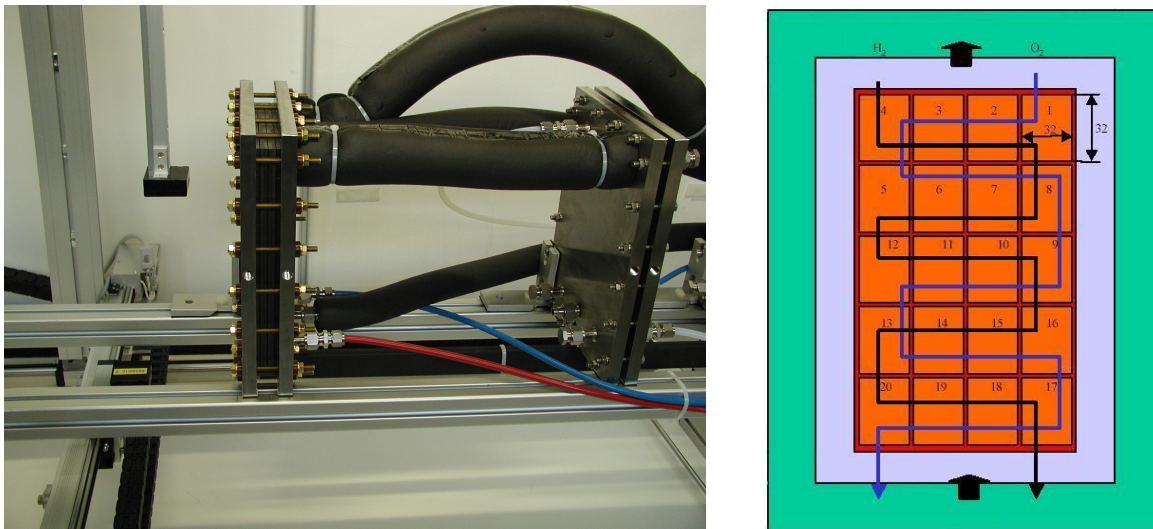


Figure 2.10: Fuel cell (left) and segmentation of the graphite layer

The left image of the Figure 2.10 shows a fuel cell in the measurement device. The black tubes are the supply pipes which provide the fuel cell with oxygen, hydrogen and take the water/steam away from the cell. The right image reflects the supply of the oxygen and hydrogen, the lines show the way of the gases through the cell. Moreover, it illustrates a segmentation into 20 segments which is the main idea of the *segmentation method*. Here, a graphite layer between the anode and cathode which usually carries the membrane with the catalyst is segmented into a number of segments. Further information as well as reconstruction results for real fuel cells can be found in [HPSW].

In the following "dummy" reconstructions -in contradiction to a real fuel cell- the current is not produced by the cell but injected. For these examples we again use the difference reconstruction algorithm.

First example: First, we take the segmented layer, feed a current of 73A into the cell, and measure the magnetic field of the resulting current distribution. Second, we cut off two segments such that these areas are non-conducting segments and measure the magnetic field. The left image of Figure 2.11 shows that we cut off the segments no. 7 and 20, i.e. we have an interior defect and a defect close to the boundary. For both situations we measure the currents of each segment. The difference of both currents is represented by the color-plot in the middle of Figure 2.11. The right image shows the difference reconstruction by the stabilized inversion.

As we can see both methods reflect the defects in general, but the interior defect is a

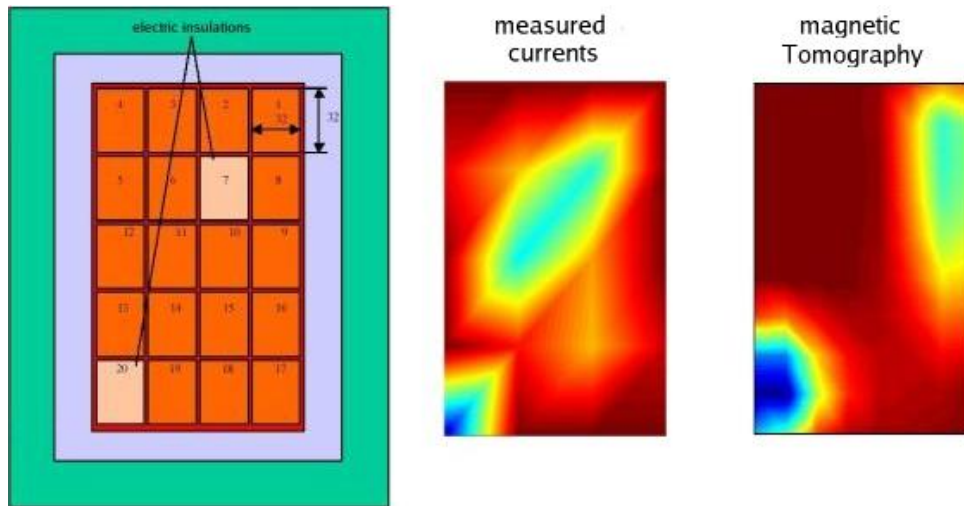


Figure 2.11: Segmented fuel cell (left), measured currents from the segmentation method and the reconstructed currents (right)

little bit out of place. Even for the segmentation method this defect is blurred. As we mentioned in the introduction, we are not sure whether the segmented fuel cell do behave like a real fuel cell and it is not clear today if the segmentation method do reflect the true currents in a fuel cell.

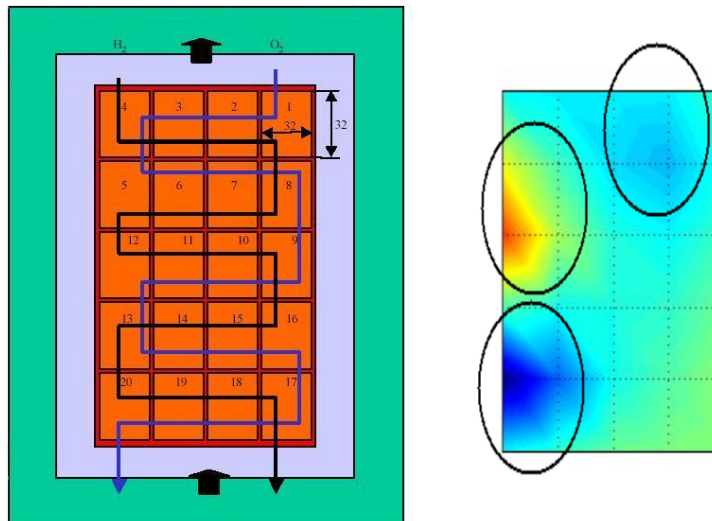


Figure 2.12: Difference reconstruction where the graphite layer has defects at segments 2, 13 and 5 respectively

Second example: In the first situation we take the segmented layer with defect segments no. 2 and 13. For the second situation we cut off the segment 5. We reconstruct the current of the difference of the magnetic fields $\mathbf{H}_1 - \mathbf{H}_2$. The reconstruction in Figure 2.12 shows the three defects with the right sign.

2.4 Exterior Field Calculation from Boundary Data

As the last basic question for magnetic tomography we asked

6. How much data do we need to measure on ∂G to uniquely determine the magnetic field \mathbf{H} in the exterior B^e ?

Here, we will investigate three different settings, where different types of data are measured on some surface $\partial G \in C^2$ surrounding the domain B .

For practical applications of magnetic tomography it is important to reduce the number of measurements and the number of different field components which are measured. In our first setting we need to know three scalar functions. Our second and third settings require less information in the sense that we need to measure two scalar functions on the boundary.

First setting: full magnetic field $\mathbf{H}|_{\partial G}$. We assume the knowledge of the boundary values $(\mathcal{W}\mathbf{j})|_{\partial G}$. The relations $\text{curl } \mathcal{W}\mathbf{j} = -\mathcal{S}^\nabla \mathbf{j}$ from (2.9) and $\text{curl } \text{curl } \mathcal{W}\mathbf{j} = -\Delta \mathcal{W}\mathbf{j} + \text{grad } \text{div } \mathcal{W}\mathbf{j}$ imply $\Delta \mathcal{W}\mathbf{j} = \mathbf{0}$, i.e. $\mathcal{W}\mathbf{j}$ has harmonic components in B^e . Together with the analyticity and the decay at infinity, we have an exterior Dirichlet problem for classical harmonic functions in G^e for every magnetic field component. This problem is uniquely solvable and the magnetic field is uniquely determined in G^e by its boundary values on ∂G .

Second setting: normal component $\nu \cdot \mathbf{H}|_{\partial G}$ and current flux $\nu \cdot \mathbf{j}|_{\partial B}$. We assume that we know the current flux $f := \nu \cdot \mathbf{j}|_{\partial B}$ and the flux of the magnetic field $h := \nu \cdot (\mathcal{W}\mathbf{j})|_{\partial G}$. We consider the following boundary value problem

BVP 10 (An exterior problem with Neumann condition) Let $\partial G \in C^2$. For some given $f \in L^2_\circ(\partial B)$ and $h \in L^2(\partial G)$

$$\text{find } \mathbf{u} \in \mathbf{C}^1(G^e) \text{ such } \begin{cases} \text{curl } \mathbf{u} = \text{grad } \mathcal{S}f & \text{in } G^e, \\ \text{div } \mathbf{u} = 0 & \text{in } G^e, \\ \nu \cdot \mathbf{u} = h & \text{on } \partial G, \\ \mathbf{u}(x) \rightarrow \mathbf{0} & |x| \rightarrow \infty. \end{cases} \quad (2.105)$$

Theorem 2.21 *The boundary value problem (2.105) admits an unique solution.*

Proof: To prove the uniqueness, let \mathbf{u} be the difference of two solutions, then \mathbf{u} is a harmonic vector field with vanishing normal component on ∂B . Theorem 1.35 together with Remark 1.36 implies that \mathbf{u} must be zero.

A solution of boundary value problem (2.105) may be constructed as follows. Let \mathbf{j}_f be a solution of

$$\begin{cases} \text{curl } \mathbf{j}_f = \mathbf{0}, & \text{div } \mathbf{j}_f = 0, & \text{in } B, \\ \gamma_\nu[B]\mathbf{j}_f = f & & \text{on } \partial B, \end{cases}$$

which is in fact the interior normal problem for harmonic vector fields with boundary data f and admits an solution \mathbf{j}_f , see Theorem 1.34. A solution of the exterior normal problem for harmonic vector fields with boundary data $h + \nu \cdot \mathcal{W}\mathbf{j}_f \in L^2(\partial G)$ is given by $\text{grad } \mathcal{S}\phi$ with density $\phi \in L^2(\partial G)$ defined by

$$\phi = -2(\mathcal{I} - \mathcal{K}^*)^{-1}(h + \nu \cdot \mathcal{W}\mathbf{j}_f). \quad (2.106)$$

For the proof we refer to Theorem A.25. Now, $\mathbf{u} = \text{grad } \mathcal{S}\phi - \mathcal{W}\mathbf{j}_f$ solves (2.105) which can be verified by

$$\begin{aligned} \text{div } \mathbf{u} &= \Delta \mathcal{S}\phi - \text{div } \mathcal{W}\mathbf{j}_f = 0, \\ \text{curl } \mathbf{u} &= -\text{curl } \mathcal{W}\mathbf{j}_f = \mathcal{S}^\nabla \mathbf{j}_f = \text{grad } \mathcal{S}(\nu \cdot \mathbf{j}_f) = \text{grad } \mathcal{S}f, \\ \nu \cdot \mathbf{u} &= \partial_\nu [G^e] \mathcal{S}\phi - \nu \cdot \mathcal{W}\mathbf{j}_f \stackrel{(A.29)}{=} \frac{1}{2}(\mathcal{K}^* - \mathcal{I})\phi - \nu \cdot \mathcal{W}\mathbf{j}_f \\ &= (h + \nu \cdot \mathcal{W}\mathbf{j}_f) - \nu \cdot \mathcal{W}\mathbf{j}_f = h. \end{aligned}$$

Moreover, the field \mathbf{u} has the required behavior at infinity. ■

Third setting: tangential components $\nu \times \mathbf{H}|_{\partial G}$. For the third way of constructing the magnetic field we assume to know the tangential component $\mathbf{h} := \nu \times (\mathcal{W}\mathbf{j})|_{\partial G}$. From $\Delta \mathcal{W}\mathbf{j} = \mathbf{0}$ and $\text{div } \mathcal{W}\mathbf{j} = 0$ we have to solve the exterior problem: For some given field $\mathbf{h} \in \mathbf{L}_{t, \text{DIV}}^2(\partial G)$

$$\text{find } \mathbf{u} \in \mathbf{C}^2(G^e) \text{ such } \begin{cases} \text{curl curl } \mathbf{u} = \mathbf{0} & \text{in } G^e, \\ \text{div } \mathbf{u} = 0 & \text{in } G^e, \\ \nu \times \mathbf{u} = \mathbf{h} & \text{on } \partial G, \\ \mathbf{u}(x) \rightarrow \mathbf{0} & |x| \rightarrow \infty, \\ \int_{\partial G} \nu \cdot \mathbf{u} \, ds = 0, \end{cases} \quad (2.107)$$

which is in fact the classical exterior Maxwell problem (A.50) we investigate in Section A.4.

Theorem 2.22 *The boundary value problem (2.107) admits an unique solution.*

Proof: A solution is given by $\text{curl } \vec{\mathcal{S}}\mathbf{b}$ with $\mathbf{b} := 2(\mathcal{I} + \mathcal{M})^{-1}\mathbf{h}$. For the proof we refer to Corollary A.31. The proof of uniqueness is much longer. We use Green's first vector identity to a domain which is the intersection of G^e and a ball B_R with sufficiently large radius R

$$\int_{G^e \cap B_R} \mathbf{u} \cdot \Delta \mathbf{v} + \text{curl } \mathbf{u} \cdot \text{curl } \mathbf{v} + \text{div } \mathbf{u} \text{ div } \mathbf{v} \, dx = \int_{\partial(G^e \cap B_R)} \nu \cdot \mathbf{u} \text{ div } \mathbf{v} + \nu \times \mathbf{u} \cdot \text{curl } \mathbf{v} \, ds. \quad (2.108)$$

We apply this relation to a solution \mathbf{u} of the corresponding homogeneous problem (2.107) and obtain

$$\int_{G^e \cap B_R} |\operatorname{curl} \mathbf{u}|^2 dx = \int_{\partial B_R} \nu \times \mathbf{u} \cdot \operatorname{curl} \mathbf{u} ds. \quad (2.109)$$

Since the field \mathbf{u} has harmonic components, we use the asymptotic behavior (1.109) together with the condition $\mathbf{u}(x) \rightarrow \mathbf{0}, |x| \rightarrow \infty$ to derive the stronger decay $\mathbf{u} = O(|x|^{-1})$. Moreover, the partial derivatives decays by $O(|x|^{-2})$. Thus, we get $\nu \times \mathbf{u} \cdot \operatorname{curl} \mathbf{u} = O(|x|^{-3}), |x| \rightarrow \infty$. We let R tend to infinity in equation (2.109) and obtain

$$\int_{G^e} |\operatorname{curl} \mathbf{u}|^2 dx = 0,$$

from where $\operatorname{curl} \mathbf{u} = \mathbf{0}$ follows, i.e. \mathbf{u} is a harmonic field. Now, let q be the scalar potential of \mathbf{u} with $\mathbf{u} = \operatorname{grad} q$. It is a harmonic function and unique up to a constant. Due to the behavior of harmonic functions we may choose q such that it vanishes at infinity. The homogeneous boundary condition $\nu \times \operatorname{grad} q = \mathbf{0}$ implies $\gamma_0[G^e]q \equiv c$ on ∂G with a $c \in \mathbb{R}$. Finally, an application of Green's first identity

$$\int_{G^e \cap B_R} |\operatorname{grad} q|^2 dx = \int_{\partial(G^e \cap B_R)} q \frac{\partial q}{\partial \nu} ds = -c \int_{\partial G} \nu \cdot \mathbf{u} ds + \int_{\partial B_R} q \frac{\partial q}{\partial \nu} ds = \int_{\partial B_R} q \frac{\partial q}{\partial \nu} ds \quad (2.110)$$

together with the asymptotics of harmonic functions (1.109), (1.110) yields $\mathbf{u} = \operatorname{grad} q = \mathbf{0}$. ■

Each of the three settings provides a way to determine the magnetic field in the exterior of the domain G by measurement data on ∂G and ∂B , respectively. Moreover, since $\mathcal{W}\mathbf{j}$ is analytic in B^e , it is just uniquely determined in all of B^e . Of course, all results are true if B and G coincides, but often in praxis the magnetic field components are measured on a different measurement surface.

Comparing the three methods, the first one assumes overdetermined data. On the one hand this increases the measurement cost but on the other hand overdetermined measurement data lead to a more stabilized calculation of the magnetic field. The second method provides a very efficient way of calculation. In our experiments, the current flux $\nu \cdot \mathbf{j}$ was given by the measurement device (in detail, by two points the current flowed out of and into the fuel cell). Therefore, for different fuel cells, we just need to measure the normal component of the magnetic field on a previously defined surface (mostly the surface of a cuboid). The third method is a theoretical example from which we will show that the current flux can be calculated from the magnetic field, i.e. $\nu \cdot \mathbf{j}|_{\partial B}$ and $\nu \times (\mathcal{W}\mathbf{j})|_{\partial B}$ are redundant information.

Theorem 2.23 *Let $\partial B \in C^2$. Furthermore, let $\mathbf{j} \in \mathbf{H}_{\operatorname{div}=0}(B)$ be a current distribution and \mathbf{a} the unique solution of the integral equation $(\mathcal{I} + \mathcal{M})\mathbf{a} = 2\nu \times (\mathcal{W}\mathbf{j})|_{\partial B}$. Then, the*

relation

$$\operatorname{DIV} \mathbf{a} = -\nu \cdot \mathbf{j} \quad (2.111)$$

is satisfied.

Proof: Let $\mathbf{j} \in \mathbf{H}_{\operatorname{div}=0}(B)$. From $\mathcal{V} : L^2(B) \rightarrow H^2(B)$ follows $\mathcal{W}\mathbf{j} \in \mathbf{H}^1(B)$. Consequently, we have $\nu \times \mathcal{W}\mathbf{j} \in \mathbf{H}_t^{1/2}(\partial B)$. In particular, $\gamma_{\times}[B^e]\mathcal{W}\mathbf{j} = \gamma_{\times}[B]\mathcal{W}\mathbf{j}$ is an element of $\mathbf{L}_t^2(\partial B)$. Now, let $\mathbf{a} \in \mathbf{L}_t^2(\partial B)$ be the unique solution of $(\mathcal{I} + \mathcal{M})\mathbf{a} = 2\nu \times (\mathcal{W}\mathbf{j})|_{\partial B}$. The fields $\mathcal{W}\mathbf{j}$ and $\operatorname{curl} \vec{\mathcal{S}}\mathbf{a}$ have free divergence, satisfy $\Delta \mathcal{W}\mathbf{j} = \mathbf{0}$ and $\Delta \operatorname{curl} \vec{\mathcal{S}}\mathbf{a} = \mathbf{0}$ in B^e , and vanish at infinity. From the jump relation (A.57) we derive $\nu \times \operatorname{curl} \vec{\mathcal{S}}\mathbf{a} = \nu \times \mathcal{W}\mathbf{j}$. Altogether, $\mathcal{W}\mathbf{j}$ and $\operatorname{curl} \vec{\mathcal{S}}\mathbf{a}$ fulfill the assumptions of the exterior Maxwell problem (2.107) with boundary data $\nu \times (\mathcal{W}\mathbf{j})|_{\partial B}$. Its unique solvability implies that both fields must agree, i.e.

$$\mathcal{W}\mathbf{j} = \operatorname{curl} \vec{\mathcal{S}}\mathbf{a} \quad \text{in } B^e.$$

From (2.9) we have $\operatorname{curl} \mathcal{W}\mathbf{j} = -\mathcal{S}^\nabla \mathbf{j} = -\operatorname{grad} \mathcal{S}(\nu \cdot \mathbf{j})$. With the aid of the formula $\operatorname{curl} \operatorname{curl} = -\Delta + \operatorname{grad} \operatorname{div}$ we get

$$\operatorname{curl} \operatorname{curl} \vec{\mathcal{S}}\mathbf{a} = \operatorname{grad} \operatorname{div} \mathcal{S}\mathbf{a} = \operatorname{grad} \mathcal{S}(\operatorname{DIV} \mathbf{a}).$$

Putting both equations together we obtain

$$-\operatorname{grad} \mathcal{S}(\nu \cdot \mathbf{j}) = \operatorname{grad} \mathcal{S}(\operatorname{DIV} \mathbf{a}) \quad \text{in } B^e.$$

or equivalent

$$\operatorname{grad} \mathcal{S}(\operatorname{DIV} \mathbf{a} + \nu \cdot \mathbf{j}) = \mathbf{0}. \quad (2.112)$$

Hence, the single layer potential $\mathcal{S}(\operatorname{DIV} \mathbf{a} + \nu \cdot \mathbf{j})$ must be constant in B^e . The behavior at infinity shows this constant to be zero. Therefore, $\mathcal{S}(\operatorname{DIV} \mathbf{a} + \nu \cdot \mathbf{j}) = 0$ on ∂B . The injectivity of \mathcal{S} completes the proof. \blacksquare

Corollary 2.24 *Let $\mathbf{j} \in \mathbf{H}_{\operatorname{div}=0}(B)$ and $\mathbf{h} := \nu \times (\mathcal{W}\mathbf{j})|_{\partial B}$. Then we have*

$$\nu \cdot \mathbf{j} = -2(\mathcal{I} - \mathcal{K}^*)^{-1} \operatorname{DIV} \mathbf{h}. \quad (2.113)$$

Proof: From Theorem 2.23 we know that the solution \mathbf{a} of $(\mathcal{I} + \mathcal{M})\mathbf{a} = 2\nu \times (\mathcal{W}\mathbf{j})|_{\partial B}$ satisfies $\operatorname{DIV} \mathbf{a} = -\nu \cdot \mathbf{j}$. Building the surface divergence we obtain

$$\operatorname{DIV} \mathbf{a} + \operatorname{DIV} (\mathcal{M}\mathbf{a}) = 2 \operatorname{DIV} \mathbf{h}. \quad (2.114)$$

Using $\operatorname{DIV} (\mathcal{M}\mathbf{a}) = -\mathcal{K}^* \operatorname{DIV} \mathbf{a}$ we derive

$$(\mathcal{I} - \mathcal{K}^*) \operatorname{DIV} \mathbf{a} = 2 \operatorname{DIV} \mathbf{h}. \quad (2.115)$$

In the proof of Theorem 2.23 we have shown $\nu \times \mathcal{W}\mathbf{j} \in \mathbf{H}_t^{1/2}(\partial B)$, therefore $\operatorname{DIV} \mathbf{h} \in H^{-1/2}(\partial B)$. Since the double layer potential operator \mathcal{D}^* maps $H^{-1/2}(\partial B)$ continuously

into $H^{1/2}(\partial B)$ and the imbedding from $H^{1/2}(\partial B)$ into $H^{-1/2}(\partial B)$ is compact, the operator \mathcal{K}^* is a compact operator on $H^{-1/2}(\partial B)$. Then we have $N(\mathcal{I} - \mathcal{K}^*) = \{0\}$ (the proof of Theorem A.21 holds for $\mathcal{K} : H^{1/2}(\partial B) \rightarrow H^{1/2}(\partial B)$ and $\mathcal{K}^* : H^{-1/2}(\partial B) \rightarrow H^{-1/2}(\partial B)$ together with the jumps from Theorem A.14). Now, we derive the statement by applying the operator $(\mathcal{I} - \mathcal{K}^*)^{-1}$ and inserting the result $\text{DIV } \mathbf{a} = -\nu \cdot \mathbf{j}$. ■

Chapter 3

Magnetic Impedance Tomography

Chapter 2 has treated the magnetic tomography problem by an inversion of the Biot-Savart integral operator. We have seen that this problem is not uniquely solvable and, in particular, the magnetic field in the exterior does not uniquely determine currents in the interior of the domain B under consideration. A natural next step is to ask what further input data or measurements, respectively, are reasonable to use to obtain more information about inhomogeneities of the underlying conductivity distribution.

For the fuel cell application, usually it is a standard procedure to measure the potential on the surface of different graphit plates. Thus, the input data

$$\nu \times \mathbf{E}|_{\partial B} \tag{3.1}$$

are natural and practically realizable measurements. In Subsection 2.4 we have shown that the normal component $\nu \cdot \mathbf{j}$ is already determined by the magnetic field \mathbf{H} in B^e . This is not the case for the electrical potential $\nu \times \mathbf{E}$ on ∂B , as can be seen from the following Section 3.1.

To start the investigation with the simplest case, in this chapter we consider piecewise constant conductivities, in particular, we investigate one inclusion or defect D inside the homogeneous ohmic conductor B . The inclusion domain D has non-negative conductivity σ_D whereas the conductivity of B denoted by σ_B is positive and known, i.e. we define the conductivity distribution $\sigma \in L^2(B)$ by

$$\sigma(x) = \begin{cases} \sigma_D & x \in D, \\ \sigma_B & x \in B \setminus \overline{D}. \end{cases} \tag{3.2}$$

The electric field \mathbf{E} in the domain B solves the equations

$$\operatorname{curl} \mathbf{E} = \mathbf{0}, \quad \operatorname{div}(\sigma \mathbf{E}) = 0, \tag{3.3}$$

which follow from Maxwell's equation $\operatorname{curl} \mathbf{E} = \mathbf{0}$, $\operatorname{curl} \mathbf{H} = \mathbf{j}$ and Ohm's law $\mathbf{j} = \sigma \mathbf{E}$. Together with the boundary values $\mathbf{e} = \nu \times \mathbf{E}|_{\partial B}$, the electric field is a solution of the

boundary value problem: For given $\mathbf{e} \in \mathbf{L}_{t, \text{DIV}=0}^2(\partial B)$

$$\text{find } \mathbf{E} \in \mathbf{H}_{\text{div}}(B) \cap \mathbf{H}_{\text{curl}}(B) \text{ such } \begin{cases} \text{curl } \mathbf{E} = \mathbf{0} & \text{in } B, \\ \text{div}(\sigma \mathbf{E}) = 0 & \text{in } B, \\ \nu \times \mathbf{E} = \mathbf{e} & \text{on } \partial B. \end{cases} \quad (3.4)$$

The goal of the Section 3.1 is to calculate the electric field determined by (3.4) where we adapt the general problem (3.4) according to both cases of inclusion. In the case of a conducting inclusion D , i.e. $\sigma_D > 0, \sigma_D \neq \sigma_B$, the problem (3.4) leads to a boundary value problem with boundary condition of *transmission* type on ∂D . This case is investigated in Subsection 3.1.1. The case of a defect D , i.e. $\sigma_D = 0$, leads to a boundary condition of *Neumann* type and its solution is presented in Subsection 3.1.2.

The representation of the magnetic field for the case of piecewise constant conductivity

$$\begin{aligned} \mathcal{W}\mathbf{j} &= (\sigma_B - \sigma_D) \vec{\mathcal{S}}_D(\nu \times \mathbf{E}) - \sigma_B \vec{\mathcal{S}}_B(\nu \times \mathbf{E}) \\ &= \vec{\mathcal{S}}_D(\nu^+ \times \mathbf{j} - \nu^- \times \mathbf{j}) - \vec{\mathcal{S}}_B(\nu \times \mathbf{j}) \end{aligned} \quad (3.5)$$

will be derivated in Subsections 3.1.1 and 3.1.2 below. The representation also reflects the importance of the boundary data $\nu \times \mathbf{E}$, which completes the magnetic measurements \mathbf{H} – similar to the Cauchy data u and $\partial u / \partial \nu$ for the acoustic case.

There is an impressive number of different algorithms for shape reconstruction in inverse problems, see for example the books [ColtonKress], [Potthast] and the survey article [Sampling and probe methods - an algorithmical view]. Here, we will use two algorithms and adapt them to the framework of magnetic tomography. We will base both methods on the representation formula of the magnetic field (3.5) as a sum of two single layer potentials, one over ∂B with the known input data $\nu \times \mathbf{j} = \sigma_B \mathbf{e}$ and one over the unknown boundary ∂D with an unknown density.

In Section 3.2 we employ the *point source method* for the field reconstruction. The point source method has been developed by Potthast (see [Po1],[ErPo]) since 1996. We follow a recent approach to the point source method due to Liu, Potthast and Nakamura (see [ErPo]). With the aid of this approach we are able to reconstruct the magnetic field in some subset of B independent of the type of the inclusion D but we are not able to use the magnetic field to reconstruct the inclusion D which is possible for the case of a sound-hard scatterer in [ErPo].

In Section 3.3 we employ the *no response test* for the domain reconstruction. The no response test has been introduced by Luke and Potthast [LuPo] in 2003. We adapt the basic idea and describe two approaches of the no response test, a global search strategy for the detection of the location of D and a local search strategy for the shape reconstruction of D .

3.1 A Homogeneous Conductor with one Inclusion

As a motivation we consider the following situation. The conductor B contains an inclusion D with conductivity $\sigma_D \in \mathbb{R}^+ \cup \{0\}$. We prescribe a voltage on ∂B and want to calculate how the current distributes in B . The underlying equation can be derived from $\operatorname{div} \mathbf{j} = 0$, Ohm's law $\mathbf{j} = \sigma \mathbf{E}$ and the first of Maxwell's equations of magnetostatic $\operatorname{curl} \mathbf{E} = \mathbf{0}$. Together with the boundary condition $\mathbf{j} = \sigma_B \mathbf{e}$ on ∂B and the conductivity distribution $\sigma \in L^2(B)$ defined in (3.2) we have to solve the boundary value problem (3.4) which we call the *generalized transmission problem for the impedance equation* for $\sigma_D \in \mathbb{R}^+ \cup \{0\}$.

We do not consider the superconducting case where the electric resistance σ_D^{-1} vanishes. Without any detailed explanation of the physical behavior we state that the electric field as well as the current distribution vanish in D . Additionally, we have to introduce a surface current distribution \mathbf{J}_D . From the complementary principle we derive $\operatorname{DIV} \mathbf{J}_D = \gamma_\nu[D^e] \mathbf{j}$. The magnetic field of the coupled volume and surface current distribution is given by

$$\mathcal{W} \mathbf{j} = \operatorname{curl} \int_{\partial D} \Phi(x, y) \mathbf{J}_D ds(y) + \operatorname{curl} \int_B \Phi(x, y) \mathbf{j}(y) dy \quad (3.6)$$

$$= \operatorname{curl} \vec{\mathcal{S}}_D \mathbf{J}_D + \vec{\mathcal{S}}_D (\gamma_\times[D^e] \mathbf{j}) - \vec{\mathcal{S}}_B (\sigma_B \mathbf{e}). \quad (3.7)$$

Since our reconstruction algorithms are based on a formula in the shape of (3.5), we do not consider the case of a superconducting inclusion in this work.

From the generalized transmission problem (3.4) we derive two conclusions. First, we show that the normal component $\nu \cdot \mathbf{j}|_{\partial D}$ is continuous, i.e.

$$\nu^+ \cdot \mathbf{j} = \nu^- \cdot \mathbf{j} \quad \text{or} \quad \sigma_D \gamma_\nu[D] \mathbf{E} = -\sigma_B \gamma_\nu[D^e] \mathbf{E}. \quad (3.8)$$

For the proof we have $\mathbf{j} \in \mathbf{H}_{\operatorname{div}}(B)$. Let $f \in H^{\frac{1}{2}}(\partial D)$, then there exist $\phi^+ \in H^1(B \setminus \overline{D})$ vanishing on ∂B and $\phi^- \in H^1(D)$ such that $\gamma_0[D^e] \phi^+ = f$ and $\gamma_0[D] \phi^- = f$ due to the trace theorem (1.16). The function ϕ defined by

$$\phi(x) := \begin{cases} \phi^+(x) & \text{if } x \in B \setminus \overline{D} \\ \phi^-(x) & \text{if } x \in D \end{cases} \quad (3.9)$$

belongs to $H_0^1(B)$ since ϕ vanishes on ∂B and the function and its first partial differentials belong to $L^2(B)$. Hence, we have $\operatorname{div}(\phi \mathbf{j}) \in L^2(B)$, and with the aid of Gauss divergence theorem

$$\begin{aligned} \int_{\partial D} f(\gamma_\nu[D] \mathbf{j} + \gamma_\nu[D^e] \mathbf{j}) ds &= \int_D \operatorname{div}(\phi^- \mathbf{j}) dx + \int_{B \setminus \overline{D}} \operatorname{div}(\phi^+ \mathbf{j}) dx \\ &= \int_B \operatorname{div}(\phi \mathbf{j}) dx \\ &= \int_{\partial B} \phi \nu \cdot \mathbf{j} dx = 0. \end{aligned}$$

This equation holds in the sence of dual system $\langle H^{\frac{1}{2}}(\partial D), H^{-\frac{1}{2}}(\partial D) \rangle$ for each $f \in H^{\frac{1}{2}}(\partial D)$, consequently $\gamma_\nu[D]\mathbf{j} + \gamma_\nu[D^e]\mathbf{j} = 0$.

Second, we show that the tangential component $\nu \times \mathbf{E}|_{\partial D}$ is continuous in the sence of

$$\nu^+ \times \mathbf{E} = \nu^- \times \mathbf{E} \quad \text{or} \quad \gamma_\times[D]\mathbf{E} = -\gamma_\times[D^e]\mathbf{E}. \quad (3.10)$$

For the proof we consider some field $\mathbf{v} \in \mathbf{H}^{\frac{1}{2}}(\partial B)$. Then there exist fields $\mathbf{w}^+ \in \mathbf{H}^1(B \setminus \overline{D})$ vanishing on ∂B and $\mathbf{w}^- \in \mathbf{H}^1(D)$ such that $\gamma_0[D^e]\mathbf{w}^+ = \gamma_0[D]\mathbf{w}^- = \mathbf{v}$. Then the field \mathbf{w} defined by

$$\mathbf{w}(x) := \begin{cases} \mathbf{w}^+(x) & \text{if } x \in B \setminus \overline{D} \\ \mathbf{w}^-(x) & \text{if } x \in D \end{cases} \quad (3.11)$$

belongs to $\mathbf{H}_0^1(B)$. We observe $\operatorname{div}(\mathbf{E} \times \mathbf{w}) = \mathbf{E} \operatorname{curl} \mathbf{w} \in \mathbf{L}^2(B)$ and

$$\begin{aligned} \int_{\partial D} \mathbf{v} \cdot (\gamma_\times[D]\mathbf{E} + \gamma_\times[D^e]\mathbf{E}) ds &= \int_{\partial D} \mathbf{v} \cdot \gamma_\times[D]\mathbf{E} ds + \int_{\partial D} \mathbf{v} \cdot \gamma_\times[D^e]\mathbf{E} ds \\ &= \int_D \operatorname{div}(\mathbf{E} \times \mathbf{w}^-) dx + \int_{B \setminus \overline{D}} \operatorname{div}(\mathbf{E} \times \mathbf{w}^+) dx \\ &= \int_B \operatorname{div}(\mathbf{E} \times \mathbf{w}) dx \\ &= \int_B \nu \cdot (\mathbf{E} \times \mathbf{w}) ds = 0, \end{aligned}$$

consequently $\gamma_\times[D]\mathbf{E} + \gamma_\times[D^e]\mathbf{E} = \mathbf{0}$.

In the next two subsection we redefine the general transmission boundary problem (3.4) due to the transmission condition (3.8). For $\sigma_D \in \mathbb{R}^+ \setminus \{\sigma_B\}$ we will transform the problem in Subsection 3.1.1 with the aid of the scalar potential u of \mathbf{E} into a boundary value problem for the impedance equation. For $\sigma_D = 0$ the transmission condition (3.8) reduces to the Neumann condition $\nu^+ \cdot \mathbf{j} = 0$ which we treat in Subsection 3.1.2. With respect to the Lipschitz continuous boundary ∂D we show uniqueness and existence of both problems. Further, we calculate the magnetic field of the resulting current distribution. Finally, Subsection 3.1.3 shows the numerical implementation of the problems where we make use of the FEM-solver FEMLAB.

3.1.1 Transmission Boundary Condition

Here, the conductivity distribution $\sigma \in L^2(\partial B)$ defined by (3.2) is strict positive since $\sigma_D, \sigma_B \in \mathbb{R}^+$. With the electrostatic potential u with $\mathbf{E} = \operatorname{grad} u$ the generalized transmission problem (3.4) reduces to the following boundary value problem:

BVP 11 (Impedance equation with transmission and tangential condition)

Let $\partial D \in C^{0,1}$, $\partial B \in C^2$. For some given $\mathbf{e} \in \mathbf{L}_{t, \text{DIV}=0}^2(\partial B)$

$$\text{find } u \in H^1(B) \text{ such } \begin{cases} \operatorname{div}(\sigma \operatorname{grad} u) = 0 & \text{in } B, \\ \gamma_{\times} \operatorname{grad} u = \mathbf{e} & \text{on } \partial B. \end{cases} \quad (3.12)$$

Theorem 3.1 *A solution $u \in H^1(B)$ of problem (3.12) is uniquely determined up to a constant.*

Proof: Let u_1, u_2 be two solutions of (3.12), then $u := u_2 - u_1$ solves the corresponding homogeneous problem. Since $\bar{D} \subset B$ we have

$$\Delta u = 0 \quad (3.13)$$

in a neighborhood of ∂B . From the homogeneous boundary data we have $\operatorname{GRAD} u = \mathbf{0}$ on ∂B which implies $u|_{\partial B} = c$ for a $c \in \mathbb{R}$. Now, the function u solves the elliptic problem

$$\text{find } u \in H^1(B) \text{ such } \begin{cases} \operatorname{div}(\sigma \operatorname{grad} u) = 0 & \text{in } B, \\ u = c & \text{on } \partial B. \end{cases} \quad (3.14)$$

This problem has an unique solution for each boundary data (see [GiTr], Theorem 8.3), consequently $u = c$ in B and the proof is complete. \blacksquare

Theorem 3.2 *There exists a solution $u \in H^1(B)$ of problem (3.12).*

Proof: We show that a solution q of the elliptic problem

$$\text{find } q \in H^1(B) \text{ such } \begin{cases} \operatorname{div}(\sigma \operatorname{grad} q) = 0 & \text{in } B, \\ q|_{\partial B} = f & \text{on } \partial B \end{cases} \quad (3.15)$$

with boundary value $f \in H_{\circ}^{\frac{1}{2}}(\partial B)$ determined by $\Delta_{\partial B} f = \operatorname{CURL} \mathbf{e}$ is a solution of problem (3.12).

For the function $\operatorname{CURL} \mathbf{e} \in H^{-3/2}(\partial B)$ holds

$$\langle \operatorname{CURL} \mathbf{e}, 1 \rangle = \int_{\partial B} \operatorname{DIV}(\nu \times \mathbf{e}) ds = 0. \quad (3.16)$$

The isomorphism $\Delta_{\partial B} : H_{\circ}^{\frac{1}{2}}(\partial B) \rightarrow H_{\circ}^{-3/2}(\partial B)$ implies that the equation $\Delta_{\partial B} f = \operatorname{CURL} \mathbf{e}$ has an unique solution $f \in H_{\circ}^{\frac{1}{2}}(\partial B)$. Now, we use the unique solvability of the elliptic problem (3.15) shown in [GiTr], Theorem 8.3. Thus, let $q \in H_{\Delta}^1(B)$ be the unique solution of (3.15). We verify

$$\operatorname{DIV}(\nu \times \operatorname{GRAD} q|_{\partial B} - \mathbf{e}) = -\operatorname{CURL} \operatorname{GRAD} f - \operatorname{DIV} \mathbf{e} = 0, \quad (3.17)$$

$$\operatorname{CURL}(\nu \times \operatorname{GRAD} q|_{\partial B} - \mathbf{e}) = \operatorname{DIV} \operatorname{GRAD} f - \operatorname{CURL} \mathbf{e} = 0. \quad (3.18)$$

Finally, we have $\operatorname{div}(\sigma \operatorname{grad} q) = 0$ and $\nu \times \operatorname{GRAD} q|_{\partial B} - \mathbf{e} = \mathbf{0}$, consequently $\gamma_{\times} \operatorname{grad} q = \mathbf{e}$, i.e. the function q solves the problem (3.12). \blacksquare

Corollary 3.3 *The boundary value problem (3.12) admits an unique solution for each $\mathbf{e} \in \mathbf{L}_{t, \operatorname{DIV}=0}^2(B)$.*

The magnetic field caused by the current distribution \mathbf{j} is determined by

$$\begin{aligned}
\mathcal{W}\mathbf{j} &= \operatorname{curl} \int_{B \setminus \overline{D}} \Phi(\cdot, y) \mathbf{j}(y) dy + \operatorname{curl} \int_D \Phi(\cdot, y) \mathbf{j}(y) dy \\
&= - \int_{B \setminus \overline{D}} \operatorname{curl}_y \{ \Phi(\cdot, y) \sigma_B \mathbf{E}(y) \} dy - \int_D \operatorname{curl}_y \{ \Phi(\cdot, y) \sigma_D \mathbf{E}(y) \} dy \\
&= -\sigma_B \int_{\partial D} \Phi(\cdot, y) \gamma_{\times} [D^e] \mathbf{E}(y) dy - \sigma_B \int_{\partial B} \Phi(\cdot, y) \gamma_{\times} [B] \mathbf{E}(y) dy \\
&\quad - \sigma_D \int_{\partial D} \Phi(\cdot, y) \gamma_{\times} [D] \mathbf{E}(y) dy \\
&= (\sigma_B - \sigma_D) \vec{\mathcal{S}}_D(\nu \times \mathbf{E}) - \sigma_B \vec{\mathcal{S}}_B(\nu \times \mathbf{E}).
\end{aligned} \tag{3.19}$$

Thereby, we use $\gamma_{\times} [D] \mathbf{E} = -\gamma_{\times} [D^e] \mathbf{E}$ from (3.10).

3.1.2 Neumann Boundary Condition

In praxis we are often faced with the situation that a conductor has a defect or a non-conducting inclusion, respectively. Consequently, the current distribution \mathbf{j} vanishes in D . The normal component $\gamma_{\nu} [D^e] \mathbf{j}$ vanish due to the transmission condition (3.8). Thus, we have the following boundary value problem

BVP 12 (Impedance problem with Neumann and tangential condition) Let $\partial D \in C^{0,1}$, $\partial B \in C^2$. For a given field $\mathbf{e} \in \mathbf{L}_{t, \operatorname{DIV}=0}^2(\partial B)$

$$\text{find } \mathbf{E} \in \mathbf{H}_{\operatorname{div}}(B \setminus \overline{D}) \cap \mathbf{H}_{\operatorname{curl}}(B \setminus \overline{D}) \text{ such } \begin{cases} \operatorname{curl} \mathbf{E} = \mathbf{0} & \text{in } B \setminus \overline{D}, \\ \operatorname{div} \mathbf{E} = 0 & \text{in } B \setminus \overline{D}, \\ \nu \cdot \mathbf{E} = 0 & \text{on } \partial D, \\ \nu \times \mathbf{E} = \mathbf{e} & \text{on } \partial B. \end{cases} \tag{3.20}$$

Theorem 3.4 *A solution of problem (3.20) is uniquely determined.*

Proof: Let \mathbf{E} be a solution of the corresponding homogeneous problem and u its scalar potential. As already shown in the proof of Theorem 3.1 the condition $\nu \times \operatorname{grad} u = \mathbf{0}$ implies $u|_{\partial B} = c$ with $c \in \mathbb{R}^3$. For the harmonic function u we observe

$$\int_{\partial B} \frac{\partial u}{\partial \nu} ds = \int_{\partial B} \frac{\partial u}{\partial \nu} ds + \int_{\partial D} \frac{\partial u}{\partial \nu} ds = \int_{\partial(B \setminus \overline{D})} \frac{\partial u}{\partial \nu} ds = 0. \tag{3.21}$$

Together with Green's first identity we obtain

$$\int_{B \setminus \overline{D}} |\text{grad } u|^2 dx = \int_{\partial(B \setminus \overline{D})} u \frac{\partial u}{\partial \nu} ds = c \int_{\partial B} \frac{\partial u}{\partial \nu} ds = 0 \quad (3.22)$$

from which $\mathbf{E} = \text{grad } u = \mathbf{0}$ follows. ■

We show the existence of a solution by reducing the problem to the boundary value problem of Laplace' equation with mixed boundary condition of Dirichlet and Neumann type

$$\text{find } q \in H^1(B) \text{ such } \begin{cases} \Delta q = 0 & \text{in } B, \\ q|_{\partial B} = f & \text{on } \partial B \\ \frac{\partial q}{\partial \nu} = 0 & \text{on } \partial D \end{cases} \quad (3.23)$$

with $f \in H_o^{\frac{1}{2}}(\partial B)$ defined by $\Delta_{\partial B} f = \text{CURL } \mathbf{e}$. We understand the boundary condition in the sense of the trace operators $\gamma_0[B]$ and $\gamma_\nu[D^e]$. We additionally note, that we have $\partial B \in C^2$, and thus, the Laplace-Beltrami operator $\Delta_{\partial B} : H_o^{\frac{1}{2}}(\partial B) \rightarrow H_o^{-\frac{3}{2}}(\partial B)$ is well defined and an isomorphism.

Theorem 3.5 *The problem (3.20) has a solution.*

Proof: The mixed boundary value problem (3.23) has a solution $q \in H^1(B \setminus \overline{D})$. For this proof we refer to [McL], Theorem 4.10, where we use that the corresponding homogeneous problem has only the trivial solution (it follows by a simple application of Green's first identity). Then, the field $\text{grad } q$ is harmonic and it fulfills the boundary condition $\nu \cdot \text{grad } q = 0$ on ∂D . Moreover, the relation $\nu \times \text{grad } q = \mathbf{e}$ holds which we have already shown in the proof of Theorem 3.2. Finally, $\text{grad } q$ turns out to be a solution of problem 3.20. ■

Corollary 3.6 *The boundary value problem (3.20) admits an unique solution for each $\mathbf{e} \in \mathbf{L}_{t, \text{DIV}}^2(B)$ with $\text{DIV } \mathbf{e} = 0$.*

Concluding, we calculate the magnetic field by

$$\begin{aligned} \mathcal{W}\mathbf{j} &= \text{curl} \int_{B \setminus \overline{D}} \Phi(., y) \mathbf{j}(y) dy = - \int_{B \setminus \overline{D}} \text{curl}_y \{ \Phi(., y) \sigma_B \mathbf{E}(y) \} dy \\ &= -\sigma_B \int_{\partial D} \Phi(., y) \gamma_\times[D^e] \mathbf{E}(y) dy - \sigma_B \int_{\partial B} \Phi(., y) \gamma_\times[B] \mathbf{E}(y) dy \\ &= \sigma_B \vec{\mathcal{S}}_D(\nu \times \mathbf{E}) - \sigma_B \vec{\mathcal{S}}_B(\nu \times \mathbf{E}). \end{aligned} \quad (3.24)$$

3.1.3 Numerical Implementation

In this section, we describe how to compute the numerical solution of the boundary value problems and the magnetic field. Here, we present two different methods which we have used for the computation of all 4 numerical examples of the next Section. On the one hand we use the finite element method by the commercial software FEMLAB 3.1 and on the other hand the boundary element method based on an boundary integral equation. For both methods the results coincide very well up to an relative error of 0.5%. Further, we explain the numerical implementation of the single layer operators which we use to calculate the magnetic field from the electric field. Additionally, the numerical computation of the point source method as well as the no response test are based on the implementation of the single layer potential. Thus, this Subsection prepare for the numerical study of the inverse problem.

For the first method we give special boundary values on the boundary ∂B . Then, we are able to reduce the problem as already shown in the proofs of the Theorems 3.2 and 3.5. In all 4 numerical examples the boundary values \mathbf{e} have the shape $\nu \times \text{grad } u$ where u is a harmonic function on B as for instance $\Phi(\cdot, p)$ with a source point $p \in B^e$. Then, the function $f \in H_{\text{circ}}^{1/2}(\partial B)$ defined by $\Delta_{\partial B} f = \text{CURL } \mathbf{e}$ is given by $u|_{\partial B}$ because

$$\Delta f = \text{CURL } \mathbf{e} = \text{CURL}(\nu \times \text{grad } u) = \text{DIV GRAD } u = \Delta u_{\partial B}. \quad (3.25)$$

Altogether, we solve the impedance equation with Dirichlet data $u|_{\partial B}$ (3.15) and the Laplace equation with mixed Dirichlet and Neumann data (3.23), respectively. Then, we obtain the electric field by the gradient of this solution. This solution is performed by FEMLAB 3.1. For the application of the FEM we assume that consistency, stability and convergence is proven. With the aid of the numerical example 'scene 1', see 3.8, we explain the basic implementation steps. The commands

```
domainD=sphere2('0.5','pos',{'-0.5','0','0'});
domainB=sphere2('2');
domain=domainB-domainD;
```

create the domains $B, D, B \setminus \overline{D}$. By

```
fem.mesh=meshinit(fem, ...
    'hmaxfact',0.8, ...
    'hcutoff',0.008, ...
    'hgrad',1.35, ...
    'hcurve',0.35);
```

we build up a volume grid on $B \setminus \overline{D}$ with some constants that define the size and shape of the triangles. With the constants and expressions

```
fem.const={'px',0,'py',0,'pz',3};
fem.expr ={'Phi','1./4.0/pi/sqrt((x-px).^2+(y-py).^2+(z-pz).^2)'};
```

we set the boundary conditions by

```
bnd.g = {0,0};
bnd.r = {0,'Phi'};
bnd.type = {'neu','dir'};
bnd.ind = [2,2,2,2,2,2,1,1,1,1,1,1,1,2,2,1,1];
```

In detail, on the boundary ∂D represented by the 8 FEMLAB surface patches no. 7, ... 12, 15, 16 we have Neumann condition with boundary data 0. On the boundary ∂B represented by the 8 surface patches no. 1, ... 7, 13, 14 we have Dirichlet condition with boundary data Phi as defined in the FEMLAB expressions. Finally, the solution process is started by

```
fem=multiphysics(fem);
fem.xmesh=meshextend(fem);
fem.sol=femlin(fem, ...
               'solcomp',{'u'}, ...
               'outcomp',{'u'});
```

Then, we get the electric field $\mathbf{E} = (ExEyEz)^t$ at any points p on the boundary ∂D by

```
[Ex,Ey,Ex]=postinterp(fem,'ux','uy','uz',p);
```

where ux denotes the x -component of the gradient of the solution u . The magnetic field can be calculated in the same way as for the boundary element method and thus, we explain the calculation at the end of this Subsection.

For the second method we represent the electric field in terms of

$$\mathbf{E} = \text{grad } \mathcal{S}_D \phi + \text{curl } \vec{\mathcal{S}}_B \mathbf{b}. \quad (3.26)$$

We note that this method requires a C^2 boundary ∂D . For our application the boundary ∂D has regular corners and edges. Anyway, we apply the boundary element method and say that the discretized boundary $\partial \tilde{D}$ which arises from a triangulation of ∂D approximates a C^2 boundary. We assume that the numerical solution on $\partial \tilde{D}$ will approximate the true solution on the Lipschitz boundary ∂D .

Theorem 3.7 *Let $\mathbf{e} \in \mathbf{L}_{t,Div=0}^2(\partial B)$. The field $\mathbf{E} = \text{grad } \mathcal{S}_D \phi + \text{curl } \vec{\mathcal{S}}_B \mathbf{b}$ is a solution of the general transmission problem (3.4) provided (ϕ, \mathbf{b}) solves the integral equation system*

$$\left[\begin{pmatrix} \mathcal{I} & 0 \\ 0 & \mathcal{I} \end{pmatrix} - \begin{pmatrix} \frac{\sigma_B - \sigma_D}{\sigma_D + \sigma_B} \mathcal{K}_{DD}^* & 2 \frac{\sigma_B - \sigma_D}{\sigma_D + \sigma_B} \nu \cdot \text{curl } \vec{\mathcal{S}}_{BD} \\ 2\nu \times \text{grad } \mathcal{S}_{DB} & \mathcal{M}_{BB} \end{pmatrix} \right] \cdot \begin{pmatrix} \phi \\ \mathbf{b} \end{pmatrix} = \begin{pmatrix} 0 \\ -2\mathbf{e} \end{pmatrix}. \quad (3.27)$$

The first subscript of the operators denotes the domain whose boundary is the boundary of integration, the second one denotes the domain on whose boundary the potential is evaluated.

Proof: Let (ϕ, \mathbf{b}) solve the integral equation (3.27). We define $\mathbf{E} := \text{grad } \mathcal{S}_D \phi + \text{curl } \vec{\mathcal{S}}_B \mathbf{b}$. The field \mathbf{E} is analytic in D and in $B \setminus \overline{D}$ since $\mathcal{S}_D \phi$ and $\vec{\mathcal{S}}_B \mathbf{b}$ are analytic therein. From the second equation of (3.27) together with the jump relation (A.57) of $\text{curl } \vec{\mathcal{S}}_B \mathbf{b}$ we derive

$$(\mathcal{I} - \mathcal{M}_{BB})\mathbf{b} = -2\mathbf{e} + 2\nu \times \text{grad } \mathcal{S}_{DB} \phi$$

and $\gamma_\times[B]\mathbf{E} = \mathbf{e}$. Using $\text{DIV}(\nu \times \mathbf{v}) = -\nu \cdot \text{curl } \mathbf{v}$ for a field continuously differentiable in a neighborhood of ∂B , we see that the right hand side is an element of $\mathbf{L}_{t, \text{Div}=0}^2(\partial B)$. The operator $\mathcal{I} - \mathcal{M}_{BB}$ is bijective on this space (see Theorem A.30), and thus, we have $\text{DIV } \mathbf{b} = 0$. Now, with the relation

$$\begin{aligned} \text{curl } \text{curl } \vec{\mathcal{S}}_B \mathbf{b} &= (-\Delta + \text{grad } \text{div}) \vec{\mathcal{S}}_B \mathbf{b} = \text{grad } \vec{\mathcal{S}}_B \text{DIV } \mathbf{b} = \mathbf{0}, \\ \text{div } \text{curl } \vec{\mathcal{S}}_B \mathbf{b} &= 0 \end{aligned}$$

we deduce that \mathbf{E} is a harmonic field. Finally, the first equation of (3.27) together the jump relation (A.29) yield $\sigma_D \nu [D]\mathbf{E} = \sigma \nu [D^e]\mathbf{E}$ and the proof is complete. \blacksquare

Theorem 3.8 *For each $\sigma_D \leq 0, \sigma_D \neq \sigma_B$ and for each tangential field $\mathbf{e} \in \mathbf{L}_{t, \text{Div}=0}^2(\partial B)$, the integral equation system (3.27) has one and only one solution $(\phi, \mathbf{b})^t$ with $\phi \in L^2(\partial D)$ and $\mathbf{b} \in \mathbf{L}_{t, \text{Div}=0}^2(\partial B)$.*

Proof: In order to apply Riesz' theory, we have to make sure that the operator

$$\mathcal{A} := \begin{pmatrix} \frac{\sigma_B - \sigma_D}{\sigma_D + \sigma_B} \mathcal{K}_{DD}^* & 2 \frac{\sigma_B - \sigma_D}{\sigma_D + \sigma_B} \nu \cdot \text{curl } \vec{\mathcal{S}}_{BD} \\ 2\nu \times \text{grad } \mathcal{S}_{DB} & \mathcal{M}_{BB} \end{pmatrix} \quad (3.28)$$

is compact. Since $\sigma_D \neq \sigma_B$ the scalar $\frac{\sigma_B - \sigma_D}{\sigma_D + \sigma_B}$ does not vanish. \mathcal{M}_{BB} and \mathcal{K}_{DD}^* are compact operators by Lemma A.28 and Theorem A.21. The linear operators $\nu \cdot \text{curl } \vec{\mathcal{S}}_{BD}$ and $\nu \times \text{grad } \mathcal{S}_{DB}$ have analytic kernels and are compact, too. Altogether, \mathcal{A} is a compact operator from $L^2(\partial D) \times \mathbf{L}_{t, \text{Div}=0}^2(\partial B)$ into itself. It remains to show that $\mathcal{I} - \mathcal{A}$ is injective, afterwards Riesz' theory ensures the bijectivity of $\mathcal{I} - \mathcal{A}$.

Let (ϕ, \mathbf{b}) satisfy the homogeneous equation (3.27), then the field $\mathbf{E} := \text{grad } \mathcal{S}_D \phi + \text{curl } \vec{\mathcal{S}}_B \mathbf{b}$ must vanish from the uniqueness Theorems 3.1 and 3.4 for $\sigma_D = 0$, respectively. With respect to the continuity of $\nu \times \mathcal{S}_D$ across ∂D we derive

$$(\sigma_B - \sigma_D)\nu \times \text{grad } \mathcal{S}_D \phi = \sigma_B \nu \times \text{grad } \mathcal{S}_D \phi - \sigma_D \nu \times \text{grad } \mathcal{S}_D \phi = \sigma_B \nu^+ \times \mathbf{E} - \nu^- \sigma_D \times \mathbf{E} = 0$$

Since $\sigma_B \neq \sigma_D$, we obtain $\nu \times \text{grad } \mathcal{S}_D \phi = \mathbf{0}$. Hence, $\text{GRAD } \mathcal{S}_D \phi = \mathbf{0}$ and $\mathcal{S}_D \phi = c$ on ∂D with a $c \in \mathbb{R}$. Now, the function $\mathcal{S}_D \phi$ solves the interior Dirichlet problem for Laplace's equation in D and must be constant therein, consequently $\nu^- \cdot \text{grad } \mathcal{S}_D \phi = 0$. The jump relation of the gradient of the single layer potentials (A.24) leads to

$$0 = \nu^+ \cdot \mathbf{E} - \nu^- \cdot \mathbf{E} = \nu^+ \cdot \text{grad } \mathcal{S}_D \phi - \nu^- \text{grad } \mathcal{S}_D \phi = -\phi.$$

Finally, we have $\mathbf{E} = \text{curl } \vec{\mathcal{S}}_B \mathbf{b}$ satisfying $(\mathcal{I} - \mathcal{M}_{BB})\mathbf{b} = \mathbf{0}$ which is true only for $\mathbf{b} = \mathbf{0}$ from Lemma A.30. \blacksquare

Now, we turn to the implementation of the boundary integrals and explain the computation of the operator \mathcal{A} . We produce a surface grid with a similar command as meshioned above. Let $\{t_k\}_{k=1\dots N}$ be the set of surface triangles and $p_{k,1}, p_{k,2}, p_{k,3}$ the corners of the k -th triangle. We calculate the centers c_k and the area A_k

$$c_k = \frac{1}{3} \sum_{n=1}^3 p_{k,n}, \quad A_k = \frac{(p_{k,1} - p_{k,3}) \cdot (p_{k,2} - p_{k,3})}{2} \quad (3.29)$$

of each triangle. Then we compute the single layer potential on ∂B with density ϕ by

$$(\mathcal{S}_B \phi)(x) = \int_{\partial B} \Phi(x, y) \phi(y) ds(y) \approx \sum_{k=1}^N A_k \Phi(x, c_k) \phi_k, \quad x \in \mathbb{R}^3 \setminus \partial B. \quad (3.30)$$

where $\phi_k = \sum_{n=1}^3 \phi(p_{k,n})/3$. Altogether, we first approximate the boundary by a 3d-polygon and apply the integral operator on the polygon, then we approximate the integral by the midpoint rule. One can show that the sum converges to the exact integral value for $h_{max} \searrow 0$, it is a linear convergence rate. Anyway, it is the most easiest way of implementation and that's why we use this integration formula for our numerical study. Of course, there are many ways to increase the performance but our intention is just to give a proof of concept.

The cost of memory is very large because we treat vector fields in three dimension. Indeed, our densities in the integral equation (3.27) are tangential vector fields, thus we are able to decrease the size of vectors and matrices by introducing local coordinates in two tangential directions and in normal direction. Let $(\vec{e}_1(x), \vec{e}_2(x), \vec{e}_3(x))$ be local coordinates with $\vec{e}_3(x) = \nu(x)$ on the boundary ∂B , then $\mathbf{b} \in \mathbf{L}^2(\partial B)$ has an unique representation

$$\mathbf{b}(x) = b_1(x)\vec{e}_1(x) + b_2(x)\vec{e}_2(x) + b_3(x)\vec{e}_3(x), \quad x \in \partial B, \quad (3.31)$$

where $b_3(x) = 0$ if \mathbf{b} is a tangential vector field. Applying the midpoint rule, we compute the vectorial single layer potential by

$$(\vec{\mathcal{S}}\mathbf{b})(x) = \int_{\partial B} \Phi(x, y) \mathbf{b}(y) ds(y) \approx \sum_{k=1}^N A_k \Phi(x, c_k) (b_1 \vec{e}_{1,k} + b_2 \vec{e}_{2,k} + b_3 \vec{e}_{3,k}) \quad (3.32)$$

We determine the local coordinates $\vec{e}_{1,k}, \vec{e}_{2,k}, \vec{e}_{3,k}$ of each triangle such that $\vec{e}_{3,k} = \nu_k$ is the exterior normal vector of the k -th triangle, $\vec{e}_{1,k}$ the normalized vector $c_k - p_{k,1}$, and $\vec{e}_{2,k} := \vec{e}_{3,k} \times \vec{e}_{1,k}$. Now, we are able to implement the operators $\nu \cdot \text{curl } \vec{\mathcal{S}}_{BD} : \mathbf{L}^2(\partial B) \rightarrow$

$L^2(\partial D)$ by

$$\nu(x) \cdot \operatorname{curl}(\vec{\mathcal{S}}_{BD}\mathbf{b})(x) = \int_{\partial B} \nu(x) \cdot \operatorname{grad}_x \Phi(x, y) \times \mathbf{b}(y) ds(y) \quad (3.33)$$

$$\approx \sum_{k=1}^N A_k \sum_{i=1}^3 \operatorname{grad}_x \Phi(x, c_k) \cdot \vec{T}_n(x) b_{i,k} \quad (3.34)$$

with

$$\vec{T}_i(x) := \vec{e}_i \times \nu(x), \quad i = 1 \dots 3. \quad (3.35)$$

Furthermore, we implement the operator $\nu \times \operatorname{grad} \mathcal{S}_{DB} : L^2(\partial D) \rightarrow \mathbf{L}^2(\partial B)$ by

$$\nu(x) \times \operatorname{grad}(\mathcal{S}_{DB}\phi)(x) = \int_{\partial B} \nu(x) \times \operatorname{grad}_x \Phi(x, y) \phi(y) ds(y) \quad (3.36)$$

$$\approx \sum_{k=1}^N A_k \nu(x) \times \operatorname{grad}_x \Phi(x, c_k) \phi_k. \quad (3.37)$$

If we evaluate the operators $\mathcal{I} - \mathcal{K}_{DD}^*$ and $\mathcal{I} - \mathcal{M}_{BB}$ in this way, we get problems because of the weakly singular integral kernels. We deal with this problem by cutting off the singularities. Consider for example the weakly integral operator

$$(\mathcal{K}_D^*\phi)(x) = \int_{\partial D} \nu(x) \cdot \operatorname{grad}_x \Phi(x, y) \phi(y) ds \approx \sum_{k=1}^N A_k \nu(x) \cdot \operatorname{grad}_x \Phi(x, c_k) \phi_k \quad (3.38)$$

which we evaluate at the discretization points $c_n, n = 1 \dots N$ by setting the diagonal matrix entries to zero. Then, the matrix entries $(\mathbf{I} - \mathbf{K}^*)_{n,k}, n = 1 \dots N, k = 1 \dots N$ are

$$(\mathbf{I} - \mathbf{K}^*)_{n,k} := \begin{cases} \frac{A_k \nu_n \cdot (c_k - c_n)}{4\pi |c_n - c_k|^3}, & \text{if } n \neq k, \\ 0, & \text{if } n = k \end{cases} \quad (3.39)$$

Next, we explain how to build the matrix $\mathbf{I} - \mathbf{M}$ associated to the operator $\mathcal{I} - \mathcal{M}_{BB}$ in local surface coordinates. Assume that $\mathbf{a} \in \mathbf{L}_{t, \operatorname{Div}=0}^2(\partial B)$. Using the local surface coordinates, the equation $(\mathcal{I} - \mathcal{M}_{BB})\mathbf{b} = -2\mathbf{a}$ can be written as

$$\begin{aligned} -2a_1(x)\vec{e}_1(x) - 2a_2(x)\vec{e}_2(x) &= b_1(x)\vec{e}_1(x) + b_2(x)\vec{e}_2(x) + b_3(x)\vec{e}_3(x) \\ -2 \int_{\partial B} \vec{e}_3(x) \times \left\{ \operatorname{grad}_x \Phi(x, y) \times \left\{ b_1(y)\vec{e}_1(y) + b_2(y)\vec{e}_2(y) + b_3(y)\vec{e}_3(y) \right\} \right\} ds(y) \end{aligned}$$

The integral on the right hand side is orthogonal to $\vec{e}_3(x)$, therefore $b_3(x) = 0, x \in \partial B$ and \mathbf{b} must be a tangential vector field. Defining $\vec{g}^{(i)}(x, y) := \operatorname{grad}_x \Phi(x, y) \times \vec{e}_i(y), i = 1, 2$

we simplify the equation system further

$$\begin{aligned} -2a_1(x)\vec{e}_1(x) - 2a_2(x)\vec{e}_2(x) &= b_1(x)\vec{e}_1(x) + b_2(x)\vec{e}_2(x) \\ -2 \int_{\partial B} \vec{e}_3(x) \times \left\{ b_1(y)\vec{g}^{(1)}(x, y) + b_2(y)\vec{g}^{(2)}(x, y) \right\} ds(y) & \end{aligned}$$

The terms

$$\begin{aligned} \vec{e}_3(x) \times \vec{g}^{(i)}(x, y) &= \vec{e}_3(x) \times \sum_{j=1}^3 \{ \vec{g}^{(i)}(x, y) \cdot \vec{e}_j(x) \} \vec{e}_j(x) \\ &= \{ \vec{g}^{(i)}(x, y) \cdot \vec{e}_1(x) \} \vec{e}_2(x) - \{ \vec{g}^{(i)}(x, y) \cdot \vec{e}_2(x) \} \vec{e}_1(x) \end{aligned} \quad (3.40)$$

for $i = 1, 2$, lead to a representation of the integral in tangential coordinates. By a comparison of coordinates we obtain the equation system

$$b_1(x) + 2 \int_{\partial B} b_1(y)\vec{g}^{(1)}(x, y) \cdot \vec{e}_2(x) + b_2(y)\vec{g}^{(2)}(x, y) \cdot \vec{e}_2(x) ds(y) = -2a_1(x), \quad (3.41)$$

$$b_2(x) - 2 \int_{\partial B} b_1(y)\vec{g}^{(1)}(x, y) \cdot \vec{e}_1(x) + b_2(y)\vec{g}^{(2)}(x, y) \cdot \vec{e}_1(x) ds(y) = -2a_2(x). \quad (3.42)$$

We define the kernels of the integrals by

$$G^{i,j}(x, y) := \vec{g}^{(i)}(x, y) \cdot \vec{e}_j(x) = (\vec{e}_i(y) \times \vec{e}_j(x)) \cdot \text{grad}_x \Phi(x, y), \quad i, j = 1, 2. \quad (3.43)$$

Using this notation and the discretization from above, by an application of the midpoint rule, we obtain the full discretized system

$$b_{1,n} + 2 \sum_{k=1}^N G^{1,2}(c_n, c_k) A_k b_{1,k} + G^{2,2}(c_n, c_k) A_k b_{2,k} = -2a_{1,n}, \quad (3.44)$$

$$b_{2,n} - 2 \sum_{k=1}^N G^{1,1}(c_n, c_k) A_k b_{1,k} + G^{2,1}(c_n, c_k) A_k b_{2,k} = -2a_{2,n}. \quad (3.45)$$

Here, we set $G^{i,j}(c_n, c_k) = 0, \forall i, j = 1, 2$ if $n = k$ accordant to the singularity cut off.

Remark 3.9 We do not arbitrarily set the matrix elements $\underline{K}_{n,n}^*, n = 1 \dots N$ and $\underline{M}_{n,n}$ resp. to zero. Let Tr_k be the k -th triangle of the surface grid of ∂D , then for $x \in \text{Tr}_k$

$$\int_{\text{Tr}_k} \nu(x) \cdot \text{grad}_x \Phi(x, y) \phi(x) ds(y) = 0, \quad (3.46)$$

since $\nu(x) = \nu_k \perp x - y, \forall y \in \text{Tr}_k \setminus \{x\}$. Furthermore, we have

$$\int_{\text{Tr}_k} G^{i,j}(x, y) b_i(y) ds(y) = 0, \quad (3.47)$$

for all $i, j = 1 \dots 2$ and $x \in \text{Tr}_k$. This can be deduced by the definition of $G^{i,j}(x, y)$ and

$$\begin{aligned}\vec{e}_i(y) \times \vec{e}_j(x) &= \vec{e}_i \times \vec{e}_j \perp x - y, \quad \forall y \in \text{Tr}_k, y \neq x \text{ if } i \neq j \\ \vec{e}_i(y) \times \vec{e}_i(x) &= \vec{e}_i \times \vec{e}_i = 0, \quad \forall y \in \text{Tr}_k, i = 1, 2.\end{aligned}$$

Anyway, the method of singularity cut off works also in the case where above integrals over a triangle are bounded only. However, if the diagonal elements do not vanish, we expect a slower convergence.

Now, we are able to evaluate the electric field and the current distribution by the corresponding ansatz field. To evaluate the magnetic field

$$\mathcal{W}\mathbf{j} = (\sigma_B - \sigma_D)\vec{\mathcal{S}}_D(\nu \times \mathbf{E}) - \sigma_B\vec{\mathcal{S}}_B(\nu \times \mathbf{E}). \quad (3.48)$$

we just calculate $\nu \times \mathbf{E}|_{\partial D} = \nu \times (\text{grad } \mathcal{S}_D\phi + \text{curl } \vec{\mathcal{S}}_B\mathbf{b})$ since $\nu \times \mathbf{E}|_{\partial B}$ is given by the boundary data \mathbf{e} . To avoid the difficulties arising with calculating the integral $\text{grad } \mathcal{S}_D\phi$ on the same discretization points we suggest the following calculation. For every triangle Tr_k we evaluate $\nu_{\partial D} \times \mathbf{E}$ which is continuous across ∂D on the corners $p_{k,i}, i = 1 \dots 3$ and take the average of these three results

$$(\nu_{\partial D} \times \mathbf{E})(c_k) \approx \frac{1}{3} \sum_{i=1}^3 (\nu_k \times \mathbf{E})(p_{k,i}).$$

We note that $\mathcal{W}\mathbf{j}$ is a continuous field in \mathbb{R}^3 and the evaluation on ∂B can be done without giving attention to jumps. But again we avoid the numerical difficulties when evaluating $\mathcal{W}\mathbf{j}$ at the center of the grid triangles by the approximation

$$(\mathcal{W}\mathbf{j})(c_k) \approx \frac{1}{3} \sum_{i=1}^3 (\mathcal{W}\mathbf{j})(p_{k,i}).$$

3.2 Field Reconstruction by the Point Source Method

In this chapter we have focussed on a homogeneous conductor with one homogeneous inclusion, i.e. the conductivity distribution is given by

$$\sigma(x) = \begin{cases} \sigma_D & x \in D, \\ \sigma_B & x \in B \setminus \overline{D}. \end{cases} \quad (3.49)$$

with $\sigma_D \in \mathbb{R}^+ \setminus \{\sigma_B\}$. The magnetic field of an ohmic current distribution based on the conductivity distribution σ can be calculated by the formula

$$\mathcal{W}\mathbf{j} = (\sigma_B - \sigma_D)\vec{\mathcal{S}}_D(\nu \times \mathbf{E}) - \sigma_B\vec{\mathcal{S}}_B(\nu \times \mathbf{E}) \quad (3.50)$$

which is derived in the last subsections. This representation formula together with the mapping properties of the single layer potential imply that the magnetic field is continuous in \mathbb{R}^3 and analytic in $D, B \setminus \overline{D}$ and B^e . We have observed in Section 2.4 that we can calculate the exterior field from the boundary data $\nu \times (\mathcal{W}\mathbf{j})|_{\partial B}$. The goal of this section is to continue the field $\mathcal{W}\mathbf{j}$ from the boundary value on ∂B in the interior of B .

For simplicity we assume that $\mathbf{h} := (\mathcal{W}\mathbf{j})|_{\partial B}$ is known. Since the continuation is not uniquely determined we additionally assume the knowledge of the tangential component of the electric field $\mathbf{e} := \nu \times \mathbf{E}|_{\partial B}$. In this case, the left side of equation (3.50) and the second term on the right side are known on ∂B , i.e. the boundary values on ∂B of the field

$$\mathbf{w}(x) := (\mathcal{W}\mathbf{j})(x) + \vec{\mathcal{S}}_B(\sigma_B \mathbf{e})(x) \quad (3.51)$$

are given. From (3.50), the field \mathbf{w} is a single layer potential

$$\mathbf{w}(x) = (\sigma_B - \sigma_D)\vec{\mathcal{S}}_D(\nu \times \mathbf{E})(x) = (\vec{\mathcal{S}}_D \mathbf{t})(x) = \int_{\partial D} \Phi(x, y) \mathbf{t}(y) ds(y) \quad (3.52)$$

with the density $\mathbf{t} = (\sigma_B - \sigma_D)(\nu \times \mathbf{E}) = \nu^+ \times \mathbf{j} - \nu^- \times \mathbf{j}$ which is the difference of the tangential components of the current distribution from the exterior and the interior. Hence, we can only expect a continuation of \mathbf{w} and $\mathcal{W}\mathbf{j}$ from ∂B into $B \setminus \overline{D}$.

The problem is neither the boundary ∂D nor the density \mathbf{t} are known. Therefore, we cannot use standard continuation calculations. Instead, we choose a recently developed algorithm called *point source method* to calculate the field \mathbf{w} and $\mathcal{W}\mathbf{j}$ respectively, in $B \setminus \overline{D}$ from the data $\mathbf{w}|_{\partial B}$. For a function $a \in L^2(\partial B)$, we observe

$$\begin{aligned} \int_{\partial B} \mathbf{w}(x) a(x) ds(x) &= \int_{\partial B} a(x) \left\{ \int_{\partial D} \Phi(x, y) \mathbf{t}(y) ds(y) \right\} ds(x) \\ &= \int_{\partial D} \mathbf{t}(y) \left\{ \int_{\partial B} \Phi(x, y) a(x) ds(x) \right\} ds(y) \\ &= \int_{\partial D} (\mathcal{S}_{BD} a)(y) \mathbf{t}(y) ds(y). \end{aligned} \quad (3.53)$$

The value of the last integral can be calculated for each function a from the known data $\mathbf{w}|_{\partial B}$. If we choose a such that $\mathcal{S}_{BD}a$ approximates the fundamental solution with a point source at $z \in B \setminus \overline{D}$

$$\Phi(x, z) = \frac{1}{4\pi} \frac{1}{|x - z|} \quad (3.54)$$

on the boundary ∂D , i.e. for $x \in \partial D$, then by a comparison of (3.53) and (3.52) the expression $\int_{\partial B} \mathbf{w} a \, ds$ is an approximation of $\mathbf{w}(z)$. This approximation called *point source approximation* is the basic idea of the point source method. We describe the details of the point source approximation applied on a test domain G with $\overline{D} \subset G$ in Subsection 3.2.1. We will illustrate the quality of the approximation in the light of a numerical example where we choose a spherical non-conducting inclusion. Moreover, we show what happens when D is not included in the test domain.

In Subsection 3.2.2 we describe the numerical realization of the point source method. We show that the algorithms work for a non-conducting as well as for a conducting inclusion. Thus, we choose a second example, where we have a cuboid-like inclusion with $\sigma_D = 2\sigma_B$. For each scene we employ a *shift algorithm* where we shift a test domain along different lines. The results of these shifts for various lines and test domains can be sampled and yield a approximation of the magnetic field $(\mathcal{W}\mathbf{j})(x)$ for (almost) all $x \in B \setminus \overline{D}$.

3.2.1 The Point Source Approximation

The equation (3.52) imply that if we have a function $a \in L^2(\partial B)$ satisfying $\mathcal{S}_{BD}a = \Phi(\cdot, z)$ on ∂D , then we are able to calculate $(\mathcal{W}\mathbf{j})(z)$ using the definition (3.51) by

$$(\mathcal{W}\mathbf{j})(z) = \int_{\partial B} \mathbf{w}(x) a(x, z) \, ds(x) + \sigma_B (\vec{\mathcal{S}}_B \mathbf{e})(z). \quad (3.55)$$

We note that σ_D is not required for this calculation. For the rest of this work we use the notation $a(\cdot, z)$ to make clear the dependency on the point source z . In order to solve $\Phi(\cdot, z) = \mathcal{S}_{BD}a(\cdot, z)$ we remark that $\Phi(\cdot, z)$ is not in the range of \mathcal{S}_{BD} . The integral operator $\mathcal{S}_{BD} : L^2(\partial B) \rightarrow L^2(\partial D)$ is compact and injective. Moreover, since its dual operator $\mathcal{S}_{DB} : L^2(\partial D) \rightarrow L^2(\partial B)$ is injective, the operator \mathcal{S}_{BD} has dense range. Therefore, we can use Tikhonov regularization to gain an approximation $\Phi(\cdot, z) \approx \mathcal{S}_{BD}a$ in the following sense: For given $\epsilon > 0$ we can find a density $a(\cdot, z) \in L^2(\partial B)$ such that

$$\|\Phi(\cdot, z) - \mathcal{S}_{BD}a(\cdot, z)\|_{L^2(\partial D)} \leq \epsilon. \quad (3.56)$$

Since the boundary ∂D is unknown, we cannot use this method for the reconstruction directly. Instead, let G be a domain with $\overline{D} \subset G$ and $\overline{G} \subset B$, then we may adapt this argumentation for the boundary ∂G . The function $\Phi(\cdot, z) - \mathcal{S}_{BG}a(\cdot, z)$ is a harmonic function on \overline{G} and depends continuously on the boundary data, i.e.

$$\|\Phi(\cdot, z) - \mathcal{S}_{BG}a(\cdot, z)\|_{L^2(\partial G)} \leq \epsilon \quad \text{implies} \quad \|\Phi(\cdot, z) - \mathcal{S}_{BD}a(\cdot, z)\|_{L^2(\partial D)} \leq C\epsilon$$

with a constant $C \in \mathbb{R}^+$. We obtain an approximation $\Phi(\cdot, z) \approx \mathcal{S}_{BG}a(\cdot, z)$, $z \notin \bar{G}$ by using Tikhonov regularization, i.e. we solve

$$(\alpha \mathcal{I} + \mathcal{S}_{BG}^* \mathcal{S}_{BG})a(\cdot, z) = \mathcal{S}_{BG}^* \Phi(\cdot, z). \quad (3.57)$$

Due to the dense range of \mathcal{S}_{BG} , there exists a regularization parameter $\alpha = \alpha(\epsilon)$ for each ϵ , and $\alpha \rightarrow 0$ for $\epsilon \rightarrow 0$. Altogether, for small ϵ , the field $\mathcal{S}_B a(\cdot, z)$ is an approximation of the point source $\Phi(\cdot, z)$ on ∂D , and we have

$$\tilde{\mathbf{w}}(z) := \int_B \mathbf{w}(x) a(x, z) ds(x) \approx \mathbf{w}(z), \quad (3.58)$$

$$\tilde{\mathbf{W}}(z) := \tilde{\mathbf{w}}(z) + \sigma_B(\tilde{\mathcal{S}}_B \mathbf{e})(z) \approx (\mathcal{W}\mathbf{j})(z). \quad (3.59)$$

This is the point source approximation on the test domain G . The point source approximation holds whenever $\bar{D} \subset G$, and then the approximation (3.58), (3.59) are valid.

Although $\tilde{\mathbf{W}}$ and $\mathcal{W}\mathbf{j}$ are the data of interest we should compare \mathbf{w} and $\tilde{\mathbf{w}}$ since the approximation affects only the calculation of $\tilde{\mathbf{w}}$. From $\tilde{\mathbf{W}} = \tilde{\mathbf{w}} + \sigma_B \tilde{\mathcal{S}}_B \mathbf{e}$, the additional term based on the known boundary data \mathbf{e} disturbs the relative error $|\tilde{\mathbf{W}} - \mathcal{W}\mathbf{j}|/|\mathcal{W}\mathbf{j}|$. That is why we focus on the comparison of \mathbf{w} and $\tilde{\mathbf{w}}$. We show that both fields coincide very well with the following setting

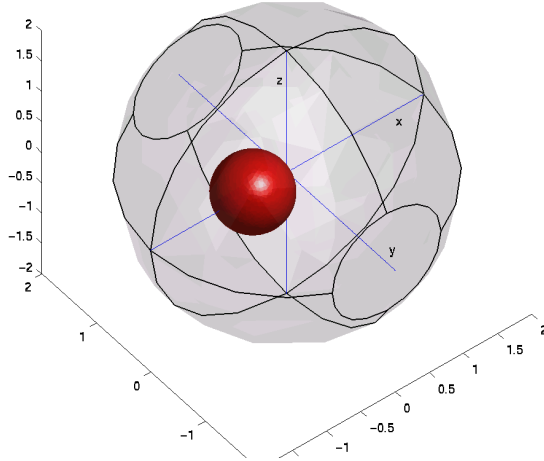


Figure 3.1: Scene 1

Let B be a ball with radius 2 centered at origin, and D a ball of radius 0.5 centered at $(-0.5, 0, 0)^t$. The domain D models a non-conducting inclusion, i.e. the field \mathbf{E} satisfies the Neumann boundary condition on ∂D . On ∂B , we require boundary data $\nu \times \mathbf{E} = \nu \times \text{grad } \Phi(\cdot, p)$ with source point $p = (0, 0, 3)^t$ on ∂B .

The Figure 3.2 shows a color-plot of the fields $\mathcal{W}\mathbf{j}$ and \mathbf{w} on the xy-plane, that means we see a slice of $\mathcal{W}\mathbf{j}$ and \mathbf{w} .

For the point source approximation we choose the test domain G as the ball with radius 0.65 centered at $(-0.5, 0, 0)^t$. The Figure 3.3 shows the three components of $\tilde{\mathbf{w}}$ as a color-plot in comparison to \mathbf{w} . In addition, the values $\frac{\tilde{\mathbf{w}}(z_k)}{\mathbf{w}(z_k)}$ are shown from which we obtain the relative error $\frac{|\mathbf{w}(z_k) - \tilde{\mathbf{w}}(z_k)|}{|\mathbf{w}(z_k)|}$ by $\left| 1 - \frac{\tilde{\mathbf{w}}(z_k)}{\mathbf{w}(z_k)} \right|$. Moreover, Figure 3.3 shows the slice of the scene. The slice of ∂D is black colored whereas the slice of G is white colored. The

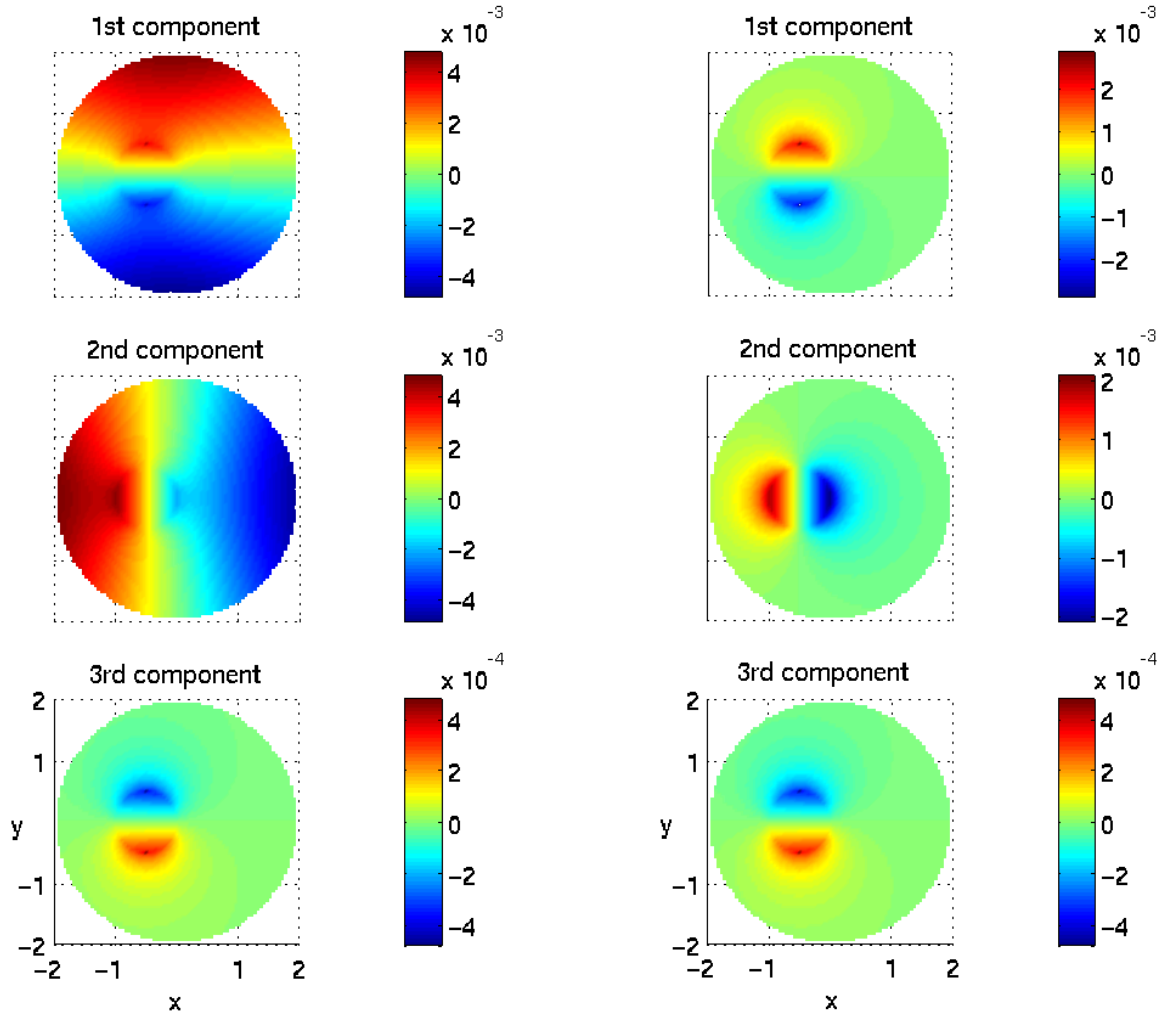


Figure 3.2: Representation of $\mathcal{W}\mathbf{j}$ (left) and \mathbf{w} (right) on the xy -plane

scales of the colorbar of first and second column are set to $[-C_m, C_m]$, $m = 1 \dots 3$ where C_m is the absolute maximum of the m -th component

$$C_m = \max_{z_k} |(\mathbf{w}(z_k))_m|. \quad (3.60)$$

The scales of the subplots in the last column are set to $[0.98; 1.02]$, i.e. we look at the errors in a 2-percent range.

Numerical Details: For the direct problem, we calculate the electric field \mathbf{E} and the magnetic field $\mathcal{W}\mathbf{j}$ as described in Subsection 3.1.2. The numerical computation is done with 3156 triangles on ∂D and 2862 on ∂B . For the numeric computation of the point source approximation we perform a surface grid of ∂G consisting of 3156 triangles by the commands

```
testdomain=sphere2(0.65, [-0.5,0,0]);
```

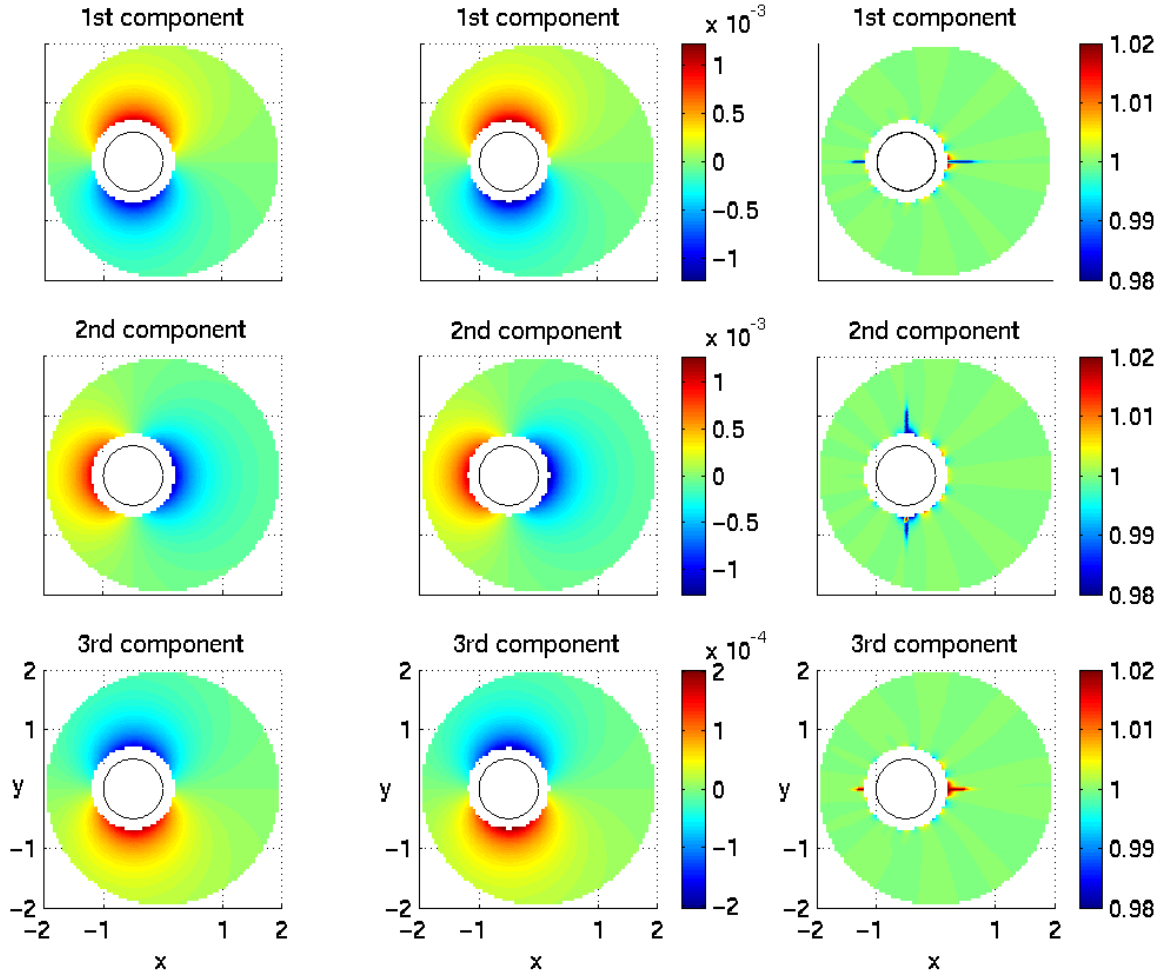



Figure 3.3: components of $\tilde{\mathbf{w}}$ (left) compared to the components of \mathbf{w} (middle) on the xy -plane and $\frac{\tilde{\mathbf{w}}(z_k)}{\mathbf{w}(z_k)}$ for a spherical test domain (white)

```
tdgrid=meshinit(fem,'Hmax',0.065);
```

We compare the fields \mathbf{w} and $\tilde{\mathbf{w}}$ on the xy -plane. Thus, we produce an equally spaced grid of 81×81 points in the plane $\{(x, y, 0)^t \mid x, y \in [-2, 2]\}$ and pick out the points in G . For each of these grid points numbered by z_k we compute

$$a(\cdot, z_k) = (\alpha \mathcal{I} + \mathcal{S}_{BG}^* \mathcal{S}_{BG})^{-1} \mathcal{S}_{BG}^* \Phi(\cdot, z_k) \quad (3.61)$$

and $\tilde{\mathbf{w}}(z_k)$ as defined by (3.58). The regularization parameter α is set to 10^{-13} .

As we can see, these are very good approximations. Whenever $\bar{D} \subset G$, the reconstructed field and the exact field coincide very well. We want to verify this statement with another choice of the test domain. For the next example let G be an ellipsoid with semiaxis 1.05 in x -direction and 0.67 in y, z -direction centered at the origin. We remark that \bar{D} is enclosed by ∂G for this configuration. Here we build up a surface grid by the FEMLAB commands

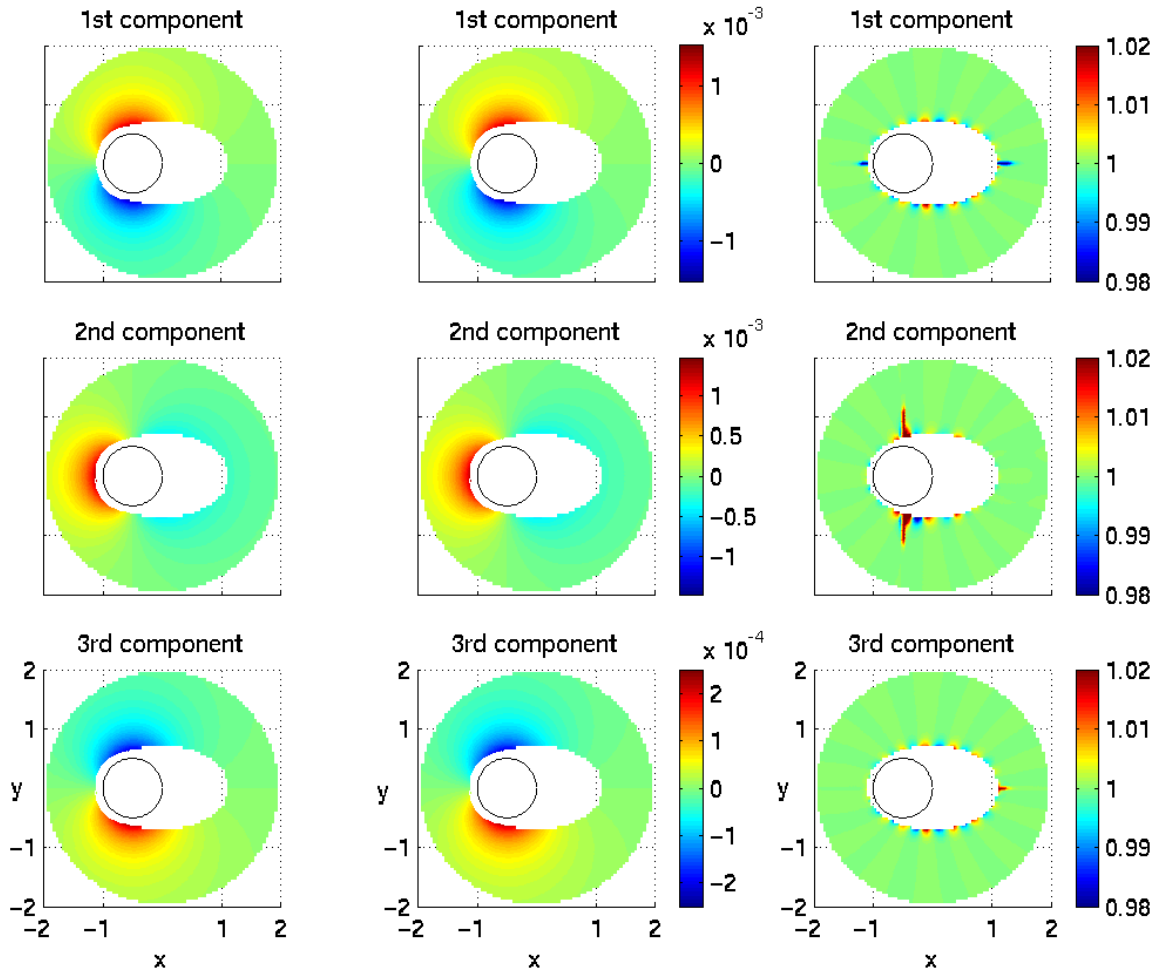


Figure 3.4: components of $\tilde{\mathbf{w}}$ (left) compared to components of \mathbf{w} (middle) and $\frac{\tilde{\mathbf{w}}(z_k)}{\mathbf{w}(z_k)}$ on the xy -plane for an elliptic test domain

```
testdomain=ellipsoid2(1.05,0.67,0.67);
tdgrid=meshinit(fem,'Hmax',0.067);
```

Figure 3.4 represents the components of $\tilde{\mathbf{w}}, \mathbf{w}$, and $\mathbf{w}(z_k)/\tilde{\mathbf{w}}(z_k)$ again. The functions $\tilde{\mathbf{w}}$ and \mathbf{w} coincide very well as we can see in columns 1 and 2. Column 3 highlights the quantity and the location of the differences which are in a 2-percent range and located close to the boundary ∂G .

The question arises what happens when $\bar{D} \not\subset G$. The two examples below show the behavior of the reconstructed field $\tilde{\mathbf{w}}$. In the first case, G is a cube of length 1 centered at the origin, and D is the ball from scene 1 again. Then we have $\bar{D} \cap G \neq \emptyset$ and $\bar{D} \not\subset G$. In the second case, we choose a spherical test domain of radius 0.5 centered at $0.4 \cdot (1, 1, 1)^t$ such that $\bar{D} \cap G = \emptyset$. Column 1 and column 2 of Figure 3.5 show the field $\tilde{\mathbf{w}}$ for the case 1 and 2 respectively on the xy -plane whereas the column 3 shows the exact field \mathbf{w} .

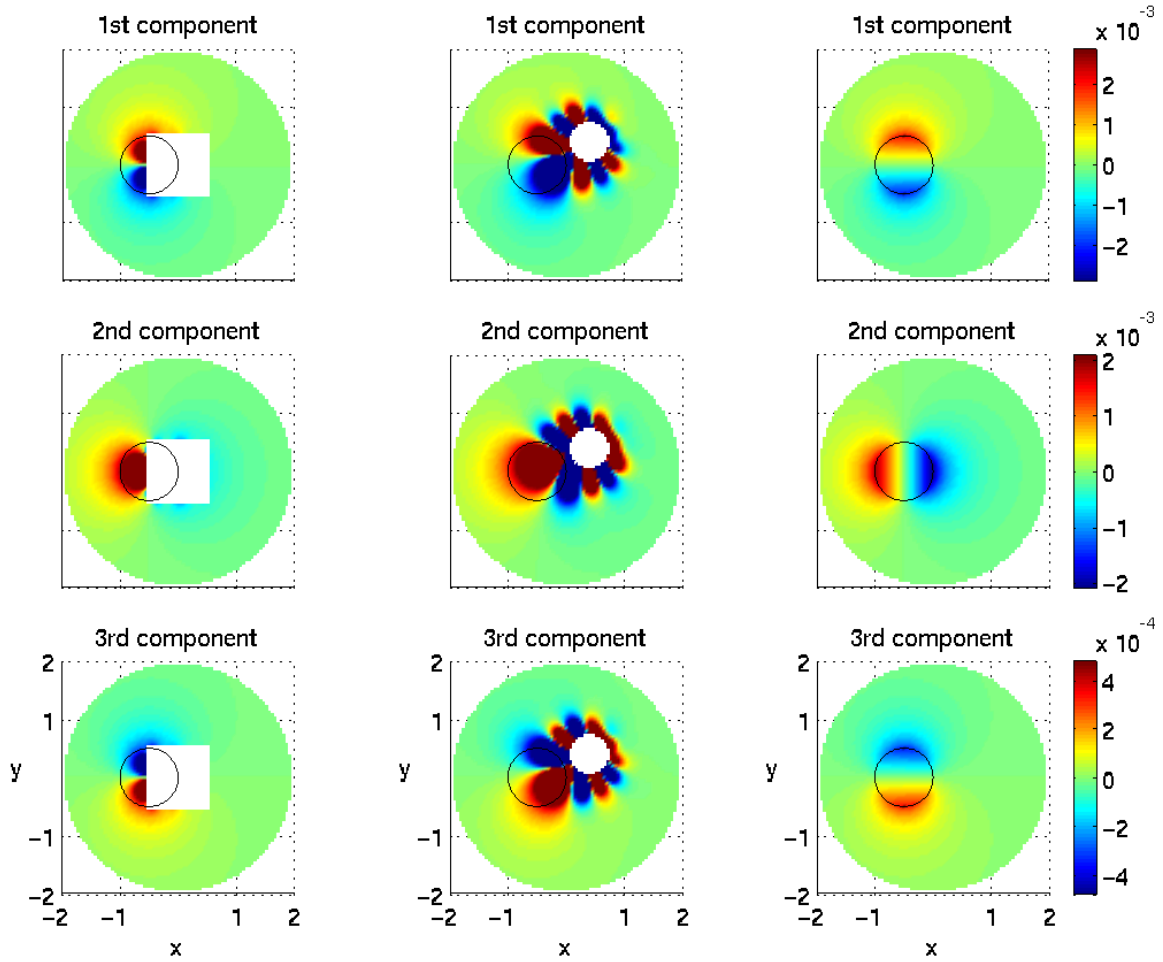


Figure 3.5: components of $\tilde{\mathbf{w}}$ for two different test domains (left,middle) compared to components of \mathbf{w} on the xy -plane

The scale of each row is set to the range of \mathbf{w} . Comparing the components $\tilde{\mathbf{w}}_i$ of the left column with the exact values $\mathbf{w}_i, i = 1..3$, we recognize that $\tilde{\mathbf{w}}$ is very enlarged. In general, it seems to reflect the behavior of the exact field in $B \setminus \{\overline{D} \cup \overline{G}\}$ but it blows up in D . Whereas $\tilde{\mathbf{w}}$ in the middle column is a completely other field and has almost nothing in common with the exact field \mathbf{w} .

3.2.2 Numerical Implementation of the Point Source Method

The fact that the field $\tilde{\mathbf{w}}$ blows up when $\overline{D} \not\subset G$ can be used to approximate \mathbf{w} in (almost) all of $B \setminus \overline{D}$. The point source method is such an algorithm. As mentioned in the introduction of this Section we want to transfer the results of the point source method applied to obstacle scattering, and thus, we should give a brief summary. The behavior of the reconstructed fields for the point source method and other applications such as inverse scattering and impedance tomography can be found in [Po1], [Po2], [Luke], [ErPo],

and many more. Firstly, the point source method was designed for field and domain reconstruction in scattering theory with the knowledge of the boundary condition. In [ErPo], the authors apply the point source method to the impedance tomography, i.e. the electric field is reconstructed from the voltages of one injected current. They choose spherical test domains G_z depending on the point source $z \notin G_z$ and attach G_z in a certain direction of z . Then they perform the point source approximation for all $z \in B$ and some directions to reconstruct the electric field. Further, they detect the boundary of a perfectly conducting inclusion as the zero-levelset of the reconstructed total electric field. For our case as well as for the impedance tomography of [ErPo], one has to decide whether the reconstruction of the single layer potential over the unknown domain ∂D is large or not. The authors of [ErPo] additionally know that the total electric field which is the sum of two boundary integrals (similar to relation (3.50)) vanishes inside D from the boundary condition, but we only know that the field $\mathcal{W}\mathbf{j}$ is bounded. Therefore, our decision whether $\tilde{\mathbf{w}}$ is large or not is much more difficult since we do not have something to compare. Altogether, transferring this algorithm, we lose the accuracy in determining the boundary curve, but we are able to perform it independently of the boundary condition on ∂D .

We assume that we have a scalar $L \in (0, 1)$ such that $\text{diam}(D) < 2L$. For every $z \in B$ let $G_z^{(n)}$ be a test domain

$$G_z^{(n)} := \{B_L(p_z) \mid p_z = z + (L + 0.01)d_n\} \quad (3.62)$$

with a normalized direction vector d_n , i.e. $G_z^{(n)}$ is a ball of radius L attached in the direction d_n from z such that $\text{dist}(z, G_z^{(n)}) = 0.01$. In the following numerical examples we take direction vectors

$$d_n := \left(\cos\left(\frac{2\pi n}{8}\right), \sin\left(\frac{2\pi n}{8}\right), 0 \right)^t, \quad n = 1 \dots 8. \quad (3.63)$$

First, let us pick up the scene 1 from Figure 3.1. We test with balls of radius 0.75. First, we calculate $\tilde{\mathbf{w}}(z)$ for the test domains $G_z^{(8)}$ with $d_8 = (1, 0, 0)^t$ for all admissible z , i.e. for all z such that $\overline{B_L(p_z)} \subset B$. The first column of Figure 3.6 illustrates the three components of $\tilde{\mathbf{w}}(z)$ on the xy-plane. The scale is set to $[-C_m, C_m]$ according to the scale of plot 3.2, so we are able to compare the results with the exact field \mathbf{w} . Next, we perform the point source approximation for the test domains $G_z^{(4)}$ with direction vector $d_4 = (-1, 0, 0)^t$. Here, the balls are attached 'left' from z with a distance 0.01. The resulting field $\tilde{\mathbf{w}}(z)$ on the xy-plane is reflected by the second column of Figure 3.6. The third and fourth columns of Figure 3.6 illustrate $\tilde{\mathbf{w}}(z)$ where we have attached the balls in positive and negative y-direction from z . For every $n = 1 \dots 8$ we call the region

$$E_n := \left\{ z \in B \mid \overline{D} \subset G_z^{(n)}, \overline{G_z^{(n)}} \subset B \right\} \quad (3.64)$$

enlighted area. It is the region where the approximation $\tilde{\mathbf{w}}(z) \approx \mathbf{w}(z)$ holds. One can see in Figure 3.6 that the values blow up outside of the enlightened areas and the sign changes very rapidly.

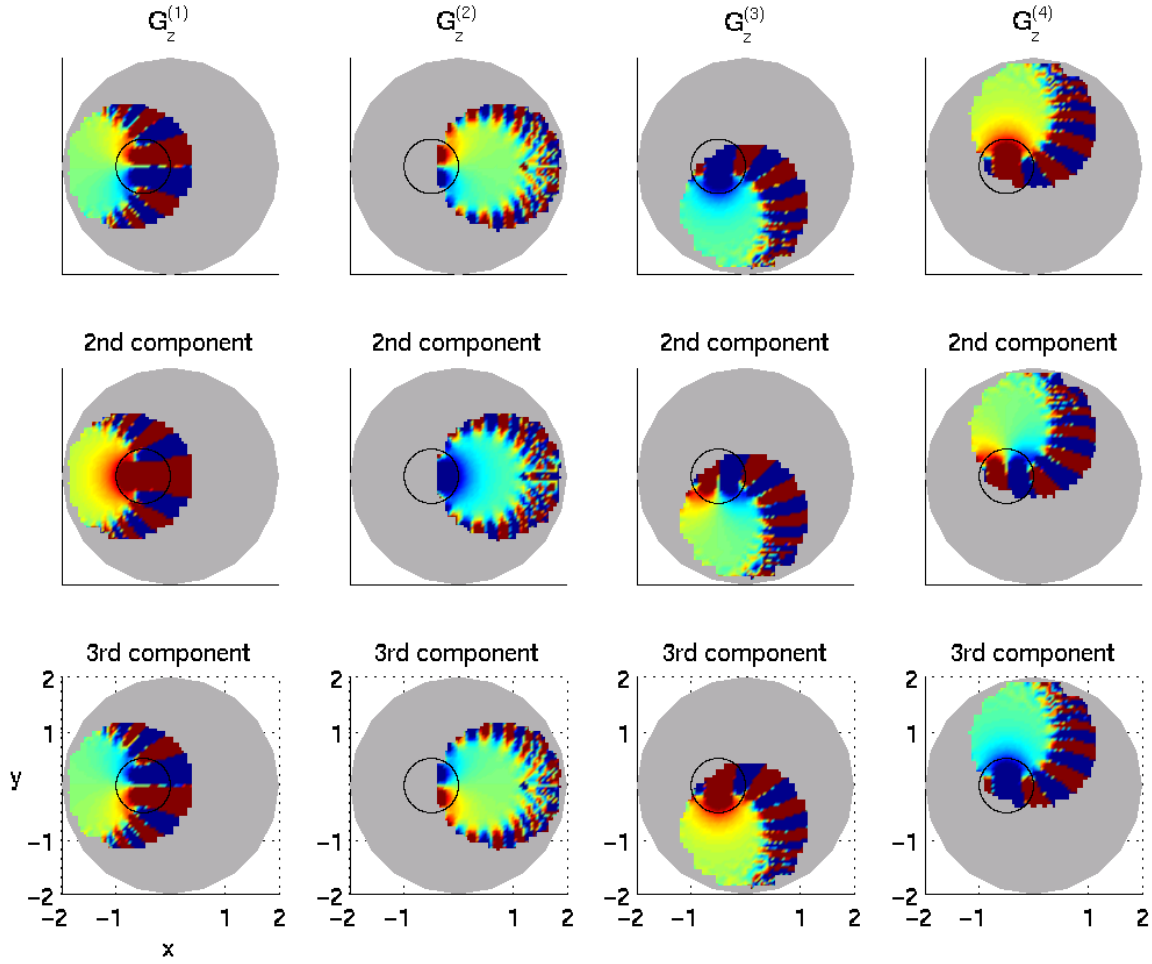


Figure 3.6: $\tilde{\mathbf{w}}(z)$ for the test domains $G_z^{(k)}$, $k = 8, 4, 2, 6$ on the xy -plane

The results for the 8 direction vectors can be sampled and yield a pretty good approximation of the exact field \mathbf{w} . Figure 3.7 shows a composition of the results for d_n , $n = 1 \dots 8$. In detail, we divide the slice in 8 areas Ω_n which are the 8 circle sectors

$$\Omega_n = \left\{ x = \begin{pmatrix} \cos t - 0.5 \\ \sin t \\ 0 \end{pmatrix} \parallel \frac{4\pi n - 1}{16} \leq t < \frac{4\pi n + 1}{16} \right\}. \quad (3.65)$$

If $z \in \Omega_n$ we take $\tilde{\mathbf{w}}(z)$ from the test with direction vector d_n . Putting \mathbf{w} into the middle column of Figure 3.7 we are able to compare the values of the enlightened area with the exact ones. The right column shows $\tilde{\mathbf{w}}(z_k)/\mathbf{w}(z_k)$. Looking at the scale, the relative error of the enlightened area is in a 5-percent range, mostly much smaller (we remark that the horizontal line in the first component of the third column is the region where the exact values are almost zero, therefore $\tilde{\mathbf{w}}/\mathbf{w}$ is increased there, the same problem occurs in the second and third component).

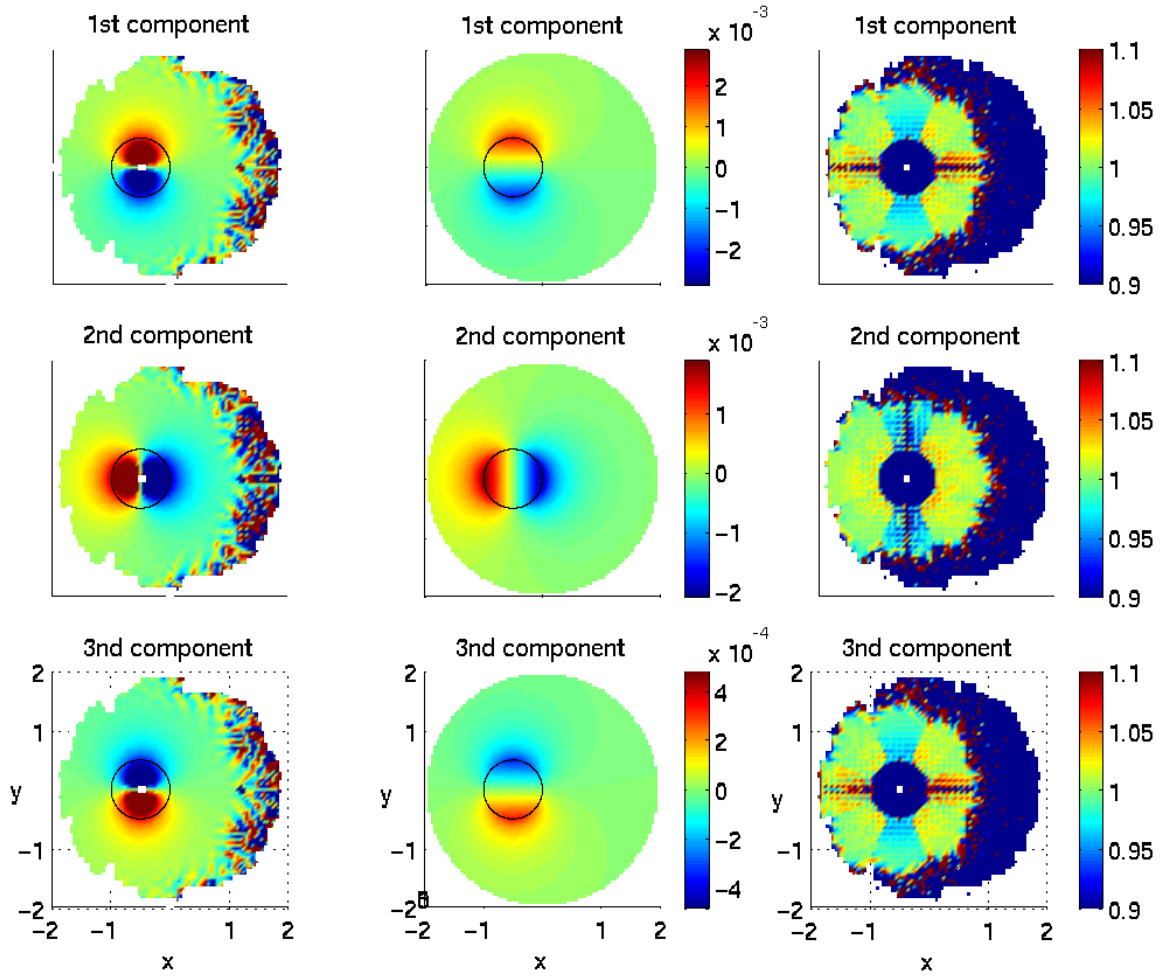
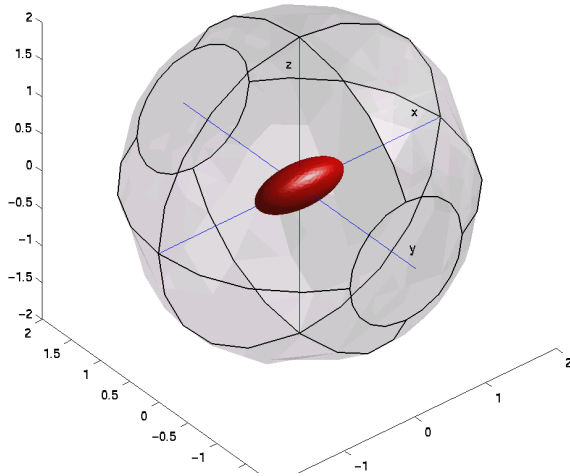


Figure 3.7: composition of the test results with the direction vectors $d_n, n = 1 \dots 8$ (left) compared to the exact field \mathbf{w} (middle) and $\frac{\tilde{\mathbf{w}}(z)}{\mathbf{w}(z)}$

At this stage we turn to the computational cost. For every $B_L(p_z) \in G_z^{(n)}, n = 1 \dots 8$ we build a surface grid of 3156 triangles and have to solve the Tikhonov regularization equation (3.61) where the matrix of discretized operator \mathcal{S}_{BG} has 3156×3156 entries. That means, for each direction vector $d_n, n = 1 \dots 8$ and for each admissible z we have to solve such an equation. On the area $[-2, 2] \times [-2, 2]$ in the xy plane, we take a discretization of 81×81 points from which about 500 admissible points z remain. Summarizing, we solve Tikhonov regularization 4000 times, and we need 3 minutes for one solution. It is not possible to manage it in a reasonable time without parallelisation. We put together more than 20 computers and assign the tests of domains $B_L(p)$ to the different processors. This way, we have decreased the time for computation to 10 hours.

One of the biggest advantages of the point source approximation is that the boundary condition is not required. Here, the method works regardless of the value of $\sigma_D \in \mathbb{R}^+$. To accomodate this, we give another numerical example.



Let D be an ellipsoid with semiaxis $0.65; 0.25; 0.25$ and center in the origin. Again, B is a ball of radius 2 also centered at the origin. The conductivities are $\sigma_B = 1, \sigma_D = 2$, so we have a typical transmission problem. The tangential components on ∂B fulfills $\nu \times \mathbf{E} = \nu \times (\text{grad } \Phi(x, p_1) - \text{grad } \Phi(x, p_2))$ with point sources at $p_1 = (0, -2, 2)^t$ and $p_2 = (0, 2, 2)^t$.

Figure 3.8: Scene 2

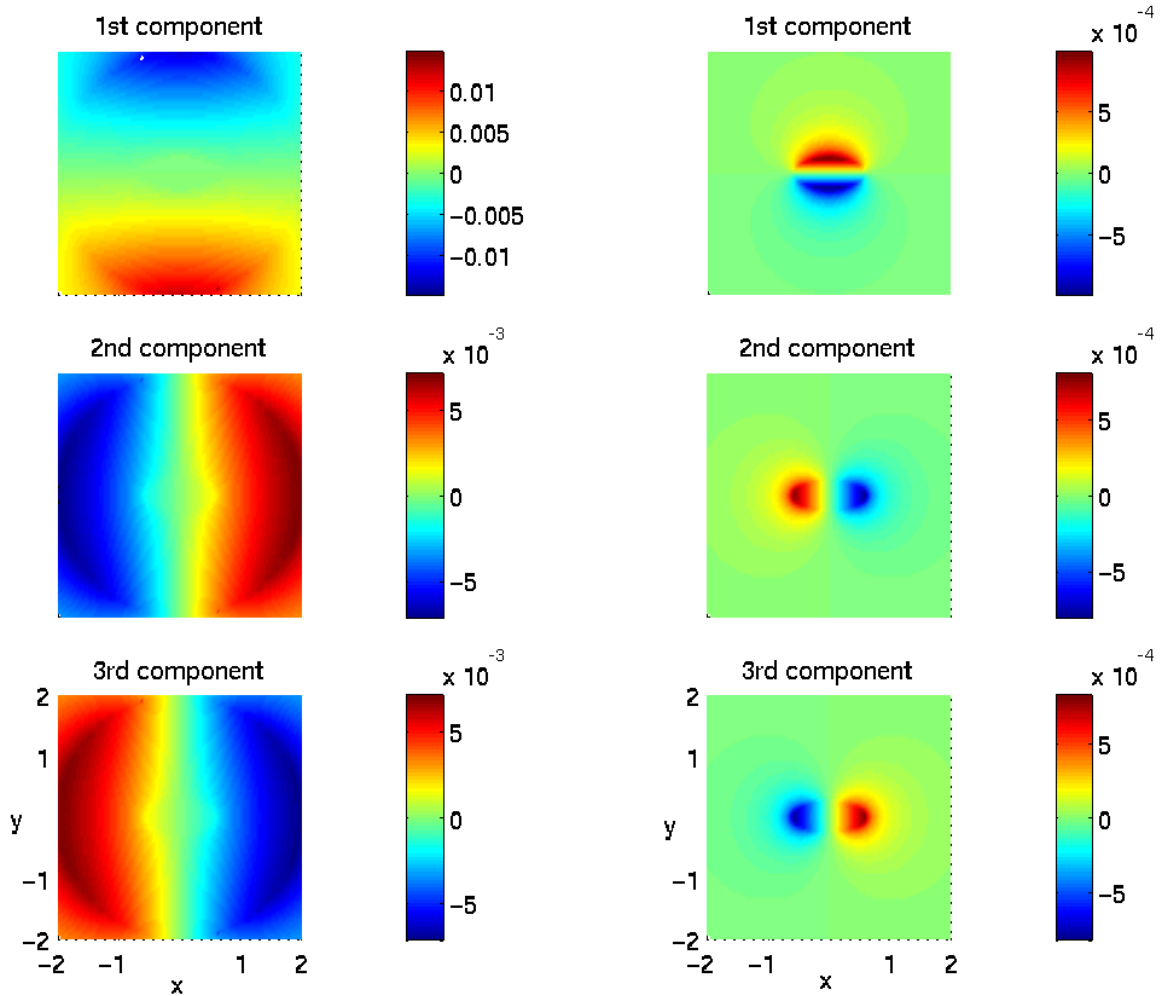


Figure 3.9: Representation of $\mathcal{W}\mathbf{j}$ (left) and \mathbf{w} (right) on the xy-plane

Numerical details: The direct problem has been solved as described in Subsection (3.1.3). For computation we use boundary grids consisting of 2452 triangles on ∂D and 3156 triangles on ∂B , thus we have $2452 + 2 \cdot 3156 = 8764$ unknowns. Afterwards, the magnetic field $\mathcal{W}\mathbf{j}$ has been calculated from equation (3.19). Figure 3.9 shows the components of the fields $\mathcal{W}\mathbf{j}$ and \mathbf{w} on the xy -plane.

The following figures show the reconstruction of the magnetic field by the point source method with spherical test domains of radius 1 which are kept fixed at a distance 0.01 from z . Figure 3.10 shows the results for direction vectors in positive and negative x and y -direction. We observe that for every direction vector the region of admissible points z is

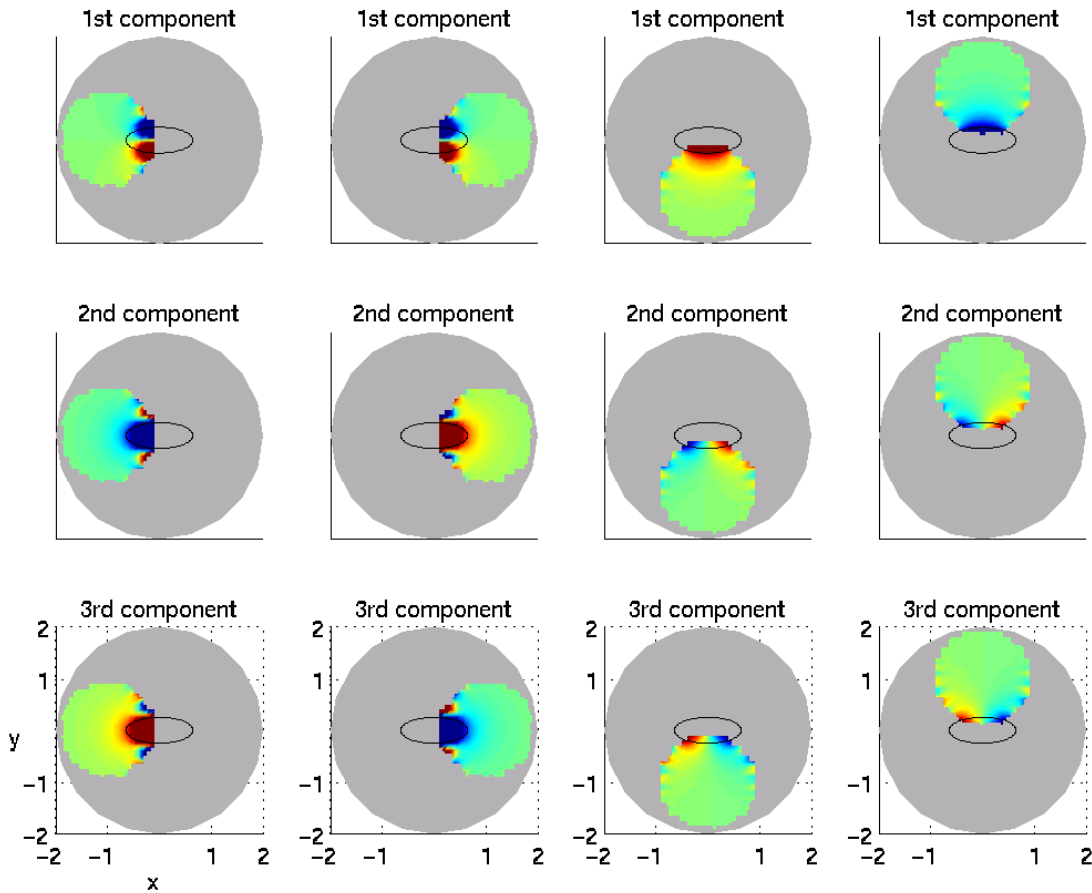


Figure 3.10: $\tilde{\mathbf{w}}$ for test domains $G_z^{(k)}$, $k = 8, 4, 2, 6$ on the xy -plane

much smaller than in scene 1 (see Fig. 3.6) because we have chosen larger test domains. Figure 3.11 illustrates a comparison of the results for the direction vectors d_n , $n = 1 \dots 8$ in comparison to the exact field in the middle column. Again, the right column indicates that the errors are small.

Here, the unknown domain D is an ellipsoid with strong ellipticity in x -direction. We note, that by testing with balls of radius 1 we can not approximate $\tilde{\mathbf{w}}$ near the boundary at all. There is a small area which is not covered by this tests. In this case, we suggest to

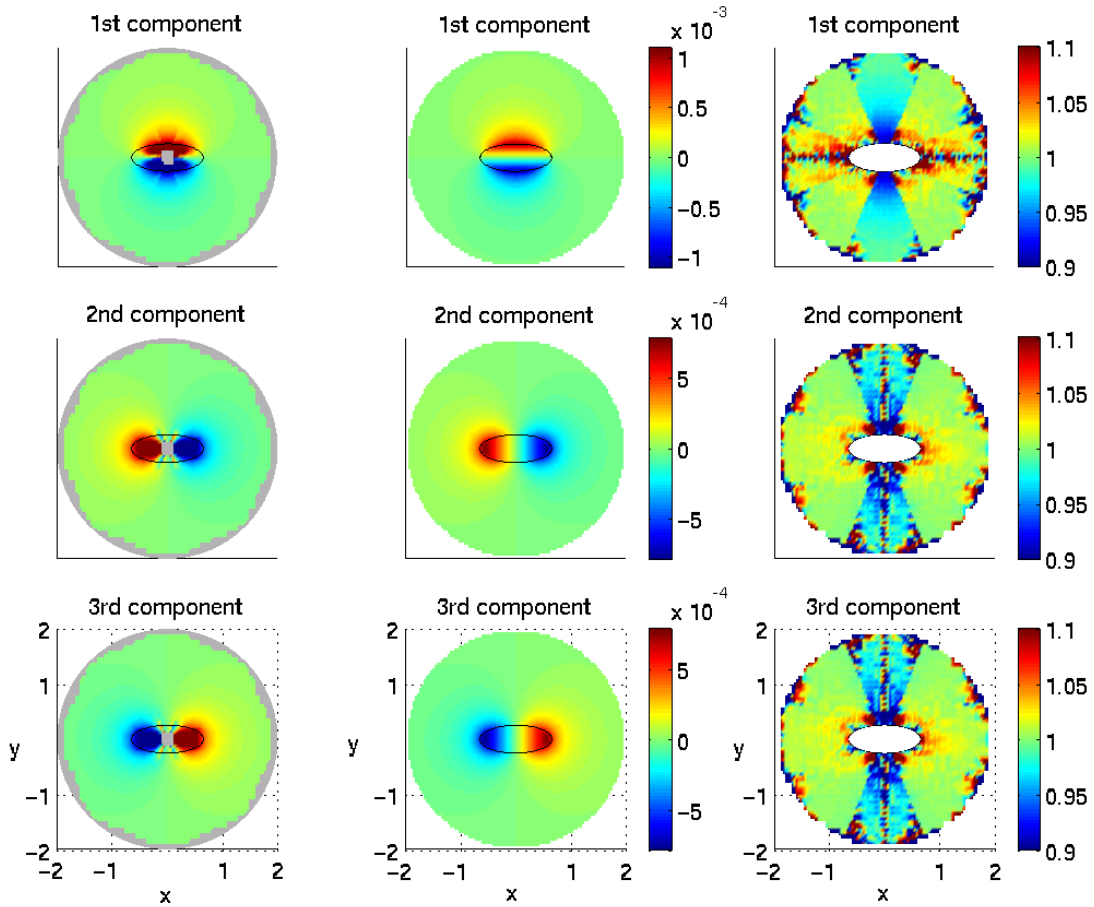


Figure 3.11: Composition of the results for $G_z^{(k)}$, $k = 1 \dots 8$ (left) in comparison to the exact field (middle) and $\frac{\tilde{\mathbf{w}}(z)}{\mathbf{w}(z)}$

choose different test domains for each direction vector. For instance we could test with cuboids or balls with radius different from 1. Furthermore, we could take more direction vectors. For above configuration, it would offer to take balls with larger radius for the negative and positive y-direction.

We conclude this section with some remarks. At present the computational cost is out of the question. Of course, we may decrease the cost by using rougher grids on $\partial G, \partial B$, and on the slices. But for a full approximation, i.e. for computing $\tilde{\mathbf{w}}(z)$ for all admissible z (not only on the xy-plane), this method is inefficient. Looking at the point source method applied to inverse scattering theory in \mathbb{R}^2 , an efficient speed-up is available. For instance in [Po2], Section 2.4, the author needs to solve one Tikhonov regularization for one direction vector when shifting the test domains. It is a consequence of the behavior of the Herglotz wave functions. The goal for future investigations is to transfer this speed-up method to the point source method in magnetic tomography, and it seems possible by choosing another fundamental function but $\Phi(\cdot, z)$.

3.3 Shape Reconstruction by the No Response Test

Originally, the no response test was developed to locate scatterers in inverse obstacle scattering (see for instance [LuPo]). Here, we transfer the basic ideas and perform the no response test to the magnetic tomography. In contrast to the computation in [LuPo], we investigate a three dimensional problem and have a different fundamental solution (here $\Phi(x, y)$). Moreover, we reconstruct the shape of the inclusion D without the knowledge of the conductivity σ_D , i.e. without the knowledge of the boundary condition on ∂D . The key for the application of the response test to the magnetic tomography are the formulas of Section 3.2 on the point source approximation

$$(\mathcal{W}\mathbf{j})(x) = (\sigma_B - \sigma_D)\vec{\mathcal{S}}_D(\nu \times \mathbf{E}) - \sigma_B\vec{\mathcal{S}}_B(\mathbf{e})(x) \quad (3.66)$$

$$\mathbf{w}(x) := (\mathcal{W}\mathbf{j})(x) + \sigma_B\vec{\mathcal{S}}_B(\mathbf{e})(x) = (\vec{\mathcal{S}}_D\mathbf{t})(x) \quad (3.67)$$

$$\int_{\partial B} \mathbf{w}(x)a(x) ds(x) = \int_{\partial D} (\mathcal{S}_{BD}a)(y)\mathbf{t}(y) ds(y), \quad (3.68)$$

where the conductivity σ_B , the tangential component of the electric field $\mathbf{e} := \nu \times \mathbf{E}|_{\partial B}$ and the magnetic field $\mathbf{h} := (\mathcal{W}\mathbf{j})|_{\partial B}$ are known. For probing with functions $a \in L^2(\partial B)$ the value $\int_B \mathbf{w}a ds$ is called the *response of a* . The relation (3.68) implies that the response is small if $\mathcal{S}_{BD}a$ is small on \overline{D} . Since the boundary of D is unknown, we again work with test domains. Let G be a test domain with $\overline{G} \subset B$. If G contains \overline{D} then for all test functions a such that $\mathcal{S}_{BD}a$ is small on G and large outside the integral $\int_{\partial B} \mathbf{w}a ds$ is small too. If $\overline{D} \not\subset G$ then there exists a function a such that (3.68) is large. Consequently, the unknown domain D is contained in all test domains for which the response of all small test functions a is small. This is the basic idea of the no response test.

In Subsection 3.3.1 we give a more detailed discription of the no response test. We explain how we perform this test algorithm to some test domain, especially we answer the question for the choice of the test functions a . The numerical examples of Subsection 3.3.2 show that in principle we are able to reconstruct the shape of conducting inlucions as well as non-conducting inclusions. We present two approaches of the no response test where we give two different strategies for the choice of the test domains.

3.3.1 Realization of the No Response Test

For a test domain G the test algorithm is given by

Algorithm 3.10 *The test algorithm decides whether a certain test domain is called positive, i.e. we mean that it contains the unknown domain D , or negative.*

- Let G with $\overline{G} \subset B$ be a test domain, for $\epsilon > 0$ define

$$M(G, \epsilon) := \left\{ a \in L^2(\partial B) \mid \|(\mathcal{S}_{BD}a)|_G\|_{C(\overline{G})} \leq \epsilon \right\}. \quad (3.69)$$

- *Calculate*

$$I(G, a) := \int_{\partial B} \mathbf{w}(x)a(x) ds(x), \quad (3.70)$$

$$I_\epsilon(G) := \sup_{a \in M(G, \epsilon)} I(G, a). \quad (3.71)$$

- *Choose a cut off parameter $C > 0$ and call G positive if $I_\epsilon(G) < C$ otherwise negative.*

Here, $M(G, \epsilon)$ is the set of all test functions a such that $\mathcal{S}_B a$ is small on G . The scalar $I(G, a)$ is called the *response* of the test function a to the test domain G . If the maximum response is smaller than a given cut off parameter then G is called positive and contains the unknown domain D . We perform this test algorithm for various test domains. The intersection of all positive test domains is an approximation on the unknown domain D , i.e. for a family of test domains \tilde{G} we calculate

$$D_{approx} := \bigcap_{\substack{G \in \tilde{G} \\ G \text{ positive}}} G. \quad (3.72)$$

In general, testing certain test domains and calculating the intersection of the positive test domains is denoted as the *no response test*.

The following theorem is a first step toward a theoretical justification.

Theorem 3.11 *If $\overline{D} \subset G$ then we have*

$$\lim_{\epsilon \rightarrow 0} I_\epsilon(G) = 0. \quad (3.73)$$

Proof: Consider the function $\mathcal{S}_B a$ which is harmonic in B . If $\|(\mathcal{S}_B a)|_G\|_{C(\overline{G})} \leq \epsilon$ and $\overline{D} \subset G$, then by the maximum-minimum principle follows that $\|(\mathcal{S}_B a)|_D\|_{C(\overline{D})} \leq \epsilon$. Using the definition of the response (3.70) and equation (3.53) we estimate

$$\begin{aligned} |I(G, a)| &\stackrel{(3.70)}{=} \left| \int_{\partial B} \mathbf{w} a ds \right| \stackrel{(3.53)}{=} \left| \int_{\partial D} (\mathcal{S}_B a) \mathbf{t} ds \right| \\ &\leq \epsilon \int_{\partial D} |\mathbf{t}| ds = \epsilon |\sigma_B - \sigma_D| \int_{\partial D} |\nu \times \mathbf{E}| ds \end{aligned} \quad (3.74)$$

for all $a \in M(G, \epsilon)$. Since the electric field \mathbf{E} is bounded, the response $I(G, a)$ vanishes for $\epsilon \rightarrow 0$ and the statement follows from definition (3.71). ■

The authors of [LuPo] are able to prove that their maximum response $I_\epsilon(G)$ is unbounded if $\overline{G} \cap \overline{D} = \emptyset$. If we have one pair of data (the far field of one incident wave or the magnetic field of one voltage, respectively), the question is open if the implication

$$D \not\subset G \implies I_\epsilon = \infty \quad (3.75)$$

is true for the obstacle scattering as well as for the magnetic tomography. The behavior of the response indicates that we should be able to reconstruct a 'minimal' or 'characteristic' set of D . For instance, in [LuPo], the authors prove that a region called corona is uniquely determined. Here, we base the no response test upon two observations. Firstly, Theorem 3.11 implies that I_ϵ is small when D is contained in the interior of the test domain G . Secondly, if $D \setminus \overline{G}$ is not empty then I_ϵ is large. The last observation can be explained by the following (heuristic) argumentation. Consider for $z \in B \setminus \overline{G}$ the point source approximation $\mathcal{S}_B a(\cdot, z) \approx \Phi(\cdot, z)$ on G calculated by the Tikhonov regularisation (3.57). If $\overline{D} \subset G$ then $\int_{\partial B} \mathbf{w} a(\cdot, z) ds$ is an approximation of $\mathbf{w}(z)$, but if $D \setminus \overline{G} \neq \emptyset$ then there exists a point $z \in D \setminus \overline{G}$. In this case, the numerical study on the point source approximation in Subsection 3.2 has shown that $\int_{\partial B} \mathbf{w} a(\cdot, z) ds$ blows up.

This observation suggests a realization of the no response test. For a test domain G , we restrict the test algorithm to functions $a(\cdot, z_k)$ approximating the fields $f_k \Phi(\cdot, z_k)$ on G of point sources $z_k \in B \setminus \overline{G}$. Thereby, the scalar f_k is a scaling factor such that

$$\|(\mathcal{S}_B a(\cdot, z_k))|_G\|_{C(\overline{G})} \leq \epsilon. \quad (3.76)$$

For an effective test, we position sufficiently many points $z_k, k = 1 \dots K$ very close to ∂G , i.e. we position the points equally distributed on a parallel surface ∂G_h with $h > 0$. Then we call the test domain G positive if

$$I_\epsilon(G) = \sup_{k=1 \dots K} I(G, a(\cdot, z_k)) \quad (3.77)$$

is smaller than a given threshold $C \in \mathbb{R}^+$ and negative otherwise.

3.3.2 Numerical Examples of the Shape Reconstruction

There are various strategies to perform the no response test, and the result as well as the convergence rate depends on the used test domains and on the strategy. A-priori information about the shape of the unknown domain or the location can be used for the no response test directly. For example, if we know that D is a cuboid then we should choose cuboid-like test domains. In this Subsection we present two strategies called *Approach A* and *Approach B*. The second one is a global search strategy, it is more suitable to find the location of the unknown domain. The first one is a local search strategy which can be used to determine the shape of D . An iterative combination of both strategies is a method which works pretty well even without a-priori information.

Algorithm 3.12 (No Response Test, Approach A) *Let $\epsilon > 0$.*

- *Choose some appropriate test domain G which is large enough, i.e. $\overline{D} \subset G + p$ for some $p \in \mathbb{R}^3$. Choose a point p_0 , N normalized directions d_n , and define the family of admissible test domains*

$$\tilde{G} := \{G + p \mid G + p \subset B, p = p_0 + t d_n, t \in \text{real}\}, \quad (3.78)$$

which are generated by the translation of G in all directions d_n from p_0 .

- Choose K points $z_k \in \partial G_h$ and calculate

$$a(\cdot, z_k) := f_k(\alpha \mathcal{I} + \mathcal{S}_{BG}^* \mathcal{S}_{BG})^{-1} \mathcal{S}_{BG}^* \Phi(z_k, \cdot), k = 1 \dots K \quad (3.79)$$

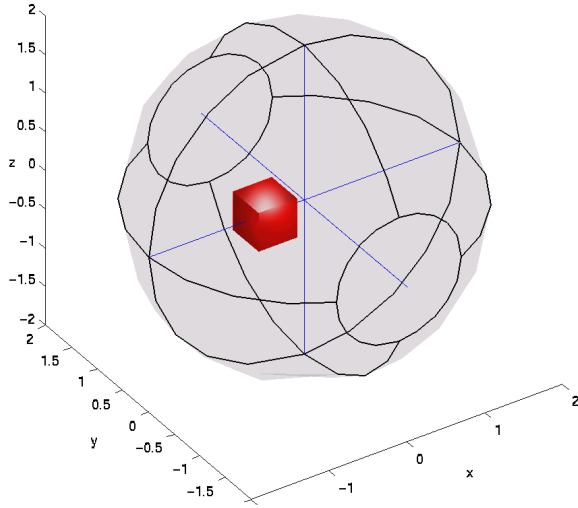
with a scaling factor $f_k \in \mathbb{R}$ such that $\|(\mathcal{S}_B a(\cdot, z_k))|_G\|_{C(\bar{G})} \leq \epsilon$.

- Choose a cut off parameter $C > 0$. For each $G \in \tilde{G}$ decide whether G is positive or negative accordant to Algorithm 3.10.

- Evaluate

$$D_{approx} := \bigcap_{\substack{G \in \tilde{G} \\ G \text{ positive}}} . \quad (3.80)$$

We illustrate the Approach A with the following example.



Let B be a ball of radius 2 centered at origin. Further, let D be a cube of length 0.5 centered at $(-0.5, 0, 0)^t$. The domain D is a conducting media with $\sigma = 1000$. Thus, the electric field satisfies the transmission boundary condition on ∂D . On ∂B , we have boundary data $\nu \times \mathbf{E} = \nu \times (\text{grad } \Phi(x, p_1) - \text{grad } \Phi(x, p_2))$ with point sources at $p_1 = (0, 0, -2.5)^t$ and $p_2 = (0, 0, 2.5)^t$.

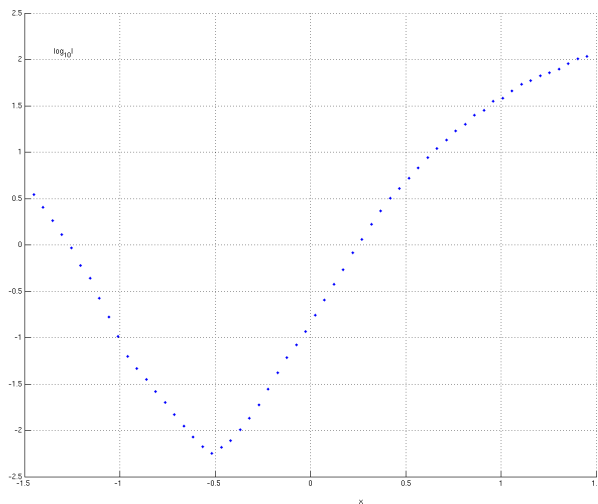
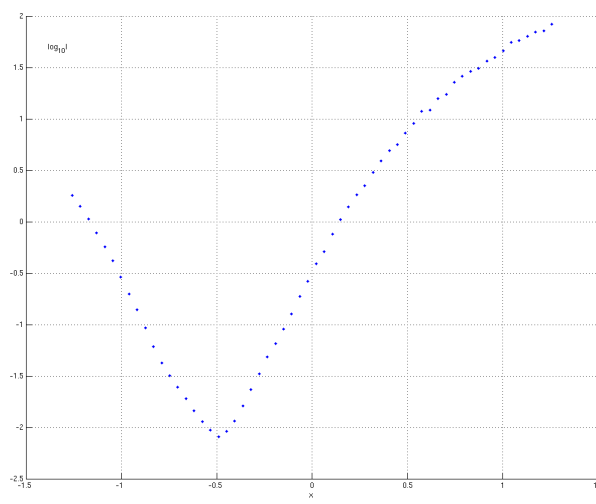
Figure 3.12: Scene 3

We test with the family of test domains

$$\tilde{G}^{(1)} = \left\{ B_R(z_k) \mid R = 0.5, z_k = (-1.5 + \frac{k}{60}, 0, 0)^t, k = 1 \dots 59 \right\}, \quad (3.81)$$

$$\tilde{G}^{(2)} = \left\{ Q_L(z_k) \mid L = 0.7, z_k = (-1.5 + \frac{k}{60}, 0, 0)^t, k = 1 \dots 59 \right\} \quad (3.82)$$

consisting of 60 balls of radius $R = 0.5$ and of 60 cubes of length $L = 0.7$, respectively, shifted along the x-direction. The following figures show the logarithmic values of $I_\epsilon(B_R(z_k))$ and $I_\epsilon(Q_L(z_k))$ for $x_k = -1.5 + k/60$.

Figure 3.13: $\log_{10} I(\tilde{G}^{(1)}, a(\cdot, z_k))$ Figure 3.14: $\log_{10} I(\tilde{G}^{(2)}, a(\cdot, z_k))$

Numerical details: In detail, we set $\epsilon = 0.001$. For each ball, we have a boundary grid of 4496 triangles. Let c_k denote the center of each triangle, then we set $z_k = c_k + 0.001 \cdot \nu_k$ and obtain 4496 point sources at a distance of (round about) 0.001 from the boundary ∂G . Then we solve the equation (3.79) for 4496 right hand sides. Afterwards we have calculated the corresponding factors f_k and $I_\epsilon(B_R(z_k))$ which is plotted in Figure 3.13 for each x_k on a logarithmic scale. The boundary grid of each cube consists of 2014 triangles. In the same manner, we have calculated point sources z_k , functions $a(\cdot, z_k)$ and $I_\epsilon(Q_L(z_k))$.

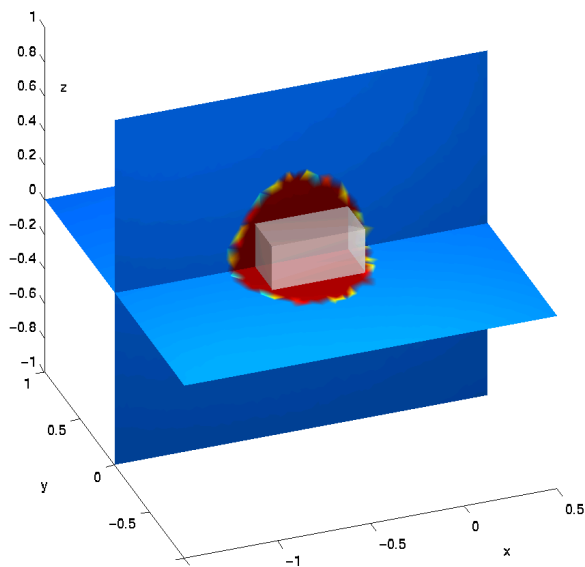


Figure 3.15: Sampling method with spherical test domains

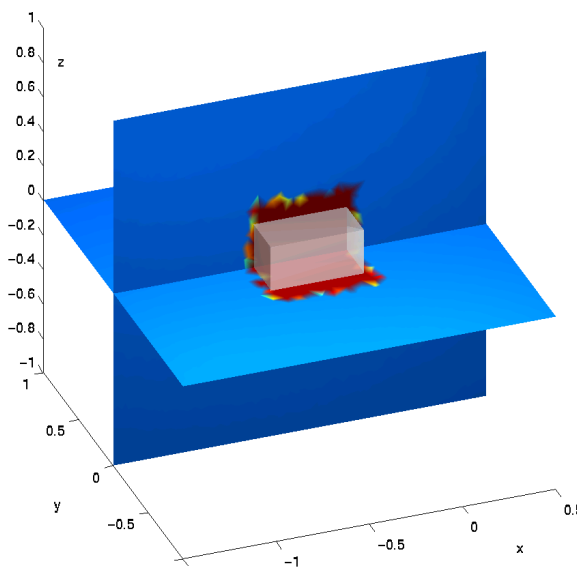


Figure 3.16: Sampling method with cubic test domains

Although there is a small interval for the cut off parameter, the crucial point for the sampling is the choice of an appropriate threshold. If we choose the parameter too small no test domain would be positive, if we choose the parameter too large, the intersection of positive test domains would be empty. Look at Figures 3.13 and 3.14 and choose cut off parameters 10^{-2} to gain an approximation D_{approx} which is represented in Figures 3.15 and 3.16, respectively.

Of course, we can not expect pretty good approximation in the case where we test with spheres and the unknown domain D is a cuboid. The comparison of Figures 3.15 and 3.16 illustrates that a-priori information about the shape of an inclusion are a big advantage for the reconstruction. Figure 3.16 shows that if we translate the test cubes defined in (3.82) along the x-direction we are able to reconstruct the side surfaces at $x = 0.25$ and $x = 0.75$ precisely.

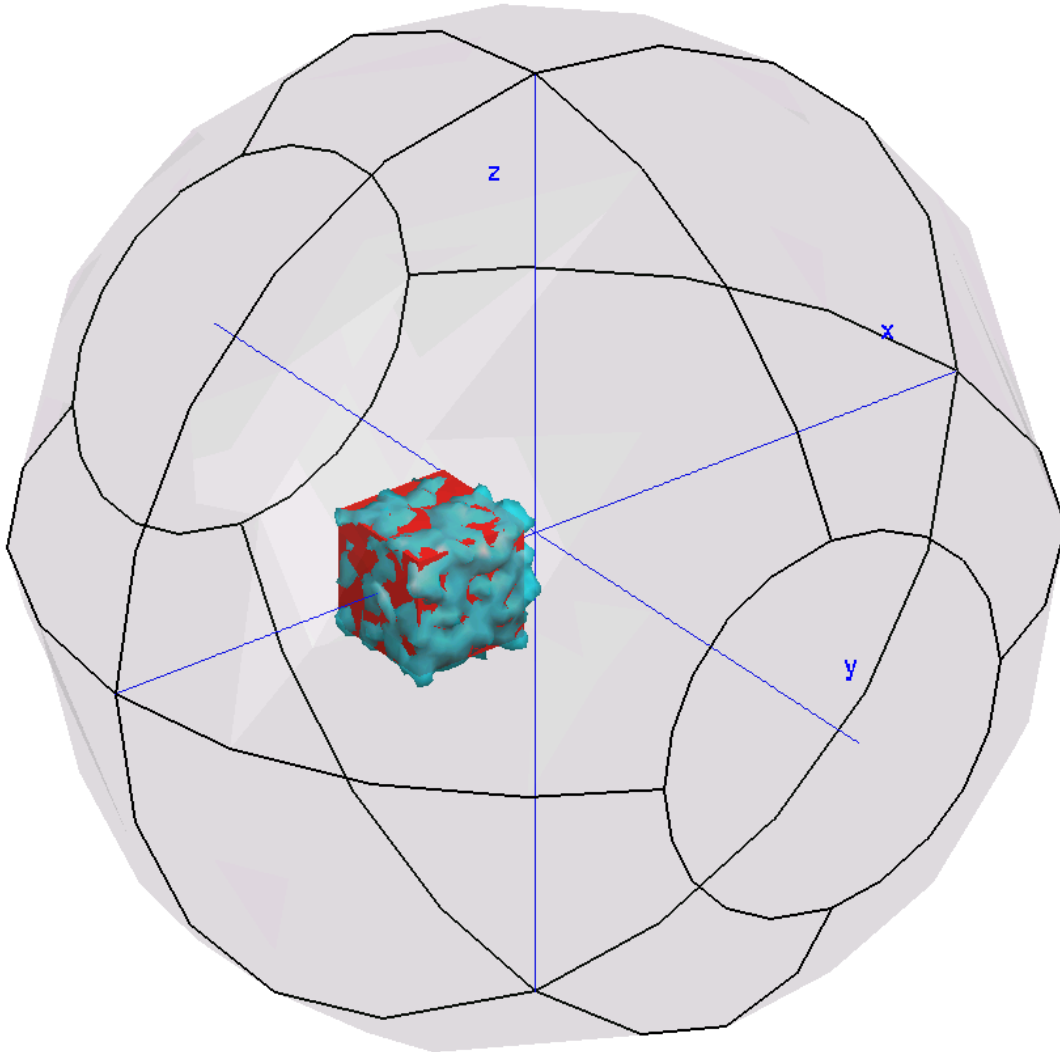


Figure 3.17: Reconstructed domain (light blue) compared to the original (red)

Next, we restart Approach A with the directions $d_1 = (0, 1, 0)^t, d_2 = (0, 0, 1)^t$. We translate test cubes of length $L = 0.7$ along the y,z-directions. Together with the result for the direction $(1, 0, 0)^t$, we obtain an accurate reconstruction D_{approx} of D . The Figure 3.17 illustrates the unknown domain D (red) compared to D_{approx} (light blue).

We turn to the computational cost for the no response test. For every test domain G , we solve the Tikhonov regularization equation (3.79). The point sources z_k close to ∂G lead to different right hand sides. Thus, we solve the equation once for 4496 right hand sides. The matrix which belongs to the operator $\mathcal{S}_{BG}^* \mathcal{S}_{BG}$ has 3156×3156 entries. This computation must be done for 3 directions and 39 domains per direction. Again we use parallelized software algorithms, so the calculations with 20 computers takes about 20 minutes.

In general, we have no information about the position of D . Since Approach A is a local method, we present the global method we call *Approach B*.

Algorithm 3.13 (No Response Test, Approach B) *We look for the minimal radius R_{min} such that $\bar{D} \subset B_{R_{min}}(p_0)$ by the following steps*

- Choose some point p_0 (if we carry out the Approach B the first time, we set $p_0 = (0, 0, 0)^t$). Let R denote the maximal radius such that $B_R(p_0) \subset B$. Calculate the response $I_\epsilon(B_{r_m}(p_0))$ for each $B_{r_m}(p_0), r_m \in (0, R)$.
- Choose a cut off parameter C , then R_{min} is the minimal radius such that $I_\epsilon(B_{r_m}(p_0)) < C$.

The goal of the Approach B is to find the location of the unknown domain D . Developing an iterative algorithm, we may restart Approach B with a new point p_0 . We explain the method by the following example.

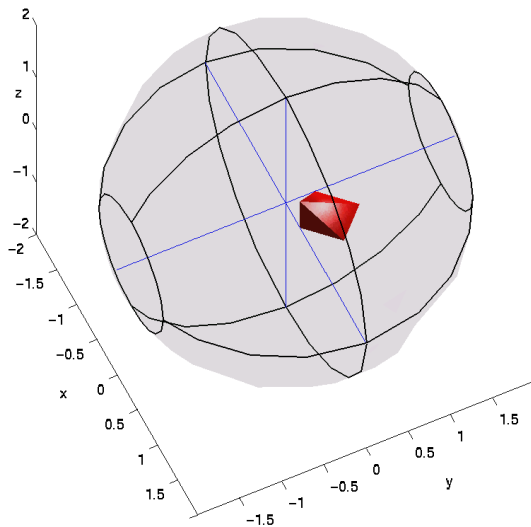


Figure 3.18: Scene 4

Again, let B be the ball with radius 2 and center at origin. Furthermore, let D be an orthogonal pyramid of height 0.5 with a squared base of length 0.5. Two corners of the base are $(\sqrt{2}/4, 0, 0)^t$ and $(0, \sqrt{2}/4, 0)^t$. We have boundary condition of Neumann type on ∂D and boundary data $\nu \times \mathbf{E} = \nu \times \text{grad } \Phi(\cdot, p)$ with source point $p = (0, 0, 3)^t$ on ∂B .

Following the Approach B, we test the family of domains

$$\left\{ B_{r_m}(0) \mid r_m = \frac{m}{30}, m = 1 \dots 59 \right\}. \quad (3.83)$$

Numerically, we build a boundary grid for every $B_{r_m}(0)$, calculate the point sources z_k as mentioned above, the functions $a(\cdot, z_k)$ and $I_\epsilon(B_{r_m}(0)) = \sup_k I(B_{r_m}(0), a(\cdot, z_k))$. These values are shown in Figure 3.19 for every r_m . Choose a cut off parameter 10^{-10} and the corresponding radius $R = 0.8$. Figure 3.20 is a color-plot of the values $\int_{\partial B} \mathbf{w} a(\cdot, z_k) ds$ plotted at the point sources z_k , i.e. we see that the point source approximation $\tilde{w}(z_k)$ blows up where $z_k \in D \setminus \overline{G}$. This way we obtain a radius R_{min} such that $\overline{D} \subset B_{R_{min}}(0)$.

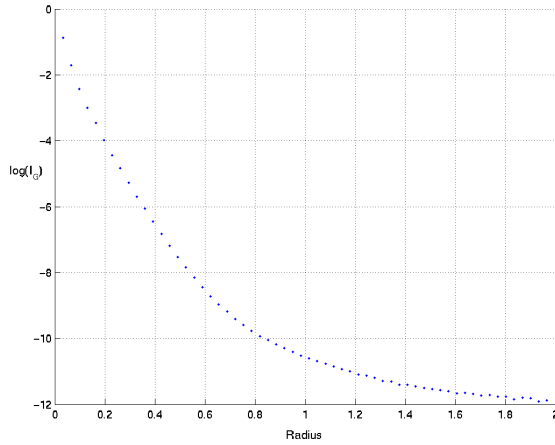


Figure 3.19: $\log_{10} I(B_{r_m}(0), a(\cdot, z_k))$

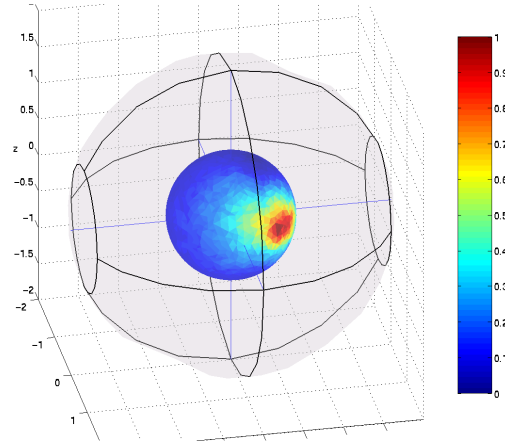


Figure 3.20: $\int_{\partial B} \mathbf{w} a(\cdot, z_k) ds$ on a parallel surface of $\partial B_{R_{min}}(0)$

Now, there are different ways to find a new point p_0 to restart the Approach B. We may continue by covering B with balls of radius R_{min} , evaluating the responses for each ball, and sampling the positive domains. This sampling will lead to a test domain G , either G is just a good approximation on D or we restart the Approach B with an appropriate p_0 in G . A shorter way is the observation that the values $\int_{\partial B} \mathbf{w} a(\cdot, z_k) ds$ evaluated at z_k , i.e. on the parallel surface of $B_{R_{min}}(p_0)$ are largest near ∂D as Figure 3.20 illustrates. We emphasize that this behavior is empirical, but it may decrease the computational cost of the search strategy. For a mathematical justification we should proof the behavior of point source approximation in future investigation. This behavior gives a hint in which region we have to look for more intensively. Then we restart the Approach B with a point p_0 in this region.

The following Figure 3.21 is an approximation we have obtained by combining Approach B and Approach A. We see that the approximation domain D_{approx} and the unknown domain D coincide very well.

Numerical details: Firstly, we take the result of Figure 3.20 to restart the Approach B with a new point $p_0 = (0.4, 0.4, 0.2)^t$. We have achieved a new minimal radius 0.6. Then we have chosen cubic test domains of length 1.2 and have translated it along x,y,z-direction from p_0 according to Approach A. Evaluating the responses we have obtained

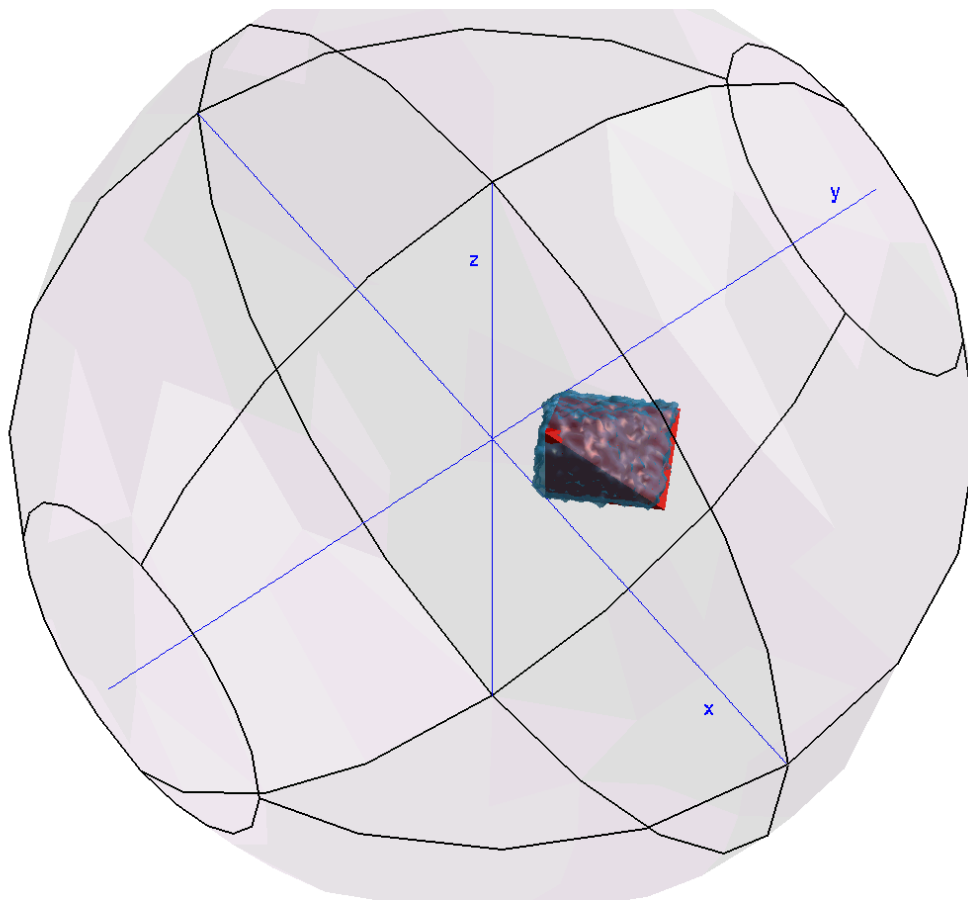


Figure 3.21: Reconstructed domain (light blue) compared to the original (red)

a new point $p_0 = (0.35, 0.35, 0.25)$. Finally, we restart the Approach A with the center p_0 and the direction vectors d_n where d_n are the normalized vectors of all possibilities of $(l, l, l)^t, l = 0, \pm 1, \pm\sqrt{2}$. We note that the surface of the reconstruction domain is not smooth which is a result of our way how we numerically build the intersection of domains. For each domain we build up a volume mesh consisting of sufficiently many points in the interior and at the surface. Then, the intersection is the set of points belonging to each of the domains. In general, this set has not a smooth surface.

Outline

The combination of the Approaches A and B is an iterative multistep method to locate the unknown domain D . In particular, the method does not depend on the type of boundary condition (we have excluded the case of a perfectly conducting inclusion). In contrast to the no response test applied to obstacle scattering as in [Po3] and [LuPo], respectively, we are not able to speed up the Approaches A and B when shifting the test domains. If one succeeds in performing this speed up in magnetic tomography, the Approaches A and B are very efficient methods to detect an unknown inclusion. However, the numerical study

of this section has shown that the no response test works in principle. It is left for future research to increase the performance, for instance by choosing a suitable fundamental solution.

In Section 3.3 we have used the no response test to reconstruct an unknown inclusion D in a conducting media B . Let D_{approx} be the reconstructed domain and G be a test domain with $\overline{D_{approx}} \subset G$, then we may apply the point source method with the test domain G to reconstruct the interior magnetic field in $B \setminus \overline{G}$. Let $\tilde{\mathbf{W}}$ denote the reconstructed magnetic field in $B \setminus \overline{G}$, then by

$$\tilde{\mathbf{j}} = \text{curl } \tilde{\mathbf{W}} + \mathcal{S}^\nabla \mathbf{j} = \text{curl } \tilde{\mathbf{W}} + \text{grad } \mathcal{S}(\nu \cdot \mathbf{j}) \quad (3.84)$$

we are able to reconstruct the current distribution in $B \setminus \overline{G}$. We have established this formula in (2.8) where we used that $\text{div } \mathbf{j} = 0$ in B . The current flux $\nu \cdot \mathbf{j}$ can be calculated by

$$\nu \cdot \mathbf{j} = -2(\mathcal{I} - \mathcal{K}^*)^{-1} \text{DIV } \mathbf{h} \quad (3.85)$$

from the magnetic field $\mathbf{h} := \nu \times (\mathcal{W}\mathbf{j})|_{\partial B}$ on the boundary ∂B (see Corollary 2.24). Summarizing, this work proposes the full reconstruction, i.e. the reconstruction of the inclusion, the interior magnetic field and the current distribution which causes the magnetic field, from the knowledge of the conductivity σ_B , the tangential component of the electric field $\mathbf{e} := \nu \times \mathbf{E}|_{\partial B}$, and the magnetic field $\mathbf{h} := (\mathcal{W}\mathbf{j})|_{\partial B}$ on the boundary ∂B independently from the nature of the inclusion.

Appendix A

Mathematical Background

A.1 Tikhonov Regularization

Reconstruction algorithms often lead to ill-posed equations of the form

$$\mathcal{A}\phi = f \tag{A.1}$$

with a compact operator \mathcal{A} . To solve the equation (A.1) we require regularization schemes as for instance Tikhonov regularization. For an introduction of ill-posed problems we refer to [Kre],[CoKr1] and [EnHaNeu]. In this section, we sum up the relevant results.

The Tikhonov regularization scheme describes a stable method for solving equation (A.1) in a Hilbert space setting, i.e. when \mathcal{A} is a linear and compact operator $\mathcal{A} : X \rightarrow Y$ between Hilbert spaces X, Y . The background is given by the singular value decomposition and Picard's theorem. In preparation for the singular value decomposition we note that an adjoint operator $\mathcal{A}^* : Y \rightarrow X$ exists in the dual space $\langle X, Y \rangle$ based on the scalar products in X, Y and \mathcal{A}^* is uniquely determined. Then the operator $\mathcal{A}^*\mathcal{A} : X \rightarrow X$ is self-adjoint and its eigenvalues form a countable set in $\mathbb{R}^+ \cup \{0\}$ accumulating at most at zero. The non-negative square roots of the eigenvalues of $\mathcal{A}^*\mathcal{A}$ are called *singular values*.

Theorem A.1 (Singular Value Decomposition) *Let $(\mu_n)_{n \in \mathbb{N}}$ be the sequence of singular values of the linear compact operator $\mathcal{A} \neq 0$ in decreasing order with repetitions according to their multiplicity. Then there exist orthonormal vectors $(\phi_n)_{n \in \mathbb{N}}$ in X and $(g_n)_{n \in \mathbb{N}}$ in Y such that*

$$\mathcal{A}\phi_n = \mu_n g_n, \quad \mathcal{A}^*g_n = \mu_n \phi_n \tag{A.2}$$

for all $n \in \mathbb{N}$. For each $\phi \in X$ we have the singular value decomposition

$$\phi = \sum_{n=1}^{\infty} \langle \phi, \phi_n \rangle_X \phi_n + \mathcal{Q}\phi \tag{A.3}$$

with the orthogonal projection operator $\mathcal{Q} : X \rightarrow N(\mathcal{A})$ mapping X into the nullspace of \mathcal{A} and

$$\mathcal{A}\phi = \sum_{n=1}^{\infty} \mu_n \langle \phi, \phi_n \rangle_X g_n. \tag{A.4}$$

Each system (μ_n, ϕ_n, g_n) of this type is called a singular system of \mathcal{A} .

Proof: For the proof we refer to Theorem 4.7 in [CoKr1]. ■

Theorem A.2 (Picard) *Let $\mathcal{A} : X \rightarrow Y$ be a linear compact operator with singular system (μ_n, ϕ_n, g_n) . Then the equation (A.1) is solvable if and only if $f \in N(\mathcal{A}^*)^\perp$ and*

$$\sum_{n=1}^{\infty} \frac{1}{\mu_n^2} |\langle f, g_n \rangle_Y|^2 < \infty. \quad (\text{A.5})$$

In this case a solution is given by

$$\phi = \sum_{n=1}^{\infty} \frac{1}{\mu_n} \langle f, g_n \rangle_Y \phi_n. \quad (\text{A.6})$$

Proof: For the proof we refer to Theorem 4.8 in [CoKr1]. ■

Theorem A.3 (Tikhonov Regularization) *Let \mathcal{A} be a linear compact operator. Then for each $\alpha > 0$ the operator $\alpha\mathcal{I} + \mathcal{A}^*\mathcal{A} : X \rightarrow X$ is bijective and has a bounded inverse. We call $\phi_\alpha := \mathcal{R}_\alpha f$ with the operator*

$$\mathcal{R}_\alpha := (\alpha\mathcal{I} + \mathcal{A}^*\mathcal{A})^{-1}\mathcal{A}^* \quad (\text{A.7})$$

the Tikhonov solution of (A.1) with regularization parameter α . If \mathcal{A} is injective and ϕ satisfies $\mathcal{A}\phi = f$, then we have

$$\phi_\alpha \rightarrow \phi, \quad \alpha \rightarrow 0. \quad (\text{A.8})$$

Proof: For the proof we refer to Theorem 4.13 in [CoKr1]. ■

Picard's theorem illustrates the ill-posedness. As noted above, the sequence $(\mu_n)_{n \in \mathbb{N}}$ of singular values accumulates only at zero. Hence, the values $1/\mu_n$ tend to infinity for $n \rightarrow \infty$. Therefore, small errors in the data are strongly enlarged. This effect is damped by regularization.

A.2 Riesz-Fredholm Theory

We now give a brief survey on the theory of operator equations

$$(\mathcal{I} - \mathcal{A})\phi = f \quad (\text{A.9})$$

of the second kind with a linear compact operator $\mathcal{A} : X \rightarrow X$ on a normed space X . We define $\mathcal{L} := \mathcal{I} - \mathcal{A}$. For the proofs of Riesz' theorems we refer to [Kre], Chapter 3.

Theorem A.4 (First Riesz Theorem) *The nullspace $N(\mathcal{L})$ of the operator \mathcal{L} is a finite-dimensional subspace of X .*

Theorem A.5 (Second Riesz Theorem) *The range of the operator \mathcal{L} is a closed linear subspace of X .*

Theorem A.6 (Third Riesz Theorem) *There exists an uniquely determined non-negative integer r , called Riesz number, such that*

$$\{0\} = N(\mathcal{L}^0) \subsetneq N(\mathcal{L}^1) \subsetneq \dots \subsetneq N(\mathcal{L}^r) = N(\mathcal{L}^{r+1}) = \dots, \quad (\text{A.10})$$

and

$$X = \mathcal{L}^0(X) \supsetneq \mathcal{L}^1(X) \supsetneq \dots \supsetneq \mathcal{L}^r(X) = \mathcal{L}^{r+1}(X) = \dots. \quad (\text{A.11})$$

Furthermore, we have the direct sum

$$X = N(\mathcal{L}^r) \oplus \mathcal{L}^r(X). \quad (\text{A.12})$$

Theorem A.7 *The operator $\mathcal{I} - \mathcal{A} : X \rightarrow X$ with a linear compact operator \mathcal{A} on a normed space X is injective if and only if it is surjective. If $\mathcal{I} - \mathcal{A}$ is injective, then the inverse operator $(\mathcal{I} - \mathcal{A})^{-1} : X \rightarrow X$ is bounded.*

If the operator \mathcal{L} is not injective and hence not surjective, the Fredholm alternative provides a criteria for the solvability of equation (A.9). This is done in a context of dual systems and adjoint operators. In particular, the Fredholm alternative is well suited for integral operators in Hilbert spaces. A comprehensive study of dual systems and Fredholm's alternative can be found in [Kre], Chapter 4.

Theorem A.8 (First Fredholm Theorem) *Let $\langle X, Y \rangle$ be a dual system and $\mathcal{A} : X \rightarrow X, \mathcal{B} : Y \rightarrow Y$ be compact adjoint operators. Then, the nullspaces of $\mathcal{I} - \mathcal{A}$ and $\mathcal{I} - \mathcal{B}$ have the same finite dimension.*

Theorem A.9 (Second Fredholm Theorem) *Let $\langle X, Y \rangle$ be a dual system and $\mathcal{A} : X \rightarrow X, \mathcal{B} : Y \rightarrow Y$ be compact adjoint operators. Then*

$$(\mathcal{I} - \mathcal{A})(X) = \{f \in X \mid \langle f, \psi \rangle = 0, \quad \forall \psi \in N(\mathcal{I} - \mathcal{B})\} \quad (\text{A.13})$$

and

$$(\mathcal{I} - \mathcal{B})(Y) = \{g \in Y \mid \langle \phi, g \rangle = 0, \quad \forall \phi \in N(\mathcal{I} - \mathcal{A})\}. \quad (\text{A.14})$$

In order to study integral operators of the form

$$(\mathcal{A}\phi)(x) := \int_B K(x, y)\phi(y) dy \quad (\text{A.15})$$

we should investigate the mapping properties of \mathcal{A} . Let $B, D \subset \mathbb{R}^3$ be two bounded domains. In the case of a continuous kernel $K(x, y), x \in D, y \in B$ we state

Theorem A.10 *The integral operator \mathcal{A} defined by (A.15) with continuous kernel K is a linear compact mapping $\mathcal{A} : L^2(B) \mapsto L^2(D)$.*

Proof: With the aid of Cauchy-Schwarz-inequality we state

$$|(\mathcal{A}\phi)(x)|^2 \leq \int_B |K(x, y)|^2 dy \int_B |\phi(y)|^2 dy$$

and

$$|(\mathcal{A}\phi)(x) - (\mathcal{A}\phi)(z)|^2 \leq \int_B |K(x, y) - K(z, y)|^2 dy \int_B |\phi(y)|^2 dy.$$

Let $U \subset L^2(B)$ be bounded, i.e. $\|\phi\|_{L^2(B)} \leq C$ for all $\phi \in U$ and a $C \in \mathbb{R}^+$. Then

$$|(\mathcal{A}\phi)(x)|^2 \leq C^2 |B| \max_{x \in D, y \in B} |K(x, y)|^2$$

for all $x \in D$ and all $\phi \in U$, i.e. $\mathcal{A}(U)$ is bounded in $C(\overline{D})$. For every $\epsilon > 0$ there exists $\delta > 0$ such that

$$|K(x, y) - K(z, y)| < \frac{\epsilon}{C\sqrt{|B|}}$$

for all $x, z \in D, y \in B$ with $|x - z| < \delta$ by the uniform continuity of K on $D \times B$. Then

$$|(\mathcal{A}\phi)(x) - (\mathcal{A}\phi)(z)|^2 < \epsilon^2$$

for all $x, z \in D$ with $|x - z| < \delta$ and all $\phi \in U$. Thus, $\mathcal{A}(U)$ is equicontinuous in $C(\overline{D})$. Hence, $\mathcal{A} : L^2(B) \rightarrow C(D)$ is compact by the Arzelà-Ascoli theorem (see for instance Theorem 1.18 in [Kre]). Finally, convergence in $C(\overline{D})$ implies convergence in $L^2(D)$ and $\mathcal{A} : L^2(B) \rightarrow L^2(D)$ is compact, too. ■

Now, we extend our investigation to weakly singular integral kernels. An integral kernel K is called *weakly singular* if K is continuous for all $x \in \overline{D}, y \in \overline{B}, x \neq y$ and there exist positive constants $C \in \mathbb{R}$ and $\alpha \in (0, 3]$ such that

$$|K(x, y)| \leq C|x - y|^{\alpha-3}, \quad x \in \overline{D}, y \in \overline{B}, x \neq y. \quad (\text{A.16})$$

It turns out that the statement of Theorem A.10 keeps valid for operators with weakly singular kernels. For the proof we need Lax' theorem.

Theorem A.11 (Lax) *Let X, Y be two normed spaces, both of which have a scalar product $\langle \cdot, \cdot \rangle_X$ resp. $\langle \cdot, \cdot \rangle_Y$. Assume that there exists a constant $c \in \mathbb{R}^+$ such that*

$$|\langle \phi_1, \phi_2 \rangle_X| \leq c \|\phi_1\| \|\phi_2\| \quad (\text{A.17})$$

for all $\phi_1, \phi_2 \in X$. Let $\mathcal{A} : X \rightarrow Y, \mathcal{B} : Y \rightarrow X$ be bounded linear operators satisfying

$$\langle \mathcal{A}\phi, \psi \rangle_Y = \langle \phi, \mathcal{B}\psi \rangle_X \quad (\text{A.18})$$

for all $\phi \in X$ and $\psi \in Y$. Then \mathcal{A} is bounded with respect to the norms $\|\cdot\|_s$ induced by the scalar products and

$$\|\mathcal{A}\|_s^2 \leq \|\mathcal{A}\| \|\mathcal{B}\|. \quad (\text{A.19})$$

Proof: The proof can be found for instance in [Kre], Theorem 4.11. ■

Theorem A.12 *The integral operator \mathcal{A} with weakly singular kernel is a linear compact map $\mathcal{A} : L^2(B) \rightarrow L^2(D)$.*

Proof: The proof of compactness of $\mathcal{A} : C(\overline{B}) \rightarrow C(\overline{D})$ in Theorem 2.22 of [Kre] also works for two domains B, D . Since $C(\overline{D})$ is a dense subset of $L^2(D)$, there exists one and only one extension operator $\tilde{\mathcal{A}}$ in $\mathcal{L}(L^2(B), L^2(D))$ with $\mathcal{A}\phi = \tilde{\mathcal{A}}\phi, \forall \phi \in C(\overline{B})$. We also denote the extension of \mathcal{A} by \mathcal{A} instead by $\tilde{\mathcal{A}}$. Now, we use Lax' theorem with $X = L^2(B), Y = L^2(D)$. It can be seen that integral operators with weakly singular kernels are compact in the completion of $C(\overline{B})$ with respect to the scalar product, i.e. in $L^2(B)$. ■

Theorem A.13 *If $\partial B \in C^1$, then the integral operator \mathcal{A} with continuous or weakly singular kernel is a linear compact map $\mathcal{A} : L^2(\partial B) \rightarrow L^2(\partial B)$.*

Proof: The theorem is shown for $\mathcal{A} : C(\overline{B}) \rightarrow C(\overline{B})$ in [Kre], Theorem 2.23. The extension to $L^2(B)$ can be made similar the proof of Theorem A.12. ■

A.3 Boundary Integral Representation of Harmonic Functions

Here, we give a detailed overview how to solve the classical boundary value problems of Laplace's equation

BVP 13 (Interior Dirichlet problem for the classical Laplace equation) Let $\partial B \in C^2$. For some given function $f \in L^2(\partial B)$

$$\text{find } u \in C^2(B) \text{ such } \begin{cases} \Delta u = 0 & \text{in } B, \\ u = f & \text{on } \partial B. \end{cases} \quad (\text{A.20})$$

BVP 14 (Interior Neumann problem for the classical Laplace equation) Let $\partial B \in C^2$. For some given function $g \in L^2_0(\partial B)$

$$\text{find } u \in C^2(B) \text{ such } \begin{cases} \Delta u = 0 & \text{in } B, \\ \frac{\partial u}{\partial \nu} = g & \text{on } \partial B. \end{cases} \quad (\text{A.21})$$

BVP 15 (Exterior Dirichlet problem for the classical Laplace equation) Let $\partial B \in C^2$. For some given function $f \in L^2(\partial B)$

$$\text{find } u \in C^2(B^e) \text{ such } \begin{cases} \Delta u = 0 & \text{in } B^e, \\ u = f & \text{on } \partial B, \\ u(x) \rightarrow 0 & |x| \rightarrow \infty. \end{cases} \quad (\text{A.22})$$

BVP 16 (Exterior Neumann problem for the classical Laplace equation) Let $\partial B \in C^2$. For some given function $g \in L^2(\partial B)$

$$\text{find } u \in C^2(B^e) \text{ such } \begin{cases} \Delta u = 0 & \text{in } B^e, \\ \frac{\partial u}{\partial \nu} = g & \text{on } \partial B, \\ u(x) \rightarrow 0 & |x| \rightarrow \infty. \end{cases} \quad (\text{A.23})$$

Their weak formulation has been treated in Subsection 1.4.2. We represent the classical solutions in the shape of single and double layer potentials, respectively. With the aid of the jump relations we may adapt the layer potentials to the different boundary conditions. The disadvantage of this boundary integral method is the requirement for more regularity of ∂B .

Theorem A.14 *Let B be a bounded simply-connected Lipschitz domain and $\phi \in H^{-\frac{1}{2}}(\partial B)$, $\psi \in H^{\frac{1}{2}}(\partial B)$, then we have*

$$\gamma_0[B^e]\mathcal{S}\phi - \gamma_0[B]\mathcal{S}\phi = 0, \quad \partial_\nu[B^e]\mathcal{S}\phi - \partial_\nu[B]\mathcal{S}\phi = -\phi, \quad (\text{A.24})$$

$$\gamma_0[B^e]\mathcal{D}\psi - \gamma_0[B]\mathcal{D}\psi = \psi, \quad \partial_\nu[B^e]\mathcal{D}\psi - \partial_\nu[B]\mathcal{D}\psi = 0. \quad (\text{A.25})$$

Proof: The general jump relations (A.24),(A.25) can be found in [Co], Lemma 4.1. ■

Both jump relations can be transformed into an equation of second kind. Setting $\mathcal{T}\phi := \partial_\nu[B^e]\mathcal{D}\psi + \partial_\nu[B]\mathcal{D}\psi$ we obtain

$$\gamma_0[B^\pm]\mathcal{D}\psi = \frac{1}{2}(\mathcal{T}\phi \pm \phi), \quad (\text{A.26})$$

and a similar equation for the single layer potential. Here, we used the syntax B^+ for the exterior of B and B^- for the interior. The crucial point is that we want to reduce (A.26) to a manageable integral equation of second kind where we can apply the comfortable Riesz theory. In this section, we focus on the Dirichlet and Neumann problems with L^2 boundary values on the C^2 boundary ∂B . The jump relations of Theorem A.14 do not change which can also be seen by the following theorem.

Theorem A.15 *For the bounded domain B with $\partial B \in C^2$ we have*

$$\gamma_0[B^\pm]\mathcal{D}\psi = \frac{1}{2}(\mathcal{K}\psi \pm \psi) \quad (\text{A.27})$$

with the operator $\mathcal{K} : L^2(\partial B) \rightarrow L^2(\partial B)$ defined by

$$(\mathcal{K}\phi)(x) := 2 \int_{\partial B} \frac{\partial \Phi(x, y)}{\partial \nu(y)} \phi(y) ds(y), \quad x \in \partial B. \quad (\text{A.28})$$

Furthermore, we have

$$\partial_\nu[B^\pm]\mathcal{S}\phi = \frac{1}{2}(\mathcal{K}^*\phi \mp \phi) \quad (\text{A.29})$$

with the adjoint operator $\mathcal{K}^* : L^2(\partial B) \rightarrow L^2(\partial B)$ of \mathcal{K} defined by

$$(\mathcal{K}^*\phi)(x) := 2 \int_{\partial B} \frac{\partial \Phi(x, y)}{\partial \nu(x)} \phi(y) ds(y), \quad x \in \partial B. \quad (\text{A.30})$$

Proof: A detailed treatment of the jump relations can be found in [Ker]. ■

Lemma A.16 *Let $\partial B \in C^2$, the linear integral operators $\mathcal{K}, \mathcal{K}^* : L^2(\partial B) \rightarrow L^2(\partial B)$ are compact operators.*

Proof: The operators \mathcal{K} and \mathcal{K}^* as defined in (A.28) and (A.30) have weakly singular kernels. Therefore, the operators $\mathcal{K}, \mathcal{K}^* : L^2(\partial B) \rightarrow L^2(\partial B)$ are compact operators in view of Theorem A.13. ■

The following theorems reduces the question for the existence of solutions of the different boundary value problems to question for the solvability of corresponding integral equations of second kind.

Theorem A.17 *The double layer potential $\mathcal{D}\psi$ with density $\psi \in L^2(\partial B)$ solves the interior Dirichlet problem for Laplace's equation with boundary data $g \in L^2(\partial B)$ provided that ψ is a solution of*

$$(\mathcal{I} - \mathcal{K})\psi = -2g. \quad (\text{A.31})$$

Proof: This is a consequence of Theorem A.15. ■

Theorem A.18 *The modified double layer potential $\tilde{\mathcal{D}}\psi$ defined by*

$$(\tilde{\mathcal{D}}\psi)(x) := \int_{\partial B} \psi(y) \left\{ \frac{\partial \Phi(x, y)}{\partial \nu(y)} + \Phi(x, 0) \right\} ds(y), \quad x \in B^e \quad (\text{A.32})$$

with density $\psi \in L^2(\partial B)$ solves the exterior Dirichlet problem for Laplace's equation with boundary data $g \in L^2(\partial B)$ provided that ψ is a solution of

$$(\mathcal{I} + \tilde{\mathcal{K}})\psi = 2g, \quad (\text{A.33})$$

where

$$(\tilde{\mathcal{K}}\psi)(x) := 2 \int_{\partial B} \psi(y) \left\{ \frac{\partial \Phi(x, y)}{\partial \nu(y)} + \Phi(x, 0) \right\} ds(y), \quad x \in \partial B. \quad (\text{A.34})$$

Here, we assume that the origin is contained in B .

Proof: From (A.27) we deduce

$$2\gamma_0[B^e]\tilde{\mathcal{D}}\psi = 2\gamma_0[B^e]\mathcal{D}\psi + 2 \int_{\partial B} \Phi(x, 0)\psi(y) ds(y) = (\mathcal{I} + \tilde{\mathcal{K}})\psi \quad (\text{A.35})$$

and the statement is evident. Observe that the modified double layer potential has the required behavior at infinity. ■

Theorem A.19 *The single layer potential $\mathcal{S}\phi$ with a density $\phi \in L^2(\partial B)$ solves the interior Neumann problem for Laplace's equation with boundary data $g \in L^2(\partial B)$ provided that ϕ is a solution of*

$$(\mathcal{I} + \mathcal{K}^*)\phi = 2g. \quad (\text{A.36})$$

Proof: This is consequence of Theorem A.15. ■

Theorem A.20 *The single layer potential $\mathcal{S}\phi$ with a density $\phi \in L^2(\partial B)$ solves the exterior Neumann problem for Laplace's equation with boundary data $g \in L^2(\partial B)$ provided that ϕ is a solution of*

$$(\mathcal{I} - \mathcal{K}^*)\phi = -2g. \quad (\text{A.37})$$

Proof: This follows from Theorem A.15. ■

Now, we have to investigate the different integral equation of second kind. Since the operators $\mathcal{K}, \mathcal{K}^*$ are compact we are able to apply Riesz-Fredholm theory. Therefore, the nullspaces $N(\mathcal{I} \pm \mathcal{K})$ as well as $N(\mathcal{I} \pm \mathcal{K}^*)$ have finite dimension. The next theorem characterizes it more precisely.

Theorem A.21 *Let $\partial B \in C^2$. The nullspaces of $\mathcal{I} \pm \mathcal{K}$ are given by*

$$N(\mathcal{I} - \mathcal{K}) = \{0\}, \quad N(\mathcal{I} + \mathcal{K}) = \text{span}\{1\}. \quad (\text{A.38})$$

Moreover, the nullspaces $N(\mathcal{I} \pm \mathcal{K}^*)$ are given by

$$N(\mathcal{I} - \mathcal{K}^*) = \{0\}, \quad N(\mathcal{I} + \mathcal{K}^*) = \text{span}\{\phi_B\}, \quad (\text{A.39})$$

with a normalized $\phi_B \in L^2(\partial B)$.

Proof: We start to prove the first statement. Let $\psi \in N(\mathcal{I} - \mathcal{K})$, then $\mathcal{D}\psi$ solves the interior Dirichlet problem with homogeneous boundary condition (see Theorem A.17). This problem has only the trivial solution, thus $\mathcal{D}\psi = 0$ in B . Hence, $\partial_\nu[B^-]\mathcal{D}\psi = 0$. From the jump relation (A.25) we have $\partial_\nu[B^+]\mathcal{D}\psi = \partial_\nu[B^-]\mathcal{D}\psi = 0$. Now, $\mathcal{D}\psi$ is a solution of the exterior Neumann problem in B^e with vanishing boundary data. Uniqueness of this problem yields $\mathcal{D}\psi = 0$ in B^e . The jump relation (A.25) leads to $\psi = \gamma_0[B^e]\mathcal{D}\psi - \gamma_0[B]\mathcal{D}\psi = 0$. The statement $N(\mathcal{I} - \mathcal{K}^*) = \{0\}$ follows from Fredholm's alternative.

Let $\psi \in N(\mathcal{I} + \mathcal{K})$, then $\mathcal{D}\psi$ is harmonic in B^e , vanishes at infinity and has boundary values $\gamma_0[B^e]\mathcal{D}\psi = 0$ by the jump relation (A.27). That means, $\mathcal{D}\psi$ solves the exterior Dirichlet problem with homogeneous boundary condition. Therefore, $\mathcal{D}\psi = 0$ in B^e since this problem has at most one solution. Then $\gamma_\nu[B^e]\mathcal{D}\psi = 0$ and $\gamma_\nu[B]\mathcal{D}\psi = 0$ by the jump relation (A.25). Now, $\mathcal{D}\psi$ is a solution of the interior Neumann problem in B with homogeneous boundary values. A solution to this problem is unique up to a constant, therefore $\mathcal{D}\psi \equiv c$ in B for a $c \in \mathbb{R}$. Now, $\gamma_0[B]\mathcal{D}\psi = c$ and $\psi = \gamma_0[B^e]\psi - \gamma_0[B]\psi = -c$. Thus, we have proven $N(\mathcal{I} + \mathcal{K}) \subset \text{span}\{1\}$. Reversely, the calculation (1.135) yields $\mathcal{D}1 = -1$ in B and $\mathcal{D}1 = 0$ in B^e . Using the jump relation (A.27) once more we obtain $\mathcal{K}1 = \gamma_0[B^+]\mathcal{D}1 + \gamma_0[B^-]\mathcal{D}1 = -1$. Therefore, $(\mathcal{I} + \mathcal{K})1 = 0$, and $N(\mathcal{I} + \mathcal{K}) = \text{span}\{1\}$ is proven. The Fredholm alternative implies that $N(\mathcal{I} + \mathcal{K}^*)$ has dimension one, thus $N(\mathcal{I} + \mathcal{K}^*) = \{\phi_B\}$ with a density $\phi_B \in L^2(\partial B)$ which can be normalized. ■

In a brief review we show that the modified double layer potential provides a solution to the exterior Dirichlet problem for every boundary data $g \in L^2(\partial B)$. Let $\psi \in L^2(\partial B)$ be a solution of $(\mathcal{I} + \tilde{\mathcal{K}})\psi = 0$, then $\tilde{\mathcal{D}}\psi$ solves the exterior Dirichlet problem with vanishing boundary values on ∂B (see Theorem A.18). By the uniqueness of this problem $\tilde{\mathcal{D}}\psi$ is zero in B^e , especially $\partial_\nu[B^e]\tilde{\mathcal{D}}\psi = 0$. With the aid of $\text{grad } \Phi(x, y) = \frac{1}{4\pi} \frac{x-y}{|x-y|^3}$ we deduce

the asymptotic

$$|x|(\tilde{\mathcal{D}}\psi)(x) = \int_{\partial B} \psi ds \cdot \left(1 + O\left(\frac{1}{|x|}\right)\right), \quad |x| \rightarrow \infty. \quad (\text{A.40})$$

From this behavior we get $\int_{\partial B} \psi ds = 0$ since $\tilde{\mathcal{D}}\psi = 0$ in B^e . By the jump relation (A.25) we obtain

$$\partial_\nu[B^e]\tilde{\mathcal{D}}\psi - \partial_\nu[B]\tilde{\mathcal{D}}\psi = \partial_\nu[B^e]\mathcal{D}\psi - \partial_\nu[B]\mathcal{D}\psi = 0. \quad (\text{A.41})$$

Inserting $\partial_\nu[B^e]\tilde{\mathcal{D}}\psi = 0$ we have $\partial_\nu[B]\tilde{\mathcal{D}}\psi = 0$. Now, $\tilde{\mathcal{D}}\psi$ solves the homogeneous interior Neumann problem, and must be constant in B . Using the jump relation (A.25) once more we obtain

$$\gamma_0[B^e]\tilde{\mathcal{D}}\psi - \gamma_0[B]\tilde{\mathcal{D}}\psi = \gamma_0[B^e]\mathcal{D}\psi - \gamma_0[B]\mathcal{D}\psi = \psi, \quad (\text{A.42})$$

and ψ must be constant. Now $\int_{\partial B} \psi ds = 0$ implies $\psi = 0$, and we have proven

Corollary A.22 $N(\mathcal{I} + \tilde{\mathcal{K}}) = \{0\}$.

Theorem A.23

The interior Dirichlet problem (A.20) is uniquely solvable for each right hand side $f \in L^2(\partial B)$.

The interior Neumann problem (A.21) with boundary values $g \in L^2(\partial B)$ has a solution uniquely determined up to a constant if and only if $\int_{\partial B} g ds = 0$.

The exterior Dirichlet problem (A.22) is uniquely solvable for each right hand side $f \in L^2(\partial B)$.

The exterior Neumann problem (A.23) with boundary values $g \in L^2(\partial B)$ has an unique solution.

Proof: Due to $N(\mathcal{I} - \mathcal{K}) = \{0\}$ the integral equation $(\mathcal{I} - \mathcal{K})\psi = -2g$ with the compact operator \mathcal{K} is uniquely solvable for each right hand side, i.e. $\mathcal{D}\psi$ is a solution of the interior Dirichlet problem. Since Theorem 1.28 shows the uniqueness for boundary values $g \in H^{1/2}(\partial B)$ we have to modify the proof of uniqueness. We use Green's first identity in the sence of

$$\int_{\partial B} u \Delta v + \text{grad } u \text{ grad } v dx = \langle u_{\partial B} \partial_\nu v, 1 \rangle. \quad (\text{A.43})$$

Now, let $u \in H^1_\Delta(B)$ be a solution of the homogeneous Dirichlet problem, then (A.43) with $v = u$ results in $\int_B |\text{grad } u|^2 dx = 0$. Hence, $\text{grad } u$ must be constant and this constant is zero according to the homogeneous boundary condition.

For the compact operator \mathcal{K}^* we have proven $N(\mathcal{I} + \mathcal{K}^*) = \text{span}\{\phi_B\}$. Fredholm's alternative implies

$$(\mathcal{I} + \mathcal{K}^*)(L^2(\partial B)) = \{f \in L^2(\partial B) \mid \langle f, \phi \rangle = 0, \quad \forall \phi \in N(\mathcal{I} + \mathcal{K})\}$$

i.e. $(\mathcal{I} + \mathcal{K}^*)\phi = 2g$ is solvable if and only if $\int_{\partial B} g ds = 0$. The necessity of this condition is a consequence of Theorem 1.24. We decompose $L^2(\partial B)$ with respect to the nullspace of $(\mathcal{I} + \mathcal{K}^*)$ and introduce

$$L_{\square}^2(\partial B) := N(\mathcal{I} + \mathcal{K}^*)^{\perp} = \left\{ \varphi \in L^2(\partial B) \mid \int_{\partial B} \varphi \phi_B ds = 0 \right\}. \quad (\text{A.44})$$

Altogether, the operator $\mathcal{I} + \mathcal{K}^* : L_{\square}^2(\partial B) \rightarrow L_{\square}^2(\partial B)$ is injective, and thus, bijective. From Theorem A.19, the function $\mathcal{S}\phi$ with $\phi = 2(\mathcal{I} + \mathcal{K}^*)^{-1}g \in L_{\square}^2(\partial B)$ is a solution of the interior Neumann problem. Theorem 1.29 shows that this solution is uniquely determined up to a constant.

We have shown $N(\mathcal{I} + \tilde{\mathcal{K}}) = \{0\}$. From the fact that $\tilde{\mathcal{K}} - \mathcal{K}$ has a continuous kernel, we observe that $\tilde{\mathcal{K}}$ is a compact operator. Then $(\mathcal{I} + \tilde{\mathcal{K}})\psi = 2g$ has a unique solution ψ for each g , that means $\tilde{\mathcal{D}}\psi$ is a solution of the exterior Dirichlet problem which vanishes at infinity. Theorem 1.107 together with Remark 1.32 shows that this solution is uniquely determined.

The exterior Neumann problem with boundary data $g \in L^2(\partial B)$ admits a solution $\mathcal{S}\phi$ with $\phi = -2(\mathcal{I} - \mathcal{K}^*)^{-1}g$. Since $N(\mathcal{I} - \mathcal{K}^*) = \{0\}$ the operator $(\mathcal{I} - \mathcal{K}^*)^{-1}$ exists and is bounded. Finally, Theorem 1.31 shows its uniqueness. ■

A.4 Boundary Integral Representation of Harmonic Fields

In this section we want to represent the classical solution of boundary value problems for harmonic fields and fields with harmonic components in terms of boundary integrals. First, we consider harmonic fields with given normal components. Here, we use the results of the previous section for the the scalar potential of an harmonic field. Next, we study divergence-free fields with given tangential components and its vector potentials. We are able to give a representation for harmonic fields as well as for fields with harmonic components. Again, we require a C^2 boundary ∂B .

BVP 17 (Interior normal problem for classical harmonic fields) Let $\partial B \in C^2$. For some given function $g \in L^2_0(\partial B)$

$$\text{find } \mathbf{u} \in \mathbf{C}^1(B) \text{ such } \begin{cases} \text{curl } \mathbf{u} = \mathbf{0} & \text{in } B, \\ \text{div } \mathbf{u} = 0 & \text{in } B, \\ \nu \cdot \mathbf{u} = g & \text{on } \partial B. \end{cases} \quad (\text{A.45})$$

BVP 18 (Exterior normal problem for classical harmonic fields) Let $\partial B \in C^2$. For some given function $g \in L^2(\partial B)$

$$\text{find } \mathbf{u} \in \mathbf{C}^1(B^e) \text{ such } \begin{cases} \text{curl } \mathbf{u} = \mathbf{0} & \text{in } B^e, \\ \text{div } \mathbf{u} = 0 & \text{in } B^e, \\ \nu \cdot \mathbf{u} = g & \text{on } \partial B, \\ \mathbf{u}(x) \rightarrow \mathbf{0} & |x| \rightarrow \infty. \end{cases} \quad (\text{A.46})$$

BVP 19 (Interior tangential problem for classical harmonic fields) Let $\partial B \in C^2$. For given $\mathbf{g} \in \mathbf{L}^2_{t, \text{DIV}=0}(\partial B)$

$$\text{find } \mathbf{u} \in \mathbf{C}^2(B) \text{ such } \begin{cases} \text{curl } \mathbf{u} = \mathbf{0} & \text{in } B, \\ \text{div } \mathbf{u} = 0 & \text{in } B, \\ \nu \times \mathbf{u} = \mathbf{g} & \text{on } \partial B. \end{cases} \quad (\text{A.47})$$

BVP 20 (classical Interior tangential problem for the 3d-Laplace equation) Let $\partial B \in C^2$. For some given field $\mathbf{g} \in \mathbf{L}^2_{t, \text{DIV}}(\partial B)$

$$\text{find } \mathbf{u} \in \mathbf{C}^2(B) \text{ such } \begin{cases} \text{curl curl } \mathbf{u} = \mathbf{0} & \text{in } B, \\ \text{div } \mathbf{u} = 0 & \text{in } B, \\ \nu \times \mathbf{u} = \mathbf{g} & \text{on } \partial B. \end{cases} \quad (\text{A.48})$$

BVP 21 (Exterior tangential problem for classical harmonic fields) Let $\partial B \in C^2$. For given $\mathbf{g} \in \mathbf{L}_{t, \text{DIV}=0}^2(\partial B)$

$$\text{find } \mathbf{u} \in \mathbf{C}^1(B^e) \cap \mathbf{H}_{\text{curl}}(B^e) \text{ such } \begin{cases} \text{curl } \mathbf{u} = \mathbf{0} & \text{in } B^e, \\ \text{div } \mathbf{u} = 0 & \text{in } B^e, \\ \nu \times \mathbf{u} = \mathbf{g} & \text{on } \partial B, \\ \mathbf{u}(x) \rightarrow \mathbf{0} & |x| \rightarrow \infty, \\ \int_{\partial B} \mathbf{u} ds = 0. \end{cases} \quad (\text{A.49})$$

BVP 22 (classical Exterior tangential problem for the 3d-Laplace equation) Let $\partial B \in C^2$. For some given field $\mathbf{g} \in \mathbf{L}_{t, \text{DIV}}^2(\partial B)$

$$\text{find } \mathbf{u} \in \mathbf{C}^2(B^e) \text{ such } \begin{cases} \text{curl curl } \mathbf{u} = \mathbf{0} & \text{in } B^e, \\ \text{div } \mathbf{u} = 0 & \text{in } B^e, \\ \nu \times \mathbf{u} = \mathbf{g} & \text{on } \partial B, \\ \mathbf{u}(x) \rightarrow \mathbf{0} & |x| \rightarrow \infty, \\ \int_{\partial B} \mathbf{u} ds = 0. \end{cases} \quad (\text{A.50})$$

The solutions of the interior and exterior normal problems (A.45) and (A.46) can be represented as $\text{grad } \mathcal{S}\phi$ which is the statement of the following theorem.

Theorem A.24 *The field $\text{grad } \mathcal{S}\phi$ solves the interior normal problem for harmonic fields with boundary values $g \in L^2_\circ(\partial B)$ if ϕ is a solution of*

$$(\mathcal{I} + \mathcal{K}^*)\phi = 2g. \quad (\text{A.51})$$

Moreover, the field $\text{grad } \mathcal{S}\phi$ solves the exterior normal problem for harmonic fields with boundary values $g \in L^2(\partial B)$ if ϕ is a solution of

$$(\mathcal{I} - \mathcal{K}^*)\phi = -2g. \quad (\text{A.52})$$

Proof: The field $\text{grad } \mathcal{S}\phi$ is a harmonic field in B and in B^e and vanishes at infinity. Then the boundary conditions follow from the jump relations (A.29). \blacksquare

Theorem A.25

The interior normal problem (A.45) is uniquely solvable for each right hand side $g \in L^2_\circ(\partial B)$.

The exterior normal problem (A.46) is uniquely solvable for each right hand side $g \in L^2(\partial B)$.

Proof: In the proof of Theorem A.23 we have shown that $\mathcal{I} + \mathcal{K}^* : L^2_\square(\partial B) \rightarrow L^2_\circ(\partial B)$ is a bijective operator with bounded inverse. Therefore, the equation $(\mathcal{I} + \mathcal{K}^*)\phi = 2g$

has an unique solution in $L^2_{\square}(\partial B)$ for each $g \in L^2_{\circ}(\partial B)$, and $\text{grad } \mathcal{S}\phi$ solves the interior normal problem. The uniqueness is shown by Theorem 1.29.

Since $N(\mathcal{I} - \mathcal{K}^*) = \{0\}$ the equation $(\mathcal{I} - \mathcal{K}^*)\phi = -2g$ has an unique solution for each $g \in L^2(\partial B)$ and $\text{grad } \mathcal{S}\phi$ solves the exterior normal problem. The uniqueness is proven by Theorem 1.31. \blacksquare

Now, we turn to the tangential problems of divergence-free fields. In particular, we consider a field \mathbf{u} that satisfies

$$\text{curl curl } \mathbf{u} = \mathbf{0}, \quad \text{div } \mathbf{u} = 0 \quad (\text{A.53})$$

in B or B^e and fulfills the boundary condition $\nu \times \mathbf{u} = \mathbf{g}$ for a given tangential field \mathbf{g} . Here, we use the jump of the tangential component of the vector potentials. At the beginning we present the jump relations and afterwards we characterize the boundary integral operator \mathcal{M} . With this operator we establish an integral equation of second order similar to those we have studied in the previous section.

Theorem A.26 *Let $\partial B \in C^2$. For $\mathbf{a} \in \mathbf{L}^2_t(\partial B)$, the vector potential $\vec{\mathcal{S}}\mathbf{a}$ has boundary values*

$$\text{div } \vec{\mathcal{S}}_{\pm}(\mathbf{a}) = \int_{\partial B} \text{grad } \Phi(\cdot, y) \mathbf{a}(y) ds \mp \frac{1}{2} \nu \cdot \mathbf{a} \quad (\text{A.54})$$

$$\text{curl } \vec{\mathcal{S}}_{\pm}(\mathbf{a}) = \int_{\partial B} \text{grad } \Phi(\cdot, y) \times \mathbf{a}(y) ds \mp \frac{1}{2} \nu \times \mathbf{a} \quad (\text{A.55})$$

where the subscript $+$ denotes the boundary values from the exterior B^e and $-$ from the interior B .

Proof: The classical version of the boundary values, i.e. in a setting of

$$\mathbf{C}^{0,\alpha}_{t,\text{DIV}}(\partial B) = \{\mathbf{v} \in \mathbf{C}^{0,\alpha}_t(\partial B) \mid \text{DIV } \mathbf{v} \in C^{0,\alpha}(\partial B)\} \quad (\text{A.56})$$

can be found in [CoKr1], Theorem 6.12. For the extension to $\mathbf{L}^2_t(\partial B)$ we refer to [Hä].

Corollary A.27 *Let $\partial B \in C^2$. For $\mathbf{a} \in \mathbf{L}^2_t(\partial B)$, the vector potential $\vec{\mathcal{S}}\mathbf{a}$ has boundary values*

$$2\gamma_{\times}[B^{\pm}] \text{curl } \vec{\mathcal{S}}\mathbf{a} = (\mathcal{M} \pm \mathcal{I})\mathbf{a}, \quad (\text{A.57})$$

$$2\gamma_{\Gamma}[B^{\pm}] \text{curl } \vec{\mathcal{S}}\mathcal{R}\mathbf{a} = -(\mathcal{M}^* \mp \mathcal{I})\mathbf{a} \quad (\text{A.58})$$

with the operator \mathcal{M} defined by

$$(\mathcal{M}\mathbf{a})(x) := 2 \int_{\partial B} \nu(x) \times \text{curl}_x \{\Phi(x, y) \mathbf{a}(y)\} ds(y), \quad x \in \partial B \quad (\text{A.59})$$

and the operator \mathcal{R} defined by

$$\mathcal{R}\mathbf{a} := \nu \times \mathbf{a}. \quad (\text{A.60})$$

Proof: The jump relation (A.57) can be concluded from (A.55). For the jump relation (A.58) we apply (A.57) to the tangential field $\mathcal{R}\mathbf{a}$ and obtain

$$2\gamma_{\times}[B^{\pm}] \operatorname{curl} \vec{\mathcal{S}}\mathcal{R}\mathbf{a} = (\mathcal{M} \pm \mathcal{I})\mathcal{R}\mathbf{a}.$$

Now, we apply the operator \mathcal{R} and use the relations

$$\mathcal{R}\mathcal{R}\mathbf{a} = -\mathbf{a}, \quad (\text{A.61})$$

$$\mathcal{R}\mathcal{M}\mathcal{R} = \mathcal{M}^*. \quad (\text{A.62})$$

(see for instance [CoKr1], page171). ■

With the aid of the vector potential basing on boundary integrals $\operatorname{curl} \vec{\mathcal{S}}\mathbf{b}$ we observe

$$\operatorname{curl} \operatorname{curl} \operatorname{curl} \vec{\mathcal{S}}\mathbf{b} = \operatorname{curl}(-\Delta + \operatorname{grad} \operatorname{div})\vec{\mathcal{S}}\mathbf{b} = \mathbf{0} \quad \operatorname{div} \operatorname{curl} \vec{\mathcal{S}}\mathbf{b} = 0. \quad (\text{A.63})$$

Together with the jump relation we are able to adapt $\operatorname{curl} \vec{\mathcal{S}}\mathbf{b}$ such that the vector potential is a solution of the interior and exterior tangential problems, respectively. To accommodate this, we recall the surface operator GRAD , DIV , CURL and the spaces $\mathbf{L}_{t,\operatorname{DIV}}^2(\partial B)$ and $\mathbf{L}_{t,\operatorname{CURL}}^2(\partial B)$ from Subsection 2.2.3 and study the mapping properties of the operator \mathcal{M} .

Lemma A.28 *Let $\partial B \in C^2$. The linear integral operator \mathcal{M} is a compact operator on $\mathbf{L}_t^2(\partial B)$, $\mathbf{L}_{t,\operatorname{DIV}}^2(\partial B)$ as well as on $\mathbf{L}_{t,\operatorname{DIV}=0}^2(\partial B)$.*

Proof: Since its kernel is weakly singular, \mathcal{M} is a compact operator from $\mathbf{L}_t^2(\partial B)$ into itself. Following [Hä], \mathcal{M} is also a compact operator on $\mathbf{L}_{t,\operatorname{DIV}}^2(\partial B)$. The statement for $\mathbf{L}_{t,\operatorname{DIV}=0}^2(\partial B)$ follows from the relation (see [CoKr1], page 169)

$$\operatorname{DIV} \mathcal{M}\mathbf{a} = -\mathcal{K}^* \operatorname{DIV} \mathbf{a} \quad (\text{A.64})$$

where \mathcal{K}^* is the adjoint operator of the double layer potential \mathcal{K} . ■

Theorem A.29 *$\mathcal{I} + \mathcal{M}$ is an one-to-one mapping on $\mathbf{L}_t^2(\partial B)$, $\mathbf{L}_{t,\operatorname{DIV}}^2(\partial B)$ as well as on $\mathbf{L}_{t,\operatorname{DIV}=0}^2(\partial B)$ whereas $\mathcal{I} + \mathcal{M}^*$ is an one-to-one mapping on $\mathbf{L}_t^2(\partial B)$, $\mathbf{L}_{t,\operatorname{CURL}}^2(\partial B)$ as well as on $\mathbf{L}_{t,\operatorname{CURL}=0}^2(\partial B)$.*

Proof: First, we prove the statements of $\mathcal{I} + \mathcal{M}$. Theorem 5.4 of [CoKr2] shows the injectivity of $\mathcal{I} + \mathcal{M}$ as a mapping from $\mathbf{C}_{t,\operatorname{DIV}}^{0,\alpha}(\partial B)$ into itself. Together with Fredholm's alternative it can be shown that the nullspace with respect to $\mathbf{L}_t^2(\partial B)$ coincides with the nullspace with respect to $\mathbf{C}_{t,\operatorname{DIV}}^{0,\alpha}(\partial B)$ (for the technique see for instance [CoKr1], page 59). The relation

$$\operatorname{DIV}(\mathcal{I} + \mathcal{M})\mathbf{a} = (\mathcal{I} - \mathcal{K}^*) \operatorname{DIV} \mathbf{a} \quad (\text{A.65})$$

and the mapping property $\mathcal{K}^* : L^2(\partial B) \rightarrow L^2(\partial B)$ from imply the bibejectivity on $\mathbf{L}_{t,\operatorname{DIV}}^2(\partial B)$. Since the nullspace of $\mathcal{I} - \mathcal{K}^*$ is trivial (see Theorem A.21), $\mathcal{I} + \mathcal{M}$ is

also a bijectiv operator on $\mathbf{L}_{t,\text{DIV}=0}^2(\partial B)$.

The Fredholm alternative asserts that $\mathcal{I} + \mathcal{M}^*$ is also bijective in the dual spaces, i.e. in $\mathbf{L}_t^2(\partial B)$ and $\mathbf{L}_{t,\text{DIV}}^2(\partial B)$ where the bilinear form is induced by

$$\langle \mathcal{R}\mathbf{a}, \mathbf{b} \rangle_{\mathbf{L}_{t,\text{CURL}}^2(\partial B)} = \langle \mathcal{R}\mathbf{a}, -\mathcal{R}\mathbf{b} \rangle_{\mathbf{L}_{t,\text{DIV}}^2(\partial B)}. \quad (\text{A.66})$$

Now, the bijectivity on $\mathbf{L}_{t,\text{CURL}=0}^2(\partial B)$ follows from

$$\begin{aligned} \text{CURL}(\mathcal{I} + \mathcal{M}^*)\mathbf{a} &= \text{CURL}(\mathcal{I} + \mathcal{R}\mathcal{M}\mathcal{R})\mathbf{a} = \text{CURL}\mathbf{a} - \text{DIV}\mathcal{M}\mathcal{R}\mathbf{a} \\ &= \text{CURL}\mathbf{a} + \mathcal{K}^* \text{DIV}\mathcal{R}\mathbf{a} = (\mathcal{I} - \mathcal{K}^*) \text{CURL}\mathbf{a}. \end{aligned}$$

and $N(\mathcal{I} - \mathcal{K}^*) = \{0\}$.

Theorem A.30 $\mathcal{I} - \mathcal{M}$ is an one-to-one mapping on $\mathbf{L}_t^2(\partial B)$, $\mathbf{L}_{t,\text{DIV}}^2(\partial B)$ as well as on $\mathbf{L}_{t,\text{DIV}=0}^2(\partial B)$. $\mathcal{I} - \mathcal{M}^*$ is an one-to-one mappings on $\mathbf{L}_t^2(\partial B)$, $\mathbf{L}_{t,\text{CURL}}^2(\partial B)$ as well as on $\mathbf{L}_{t,\text{CURL}=0}^2(\partial B)$.

Proof: First, we turn to the statement of $\mathcal{I} - \mathcal{M}$. Consider a $\mathbf{g} \in \mathbf{L}_{t,\text{CURL}}^2(\partial B)$, then $\mathbf{a} := (\mathcal{I} + \mathcal{M})^{-1}\mathcal{R}\mathbf{g} \in \mathbf{L}_{t,\text{DIV}}^2(\partial B)$. For the tangential field $\mathbf{b} = -\mathcal{R}\mathbf{a}$ we observe

$$(\mathcal{I} - \mathcal{M}^*)\mathbf{b} = -\mathcal{R}(\mathcal{I} + \mathcal{M})\mathcal{R}\mathbf{b} = -\mathcal{R}(\mathcal{I} + \mathcal{M})(\mathcal{I} + \mathcal{M})^{-1}\mathcal{R}\mathbf{g} = \mathbf{g}, \quad (\text{A.67})$$

i.e. the mapping $\mathcal{I} - \mathcal{M}^*$ is surjective. The Riesz' theory implies that $\mathcal{I} - \mathcal{M}^*$ is bijective on $\mathbf{L}_{t,\text{CURL}}^2(\partial B)$. The argumentation is also valid for $\mathbf{g} \in \mathbf{L}_t^2(\partial B)$ and for $\mathbf{g} \in \mathbf{L}_{t,\text{CURL}=0}^2(\partial B)$, therefore $\mathcal{I} - \mathcal{M}^*$ is bijective on $\mathbf{L}_t^2(\partial B)$ and on $\mathbf{L}_{t,\text{CURL}=0}^2(\partial B)$.

For the proof of the statement of $\mathcal{I} - \mathcal{M}$ we use a similar technique. Starting from some $\mathbf{g} \in \mathbf{L}_{t,\text{DIV}}^2(\partial B)$, we define $\mathbf{a} := (\mathcal{I} + \mathcal{M}^*)^{-1}\mathcal{R}\mathbf{g}$, then $\mathbf{b} = -\mathcal{R}\mathbf{a} \in \mathbf{L}_{t,\text{DIV}}^2(\partial B)$ fulfills $(\mathcal{I} - \mathcal{M})\mathbf{b} = \mathbf{g}$. Hence, $\mathcal{I} - \mathcal{M}$ is seen to be surjective, and thus, bijective on $\mathbf{g} \in \mathbf{L}_{t,\text{DIV}}^2(\partial B)$. This proof also works to verify the bijectivity on $\mathbf{L}_t^2(\partial B)$ and on $\mathbf{L}_{t,\text{DIV}=0}^2(\partial B)$. \blacksquare

Now, we are prepared to solve the Maxwell problems.

Corollary A.31 The field $\text{curl}\vec{\mathcal{S}}\mathbf{a}$ solves the problem (A.48) with boundary data $\mathbf{g} \in \mathbf{L}_{t,\text{DIV}}^2(\partial B)$ where \mathbf{a} is the unique solution of

$$(\mathcal{I} - \mathcal{M})\mathbf{a} = -2\mathbf{g}. \quad (\text{A.68})$$

Furthermore, the field $\text{curl}\vec{\mathcal{S}}\mathbf{a}$ solves the problem (A.50) with boundary data $\mathbf{g} \in \mathbf{L}_{t,\text{DIV}}^2(\partial B)$ where \mathbf{a} is the unique solution of

$$(\mathcal{I} + \mathcal{M})\mathbf{a} = 2\mathbf{g}. \quad (\text{A.69})$$

Proof: Since $N(\mathcal{I} - \mathcal{M}) = \{\mathbf{0}\}$ and \mathcal{M} compact, the equation $(\mathcal{I} - \mathcal{M})\mathbf{a} = -2\mathbf{g}$ is solvable for each $\mathbf{g} \in \mathbf{L}_{t, \text{DIV}}^2(\partial B)$. Then $\text{curl } \vec{\mathcal{S}}\mathbf{a}$ fulfills the boundary condition (see jump relation from Theorem A.30) and the first and second condition (see (A.63) of the interior tangential problem.

The nullspace of $\mathcal{I} + \mathcal{M}$ is trivial, i.e. $(\mathcal{I} + \mathcal{M})\mathbf{a} = -2\mathbf{g}$ is solvable for each $\mathbf{g} \in \mathbf{L}_{t, \text{DIV}}^2(\partial B)$. The jump relation imply that $\text{curl } \vec{\mathcal{S}}\mathbf{a}$ fulfills the boundary condition of the exterior tangential problem. Moreover, the equations (A.63) show that the first and second condition are satisfied. ■

With a small modification we are able to solve the tangential problems for classical harmonic fields.

Corollary A.32 *The field $\text{curl } \vec{\mathcal{S}}\mathbf{a}$ solves the interior problem (A.47) with boundary data $\mathbf{g} \in \mathbf{L}_{t, \text{DIV}=0}^2(\partial B)$ where \mathbf{a} is the unique solution of $(\mathcal{I} - \mathcal{M})\mathbf{a} = -2\mathbf{g}$. Furthermore, it is a solution of the exterior problem (A.49) with boundary data $\mathbf{g} \in \mathbf{L}_{t, \text{DIV}=0}^2(\partial B)$ where \mathbf{a} is the unique solution of $(\mathcal{I} + \mathcal{M})\mathbf{a} = 2\mathbf{g}$.*

Proof: In a view of Corollary A.31 it remains to prove that $\text{curl } \vec{\mathcal{S}}$ is curl-free. Theorem A.30 implies that for the solution of $(\mathcal{I} - \mathcal{M})\mathbf{a} = -2\mathbf{g}$ with $\text{DIV } \mathbf{g} = 0$ holds $\text{DIV } \mathbf{a} = 0$. With the relation

$$\text{div } \vec{\mathcal{S}}\mathbf{a} = \vec{\mathcal{S}} \text{DIV } \mathbf{a} \tag{A.70}$$

we observe

$$\text{curl } \text{curl } \vec{\mathcal{S}}\mathbf{a} = (-\Delta + \text{grad } \text{div}) \vec{\mathcal{S}}\mathbf{a} = \text{grad } \vec{\mathcal{S}} \text{DIV } \mathbf{a} = \mathbf{0}.$$

Analogous, Theorem A.29 implies $\text{DIV } \mathbf{a} = 0$ for the solution of $(\mathcal{I} + \mathcal{M})\mathbf{a} = 2\mathbf{g}$ with $\text{DIV } \mathbf{g} = 0$, and $\text{curl } \vec{\mathcal{S}}\mathbf{a}$ is curl-free. ■

A.5 Formulas of Vector Analysis

\mathbf{a} twice continuously differentiable vector field,

$$\operatorname{curl} \operatorname{curl} \mathbf{a} = \operatorname{grad} \operatorname{div} \mathbf{a} - \Delta \mathbf{a} \quad (\text{A.71})$$

a continuously differentiable function, \mathbf{b} continuously differentiable vector field

$$\operatorname{div} (a\mathbf{b}) = \mathbf{b} \cdot \operatorname{grad} a + a \operatorname{div} \mathbf{b} \quad (\text{A.72})$$

$a \in H^1(B)$, $\mathbf{b} \in \mathbf{H}_{\operatorname{div}}(B)$

$$\int_{\partial B} a \nu \cdot \mathbf{b} \, ds = \int_B \mathbf{b} \cdot \operatorname{grad} a + a \operatorname{div} \mathbf{b} \, dx \quad (\text{A.73})$$

\mathbf{a} , \mathbf{b} continuously differentiable vector fields

$$\operatorname{div} (\mathbf{a} \times \mathbf{b}) = \mathbf{b} \operatorname{curl} \mathbf{a} - \mathbf{a} \operatorname{curl} \mathbf{b} \quad (\text{A.74})$$

$\mathbf{a} \in \mathbf{H}_{\operatorname{curl}}(B)$, $\mathbf{b} \in \mathbf{H}^1(B)$

$$\int_{\partial B} \mathbf{b} \cdot (\nu \times \mathbf{a}) \, ds = \int_B \mathbf{b} \operatorname{curl} \mathbf{a} - \mathbf{a} \operatorname{curl} \mathbf{b} \, dx \quad (\text{A.75})$$

a continuously differentiable function, \mathbf{b} continuously differentiable vector field

$$\operatorname{curl} (a\mathbf{b}) = a \operatorname{curl} \mathbf{b} - \mathbf{b} \times \operatorname{grad} a \quad (\text{A.76})$$

$a \in H^1(B)$, $\mathbf{b} \in \mathbf{H}_{\operatorname{curl}}(B)$

$$\int_{\partial B} a \nu \times \mathbf{b} \, ds = \int_B a \operatorname{curl} \mathbf{b} - \mathbf{b} \times \operatorname{grad} a \, dx \quad (\text{A.77})$$

\mathbf{a} , \mathbf{b} continuously differentiable vector fields

$$\operatorname{curl} (\mathbf{a} \times \mathbf{b}) = (\mathbf{a} \cdot \operatorname{grad}) \mathbf{b} - (\mathbf{b} \cdot \operatorname{grad}) \mathbf{a} + \mathbf{a} \operatorname{div} \mathbf{b} - \mathbf{b} \operatorname{div} \mathbf{a} \quad (\text{A.78})$$

\mathbf{a} continuously differentiable vector field, then the formulas

$$\operatorname{div} \{ \Phi(x, y) \mathbf{a}(y) \} = \operatorname{grad} \Phi(x, y) \cdot \mathbf{a}(y) + \Phi(x, y) \operatorname{div} \mathbf{a}(y) \quad (\text{A.79})$$

$$\operatorname{curl} \{ \Phi(x, y) \mathbf{a}(y) \} = \operatorname{grad} \Phi(x, y) \times \mathbf{a}(y) + \Phi(x, y) \operatorname{curl} \mathbf{a}(y) \quad (\text{A.80})$$

are true for both differentiation with respect to x and y .

$$\operatorname{div}_x \{ \Phi(x, y) \mathbf{a}(y) \} = -\operatorname{div}_y \{ \Phi(x, y) \mathbf{a}(y) \} + \Phi(x, y) \operatorname{div}_y \mathbf{a}(y) \quad (\text{A.81})$$

$$\operatorname{curl}_x \{ \Phi(x, y) \mathbf{a}(y) \} = -\operatorname{curl}_y \{ \Phi(x, y) \mathbf{a}(y) \} + \Phi(x, y) \operatorname{curl}_y \mathbf{a}(y) \quad (\text{A.82})$$

List of Figures

1.1	Basic principle of a hydrogen fuel cell	3
1.2	Stack consisting of 8 fuel cells	4
1.3	Fuel cell, wire grid model and measurement device for magnetic tomography	7
2.1	Discretization model with 5 points in each direction	55
2.2	Magnetic field on the shell of a cylinder	58
2.3	Our way of the current representation in $3d$	58
2.4	Simulated and reconstructed currents for a defect near the boundary	59
2.5	Simulated and reconstructed currents for two defects	59
2.6	Wire grid with 125 resistors	60
2.7	Wire grid and simulated magnetic field	60
2.8	Simulated and reconstructed currents in a small wire grid	61
2.9	Comparison of a difference reconstruction with the simulated z -currents	61
2.10	Fuel cell and segmentation of the graphite layer	62
2.11	Segmented fuel cell, measured and reconstructed currents	63
2.12	Difference reconstruction with three defects	63
3.1	Scene 1	85
3.2	Representation of $\mathcal{W}\mathbf{j}$ and \mathbf{w} on the xy-plane	86
3.3	Comparison of $\tilde{\mathbf{w}}$ and \mathbf{w} for a spherical test domain	87
3.4	Comparison of $\tilde{\mathbf{w}}$ and \mathbf{w} for an elliptic test domain	88
3.5	Comparison of $\tilde{\mathbf{w}}$ and \mathbf{w} for different test domains	89
3.6	$\tilde{\mathbf{w}}(z)$ for the test domains $G_z^{(k)}, k = 8, 4, 2, 6$	91
3.7	Composition of the test results for $d_n, n = 1 \dots 8$	92
3.8	Scene 2	93
3.9	Representation of $\mathcal{W}\mathbf{j}$ and \mathbf{w} on the xy-plane	93
3.10	$\tilde{\mathbf{w}}$ for test domains $G_z^{(k)}, k = 8, 4, 2, 6$	94
3.11	Composition of the results for $G_z^{(k)}, k = 1 \dots 8$	95
3.12	Scene 3	99
3.13	Logarithmic values of the responses for spherical test domains	100
3.14	Logarithmic values of the responses for cubic test domains	100
3.15	Sampling method with spherical test domains	100
3.16	Sampling method with cubic test domains	100

3.17 Reconstructed domain (light blue) compared to the original (red)	101
3.18 Scene 4	102
3.19 Logarithmic values of the responses for the balls	103
3.20 Colored plot of $\tilde{\mathbf{w}} = \int_{\partial B} \mathbf{w} a(\cdot, z_k) ds$ on a parallel surface of $\partial B_{R_{min}}(0)$. .	103
3.21 Reconstructed domain (light blue) compared to the original (red)	104

List of Boundary Value Problems

1 Interior Dirichlet problem for Laplace's equation	27
2 Interior Neumann problem for Laplace's equation	27
3 Exterior Dirichlet problem for Laplace's equation	28
4 Exterior Neumann problem for Laplace's equation	28
5 Interior normal problem for harmonic fields	29
6 Exterior normal problem for harmonic fields	29
7 Interior tangential problem for harmonic fields	47
8 Interior tangential problem for the 3d-Laplace equation	49
9 Interior Neumann problem for the impedance equation	51
10 An exterior problem with Neumann condition	64
11 Impedance equation with transmission and tangential condition	72
12 Impedance problem with Neumann and tangential condition	74
13 Interior Dirichlet problem for the classical Laplace equation	112
14 Interior Neumann problem for the classical Laplace equation	112
15 Exterior Dirichlet problem for the classical Laplace equation	112
16 Exterior Neumann problem for the classical Laplace equation	112
17 Interior normal problem for classical harmonic fields	118
18 Exterior normal problem for classical harmonic fields	118
19 Interior tangential problem for classical harmonic fields	118
20 classical Interior tangential problem for the 3d-Laplace equation	118
21 Exterior tangential problem for classical harmonic fields	118
22 classical Exterior tangential problem for the 3d-Laplace equation	119

Bibliography

- [Adams] R. A. Adams: *Sobolev Spaces*, Academic Press, London, 1997
- [BaKo] Bank, H.T. and Kojima, F.: *Boundary shape identification in two-dimensional electrostatic problems using SQUIDS*, J. Inverse Ill-Posed Probl. 8 (2000), No. 5, 487-504
- [CoKr1] D. Colton and R. Kress: *Inverse Acoustic and Electromagnetic Scattering Theory*, Springer-Verlag, Berlin Heidelberg, 1992
- [CoKr2] D. Colton and R. Kress: *Integral Equation Methods in Scattering Theory*, Wiley-Interscience Publication, New York, 1983
- [Co] M. Costabel: *Boundary Integral Operator on Lipschitz Domains: Elementary Results*, SIAM J. Math. Anal. 19 (1988), 613-626
- [EnHaNeu] H. W. Engl, M. Hanke and A. Neubacher: *Regularization of Inverse Problems*, Kluwer Academic Publisher, Dordrecht, 1996.
- [ErPo] K. Erhard, R. Potthast: *The point source method for reconstructing an inclusion from boundary measurements in electrical impedance tomography and acoustic scattering*, Inverse Problems 19 (2003), No. 5, 1139-1157.
- [GiTr] D. Gilbart and N. S. Trudinger: *Elliptic Partial Differential Equations of Second Order*, 2nd Edition, Springer Verlag, New York, 1983
- [GiRa] V. Girault and P.-A. Raviart: *Finite Element Approximation of the Navier Stokes Equations*, Springer Verlag, Berlin, 1986
- [Gri] P. Grisvard: *Elliptic Problems in nonsmooth domains*, Pitman Advanced Publishing Program, London, 1985
- [Hä] P. Hähner: *An exterior boundary-value problem for the Maxwell equations with boundary data in a Sobolev space*, Proc. Roy. Soc. Edinburgh **109 A**, 213-224
- [HaKüPo] K.-H. Hauer, L. Kühn, R. Potthast: *On uniqueness and non-uniqueness for current reconstruction from magnetic fields*, Inverse Problems, to appear

- [HPSW] K.-H. Hauer, R. Potthast, D. Stolten, T. Wüster: *Magnetotomography - A New Method for Analysing Fuel Cell Performance and Quality*, Journal of Power Sources, to appear.
- [Jost] J. Jost: *Partielle Differentialgleichungen: elliptische (und parabolische) Gleichungen*, Springer-Verlag, Berlin, 1998
- [Ker] H. Kersten: *Grenz - und Sprunrelationen für die Potentiale mit quadratintegrierbarer Dichte*, Res. d. Math. 3, 17-24 (1980)
- [Ma] E. Martensen: *Potentialtheorie*, B.B Teubner, Stuttgart, 1968
- [McL] W. McLean: *Strongly Elliptic System and Boundary Integral Equation*, Cambridge University Press, 2000
- [MeySe] N. Meyers and J. Serrin : $H=W$, Proc. Nat. Acad. Sci. USA **51** (1964), 1055-1056
- [Kre] R. Kress: *Linear Integral Equations*, 2nd ed. Springer-Verlag, New York, 1999
- [KrKüPo] R. Kress, L. Kühn and R. Potthast: *Reconstruction of a current distribution from its magnetic field*, Inverse Problems 18 (2002), No. 4, 1127-1146.
- [KüPo] L. Kühn and R. Potthast: *On the convergence of the finite integration technique for the anisotropic boundary value problem of magnetic tomography*, Math. Meth. Appl. Sci. 26 (2003), No. 9, 739-757
- [Luke] D. R. Luke: *Multifrequency inverse obstacle scattering: the point source method and generalized filtered backprojection*, IMACS Math. Sim. Sci., Vol. 66 (2004), 297-314
- [LuPo] D. R. Luke, R. Potthast: *The no response test - a sampling method for inverse scattering problems*, SIAM J. Appl. Math. 63 (2003), No. 4, 1292-1312 (electronic)
- [Ned] J.-C. Nedelec: *Acoustic and Electromagnetic Equations - Integral Representations for Harmonic Problems* Springer-Verlag, New York, 2001
- [Po1] R. Potthast: *Point-sources and Multipoles in Inverse Scattering*, Chapman and Hall, London, 2001
- [Po2] R. Potthast: *A point-source method for inverse acoustic and electromagnetic obstacle scattering problems*, IMA Journal of Appl. Math 61 (1998), 119-140
- [Po3] R. Potthast: *A set-handling approach for the no-response test and related methods*, IMACS Math. Sim. Sci., Vol. 66 (2004), 281-295
- [Ra1] Ramon, C. Marks R. J., Nelson, A. C. and Meyer, M. G.: *Resolution Enhancement of Biomagnetic Images Using the Method of Alternating Projections*, IEEE Trans. Biomed. Eng., Vol. 40, No. 4, 323-328 (1993).

-
- [Ra2] Ramon, C., Meyer, M. G., Nelson, A. C., Spelman, F. A., Lamping, J.: *Simulation Studies of Biomagnetic Computed Tomography*, IEEE Trans. Biomed. Eng., Vol. 40, No. 4, 317-322 (1993).
- [deRham] G. de Rham: *Varietes Differentiables*, Hermann (1960)
- [Sa] Sarvas, J.: *Basic mathematical and electromagnetic concepts of the biomagnetic inverse problem* Phys. Med. Biol. Vol. 32, No. 1, 11-22 (1987)
- [Str] Stroink, G.: *Cardiomagnetic Imaging*. in *Frontiers in Carciovascular Imaging* by Zaret, B. L., Kaufman, L., Berson, A. S. and Dunn, R. A. (Eds.), Raven Press, New York, 1993.
- [TiWa] Tilg, B. and Wach, P.: *An iterative approach on magnetic source imaging within the human cortex - a simulation study*, Int. J. Bio-Medical Computing 40, 51-57 (1995)

Lebenslauf

persönliche Daten

Name	Lars Kühn
Geburtstag	16.09.1976
Geburtsort	Dresden
Eltern	Kersti Kühn, geb. Puschbeck, DV-Administrator Reinhard Kühn, stellv. Studienseminarleiter
Anschrift	An der Koppel 160, 99100 Bienstädt
E-Mail	Kuehn.L@gmx.de

Schulausbildung

09.1983-07.1991	45. Polytechnische Oberschule Erfurt
08.1991-06.1995	Gymnasium 7, Erfurt Spezialschuleteil mathematisch-naturwissenschaftlicher Richtung
20.06.1995	Abitur

Wehrdienst

10.1995-09.1996	verlängerter Grundwehrdienst in der Stabskompanie der Panzerbrigade 39 in Erfurt
-----------------	--

Studium an der Georg August Universität zu Göttingen

10.1996-07.2001	Diplomstudiengang Mathematik
10.1996-09.2003	Diplomstudiengang Physik

Prüfungen/Abschlüsse

16.10.1998	Vordiplom Mathematik
11.02.1999	Vordiplom Physik
05.07.2001	Diplom Mathematik

Tätigkeiten

10.2000-09.2004	wissenschaftlicher Mitarbeiter in der Nachwuchsforschergruppe <i>Neue Numerische Verfahren zur Lösung Inverser Probleme</i> am Institut für Numerische und Angewandte Mathematik der Universität Göttingen
-----------------	--